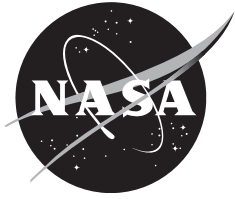


NASA/CR – 2013 - 218304



Environmentally Responsible Aviation N+2 Advanced Vehicle Study

Final Technical Report

*Aaron Drake, Christopher A. Harris, Steven C. Komadina, Donny P. Wang, and Anne M. Bender
Northrop Grumman Systems Corporation, Aerospace Systems, El Segundo, California*

April 2013

NASA STI Program ... in Profile

Since its founding, NASA has been dedicated to the advancement of aeronautics and space science. The NASA scientific and technical information (STI) program plays a key part in helping NASA maintain this important role.

The NASA STI program operates under the auspices of the Agency Chief Information Officer. It collects, organizes, provides for archiving, and disseminates NASA's STI. The NASA STI program provides access to the NTRS Registered and its public interface, the NASA Technical Reports Server, thus providing one of the largest collections of aeronautical and space science STI in the world. Results are published in both non-NASA channels and by NASA in the NASA STI Report Series, which includes the following report types:

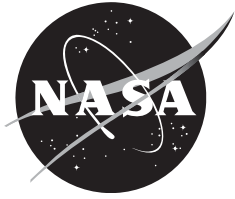
- **TECHNICAL PUBLICATION.** Reports of completed research or a major significant phase of research that present the results of NASA Programs and include extensive data or theoretical analysis. Includes compilations of significant scientific and technical data and information deemed to be of continuing reference value. NASA counterpart of peer-reviewed formal professional papers but has less stringent limitations on manuscript length and extent of graphic presentations.
- **TECHNICAL MEMORANDUM.** Scientific and technical findings that are preliminary or of specialized interest, e.g., quick release reports, working papers, and bibliographies that contain minimal annotation. Does not contain extensive analysis.
- **CONTRACTOR REPORT.** Scientific and technical findings by NASA-sponsored contractors and grantees.
- **CONFERENCE PUBLICATION.** Collected papers from scientific and technical conferences, symposia, seminars, or other meetings sponsored or co-sponsored by NASA.
- **SPECIAL PUBLICATION.** Scientific, technical, or historical information from NASA programs, projects, and missions, often concerned with subjects having substantial public interest.
- **TECHNICAL TRANSLATION.** English-language translations of foreign scientific and technical material pertinent to NASA's mission.

Specialized services also include organizing and publishing research results, distributing specialized research announcements and feeds, providing information desk and personal search support, and enabling data exchange services.

For more information about the NASA STI program, see the following:

- Access the NASA STI program home page at <http://www.sti.nasa.gov>
- E-mail your question to help@sti.nasa.gov
- Phone the NASA STI Information Desk at 757-864-9658
- Write to:
NASA STI Information Desk
Mail Stop 148
NASA Langley Research Center
Hampton, VA 23681-2199

NASA/CR – 2013 - 218304



Environmentally Responsible Aviation N+2 Advanced Vehicle Study

Final Technical Report

*Aaron Drake, Christopher A. Harris, Steven C. Komadina, Donny P. Wang, and Anne M. Bender
Northrop Grumman Systems Corporation, Aerospace Systems, El Segundo, California*

National Aeronautics and
Space Administration

*Dryden Flight Research Center
Edwards, CA 93523-0273*

April 2013

Available from:

NASA Center for AeroSpace Information
7115 Standard Drive
Hanover, MD 21076-1320
443-757-5802



Environmentally Responsible Aviation

N+2 Advanced Vehicle Study

Final Technical Report

Aaron Drake, Christopher A. Harris, Steven C. Komadina, Donny P. Wang and Anne M. Bender

Northrop Grumman Systems Corporation, Aerospace Systems, El Segundo, California

April 30, 2013

NASA Dryden Flight Research Center
P.O Box 273
M/S 1422
Edwards, CA 93523-0273

Prepared for Dryden Flight Research
Center Under Contract NND11AG02C

Abstract

This is the Northrop Grumman final report for the Environmentally Responsible Aviation (ERA) N+2 Advanced Vehicle Study performed for the National Aeronautics and Space Administration (NASA). Northrop Grumman developed advanced vehicle concepts and associated enabling technologies with a high potential for simultaneously achieving significant reductions in emissions, airport area noise, and fuel consumption for transport aircraft entering service in 2025. A Preferred System Concept (PSC) conceptual design has been completed showing a 42% reduction in fuel burn compared to 1998 technology, and noise 75dB below Stage 4 for a 224-passenger, 8,000 nm cruise transport aircraft. Roadmaps have been developed for the necessary technology maturation to support the PSC. A conceptual design for a 55%-scale demonstrator aircraft to reduce development risk for the PSC has been completed.

Contents

Abstract..... ii

Figures..... vii

Tables..... xi

1. INTRODUCTION 1

 1.1. Objectives..... 1

 1.2. Approach 1

 1.2.1. Task 1: 2025 EIS Projected Future Scenario 1

 1.2.2. Task 2: Preferred Systems Concepts Data Packages 3

 1.2.3. Task 3: Technology Maturation Plans: 15-Year Roadmaps..... 6

 1.2.4. Task 4: Prioritized List of Time-Critical Technology Demonstrations 7

 1.2.5. Task 5: Conceptual Design of an ERA/UAS Subscale Testbed Vehicle..... 8

2. PROJECTED FUTURE SCENARIO..... 10

 2.1. Update of Twin-Aisle Service Volume Forecast for NextGen 2025 10

 2.2. Update of Forecast Twin-Aisle Fleet Assumption in NextGen 2025 12

 2.2.1. PSC Fleet Integration Methodology 14

 2.3. System-level Environmental Modeling..... 17

 2.3.1. AEDT Model Overview..... 17

 2.3.2. AEDT Model Setup 18

 2.3.3. AEDT/BADA Performance Modeling 19

 2.3.4. AEDT Emissions Modeling..... 20

 2.4. AEDT Single Mission Modeling and Assessments 21

 2.5. System-Level Assessments and Metrics 24

 2.6. Aircraft Noise Analysis..... 31

 2.6.1. AAM Model Overview 31

 2.6.2. Noise Model Assessments 31

 2.7. PSC Technology Requirements on NextGen 45

3. PREFERRED SYSTEM CONCEPTS..... 47

 3.1. Overview of Vehicle Designs 47

 3.1.1. Task 2 Concept Vehicle Designs 47

 3.1.2. Configuration Descriptions..... 48

 3.1.3. General Parameters and Performance Summary 49

 3.2. Assessment of ERA Goals 51

3.2.1. Summary of ERA Goals 51

3.3. Comparison of Vehicles 52

 3.3.1. Configuration Effects on Goals 53

3.4. Mission Requirements, Constraints, and Assumptions 53

 3.4.1. NASA ERA Requirements 54

 3.4.2. Additional Requirements, Constraints and Assumptions 54

3.5. Integration of Technologies into Task 2 Vehicle Models 55

 3.5.1. Technologies Applied, Benefits, and Penalties Implementation into Models 55

 3.5.2. Technology Trade Studies 56

3.6. Vehicle Configuration Designs and Trade Studies 58

 3.6.1. 1998 EIS Reference Wing-Body-Tail Vehicles 58

 3.6.2. 2025 EIS Baseline Wing-Body-Tail Vehicles 59

 3.6.3. Flying Wing Centerbody and Wing Design 59

 3.6.4. Flying Wing Propulsion Integration 60

 3.6.5. Flying Wing Acoustics Considerations 62

 3.6.6. Flying Wing Payload Integration 63

 3.6.7. Multibody Configuration 66

 3.6.8. Multibody Configuration Design and Layout 67

 3.6.9. Multibody Propulsion Integration and Acoustic Considerations 69

 3.6.10. Multibody Payload Integration 69

3.7. Propulsion System Design 71

 3.7.1. Propulsion System Design Process 72

 3.7.2. 1998 EIS Reference Vehicles Engine Design 74

 3.7.3. 2025 EIS Baseline Vehicles and Multibody Vehicles Engine Design 74

 3.7.4. 2025 EIS Flying Wing Vehicles Engine Design 76

3.8. Vehicle Sizing and Results 77

 3.8.1. 1998 EIS Reference Vehicles Sizing 77

 3.8.2. 2025 EIS Baseline Vehicles Sizing 79

 3.8.3. 2025 EIS PSC Flying Wing Vehicles Sizing 82

3.9. Acoustic Analysis 85

 3.9.1. Vehicle Approach and Departure Profiles 85

 3.9.2. Acoustic Analysis Tools and Process 85

 3.9.3. 1998 EIS Comparison Vehicle Acoustic Analysis 87

 3.9.4. 1998 EIS Reference Vehicles Acoustic Analysis 88

3.9.5.	2025 EIS Baseline Vehicles Acoustic Analysis.....	88
3.9.6.	2025 EIS Multibody Vehicles Acoustic Analysis	89
3.9.7.	2025 EIS PSC Flying Wing Vehicles Acoustic Analysis.....	89
4.	TECHNOLOGY MATURATION PLANS.....	94
4.1.	Technology Assessment Approach	94
4.2.	Structures Technology.....	95
4.2.1.	Sizing Methodology.....	96
4.2.2.	Structures Trade Study Results.....	100
4.3.	Aerodynamic Technology	103
4.4.	Propulsion Airframe Integration	104
4.5.	Acoustic Technology.....	105
4.5.1.	Airframe Propulsion Source Shielding	105
4.6.	Subsystems Technology.....	106
4.7.	Propulsion Technology	106
4.8.	Technology Performance and Pareto Analysis	107
4.8.1.	2025 Baseline System Level Benefits – Fuel Burn	107
4.8.2.	PSC System Level Benefits – Fuel Burn	108
4.9.	System Readiness Level for PSC.....	109
5.	TIME-CRITICAL TECHNOLOGY DEMONSTRATIONS	111
5.1.	Prioritized Technology Demonstrations.....	112
5.1.1.	Benefit to Vehicle, Task 4 technologies	112
5.1.2.	Time-criticality, Task 4 technologies	114
5.1.3.	Prioritization of Task 4 technologies	114
6.	SUBSCALE TESTBED VEHICLE	116
6.1.	Introduction	116
6.2.	System Requirements.....	118
6.2.1.	NASA Defined System Requirements.....	119
6.2.2.	Concept of Operations and Derived Requirements	120
6.2.3.	Validation and Verification.....	121
6.3.	Performance Sizing Trade Studies	121
6.3.1.	Configuration Trade Space Overview	122
6.3.2.	Results for 55% Scale STV.....	123
6.4.	Configuration Integration and Structures.....	124
6.4.1.	Configuration Design.....	124

6.4.2.	Key Design Features	126
6.4.3.	STV Subsystems Integration.....	126
6.4.4.	Key Structures Design Drivers	128
6.4.5.	1.4.5 Cockpit Design and Structures Integration	129
6.4.6.	Landing Gear Design and Structures Integration.....	130
6.4.7.	Environmental Control System Structures (ECS) Integration	132
6.4.8.	Payload Structures Integration.....	133
6.4.9.	Payload Cargo Loading Integration	133
6.4.10.	Propulsion Design and Structures Integration.....	134
6.4.11.	STV Configuration Integration Summary.....	135
6.5.	Propulsion System.....	136
6.5.1.	Overall Propulsion System Layout	136
6.5.2.	Propulsion Flow Path Integration and Installation Parameters.....	137
6.6.	Vehicle Subsystems.....	137
6.7.	Vehicle Management Systems	138
6.7.1.	VMS Subsystem Equipment.....	140
6.7.2.	Cockpit Location and Layout.....	140
6.8.	Mass Properties	141
6.8.1.	STV Weight Estimate	141
6.8.2.	Technology Weight Savings or Impacts	142
6.8.3.	Weight Estimation Assumptions.....	142
6.9.	Baseline STV.....	143
6.9.1.	Baseline STV Aerodynamics.....	144
6.9.2.	Baseline STV Propulsion.....	146
6.9.3.	Baseline STV Performance.....	146
7.	Conclusions.....	149
7.1.	Significance of the AVC Study.....	150
7.2.	Perceived Impact of Work.....	150

Figures

Figure 1 Twin-Aisle Vehicle Class Operation and Distance Network Comparisons 11

Figure 2 Updated Twin-Aisle Vehicle Class Operation and Distance Network 12

Figure 3 Original vs. Adjusted Distance Networks for modeled Twin-Aisle Aircraft 13

Figure 4 PSC Payload and Range Comparisons existing Aircraft Types 14

Figure 5 Historical Retirement and Replacement of Selected Wide-Body Aircraft 16

Figure 6 Aggregated Replacements and Retirements of Selected Wide-Body Aircraft 17

Figure 7 Data-Flow Overview of AEDT 18

Figure 8 EI and Fuel Flow Log-Log Relationship as used in BFFM2 21

Figure 9 Comparison of Single Mission LTO Fuel Burn and Emissions at Nominal 40,000 ft
Cruise Altitude 22

Figure 10 Comparison of Single Mission Full Flight FB and Emissions at Nominal 40,000 ft
Cruise Altitude 22

Figure 11 Comparison of Single Mission Full Flight Fuel Burn and Emissions at Optimal
Altitudes 23

Figure 12 Percent Contributions by 2025 PSC and the 2025 Baseline Vehicle 25

Figure 13 Comparison of System Level LTO Fuel Burn and Emissions 26

Figure 14 Comparison of System Level Full Flight Fuel Burn and Emissions 26

Figure 15 System Level Full Flight Fuel Burn and Emissions Normalized Metrics 27

Figure 16 System Level Aircraft Comparisons of Percent ASM versus Percent CO₂ Emissions 28

Figure 17 System Level Aircraft Comparisons of CO₂ emissions per RPM versus Seating
Capacity and Average Trip Distance for Twin Aisle Aircraft Only 29

Figure 18 Altitude Distributions of CO₂ Emissions Loadings for all 2025 Scenarios 30

Figure 19 Altitude Distributions of NO_x Emissions Loadings for all 2025 Scenarios 30

Figure 20 PSC Passenger Noise Spheres for Takeoff Conditions 33

Figure 21 PSC Passenger Noise Spheres for Takeoff Conditions 34

Figure 22 PSC Passenger Noise Spheres for Approach Conditions 35

Figure 23 PSC Passenger Noise Spheres for Approach Conditions 36

Figure 24 PSC Passenger Noise Spheres for Approach Conditions 37

Figure 25 PSC Takeoff & Approach Ground Contours (SEL-dBA) 38

Figure 26 PSC Approach Ground Values at Computational Notes (SEL-dBA) 38

Figure 27 Time history SEL-dBA at 3 Points of Interest (40k,20k), (40k,22k), (40k,24k)Ft. 39

Figure 28 Sphere Slices at different theta locations, SEL-dBA (PSCpx004) 39

Figure 29 High resolution receiver mesh (200ft spacing) – PSC passenger, Approach, SEL-dBA
..... 40

Figure 30 SFO Runway Configuration 41

Figure 31 Single-Event Departure SEL Noise Gradient of 2025 Baseline Vehicle at SFO 42

Figure 32 Single-Event Departure SEL Noise Gradient of PSC at SFO 42

Figure 33 Difference SEL gradient comparing 2025 Baseline Vehicle and PSC on Departure at
SFO 43

Figure 34 Single-Event Arrival SEL Noise Gradient of 2025 Baseline Vehicle at SFO 43

Figure 35 Single-Event Arrival SEL Noise Gradient of PSC Vehicle at SFO 44

Figure 36 Difference SEL gradient comparing 2025 Baseline Vehicle and PSC on Arrival at
SFO 44

Figure 37 Concept Vehicle Design Process 47

Figure 38 Task 2 Final Concept Vehicle Designs 48

Figure 39	Multibody Configuration Vehicles.....	49
Figure 40	2025 PSC Passenger Version 3-View	50
Figure 41	2025 PSC Cargo Version 3-View.....	51
Figure 42	Comparison of Fuel Burn and Noise Margin for ERA Vehicles.....	53
Figure 43	NASA ERA Mission Profile	54
Figure 44	Conventional Wing-Body-Tail Configuration for 1998 EIS Reference Vehicles.....	58
Figure 45	Schematic Layout of Flying Wing Configuration	59
Figure 46	Flying Wing Propulsion Integration Approach Selection	61
Figure 49	Flying Wing Configuration with Acoustics Considerations	63
Figure 50	Example of Integrated Passenger Baggage	64
Figure 51	Flying Wing Passenger Internal Arrangement	65
Figure 52	Flying Wing Passenger Internal Arrangement	66
Figure 53	2025 Multibody Vehicle Configuration	66
Figure 54	Multibody Configuration Design Trades.....	68
Figure 55	Multibody Acoustic Considerations.....	69
Figure 56	Multibody Passenger and Cargo Payload Cabins.....	69
Figure 57	Multibody Passenger Cross Section Views.....	70
Figure 58	Multibody Passenger Interior Arrangement	70
Figure 59	Multibody Cargo Cross Section and Interior Arrangement	71
Figure 60	1998 Reference Vehicles Propulsion Installation Requirements	71
Figure 61	2025 Baseline Vehicles Propulsion Installation Requirements.....	72
Figure 62	2025 PSC Vehicles Propulsion Installation Requirements	72
Figure 63	Engine Cycle Optimization Process	73
Figure 64	Parametric models included in Modeling & Simulation	74
Figure 65	2025 Baseline Engine Overview	75
Figure 66	2025 Baseline Engine Optimization.....	75
Figure 67	2025 PSC Engine Optimization.....	76
Figure 68	2025 PSC Engine Technologies	77
Figure 69	Wing Aspect Ratio Study for 1998 Reference Vehicles	78
Figure 70	Wing Leading Edge Sweep Study for 1998 Reference Vehicles	78
Figure 71	Wing Area and Engine Scale Carpet Plot Study for 1998 Reference Passenger	79
Figure 72	Wing Area and Engine Scale Carpet Plot Study for 1998 Reference Cargo.....	79
Figure 73	Wing Aspect Ratio Study for 2025 Baseline Vehicle	80
Figure 74	Wing Leading Edge Sweep Study for 2025 Baseline Vehicles	80
Figure 75	Wing Area and Engine Scale Carpet Plot Study for 2025 Baseline Passenger (Note that all designs shown in plot meet balanced field length requirement).....	81
Figure 76	Wing Area and Engine Scale Carpet Plot Study for 2025 Baseline Cargo (Note that all designs shown in plot meet balanced field length requirement).....	81
Figure 77	Payload Cabin and Centerbody Study for 2025 PSC Passenger	82
Figure 78	Schematic Layouts of Selected Centerbodies for 2025 PSC vehicles.....	82
Figure 79	Leading Edge Sweep and Balancing Study Results for 2025 PSC Vehicles	83
Figure 80	Span Study Results for 2025 PSC Vehicles	84
Figure 81	Taper Ratio Study Results for 2025 PSC Vehicles	84
Figure 82	Pitch Up Limits Applied to 2025 PSC Vehicles	85
Figure 83	FAR Part 36 Take-off/Climb-out and Approach/Landing Profiles for Passenger Configurations.....	85

Figure 84 FAR Part 36 Stage 3 Certification Limits	87
Figure 85 FAR Part 36 Stage 3 Certification Levels and Limits for 777-300	88
Figure 86 (L) Fan Component Noise Point Source Location (R) Jet Exhaust Component Noise Point Apparent Source Location Relative to the Passenger PSC Configuration OML	91
Figure 87 FAR Part 36 Stage 3 Certification Levels	92
Figure 88 FAR Part 36 Stage 3, Stage 4, and N+2 ERA Certification Margins.....	92
Figure 89 Technology Assessment Approach	94
Figure 88 Major Components for Structural & Material Technologies Benefit Study	95
Figure 91 Set-up For Internal Loads Analysis of Wing Box	97
Figure 92 Set-up For Internal Loads Analysis of Fuselage Shell	98
Figure 93 Wing Component Weight Reduction Due to Composite Structures Technology	101
Figure 94 Fuselage Component Weight Reduction Due to Composite Structures Technology	102
Figure 95 Effect of Maneuver Load Alleviation on Wing Weight	103
Figure 96 Typical Drag Breakdown for Wide Body Aircraft.....	104
Figure 97 Pareto Analysis of Technology Benefits for 2025 Baseline Passenger.....	108
Figure 98 Pareto Analysis of Technology Benefits for 2025 Baseline Cargo.....	108
Figure 99 Pareto Analysis of Technology Benefits for Passenger PSC	109
Figure 100 Pareto Analysis of Technology Benefits for Cargo PSC.....	109
Figure 101 Vehicle Concept Lineage	116
Figure 102 STV Enables Flight Demonstration of Advance Configuration, Key Efficiency Technologies, and Noise/Emissions Reduction by 2017	117
Figure 103 Frequency of Cargo Densities Transported on Operational Aircraft	118
Figure 104 STV System Requirements and Document Tree.....	119
Figure 105 Sizing Trade Study Assumptions	122
Figure 106 Configuration Trade Space Overview	123
Figure 107 55% STV Overview	124
Figure 108 Baseline STV (55% Scale of PSC Cargo).....	125
Figure 109 Baseline STV (3-View).....	125
Figure 110 Baseline STV Key Features.....	126
Figure 111 STV Subsystems (Plan View)	127
Figure 112 STV Subsystems (Bottom View)	128
Figure 113 STV Key Structural Design Drivers.....	129
Figure 114 STV Cockpit (Centerline cross section).....	130
Figure 115 STV Cockpit (Isometric view)	130
Figure 116 STV Landing Gear (left side view)	131
Figure 117 STV Landing Gear Structural Integration	132
Figure 118 Environmental Control System (ECS) Structural Integration.....	132
Figure 119 STV Payload Structural Integration	133
Figure 120 STV Cargo Loading (463L Military Pallets).....	134
Figure 121 Propulsion Structural Integration	135
Figure 122 Baseline STV.....	135
Figure 123 Baseline STV 4-Engine Propulsion Layout [Bifurcated Inlet Ducting (Blue), Engines (Gray), and Exhaust Ducting (Orange)] Are Shown With Top OML Removed.....	136
Figure 124 STV Propulsion Flow Path Cross-Section at Outboard Engine Location.....	137
Figure 125 Key Vehicle Features	138
Figure 126 VMS Systems Avionics Architecture Interface	139

Figure 127 STV VMS Architecture.....	140
Figure 128 Crew Compartment Location on STV.....	141
Figure 129 Cockpit Layout - External View.....	141
Figure 130 STV Group Weight Statement.....	142
Figure 131 STV Weight Impact of Technologies.....	142
Figure 132 Baseline STV 3-View.....	144
Figure 133 STV Baseline Laminar Flow.....	145
Figure 134 STV Baseline L/D.....	145
Figure 135 M=0.80, 40,000 ft. Altitude STV L/D Correlation.....	146
Figure 136 STV Baseline Mission Profiles.....	147
Figure 137 STV Baseline Fuel and Time Spent.....	147
Figure 138 STV Baseline Flight Envelope.....	148

Tables

Table 1 SEL Noise Contour Area Change from Baseline Vehicle to PSC..... 45

Table 2 Task 2 Vehicles Geometry and Performance Parameters Summary 50

Table 3 N+2 Goals Assessment for ERA Vehicles 52

Table 4 Summary of 2025 Technologies Applied in Vehicle Models..... 56

Table 5 SWLFC Technology Trade for 2025 Baseline Vehicles 57

Table 6 Advanced Subsystems Technology Trade for 2025 Vehicles 57

Table 7 Passenger Class Distribution and Seat Pitch..... 63

Table 8 2025 Multibody Vehicles Geometry and Performance Summary..... 67

Table 9 FAR Part 36 Stage 3, Stage 4, and N+2 ERA Certification Margins 93

Table 10 Structures Technology Candidates 96

Table 11 Sizing Constraints and Failure Modes 99

Table 12 Aerodynamic Technology Candidates..... 104

Table 13 Propulsion Airframe Technology Candidates..... 105

Table 14 Acoustic Technology Candidates 105

Table 15 Subsystems Technology Candidates..... 106

Table 16 Propulsion Technology Candidates 107

Table 17 System Readiness Level Definition and Exit Criteria 110

Table 18 Task 4 Technologies 112

Table 19 2025 Cargo PSC..... 113

Table 20 2025 Passenger PSC 113

Table 21 Fuel Burn Reduction Benefit of Technologies on the PSC Vehicles 113

Table 22 Task 4 Technologies and STV Demonstration 114

Table 23 Prioritization of Task 4 Technologies..... 114

Table 24 55% STV Performance Summary..... 124

Table 25 STV Baseline Performance Summary (*NGC Estimated)..... 148

1. INTRODUCTION

The Northrop Grumman Systems Corporation, Aerospace Systems (NGAS), team has completed the National Aeronautics and Space Administration (NASA) N+2 Advanced Vehicle Concepts (AVC) Study developing conceptual designs for transport aircraft that could enter service in the 2025 (N+2) time frame. Northrop Grumman completed this work using a select team to execute the program including Rolls-Royce Liberty Works (RRLW), Wyle Laboratories, and Iowa State University (ISU).

1.1. Objectives

The main objective of this AVC study program was to conduct research into technologies and integrated aircraft systems that will allow subsonic transport aircraft entering into service in the 2025 or beyond time frame to simultaneously meet the NASA system-level goals of reduced noise, emissions, and fuel burn. Two critical objectives were to define two PSC conceptual designs, one passenger and one cargo aircraft, for EIS 2025 and determine through analysis how they will integrate efficiently within the NextGen airspace environment. An objective was to have this study be complementary to a number of ongoing and planned government programs. A significant objective of this study was to develop technology maturation plans that identify the required PSC technologies and develop roadmaps for maturing these technologies over the next 15 years while maturing all critical enabling technologies to TRL 6 by 2020. In order to demonstrate time-critical key technologies, an objective was to develop a subscale testbed conceptual design for future flight campaigns and begin reducing the risks of this demonstrator aircraft in two follow-on options.

Overall objectives of the two follow-on options are to reduce the risk for the technologies and integration that are critical enablers for the proposed 2025 EIS of the PSCs and provide critical validation data for predictive methods required for design of full-scale PSCs. A specific objective of Option 1 is to continue development of the flexible subscale testbed vehicle to a preliminary design level of maturity. These flight campaigns of the testbed will provide quantitative evidence that the N+2 fuel-burn, emissions, and noise goals can be met by the PSC designs and will evaluate technologies needed for integrating the cargo PSC as a UAS into the NAS. The Option 2 objective is to begin risk reduction activities associated with the preliminary design of the testbed aircraft.

1.2. Approach

The AVC study was divided into five tasks to accomplish the objectives. These tasks were interrelated, with information flowing between each of the various tasks.

1.2.1. Task 1: 2025 EIS Projected Future Scenario

Integration of the PSC into the projected 2025 NAS under the anticipated market conditions was performed by a Wyle Laboratories and Northrop Grumman team. The top-level tasks of defining the future scenario (operational environment caused by NextGen and market conditions) and assessing the operational efficiency of the PSC was performed with tools extensively used and/or developed by Wyle. This was backed up by extensive nonconventional concepts of operations (CONOPS) development and acoustics simulations performed by Northrop Grumman on advanced transport aircraft – both manned and unmanned. The PSC must not only operate in the NextGen environment but should take advantage of new operational procedures such as unmanned operations and dynamic wake vortex standoff distances. The effects of the PSC on

system-level acoustics, exhaust emissions, and passenger and cargo delivery was examined to directly compare advances in concept configuration, in technology levels, and in operational capabilities enabled by NextGen. The goal was to determine the real-world NAS system environmental impact while improving passenger and operator safety and reducing delays (increasing throughput). With infrastructure assets in 2025 projected to expand weakly, these goals are crucial for effective PSC vehicle design.

The Northrop Grumman team evaluated the planned NextGen improvements for the 2025 time frame and the impact of these advancements on the capability of the future NAS. Expected areas of impact were increased passenger throughput brought about by increases in both sector capacities and allowable airport operations per hour. Some of these improvements were dependent on NextGen capabilities alone, i.e., any airframe can take advantage of the future system. However, additional advantages were gained by investigating higher throughputs for large-class transport craft with weaker wake vortices and through turnaround time reductions. Likewise, optimized approaches for continuous descent revealed potential for fuel and emissions performance and impact on passenger delivery. The team took into account interdependencies and trade-off imbalances between system-level benefits (e.g., reduction in NAS-wide fuel burn/emissions) and local constraints (e.g., adverse noise impacts in select local areas) that challenged effective implementation of both technology integration and advanced operational concepts. For instance, vehicle cruise speed had a direct effect on throughput and/or the number of airframes required to perform the same payload delivery mission. The proper analysis of the environmental benefits (both system-level impacts and local/regional constraints) and operational efficiencies of NextGen vehicle concepts was important in order to understand their contribution to achieving and defining an optimal NAS solution.

Advanced environmental modeling tools were used, including the AEDT and the AAM to conduct system-level analysis of the environmental effects resulting from the integration of N+2 vehicle concept into the NAS under NextGen 2025 conditions. The AEDT is an integrated tool developed by the FAA for the modeling of environmental impacts, constraints, and tradeoffs resulting from airspace and airport operations. The AEDT integrates several legacy environmental tools including:

- Integrated noise model (INM)
- Model for assessing global exposure to the noise of transport aircraft (MAGENTA)
- Noise-integrated routing system (NIRS)
- Emissions and dispersion modeling system (EDMS)
- System for assessing aviation's global emissions (SAGE).

Inputs such as socioeconomic projections and assumptions regarding the progress in NextGen capabilities were justified and documented. Wyle took advantage of recent advances in modeling technology and technical synergies from ongoing NASA and FAA programs to model environmental (noise and emissions) and fuel-burn effects for both en route and terminal operations for the PSC. This identified trade-off benefits and requirements/constraints of the optimal deployment scenario for the N+2 vehicle concept.

The AAM tool is a suite of computer programs developed by Wyle for the DoD that predicts far-field noise for single or multiple flight vehicle operations of fixed-wing or rotary-wing aircraft. The AAM calculates the noise levels in the time domain and with a variety of integrated metrics at receiver positions on or above the ground at specific points of interest and over a

uniform grid. The AAM is based on three-dimensional noise sources defined about a vehicle moving along a trajectory. Three-dimensional source modeling includes the effect of thrust vectoring, implicit for rotorcraft and present on certain fixed-wing aircraft.

Wyle, a key developer of the AEDT, has worked closely with NASA, the Volpe Center, and the FAA to develop and test an operational AEDT V5 to conduct NextGen assessments. Prior to program start, the team updated the application reference fleet database with source characteristics for the advanced vehicles.

The acoustic impact assessment of advanced aircraft concepts employing engine shielding and other complex design features that aim to reduce the noise footprint of the vehicle generally require advanced simulation techniques for accurate modeling beyond the integrated capabilities of the AEDT. Wyle used its internal processes that work in tandem with the AEDT modeling infrastructure to permit the use of AAM single-event noise grids with the use of an event-based methodology to produce cumulative airport noise footprints for the PSC. Wyle worked with the rest of the Northrop Grumman team to ensure that the NextGen acoustic modeling fidelity was commensurate with vehicle design characteristics. Limitations present in the AEDT noise engine, encompassed by a single spectral class and set noise power-distance (NPD) of curves with lateral directivity modeling based on conventional tube-and-wing aircraft, were bypassed using such tools. It was determined that such an approach for advanced configuration PSC noise modeling was inaccurate, therefore Wyle provided the higher fidelity effort/analysis for this task to ensure that acoustic fidelity was sufficient. The availability of this multi-fidelity approach ensured that the analysis products were credible across all environmental impact metrics, including noise, emissions, and fuel burn.

1.2.2. Task 2: Preferred Systems Concepts Data Packages

The Northrop Grumman team produced six total aircraft conceptual designs for the AVC study. For each of the three time frame/assumption sets (1998 EIS, 2025 EIS, and 2025 EIS with configuration innovations), a passenger transport (50,000-pound payload, 8,000 nm range, 0.85 cruise Mach) and a cargo transport (100,000-pound payload, 6,500 nm range, 0.85 cruise Mach) were designed. Detailed mission characteristics specified by NASA were used. The degree of commonality between corresponding passenger and cargo versions was a result of the requirements and analysis process. In addition to designing these six aircraft, the team had the tools, methods, and designs to analyze these configurations for operation in the NAS.

A set of air vehicle design parameters and characteristics for each of the six configurations are described in this report. First, the given mission requirements applied to each aircraft are presented. A configuration description including a three-view drawing and an interior arrangement along with descriptions of the subsystems and sizing constraints are included herein. The aerodynamic characteristics of the air vehicles are represented by data and parameters of interest such as drag polars and drag buildups. Full group weights statements are provided that estimate the weight of the components of the aircraft and the entire aircraft in various operating conditions. Mission performance characteristics are provided for key segments of the mission and include contour plots displaying these characteristics in Mach-altitude space. A detailed description of the physical characteristics of the propulsion system and propulsion performance data for various flight conditions and mission segments is provided.

The AVC study was conducted using Northrop Grumman's Air Vehicle Multi-Disciplinary Optimization (AVMDO) methods. The AVMDO methods and toolset developed at Northrop

Grumman allowed the team to successfully execute the AVC study portion of the ERA program for configurations that vary from traditional to revolutionary, at a level of combined complexity and fidelity not achievable with a conventional aircraft design process.

This modern and validated AVMDO capability combines various tools, methods, and models used across multiple disciplines in the traditional air vehicle design process. These components of the overall AVMDO toolkit and process are designed to integrate together to rapidly produce a closed air vehicle design in a semi-automated, engineer-in-the-loop manner. This set of tools and models have been integrated using the *ModelCenter* environment. This allows the various tools and models to be linked together and to pass and receive input and output variables. Large-scale trade studies can be easily automated with this environment, and it further aids the engineer in collecting and visualizing these data.

Each given air vehicle design had associated with it a set of data files and variables relating to each of the tools and models from each discipline. These data files provided the majority of the above-mentioned air vehicle design parameters and characteristics. Other files provided the team with further design insight and rationale.

The AVC study team used CATIA as the computer-aided design (CAD) tool for its geometric representation of the air vehicles being designed. In the AVMDO process, a library of parametric aircraft models exists with each aircraft being of a unique “configuration type.” Within each configuration type, the AVMDO tools was automated to vary geometry parameters while still maintaining the same overall configuration type. Major configuration changes warranted use of a different configuration-type model (e.g., wing body tail, flying wing).

With these parametric CAD models connected to the set of AVMDO tools, each candidate air vehicle design had an associated CAD model capturing the geometric parameters, key dimensions, and underlying sizing constraints. The CAD model itself included parametric geometrical representations of the major interior components including passenger accommodations, cargo, the flight deck, and subsystems.

An aerodynamics database was created for each configuration in the study using a combination of empirical methods and a vortex lattice method. Lift-independent drag was estimated using the “delta method,” an empirical drag estimation procedure that is used in the respected government sizing code, the Flight Optimization System (FLOPS) while lift and lift-dependent drag were computed using a vortex lattice method. Northrop Grumman revised some aspects of the delta method as necessary to be more suitable for the type of configurations and advanced technologies studied in the ERA program. Furthermore, modifications were made to more accurately estimate the drag on flying wing configurations characterized by wings with any combination of low aspect ratio, high thickness-to-chord ratio, large sweep angles, or high taper ratios.

A wing design toolkit was used that automatically-created input models for the vortex lattice method. The wing design toolkit allocated a wing section thickness and twist for several spanwise stations along the wing based on given mission requirements such as cruise Mach number and maximum takeoff weight.

The above-mentioned aerodynamic database was used by the mission performance models in the AVMDO. Also, from this database aerodynamic parameters or plots of interest were quickly generated for review.

Parametric models of the various configuration topologies were established to determine mass properties for use in the AVMDO modeling. The initial data provided by the parametric analysis was weight and longitudinal center-of-gravity (CG). The weight estimation tool is a modified version of the Northrop Grumman conceptual mass properties (CONMAP) methods. CONMAP is a Northrop Grumman system of parametric weight estimation equations derived from statistical regression analyses. These analyses were performed over a 2-decade period on Northrop Grumman's weight database of over 120 aircraft. Impacts of technologies on weight were assessed in the model by modifying the input parameters. CONMAP also tracks longitudinal CG by component, allowing for a rapid balance estimate.

To address the challenges of the ERA program, the CONMAP system of equations provided the capability to customize and adjust for unconventional configurations (e.g., multi-body concept). Techniques for application to flying wings, oblique wings, tandem wing configurations, and other special designs were used in prior projects and similarly were applied to configurations in this program.

The CONMAP tool was linked to the parametric CAD models mentioned earlier and was integrated into the overall AVMDO toolset. Hence, each configuration had an associated CONMAP file that provided a full standard group weights statement.

Propulsion information was determined by working directly with RRLW to select a series of engine models for the AVC study and produced a set of associated five-column data files for these engines. These various engine cycles were representative of the 1998 EIS date and the 2025 EIS date with associated technology benefits. Appropriate installation losses were developed for each configuration based on the propulsion integration concepts. Engine thrust and specific fuel consumption (SFC) scalars were incorporated into the AVMDO toolset. With recommendations from RRLW, study engines were scaled in thrust and/or SFC as needed directly through the five-column data files. Geometrical and mass properties scale factors for the engines corresponding to these thrust and/or SFC scalings were provided by RRLW. With these, geometrical descriptions of the propulsion system and propulsion performance parameters were provided.

The Northrop Grumman team conducted sizing and mission performance trades using proprietary mission performance and field performance tools. These tools combined the aerodynamic and propulsion data with a mission profile input file. The mission performance code computed and tracked mission performance parameters as it performed the specified mission profiles. A point-performance code computed and displayed performance parameters such as specific range, specific endurance, and rate of climb as a function of Mach number, weight, and altitude.

The Northrop Grumman team performed takeoff and landing simulations using tools in the AVMDO environment. These tools provide a physics-based simulation built around the Federal Aviation Regulations (FAR) Part 25 takeoff and landing rules to calculate the balanced field length (BFL) of an aircraft. The takeoff and landing analysis used the same five-column engine data as the other AVMDO performance codes, along with a low-speed aerodynamics database and takeoff- and landing-specific configuration parameters. The output included BFL and associated queue speeds in weight-altitude space. Using this tool, the team evaluated the vehicle design space to understand the vehicle sizing and mission performance impacts of meeting the balanced field length goal.

Noise analysis was performed on all the configurations using Model for Investigating Detectability of Acoustic Signatures (MIDAS). MIDAS used propulsion cycle parameters and aero-performance-determined trajectory data to generate noise source signatures for each significant component noise source. These were compiled into the system-level noise source characterization, which integrates shielding and propulsion-airframe interaction effects. The combined noise source characterization and trajectory data were inputs to the exposure calculations of MIDAS, which computed the EPNL according to the FAR Part 36 prescription.

1.2.3. Task 3: Technology Maturation Plans: 15-Year Roadmaps

The approach to developing a robust set of 15-year technology maturation plans (TMPs) was to leverage related products developed during previous NASA and U.S. Air Force Research Laboratory (AFRL) efforts. These large sets of technologies were applicable to future subsonic transport concepts, both passenger (NASA N+3 Phase 1, NASA Extreme Short Takeoff and Landing [ESTOL]) and cargo (AFRL Revolutionary Concepts for Energy Efficiency [RCEE]). The set was updated and expanded to include those specifically applicable to the NASA ERA goals for the 2025 PSC. The process collected all inputs into the Northrop Grumman quality function deployment (QFD) database. Northrop Grumman performed an analysis of the value of each technology to the PSC with a transparent weighting and ranking system that honed the value of each weighting factor corresponding to the N+2 metrics. This ensured that trade-offs to overall system performance were in line with the NASA ISRP goals.

For the passenger and cargo PSCs defined in Task 2, 15-year look-ahead TMPs were developed outlining the required research to develop technologies and integrated aircraft systems critical to achieving the noise, emission, and fuel-burn goals. These were identified using the QFD process with a goal of TRL 6 for the 2020 date. The maturation plans highlighted the TRL and SRL progression (start and end points) along with the intermediate development steps to address the technology's technical, schedule, and cost challenges. Intermediate criteria for determining progress (go/no go) were provided to allow for credible future decisions for potential technology development activities. The TRLs followed Northrop Grumman's standards used in previous programs, which essentially adhere to the NASA TRL definitions. SRL definitions were developed by the team for use on this program. The technologies in the database fell into three key discipline areas being explored under this program: (1) airframe technology, including research into lightweight structures, flight dynamics and control, drag reduction, and noise reduction, (2) propulsion technology, including research into combustors, fan module concepts, distributed propulsion, boundary-layer ingestion (BLI), and the core; and (3) vehicle systems integration, including systems analysis, propulsion airframe integration, propulsion airframe aeroacoustics, and advanced vehicle concepts.

A rigorous QFD analysis was used to provide qualitative assessment to select the candidate N+2 technologies. Analyses that encompassed system and discipline sensitivity studies ultimately led to a ranking of the different technologies for which technology maturation plans were developed. Each technology was assigned a figure of merit with respect to the ERA N+2 goals through collaboration with subject matter experts (SMEs). A TRL risk factor was applied to each technology based on the respective TRL qualified for the PSC EIS of 2025. Additionally, an interaction quotient that captures and quantifies the technology's compatibility and interaction with different combinations of technologies to produce a final technology effectiveness rating (TER) was calculated. Technologies were prioritized by TER and used to minimize absolute

design uncertainty by identifying modeling accuracy needs between high-payoff and low-payoff (low-fidelity, high-relative-uncertainty) technologies.

The TMP activity involved 15-year time-phased plans that outlined the research required to develop the highly ranked technologies and integrated aircraft system critical to simultaneously meeting the noise, emission and fuel-burn goals for both the passenger and cargo PSCs. The selected candidate technologies were assessed for their applicability to the PSC vehicles along with the degree of benefit it provided to meeting each of the program goals, risk mitigation tasks, and associated TRL. The individual technology maturation roadmaps were integrated together to ensure that ERA system goals are simultaneously met by 2025. This integration identified synergies among individual maturation roadmaps providing opportunities for common and/or multipurpose demonstrations among individual roadmaps. The process of developing an integrated technology roadmap was iterative to factor in the increasing maturity of the various key systems, requirements, and technologies and the cost of these as the program progressed.

1.2.4. Task 4: Prioritized List of Time-Critical Technology Demonstrations

Based on the results of the time-phased 15-year technology maturation plan effort performed in Task 3, a prioritized list of time-critical technology demonstrations considered necessary for the development of the PSC vehicles was identified. This list was directed towards demonstrations of high-benefit/pay-off technologies and/or enabling technologies that must be performed in the FY 2013 to 2015 time frame or addressed initially within Phase 2 of the ERA program in order to meet TRL 6 goals in 2020 and EIS in 2025. The technology demonstration identification process used the QFD results from Task 3 in combination with the TER rankings to target high-payoff or enabling technologies that also provided a high level of technology interactions and compatibility with one another. The technology selection process assessed each technology's effect on the overall vehicle system. Each of the systems' technologies was evaluated and ranked against its resultant measures of merit. Measures of merit were weighted and summarized into an overall system effectiveness rating. Enabling technologies were analytically assessed for each PSC system concept. The results arrived at an overall system effectiveness rating and cost effectiveness to rank the best-value time-critical technologies for demonstration.

Each of the time-critical technology demonstrations has updated roadmaps with detailed development plans including: (1) cost; (2) technology maturation plan with key research, analyses, tool and method development, and ground and flight tests; (3) background information to set the context; (4) current status including TRL level; (5) risk assessment; and (6) applicability across vehicle classes. Sensitivity and trade analysis were carried out to quantify the critical technologies' contributions in simultaneously meeting the N+2 noise, fuel-burn, and emission performance metrics and ascertained the relative merits of each technology. The key technologies and technical challenges were classified and ranked under each of the following four major subgroups: (1) propulsion only, (2) airframe only, (3) integrated propulsion and airframe, and (4) integrated vehicle testbed.

The roadmaps for each of the four major subgroups were integrated to provide a comprehensive overall PSC technology maturation plan with detailed cost, performance, and schedule information. The overall TMP was designed to be a valuable deliverable to help guide future NASA ISRP investment decisions, including those for future phases of the ERA program and well beyond.

1.2.5. Task 5: Conceptual Design of an ERA/UAS Subscale Testbed Vehicle

An important step in reducing the risk associated with development of the full-scale version of the PSC vehicle is the development and flight demonstration of a subscale testbed vehicle (STV). The testbed vehicle was designed to test integrated technologies that are critical to the success of the PSC. In order to provide NASA with greater value from the testbed vehicle, it was designed for subsequent studies of UAS operations in the NAS. It was determined that the technology demonstration and risk reduction objectives for the testbed vehicle were best served by a manned aircraft. However, demonstrations of UAS operations in the NAS necessarily required an optionally-manned vehicle. To meet these objectives, the testbed was designed to initially be a manned aircraft with designed-in and built-in provision for conversion to autonomous operation. To provide maximum flexibility and utility, the autonomous control system for the testbed will include a remotely-piloted mode.

During the AVC study, the conceptual design of the testbed vehicle was completed. The conceptual design of the testbed included determining the vehicle and system requirements, sizing and analyzing the vehicle design, determining the concept of operations and specific mission attributes, developing cost and schedule estimates for the testbed vehicle, planning the preliminary design phase of the testbed's development, and planning the risk reduction testing that will occur as part of the preliminary design phase.

The functional and performance requirements for the testbed were determined directly from the design of the PSC and the prioritization of critical technologies. Determination of these requirements lent itself directly to identification of the verification and/or validation approaches that can be employed in the design and testing of the testbed. In order to have the most efficient testbed development program and the best-designed testbed vehicle, these requirements were determined as inputs to the initial sizing and design of the testbed vehicle.

The conceptual design of the testbed was done using existing Northrop Grumman conceptual design tools such as those employed in Task 2. Additionally, specific information about the characteristics and integration details for key technologies to be included in the testbed that were developed in Task 3 and Task 4 were used, including consideration of the scalability of the technologies to the subscale size of the testbed. The requirements for the testbed provided specific performance and system capabilities against which the sizing studies were measured. Initially, the testbed was assumed to be a 50 percent-scale version of the PSC. However, sizing studies allowed the scale of the testbed to be explored, ensuring that the resulting testbed design was optimally sized to accomplish the objectives. Because of the speed capability (Mach number matching the PSC) of the testbed, systems such as retractable landing gear were necessary.

The propulsion system for the testbed used existing off-the-shelf turbofan engines. However, this engine will be used to demonstrate the propulsion integration aspects of the PSC by designing the integration of the propulsion system to use the same approaches embodied in the PSC. As a result, the actual measured efficiency of the testbed will not match that predicted for the PSC; however, correcting for the difference in the engine's efficiency is straightforward and will allow validation of the predicted efficiency of the PSC.

Planning for autonomous and remotely piloted operation of the testbed was done during the conceptual design task. Building on experience with autonomous aircraft over the last decade, Northrop Grumman has used internal funding to develop a standardized approach to converting existing manned aircraft to autonomous operations. While this work has focused on fully-

autonomous vehicles due of their significant operational benefits over remotely-piloted vehicles, the approaches and architectures employed were modified to also provide the remotely piloted capability desired in the testbed.

Based on the conceptual design of the testbed and its performance characteristics, the mission and operational characteristics of the vehicle were determined. The concept of operations developed from this identified how to meet the requirements identified for the testbed system using the expected characteristics of the testbed vehicle. A design reference flight mission (DRFM) for the testbed vehicle was assembled to include the flight test objectives for each stage of testing. To validate the DRFM, a description of the testbed vehicle characteristics that facilitate addressing those objectives was used together with the applicable flight envelope.

Based on the conceptual design of the testbed vehicle, a development schedule was determined. Rough-order-of-magnitude (ROM) costs for the development stages of the testbed and unique resource requirements were determined. This estimating activity looked at the preliminary design phase, the detailed design phase, manufacturing, and all test phases.

Specific detailed planning of the preliminary design activities were undertaken for the specific purpose of allowing the conceptual design work to flow smoothly and efficiently into the next phase of development. The specifics of the approach to preliminary design included a ROM cost estimate, schedule, and resource requirements to develop the testbed vehicle for the Preliminary Design Review (PDR). A plan based on the NASA-specified tasks contained in the NRA ROA-2010 Appendix D and tailored to include Northrop Grumman best practices, was developed to accomplish the testbed preliminary design.

To accompany the planning for the preliminary design of the testbed, planning for the associated risk reduction testing were performed. This risk reduction testing included both technology-specific testing needed to ensure that the design of the testbed provides an appropriate demonstration environment and typical testing activities that are part of preliminary design.

2. PROJECTED FUTURE SCENARIO

The analysis to assess the system-level effects of the PSC integrated into the projected 2025 National Airspace System (NAS) was performed using updated 2025 fleet and operations forecasts. These operations databases were previously modeled for the NextGen Advanced Vehicles & Concepts NRA. The forecast represents a 2025 NextGen end-state and was derived from analysis produced by the Joint Planning and Development Office (JPDO) and the Federal Aviation Administration (FAA). The initial forecasts for NextGen assessments were based on a single day of operations in the NAS¹, which was projected into a NextGen end-state for the Year 2025. Both domestic and international operations were included in the database, originating from within the CONUS. A range of typical vehicles that operate in the US airspace is included in this fleet mix, from large transports to GA vehicles. Projections include phasing out of existing airframes, and inclusion of planned new airframes just entering the market.

The JPDO/FAA NextGen forecast was updated and modeled in the Airspace Concept Evaluation System (ACES) to perform system-level assessments of various advanced vehicles and NextGen operational concept in a previous NRA. For this analysis, a new assessment and further updates were performed to take into account current conditions in the air transportation system as well as the effects of recent events (e.g., economic downturn, fuel price volatility, security challenges) on operational levels in the NAS. The study team used this basis to update the overall 2025 baseline operational levels to reflect current conditions within the market and vehicle class of interest to the study, namely the twin-aisle long-haul vehicle class.

The evaluation of the NextGen dataset was performed by comparing the fleet composition and operational volumes against other datasets maintained by the FAA that provide detailed information on fleet composition and number of operations for the entire NAS. Enhanced Traffic Management System (ETMS) data for the year 2009 were used as a reference and anchor for the assessment of 2025 forecast conditions in terms of overall service volumes. Forecasts performed for the International Civil Aviation Organization's (ICAO's) Committee on Aviation and Environmental Protection (CAEP)² were used to compare overall assumptions in fleet forecasting for the twin-aisle vehicle class under 2025 NextGen conditions. The value of this assessment, within the resource constraints of the study, is twofold: (a) the injection of market realism in overall twin-aisle forecasts for modeled 2025 baseline conditions and (b) the inclusion of ICAO/CAEP forecasting knowledge into the modeling assessments of the study.

2.1. Update of Twin-Aisle Service Volume Forecast for NextGen 2025

The review of the 2025 baseline data for the Twin-Aisle category was performed for both domestic and international operations based on key attributes including total operational volumes, total distance flown, average trip distance, payload, and relative mix of aircraft types. These attributes were assessed due to their relative influence on environmental effects including noise and emissions, as well as their relevance to the mission capability goals of the PSC. This served as a guiding rationale and methodology for PSC integration into the projected 2025 NextGen fleet.

The domestic and international Twin-Aisle total distance and number of flights comparisons were performed using the CAEP 2006, ETMS 2009, and CAEP 2026 dataset. Each dataset was

¹ The seed day for the initial forecast leading to NextGen baseline is 13 July 2006

² 2026 forecast Movements databases developed for CAEP 8 cycle and now used for the ongoing CAEP 9 cycle

first loaded into a relational database to add fleet and airport information; these were then used to facilitate the identification and grouping of the data. The CAEP 2006 data were used to represent the source (seed) of the forecasted JPDO baseline since that dataset is also based on the 2006 ETMS data. A comparison of seed data representing 2006 and 2009 operations reveals a 6-percent decrease in the number of flights within the Twin-aisle vehicle class, most likely due to overall market responses and airline adjustments resulting from recent conditions including global fuel price volatility and the economic downturn. Notably, the comparison reveals that, within this vehicle class, fewer flights served longer distances in 2009 than in 2006, potentially reflecting a fleet and O/D pair adjustment made by airlines more recently in response to market conditions. A comparison of forecast CAEP 2026 and NextGen 2025 data shows the latter projecting significantly less operations, but serving more distant O/D pairs on international routes. The differences in overall service volumes between seed and projected reference datasets are presented in Figure 1.

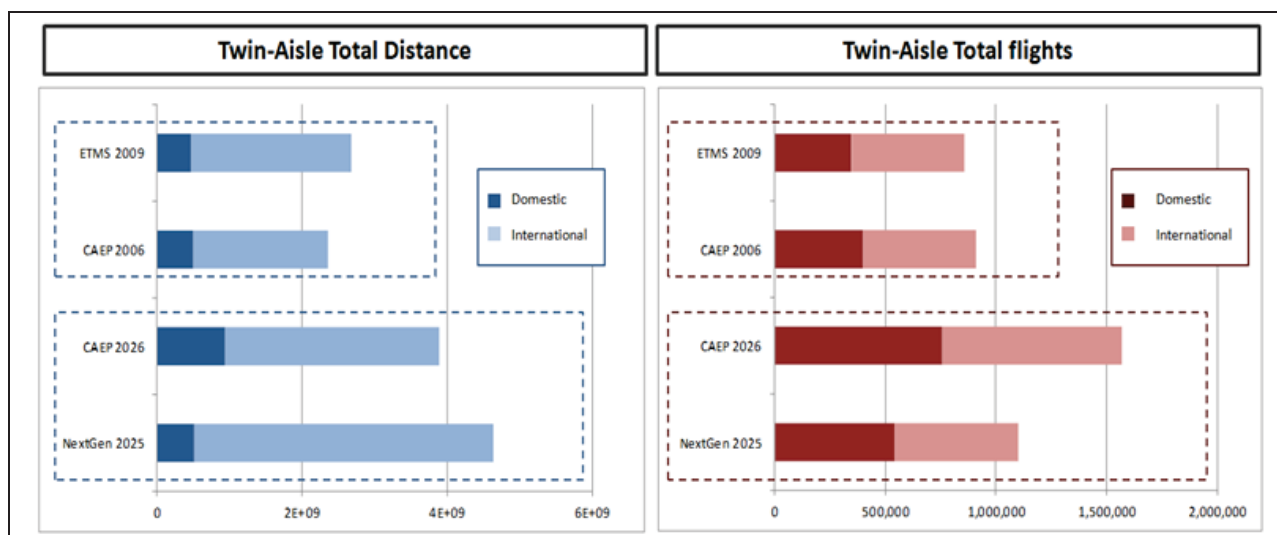


Figure 1 Twin-Aisle Vehicle Class Operation and Distance Network Comparisons

Based on the observed variance between the seed data (2006) for the NextGen forecasts and more recent data (2009) reflecting total NAS operations, the study team applied aggregate in-class growth rates from current commercial sources³ as well as ICAO/CAEP to current operational levels to define updated NextGen service volumes and total distance network for the Twin-Aisle vehicle class. Figure 2 shows the updated 2025 NextGen operational levels for the Twin-aisle vehicle class compared to previously modeled NextGen levels as well as forecasts projected by ICAO/CAEP. The update provides a more current projection of overall operations within the vehicle class of interest to the study, but does not update forecasts previously developed for other vehicle classes under NextGen. It also does not alter the trajectory information simulated for the 2025 NextGen end state for all modeled aircraft.

³ Data published by Boeing and Airbus in their respective 2010-2011 market outlook reports was used

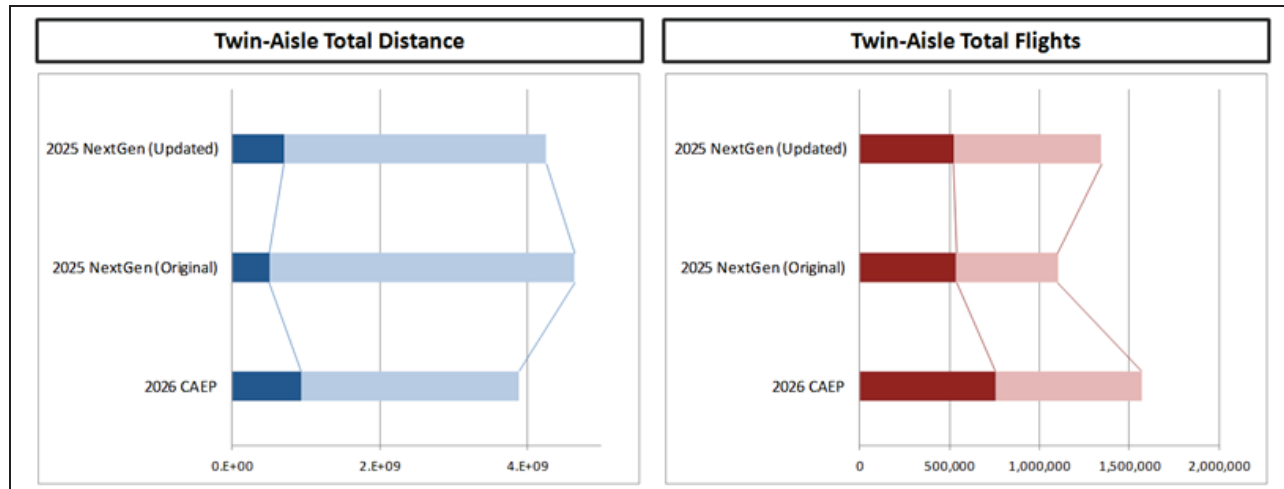


Figure 2 Updated Twin-Aisle Vehicle Class Operation and Distance Network

2.2. Update of Forecast Twin-Aisle Fleet Assumption in NextGen 2025

Projected Twin-Aisle vehicle class fleet mix data was also examined through a comparative analysis of CAEP and NextGen service volumes of each major aircraft type within the class. Note that the forecast JPDO/FAA NextGen and CAEP fleet projections vary in terms of methodology. The 2026 CAEP forecasts are developed by incorporating internationally approved fleet retirement and replacement schedules that have been reconfirmed in the ongoing CAEP 9 work cycle, and make equitable assumptions of fleet growth for competing aircraft types (ICAOa 2010).

A comparison of fleet service volumes for both the domestic and international segments for the twin-aisle vehicle class revealed differences between the assumptions originally used in the NextGen 2025 baseline and those more recently developed by the ICAO/CAEP Forecast and Economic Analysis Support Group (FESG) for application in global assessments. Therefore, the study team applied fleet adjustments to update forecast levels for families of aircraft with the most pronounced differences in forecast levels between what is accepted as ICAO/CAEP fleet projections and what was previously modeled for NextGen 2025. The fleet adjustment process that was undertaken to realign forecasts within the Twin-Aisle class consisted of three steps:

- Generate aircraft type distribution information for both the target and reference databases;
- Develop the set of change percentages to apply to specific aircraft types to normalize overall aircraft distributions relative to source data;
- Update service volumes for specific O/D pair flights consistent with calculated change distributions.

The resulting adjustments to the Twin-Aisle aircraft class domestic and international distance network by major aircraft type are shown in Figure 3. It is also noted that flight frequency for the relevant aircraft types was adjusted in order to realign NextGen distance network with current international forecasts as well as account for the updates made to NextGen service volumes as discussed in the previous section and highlighted in Figure 2.

The extent of the prescribed updates and adjustments is limited to the scope of the study and its focus on the design class of the N+2 PSC. It is also important to note that forecasts under

ICAO/CAEP and those under NextGen use different sets of broad assumptions and different fleet forecasting methodologies. Thus, the study team did not seek to impose one methodology (or forecast) over the other, but instead apply adjustments to the NextGen baseline that are grounded in internationally-accepted assumptions about fleet evolution while preserving the general composition of NextGen fleet mix. As shown in Figure 3, this data fusion process results in a reduction in the forecasting gap between the two methodologies/sources for various aircraft types, but does not entirely close it. It is recommended that a more expanded and detailed fleet forecasting study be performed to update forecasts for all vehicle classes in NextGen based on multi-sourced projections of more recent operations in the NAS that take into account recent market conditions and current knowledge on fleet retirement, replacement, introduction, and evolution.

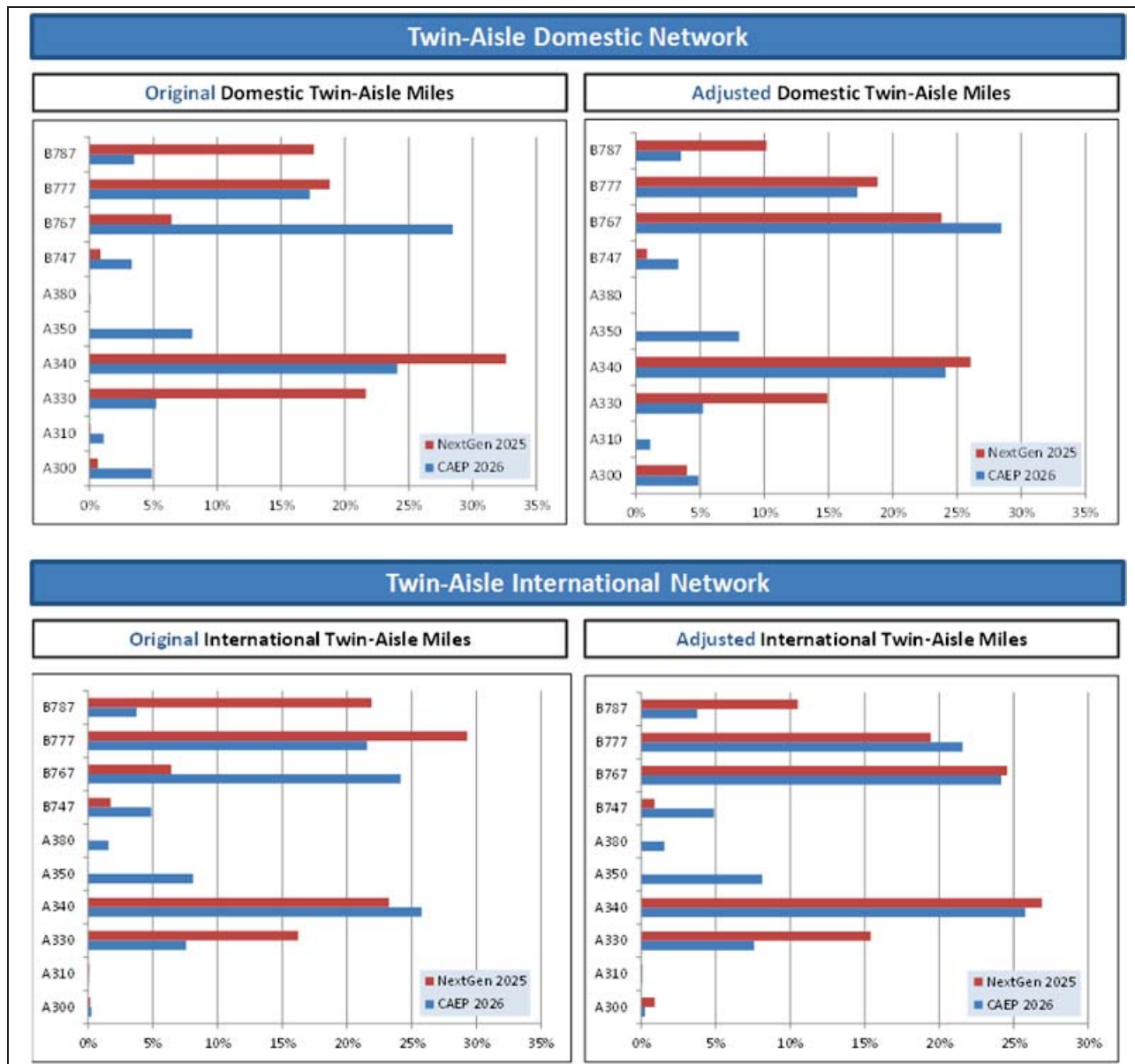


Figure 3 Original vs. Adjusted Distance Networks for modeled Twin-Aisle Aircraft

2.2.1. PSC Fleet Integration Methodology

The criteria used for the fleet integration process of replacing a portion of the 2025 projected fleet with either the PSC or Baseline vehicle was the NASA-defined ERA mission capabilities of maximum range and payload. All twin-aisle aircraft with maximum ranges and payloads that were within the ERA mission capabilities were assumed, for analysis purposes, to be candidates for one-to-one replacements. Other partial replacements of out-of-range aircraft would be dependent on specific market factors (e.g., O/D pair networks, load factors, flight frequencies). The underlying assumption is that the PSC represents both a highly successful market penetration within its class, on the order of historical new vehicle introductions, and a highly desirable technology that the market would integrate and enable to reach a mature operational state. Figure 4 provides a plot of maximum payload versus maximum range for a comprehensive list of twin aisle aircraft types. The aircraft in the dashed box in Figure 4 represent the first-tier of the replacement methodology whereby relevant aircraft types were replaced on a one-to-one basis for the PSC. As explained in forthcoming sections, partial replacements were also assumed for other aircraft outside mission box based on other criteria.

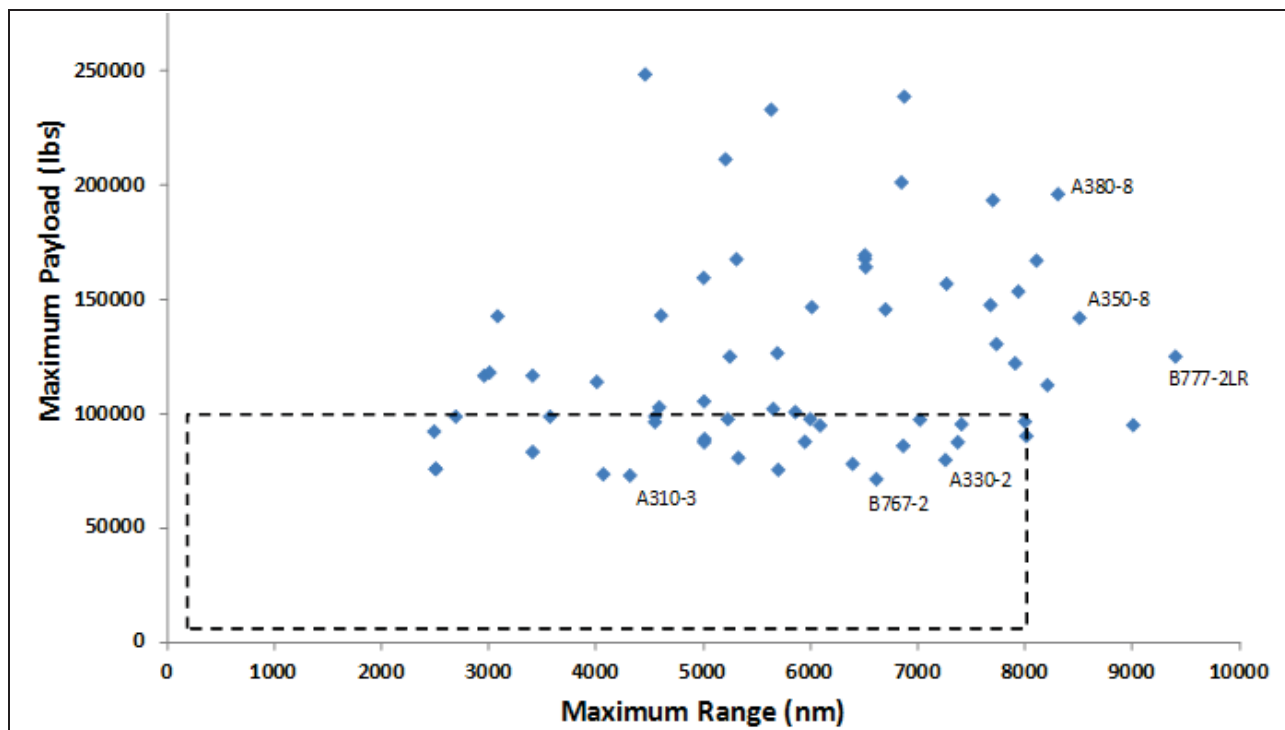


Figure 4 PSC Payload and Range Comparisons existing Aircraft Types

The first-tier replacements were conducted based on a PSC maximum range of 8,000 nm and a conservative maximum payload of 100,000 lb which encompasses the passenger version (50,000 lb maximum payload) and the cargo version (100,000 lb maximum payload) of the PSC. This was also consistent with the targeted replacement of the B787 variants with the PSC (i.e., the B787 max payload is approximately 100,000 lb).

The second tier of the PSC integration methodology considered twin-aisle aircraft types outside of the dashed box based on actual operational usage (trip distance and payload) of those aircraft in the NAS at or below PSC maximum range and payload. However, it is difficult to develop a replacement strategy that would take into account the differing magnitudes of maximum ranges

and payloads of aircraft that are outside of the PSC's capabilities. That is, for example, a replacement strategy for an aircraft with a maximum payload of 150,000 lb would likely be different than that of an aircraft with a payload of 200,000 lb. While both aircraft types could potentially be replaced by a PSC technology that provides better ROI and enhanced operational efficiency on specific O/D pairs that the PSC can serve, the process of projecting fleet replacements for such aircraft introduces complex economic and market factors that are beyond the scope of the study.

Aircraft-specific replacement ratios were developed from analyzing Form 41(T-100 Segment) flight data from the Department of Transportation (DOT) Bureau of Transportation Statistics (BTS) that contains payload information (BTS 2011). The methodology was based on summing distances flown by aircraft type with payloads above and below the PSC maximum payload. This produced replacement ratios for each aircraft based on flights performed within the NextGen baseline. Only flights with trip distances shorter than the PSC maximum range of 8,000 nm were used to develop these specific ratios.

Since the flight resolution of DOT/BTS Form 41 data does not provide any more specificity than origin-destination pairs by month, they are not as well suited for these assessments as individual flights. However, since high variability in payload is not expected among flights for the same origin-destination pair, the overall replacement ratios developed from this method are expected to be reasonably accurate.

For aircraft range, flight data from previous ACES NextGen simulations was used directly to identify the twin-aisle aircraft types performing flights with trip distances less than the PSC maximum range. Only these identified aircraft were candidates for replacement by the PSC. Although, this did not guarantee that an identified aircraft could not fly distances greater than the PSC maximum range, it provides a reasonable and somewhat conservative approximation for identifying potentially replaceable flights in a market where a game-changer like the PSC is introduced. It also ensures that no flights with ranges greater than the PSC maximum range were replaced. This clarity is possible because unlike payload, distance could readily be derived from modeled flight data in the NextGen 2025 Baseline.

In some cases, a specific ratio for an aircraft type could not be developed due to erroneous data in the DOT/BTS datasets. For these cases, a default ratio was developed by first examining 15 years of recent historical data showing the progression of selected wide-body aircraft retirements and replacements (as well as growth) as shown in Figure 5. The figure presents historical curves for in-class aircraft types with example replacement/retirement trend relationships highlighted for emphasis.

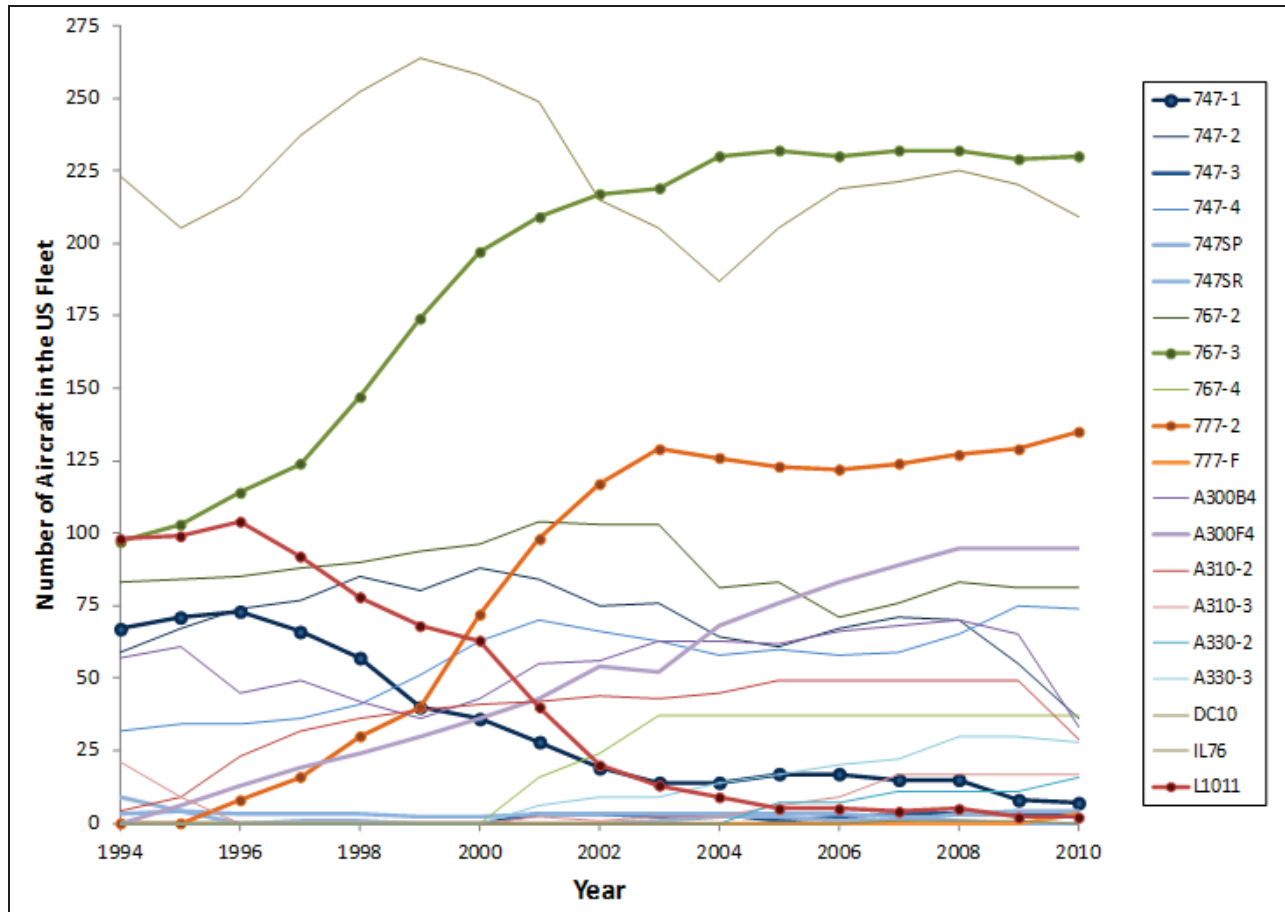


Figure 5 Historical Retirement and Replacement of Selected Wide-Body Aircraft

The referenced historical fleet evolution data was first segregated in terms of in-production aircraft with added units into the market place and retiring aircraft with declining units serving in the NAS over the past 15 years. Second, total units of each category were summed to define the degree of growth/decline and the general relationship between rates of aircraft introduction for newer aircraft and equivalent rates of retirement for older aircraft⁴. Figure 6 shows the two trend curves derived for retiring versus in-production aircraft since 1994. The resulting comparison shows that the retired aircraft account for approximately 45% of the increase in in-production aircraft with the rest accounting for growth in demand and other market-based conditions. Therefore, the study team assumed a historical replacement rate of 45% given that the PSC introduction is within a forecast NextGen 2025 end state that already provides for projected growth in air traffic and assumes, for analysis purposes, a mature operational state for the PSC.

⁴ Rate of introduction and maturity of newer aircraft into NAS not only replaces older retiring aircraft, but also accommodates growth in demand for air transportation and other market-based conditions

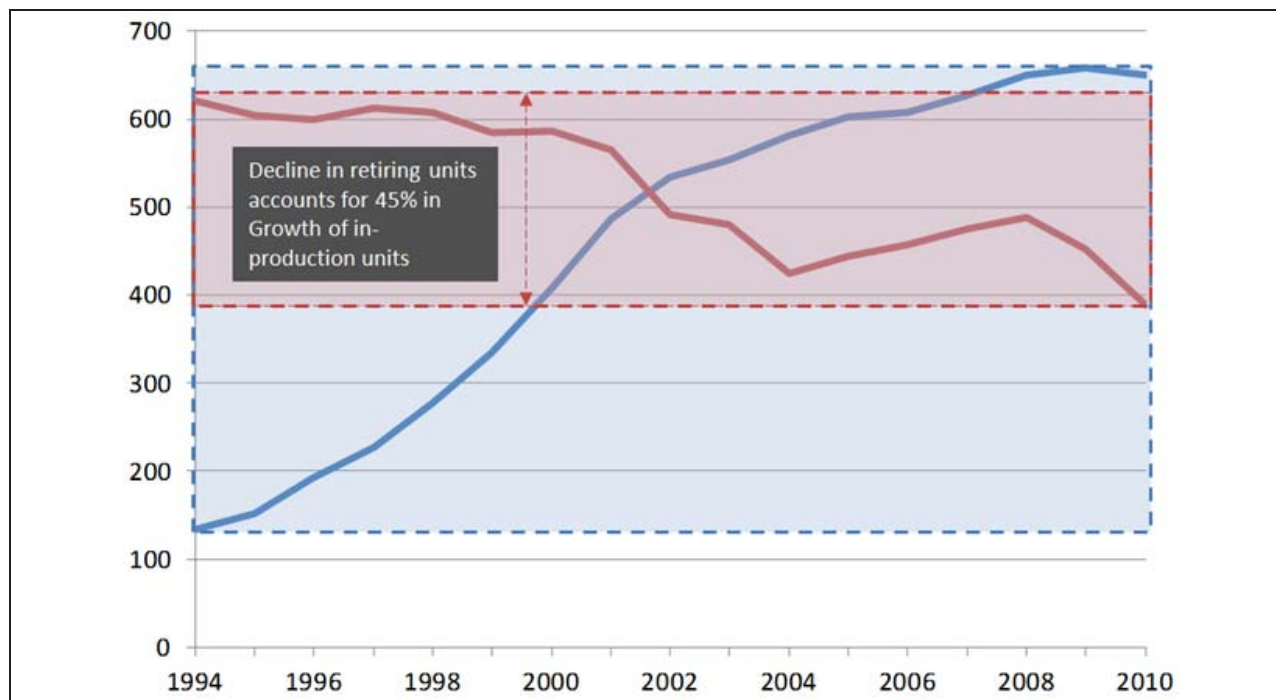


Figure 6 Aggregated Replacements and Retirements of Selected Wide-Body Aircraft

2.3. System-level Environmental Modeling

2.3.1. AEDT Model Overview

The Aviation Environmental Design Tool (AEDT) represents a comprehensive effort by the FAA to develop an integrated platform for the modeling of environmental impacts, constraints and tradeoffs resulting from airspace and airport operations (FAA 2011). The model integrates several legacy environmental tools including the Integrated Noise Model (INM), the Model for Assessing Global Exposure to the Noise of Transport Aircraft (MAGENTA), the Noise Integrated Routing System (NIRS), the Emissions and Dispersion Modeling System (EDMS), and the System for Assessing Aviation's Global Emissions (SAGE). AEDT is currently used by the FAA for domestic planning and research and to support the work of the Civil Aviation Organization (ICAO) Committee for Aviation Environmental Protection (CAEP). AEDT is currently in development and is not publicly available.

The tool is a collection of various components that allow users to perform integrated modeling of operational scenarios. The four primary components are the Aircraft Performance Module (APM), the Aircraft Emission Module (AEM), the Aircraft Acoustics Module (AAM), and the Acoustics Metrics Module (AMM). AEDT also includes various controllers that drive data creation processes and interrogate/task the application's computational modules. The AEDT data are stored in relational databases implemented using the Microsoft SQLServer platform and can be categorized into two classes: reference databases and analysis-driven databases. The first class of databases includes the information that underpins any analysis such as the aircraft performance, source noise characteristics, and emissions data, which are stored in the fleet database, and the airport and airspace information, which are found in the Airport database. The second class of databases includes analysis information like fleet, flight and trajectory data,

which are stored in the Movements database, and the output data, which are saved in the Results database. Figure 7 provides a data-flow diagram of the main AEDT modules and datasets.

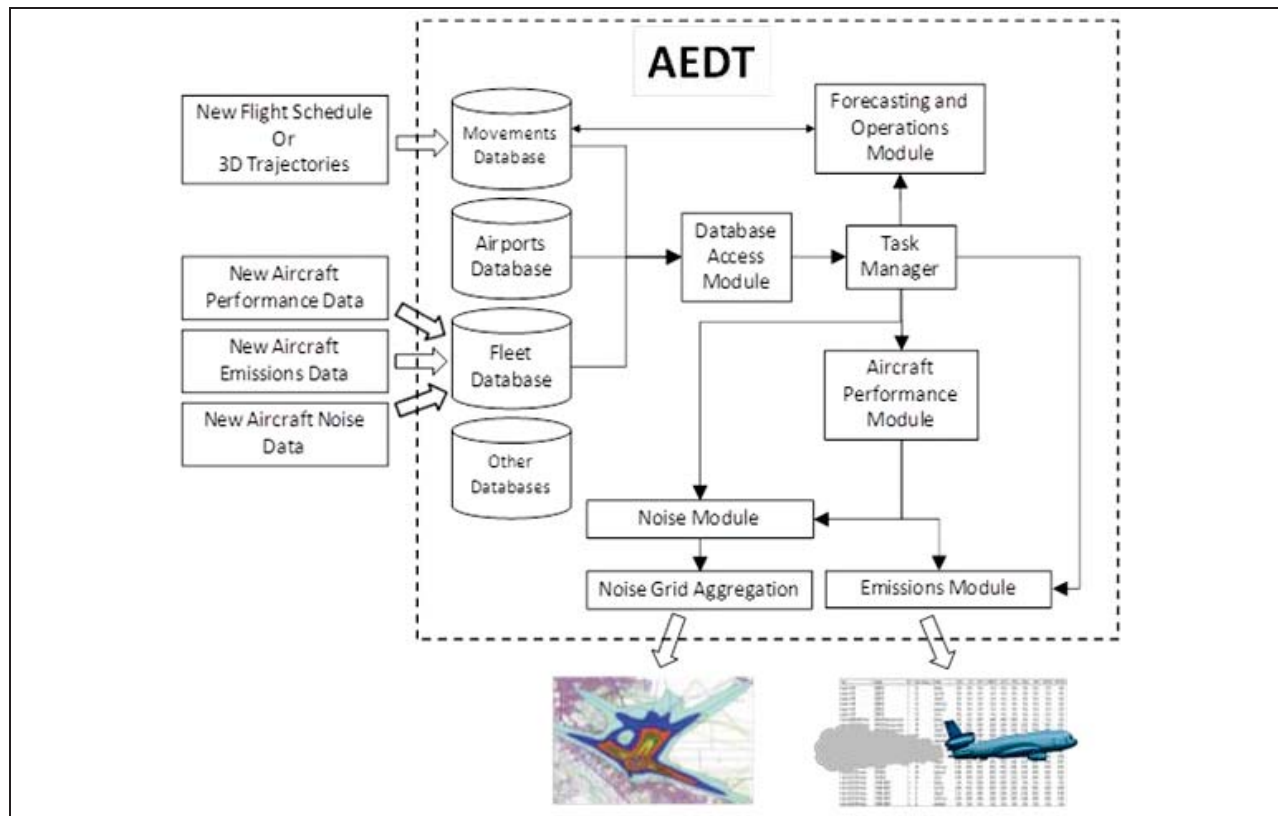


Figure 7 Data-Flow Overview of AEDT

For this study, the team exercised a research version of the AEDT tool suite designed specifically for system level assessments. The Noise and Emissions Analysis Tool (NEAT) is the application designed to replace the legacy MAGENTA and SAGE tools and is used by the agency to support the policy work done for CAEP as well as the its domestic performance assessments. While the software leverages the same computational elements of the standard AEDT (currently in its beta version), its data handling components and underlying databases are specifically designed to work with very large databases such as those required to perform NAS wide or worldwide analysis.

2.3.2. AEDT Model Setup

The NextGen 2025 forecast used for this project was previously implemented in the ACES to produce flight trajectories for NextGen end-state per JPDO Concept Of Operations (Conops) (Jawad 2009). ACES is a non-real-time, computer simulation of local, regional, and nationwide factors covering aircraft operations from gate departure to gate arrival. The objective of ACES is to provide a flexible NAS simulation and modeling environment that can assess the impact of new NAS tools, concepts, and architectures, including those that represent a significant departure from the existing NAS operational paradigm. ACES utilizes distributed architecture and agent-based modeling to create the large scale, distributed simulation framework necessary to support NAS-wide simulations based on the physics and structure of the NAS.

While AEDT/NEAT and ACES require the same type of information to operate, the data structures they rely on are different and not directly compatible. In order to perform the system level analysis for this project, the ACES trajectory data had to be first translated into the AEDT/NEAT relational database structure resulting in the necessary movement database. Once this was complete, the movement data could be used to conduct both single-flight and system-level modeling work. Copies of this data were created to develop different system level scenarios through insertion of the 2025 Baseline Conventional vehicle and the 2025 PSC.

The necessary performance data required to model these new aircraft types in AEDT were developed by Northrop Grumman and Rolls Royce. Northrop Grumman generated the BADA model of aircraft performance (e.g., fuel burn) while Rolls Royce developed the ICAO-like NO_x emissions indices. This data was implemented into the AEDT fleet database.

AEDT currently models cruise using a constant, level altitude, and uses pre-developed altitude distributions to assign cruise altitudes stochastically based on trip distance. The distribution for the B777-2 was determined to be suitable and applied to the optimal cruise altitudes of 51,000 ft and 43,000 ft for the 2025 PSC and the 2025 Baseline vehicle, respectively, where these optimal altitudes represented the approximate average point.

In modeling departures, data and methods from Northrop were used to develop a set of point-to-point profiles in AEDT that covered the range of stage lengths (or trip distances corresponding to the takeoff weight) used in AEDT. In contrast, a single profile was used to model the approach phase. Separate sets of profiles specific to the 2025 PSC and the 2025 Baseline vehicle were implemented.

To model flights of the 2025 PSC and the 2025 Baseline vehicle, Great Circle trajectories were used since they are the typical method used to model new aircraft types in AEDT. The ACES trajectories for the replaced aircraft (replaced by the new 2025 aircraft) could not be used since the 2025 PSC and the 2025 Baseline vehicle use different cruise altitudes, thus requiring new trajectories.

2.3.3. AEDT/BADA Performance Modeling

Developed by the Eurocontrol Experimental Centre, the Base of Aircraft Data (BADA), currently at Version 3.9, was originally developed to simulate trajectories for Air Traffic Management (ATM) purposes but has seen extended uses including the prediction of various performance metrics involving thrust, fuel flow, etc (EEC 2011). BADA uses the Total Energy Model (TEM) to describe the forces acting on an aircraft as indicated below:

$$(T_r - D)V_{TAS} = mg \frac{dh}{dt} + mV_{TAS} \frac{dV_{TAS}}{dt} \quad (1)$$

where T_r = Thrust acting parallel to the aircraft velocity vector

D = Aerodynamic drag

m = Aircraft mass (kg)

h = Altitude (m)

g = Gravitational acceleration = 9.81 m/s²

V_{TAS} = True air speed (m/s)

$t = \text{time (s)}$

Using the TEM, the movement of an aircraft from the beginning of its takeoff runway roll to the end of its runway landing roll are typically modeled by assessing segments of a flight. Although most of the aircraft types included in the BADA databases are jets, some turboprops and pistons are also included. In concert with the TEM, BADA provides a set of models and associated data that can be used to calculate each of the aircraft performance components (e.g., drag, thrust, fuel flow, etc.). The general form of BADA's cruise thrust specific fuel consumption model for jet aircraft is:

$$\eta = C_{cr} C_{f1} \left(1 + \frac{V_{TAS}}{C_{f2}} \right) \quad (2)$$

where $\eta = \text{Thrust specific fuel consumption (kg/min-KN)}$

$C_{cr} = \text{Cruise fuel flow correction coefficient}$

$C_{f1} = \text{1st thrust specific fuel consumption coefficient (kg/min/kN for jets)}$

$C_{f2} = \text{2nd thrust specific fuel consumption coefficient (knots)}$

$C_{f3} = \text{1st descent fuel flow coefficient (kg/min)}$

$C_{f4} = \text{2nd descent fuel flow coefficient (ft)}$

The data necessary to use each of these models is provided as part of the "BADA system," and includes formulated performance coefficients, speed schedules, and other aircraft characteristics.

2.3.4. AEDT Emissions Modeling

The Boeing Fuel Flow Method 2 (BFFM2) is a non-proprietary method that uses data from the ICAO jet engine emissions databank to derive emission indices at non-standard power settings during flight conditions. The ICAO databank provides sea-level static fuel flow and emissions indices of carbon monoxide (CO), total hydrocarbons (THC), and nitrogen oxides (NO_x) as well as Smoke Numbers for particulate matter (PM) at the standard power settings of 7%, 30%, 85%, and 100%. BFFM2 is an improvement over the standard ICAO emissions modeling method which assumes the standard power settings during the Landing and Takeoff (LTO) modes.

Using a predicted or measured fuel flow at flight conditions for a flight segment, BFFM2 uses a relationship between the fuel flow and emissions indices at standard power settings to interpolate for more appropriate emissions indices. Corrections for atmospheric effects (i.e., temperature, pressure, and humidity) and adjustments for engine installation effects are also taken into account. As shown in Figure 8, BFFM2 uses a log-log relationship between fuel flow and emissions indices (EIs) to interpolate for the EIs at non-standard power settings.

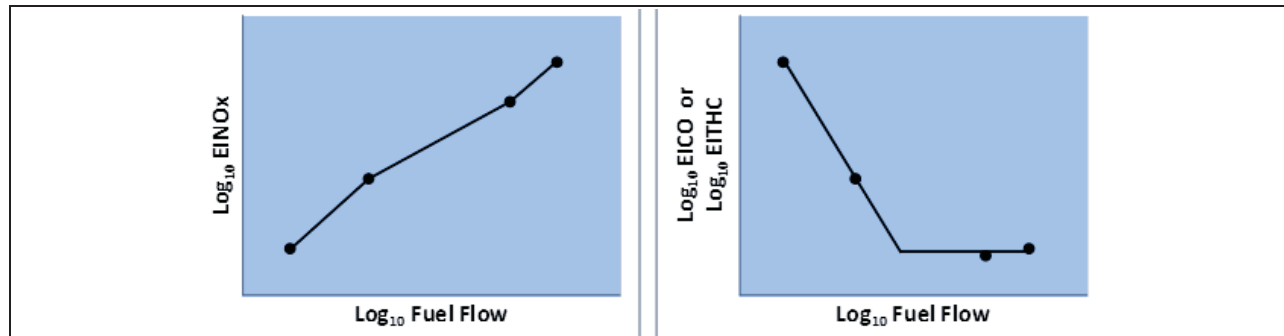


Figure 8 EI and Fuel Flow Log-Log Relationship as used in BFFM2

Once the emissions indices are determined, they are used in AEDT with the BADA-predicted fuel flow and the flight segment duration to calculate emissions for the segment. In general, as fuel burn increases, so do emissions. However, the rate of emissions generation may not increase with fuel flow. Although NO_x emissions may not be linearly related to fuel flow (or fuel burn), the NO_x emission rate generally increases with fuel flow (with more power). In contrast, rate of emissions of CO and THC generally decreases as fuel flow increases. Emissions of these pollutants are generally used to represent impacts on local air quality.

Modeling of CO₂ and other “fuel-based” pollutants are conducted using constant emission indices derived from average fuel composition data. The CO₂ emissions indices used in AEDT is 3,155 g CO₂ per kg fuel (Hadaller 1989 and 1993). This is based on the assumption that all of the carbon in the fuel is converted to CO₂ which is reasonable since most modern aircraft engines have combustion efficiencies greater than 99%. CO₂ is used to represent virtually all greenhouse gas emissions aircraft. Although other pollutants emitted from aircraft engines also exert climate change impacts, their impacts are generally smaller (e.g., as is the case with water vapor [H₂O]) and/or currently not as well understood (e.g., as with particulate matter [PM]).

2.4. AEDT Single Mission Modeling and Assessments

As a precursor to the system-level modeling work, a set of single-mission flights were modeled in AEDT to directly compare the fuel burn and emissions generated by the PSC with the 2025 Baseline vehicle and various other existing aircraft. The mission specifications are provided below:

- From Los Angeles International Airport (LAX) to Atlanta International Airport (ATL) – Approximately 1700 nm
- Nominal cruise altitude of 40,000 ft
- Constant cruise altitude (e.g., no step climbs)
- Cruise speeds specific to each vehicle’s capabilities
- Great circle trajectory as modeled in AEDT
- Takeoff and arrival profiles specific to each vehicle

As previously indicated the BADA aircraft performance data as well as the takeoff and arrive profiles for the 2025 PSC and 2025 Baseline vehicles were developed by Northrop while the ICAO-like fuel flow and NO_x emissions indices were provided by Rolls Royce Liberty Works. Modeling these datasets in AEDT, the fuel burn and emissions comparisons are presented in Figure 9 and Figure 10.

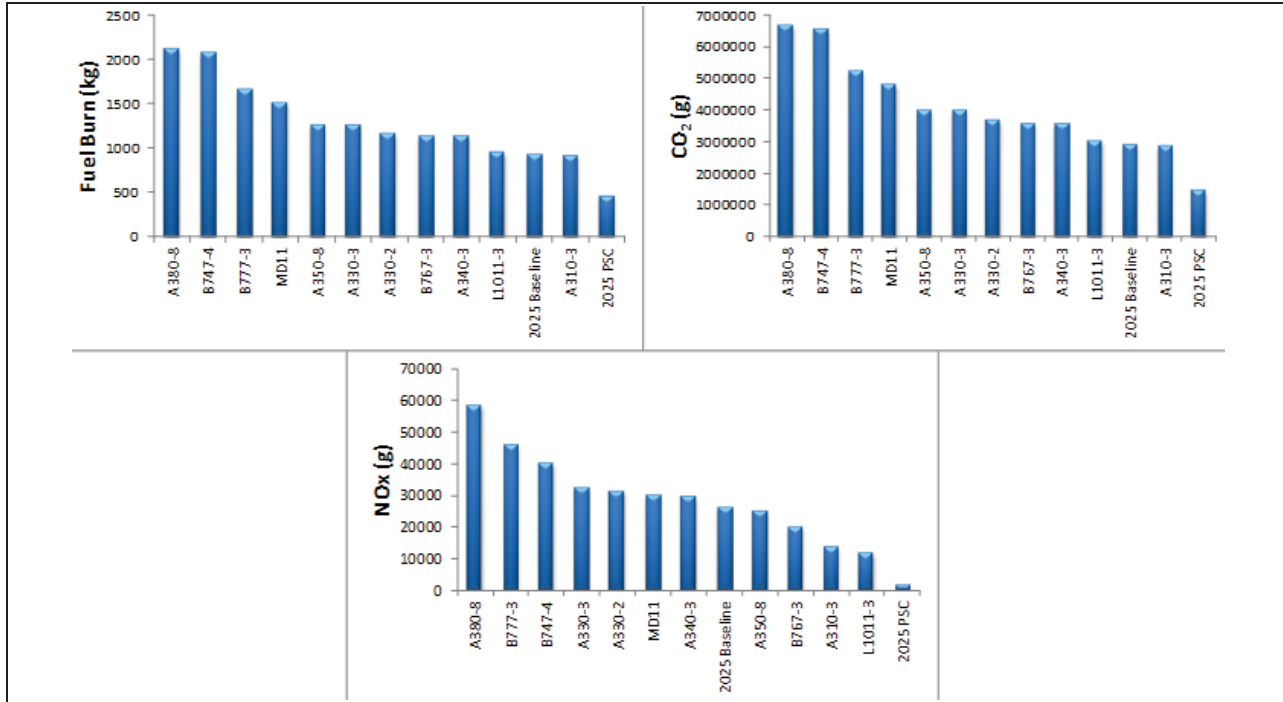


Figure 9 Comparison of Single Mission LTO Fuel Burn and Emissions at Nominal 40,000 ft Cruise Altitude

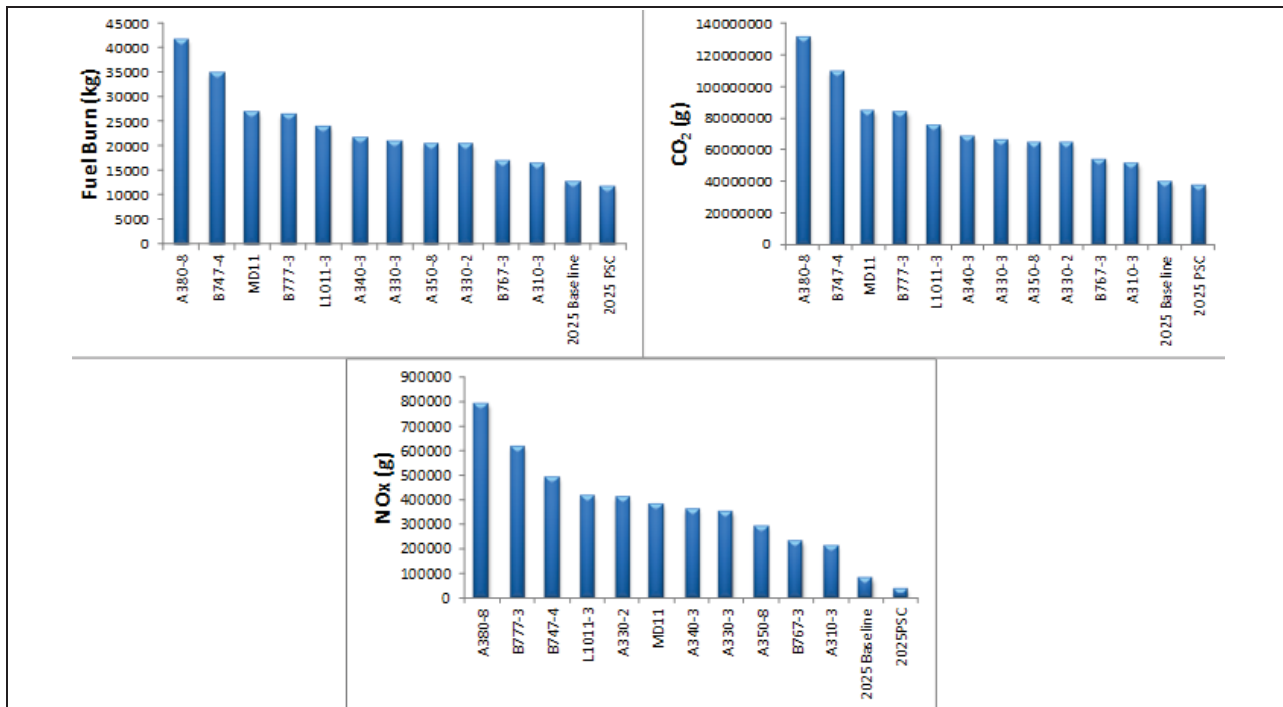


Figure 10 Comparison of Single Mission Full Flight FB and Emissions at Nominal 40,000 ft Cruise Altitude

These figures show rankings of the tested aircraft by their fuel burn and emissions for LTO and the full mission. In each case, the 2025 PSC showed significantly lower fuel burn and emissions than all other twin-aisle aircraft tested. Against the 2025 Baseline vehicle, the 2025 PSC showed approximately 6% lower fuel burn (and CO₂ emissions) and about 55% lower NO_x emissions for

the full mission. The 2025 Baseline vehicle did not have the lowest fuel burn or emissions, but was lower than most of the other aircraft.

The differences between the 2025 PSC and the 2025 Baseline vehicle are greater for the LTO modes than for the full flight. This is mainly due to the greater differences in thrust and fuel flow at the higher power settings used during takeoff (i.e., the 2025 Baseline vehicle has higher modeled thrust and fuel flow than the 2025 PSC during takeoff). As such, the lower power settings used during cruise results in lower overall differences between the two vehicles as evidenced by their full mission results.

Because of its significantly lower levels of LTO NO_x emissions, the PSC has the potential to noticeably impact local air quality. NO_x is a precursor to ozone (O₃) formation, and its reduced loading at the airport level may help provide more flexibility (more options) when conducting environmental assessments due to new airport projects – more flexibility may be afforded in dealing with emissions budget constraints imposed by State Implementation Plans (SIPs) and when trying to stay under the *de minimis* levels during a General Conformity assessment.

In addition to the nominal 40,000 ft cruise altitude, the 2025 PSC and the 2025 Baseline aircraft were flown at their respective optimal (or more representative) cruise altitudes: 51,000 ft for the 2025 PSC and 43,000 ft for the 2025 Baseline vehicle. Figure 11 provides a comparison of the resulting full mission fuel burn and emissions comparisons.

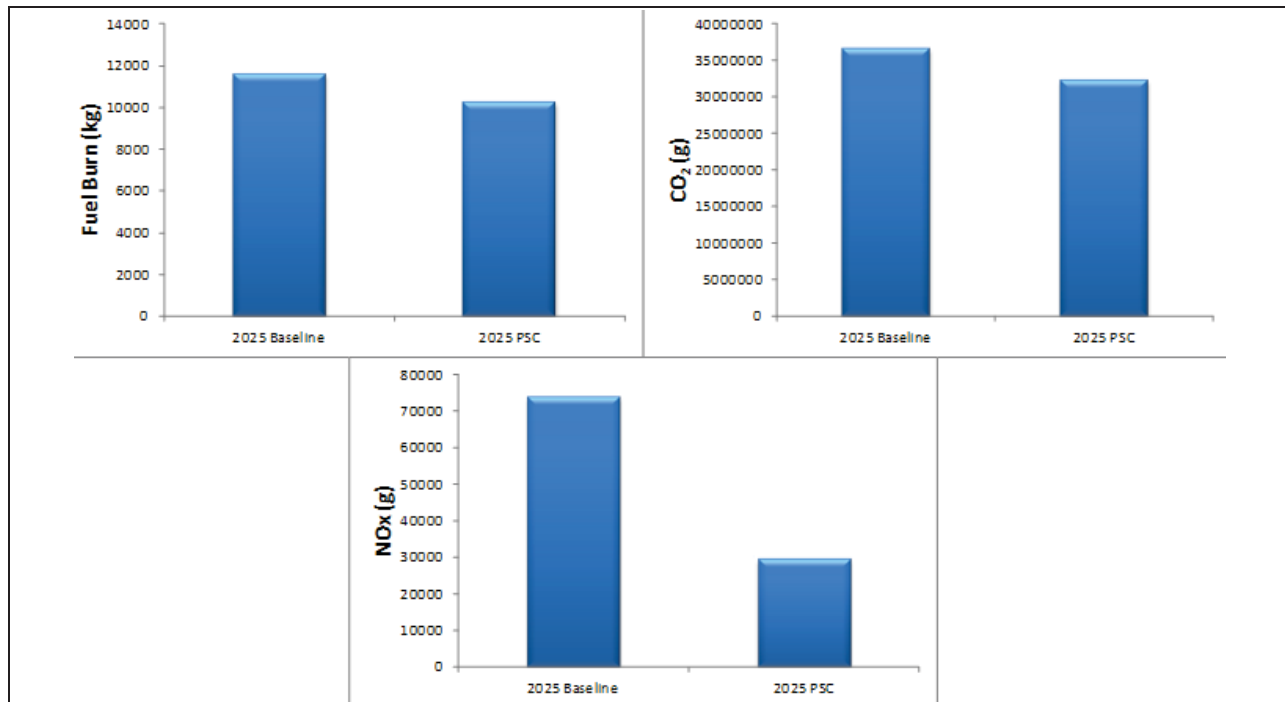


Figure 11 Comparison of Single Mission Full Flight Fuel Burn and Emissions at Optimal Altitudes

As expected, both the 2025 PSC and the 2025 Baseline vehicle produced lower fuel burn and emissions at the higher altitudes. This is due to the lower modeled drag during cruise resulting in lower thrust and lower fuel flow which also results in lower CO₂ and NO_x emissions. Although the difference levels are relatively similar, the use of the optimal altitudes also results in greater differences between the 2025 PSC and the 2025 Baseline vehicle: approximately 12% difference (as opposed to 6% at 40,000 ft) in fuel burn and about 60% difference (as opposed to 55%) in

NO_x emissions. As the change affects cruise conditions, the fuel burn and emissions for the LTO modes are not affected.

In developing these estimates for fuel burn and emissions, an adjustment to the BADA fuel flow predictions were made to improve the accuracy of BADA's predictions for the 2025 PSC. Based on comparisons to Northrop's proprietary, higher fidelity models, it was determined that at the optimized cruise altitude of 51,000 ft, the PSC's cruise fuel flow as predicted by BADA within AEDT may be under-predicted. The performance models within BADA/AEDT may be overly sensitive to altitude. Therefore, an adjustment factor of 1.311 was developed based on comparisons of the BADA/AEDT-generated fuel flows with those from the Northrop tools. The adjustment factor was applied to the 2025 PSC cruise fuel flow values. As a full investigation (e.g., sensitivity study) of BADA's methods was considered outside the scope of this project, the use of this factor was considered a reasonable correction for this project.

2.5. System-Level Assessments and Metrics

In addition to the single mission assessments, a National Airspace System (NAS)-level (or "system" level) assessment was conducted using the previously described JPDO forecasted 2025 fleet and operations. All of the fuel burn and emissions modeling was conducted in AEDT for the following scenarios:

- 2025 with no ERA aircraft (plain JPDO forecast)
- 2025 scenario with Baseline vehicle inserted according to replacement scheme previously described
- 2025 scenario with PSC inserted according to the replacement scheme previously described

In order to better understand the overall impact of the PSC and the Baseline vehicle on a system level, Figure 12 provides the percent contributions of each vehicle by flight, distance flown, and fuel burn.

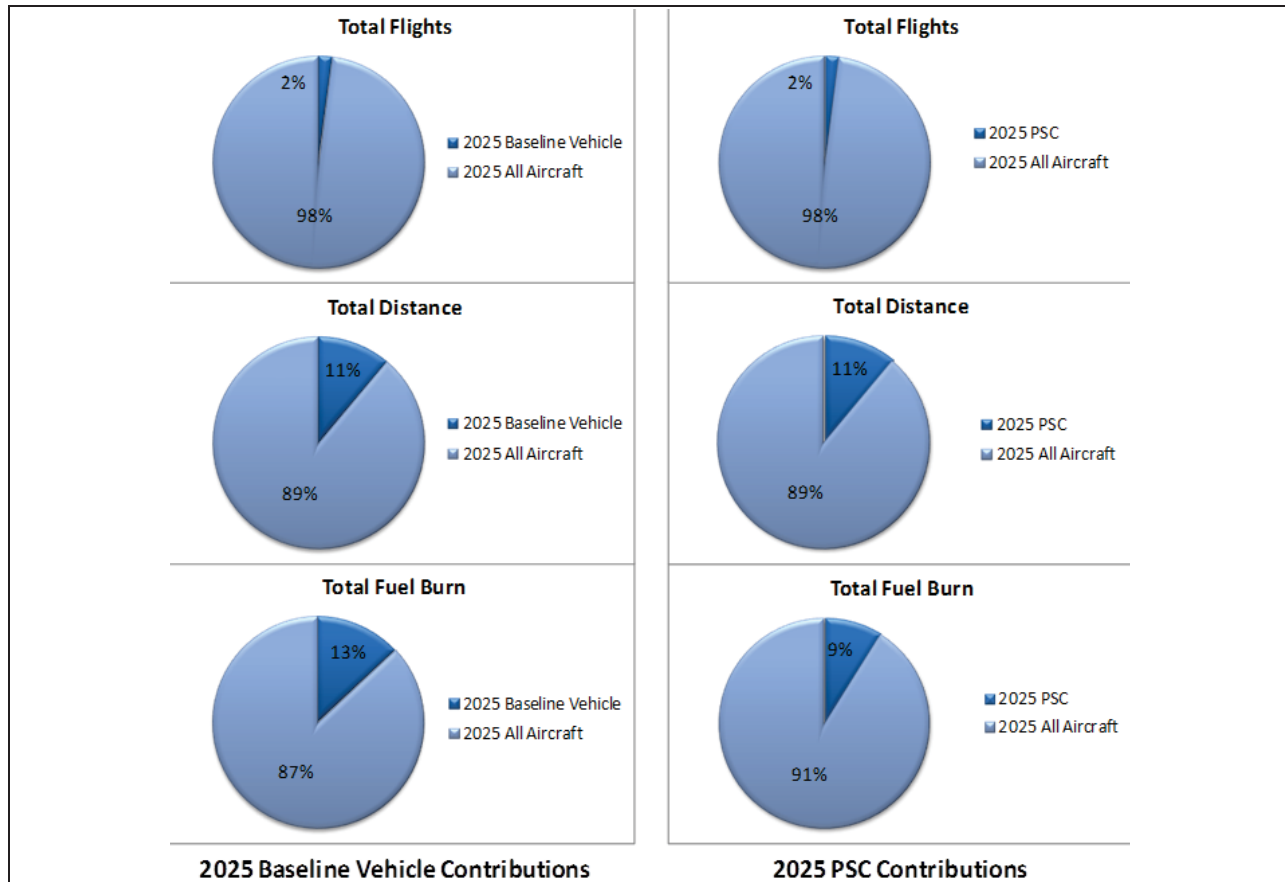


Figure 12 Percent Contributions by 2025 PSC and the 2025 Baseline Vehicle

The percent contributions by flights and distance traveled are identical for the 2025 PSC and the 2025 Baseline Vehicle because the same insertion strategy was applied to both vehicles. The disparity between percent contribution of total flights and the others (distance and fuel burn) is due to the amount of non-commercial flights (e.g., general aviation flights) included in the 2025 JPDO forecast that fly shorter distances and contribute much smaller amounts of fuel burn and emissions. The total contribution of scheduled flights by commercial aircraft is approximately 31% and the total contribution by twin aisles is over 3%. The approximate 2% contribution of flights by the 2025 PSC or the 2025 Baseline vehicle equates to 2,351 flights. With these contributions, the AEDT system level fuel burn and emissions comparisons are presented in Figure 13 and Figure 14.

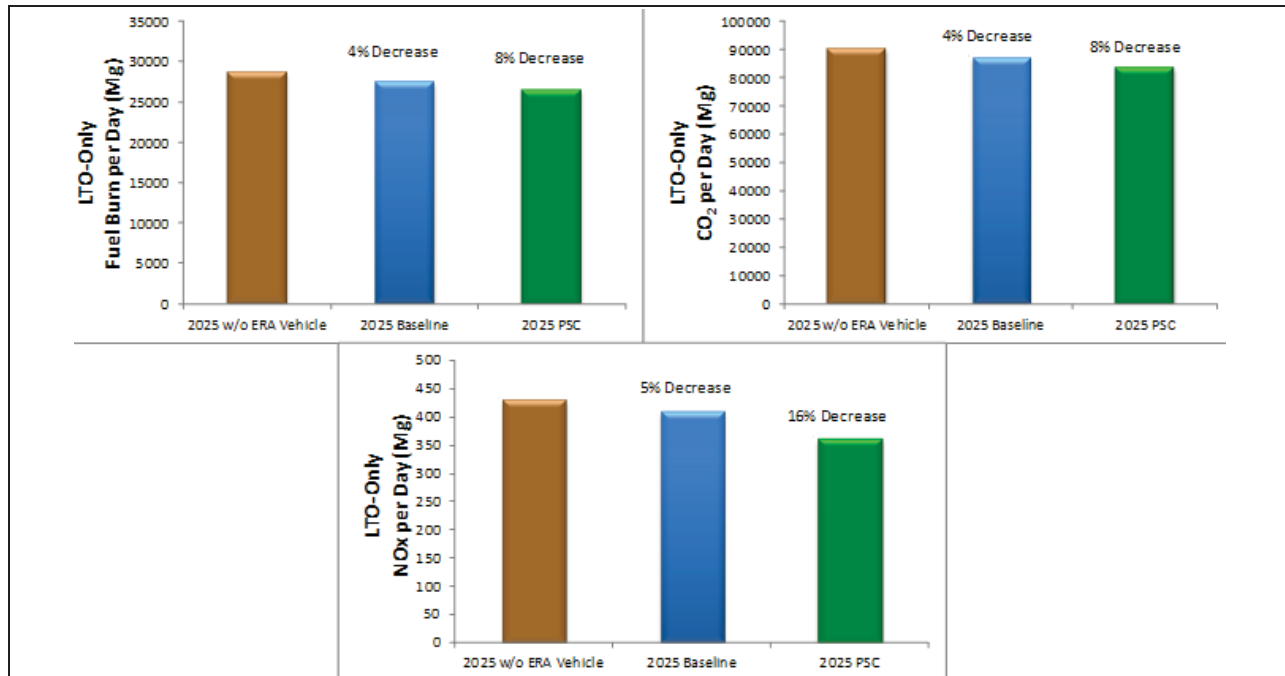


Figure 13 Comparison of System Level LTO Fuel Burn and Emissions

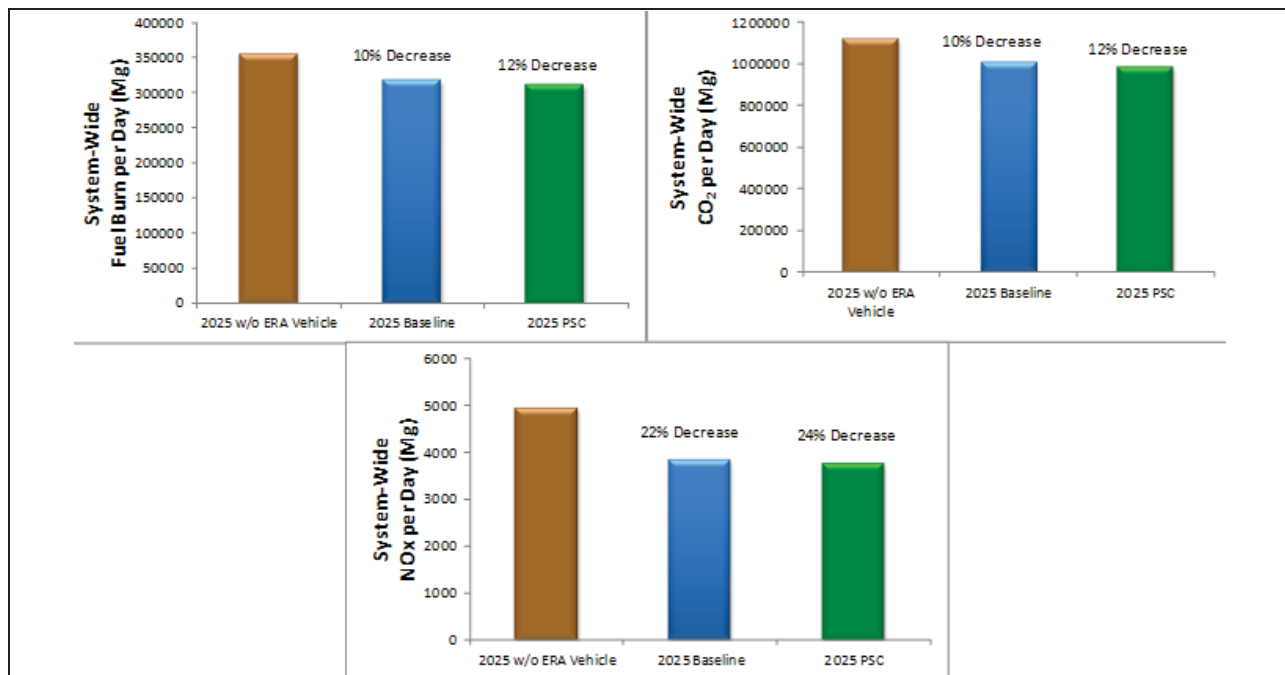


Figure 14 Comparison of System Level Full Flight Fuel Burn and Emissions

The system-level modeling in AEDT represents an expansion of the single mission assessments that included the full mix of aircraft types and operations as predicted by JPDO in their 2025 forecast, but with the previously described adjustments. Some refinements within the system level modeling work not reflected in the single mission assessments include the previously described cruise altitude distributions and the use of different takeoff profiles based on trip distance (or stage length) which are correlated to different takeoff weights.

The system level LTO fuel burn and emissions comparisons show that when compared to the 2025 scenario without any ERA vehicles, the 2025 PSC scenario produces twice as much reduction in fuel burn and CO₂ emissions than the 2025 Baseline vehicle scenario (i.e., 4% versus 8% reduction). Changes in CO₂ emissions are identical changes in fuel burn since CO₂ emissions are predicted using a constant factor in AEDT (i.e., 3,155 g CO₂/kg of fuel burn).

Due to nonlinear effects, the 8% reduction in fuel burn translates into 16% reduction in NO_x emissions. As previously indicated, this reduction has the potential to help reduce local air quality burdens by providing more flexibility with regards to SIP emissions budgets and General Conformity *de minimis* levels. The NO_x emissions reductions will mostly affect the larger airports that would be able to cater to the 2025 PSC, and will obviously depend on how many PSC operations occur at each airport.

As previously explained, the greater performance (i.e., thrust and fuel burn) differences between the 2025 Baseline vehicle and the 2025 PSC under the LTO modes (especially during takeoff) results in greater LTO fuel burn and emissions differences between the two vehicle scenarios. The smaller differences seen for the full flight mission is indicative of the relatively smaller fuel efficiency differences between the two vehicles under cruise conditions.

The single mission full flight fuel burn and emissions differences between the 2025 PSC and the 2025 Baseline vehicle are greater than the corresponding system level results. This is due to the fact that the single mission assessments were conducted over an approximately 1,700 nm trip (i.e., LAX to ATL). The system level results on average reflected longer flights with longer cruise segments which reflect the smaller differences in cruise fuel burn rates.

With the insertion of the PSC, the system level full flight comparisons show that approximately 24% decrease in NO_x emissions (for all modes) can be expected. The 12% reduction in fuel burn translates into about 97 million pounds of fuel saved per day in the NAS. The system level modeled results were used to generate some full flight fuel burn and emissions normalized (rate-type) metrics as shown in Figure 15.

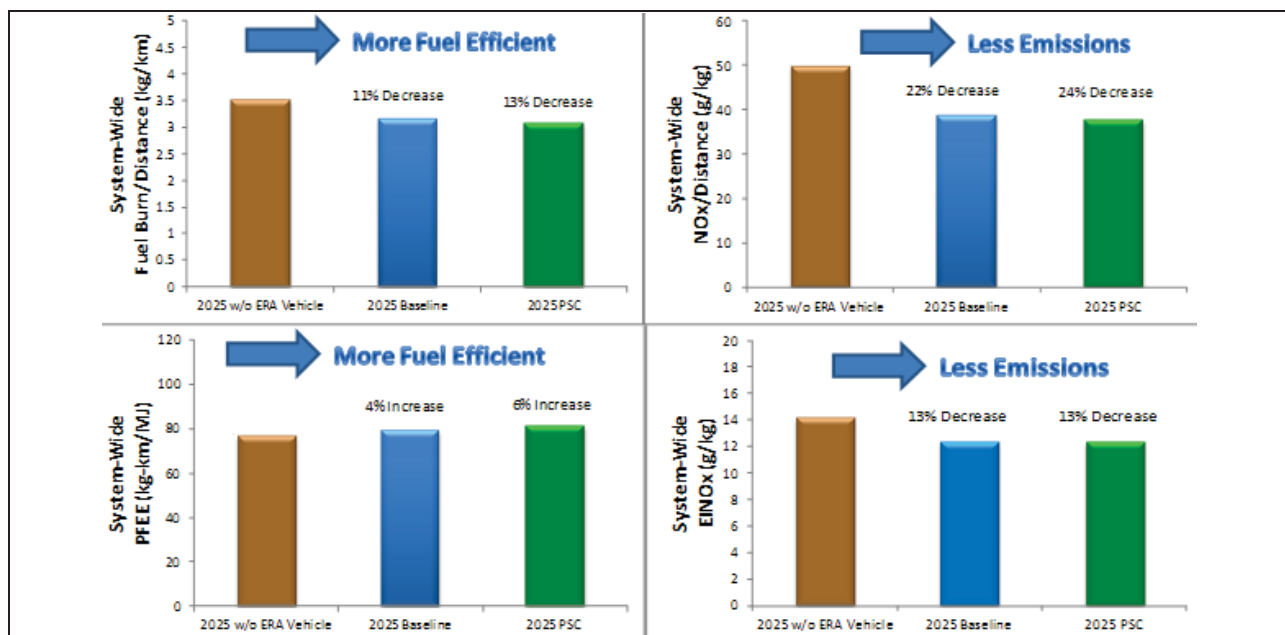


Figure 15 System Level Full Flight Fuel Burn and Emissions Normalized Metrics

The fuel burn and NO_x emissions per distance metrics indicate that the 2025 PSC scenario experiences the least amount of fuel burn and emissions. Since these metrics do not include the impact of payload, they serve to highlight the sheer influence of the performance differences between the 2025 PSC and the various other twin aisle aircraft it replaced.

The Payload Fuel Energy Efficiency (PFEE) metric (Hileman 2008) has been typically used by the FAA to assess various fuel use in modeling various future scenarios. Although it uses different units (e.g., MJ instead of mass of fuel burned) and its constituent components have been rearranged, the metric is similar in scope to the inverse of fuel burned per revenue passenger miles (mass fuel burn/RPM). Due to the difficulty of obtaining total payload data, only the weight of passengers were included using load factors of 79% and 59% for scheduled and non-scheduled flights, respectively. These load factor assumptions were derived based on actual historical data published by the U.S. Department of Transportation (DOT) Bureau of Transportation Statistics (BTS). The PFEE comparisons show that the PSC scenario is the most energy efficient – 6% more efficient than the no-ERA-vehicle scenario.

The system level full flight NO_x emission rate (EINO_x) comparisons show that the PSC and Baseline vehicle scenarios both have similar overall generation rates of NO_x emissions. This is consistent with the earlier full flight (total magnitude) comparisons of fuel burn and NO_x emissions. The lower PSC fuel burn will result in lower NO_x emissions and the higher Baseline vehicle fuel burn will result in higher NO_x emissions resulting in similar overall EINO_x values.

In addition to these normalized, efficiency-type metrics, some system level aircraft comparisons involving aircraft capacities were performed to help better understand the impact of the 2025 PSC. These comparisons are presented in Figure 16 and Figure 17.

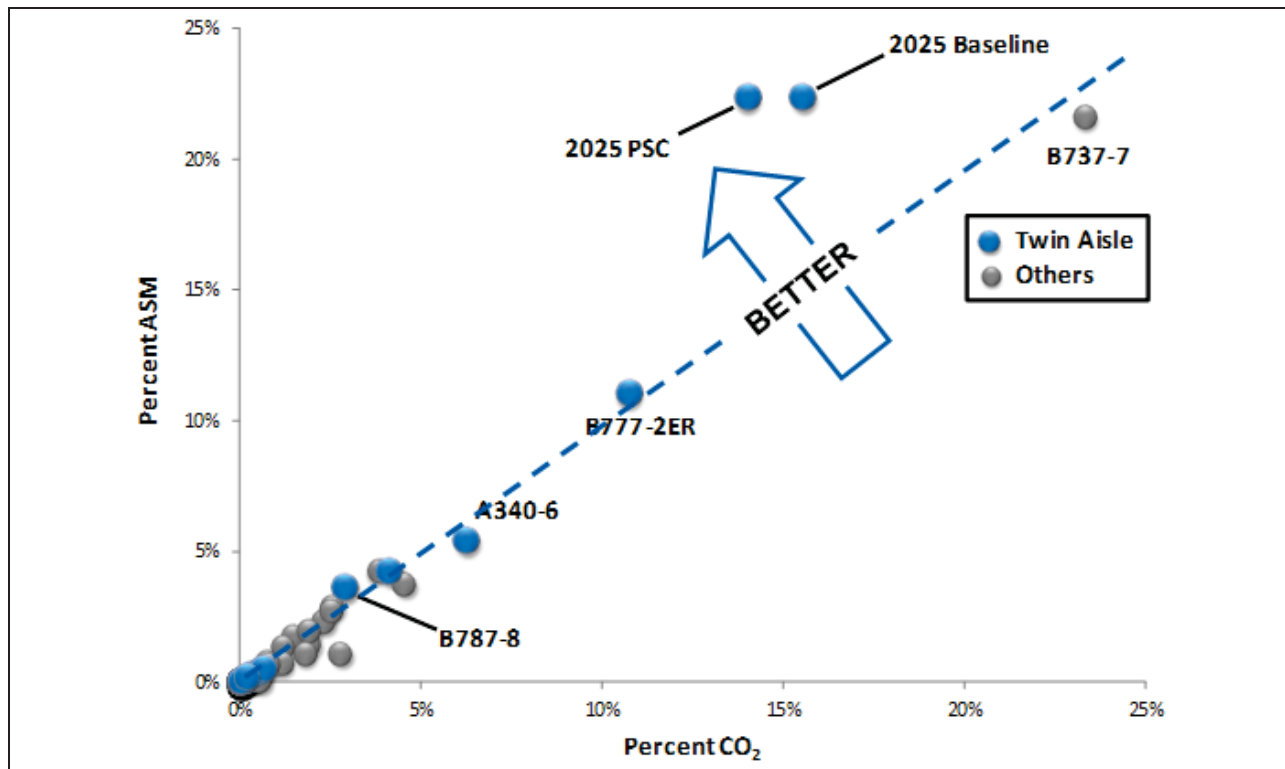


Figure 16 System Level Aircraft Comparisons of Percent ASM versus Percent CO₂ Emissions

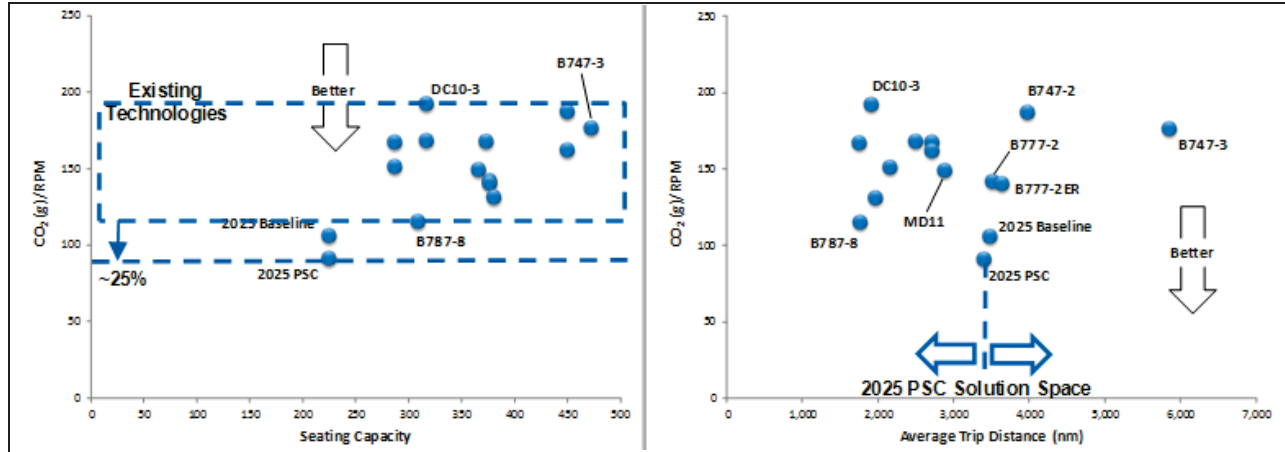


Figure 17 System Level Aircraft Comparisons of CO₂ emissions per RPM versus Seating Capacity and Average Trip Distance for Twin Aisle Aircraft Only

Figure 16 compares aircraft types by showing at the system level how much seating capacity (expressed as available seat miles [ASM]) each aircraft provides per its overall CO₂ emissions contribution. Because the 2025 PSC and the 2025 Baseline vehicle were inserted into their respective scenarios using the same insertion strategy, they have the same system level capacity contribution, but the 2025 PSC produces about 2% less CO₂ emissions. As indicated by the diagonal line, the twin aisle aircraft types appear to have similar capacity per CO₂ emission rates. As both the 2025 PSC and the 2025 Baseline vehicle are above this line, they have more capacity per CO₂ emissions than the existing twin aisle aircraft types. For example, the 2025 PSC provides slightly more capacity than the B737-7, but produces much less CO₂ emissions (about 10% less). Also, the 2025 PSC produces about 3% more CO₂ emissions than the B777-2ER, but offers about twice as much capacity.

The plots in Figure 17 provides further insights on the impact of inserting the 2025 PSC and the 2025 Baseline vehicle in the future scenarios by examining the relationship between CO₂ emissions normalized by RPM and seating capacity as well as average trip distance. Although the seating capacities of the 2025 PSC and the 2025 Baseline vehicle are lower than the other twin aisle aircraft types, the comparisons show that both aircraft types produce less CO₂ emissions/RPM than all other twin aisles with the 2025 PSC producing about 25% less than the lower limit of the twin aisle category represented by the B787-8. Comparing average trip distances, the application of the aforementioned insertion strategy for the 2025 PSC and the 2025 Baseline vehicle shows the distance solution spaces (distance traveled ranges) for both vehicles could easily support the average use of most other twin aisle aircraft types.

In addition to these assessments, there are also spatial emissions loadings that should be examined to determine potential impacts of the new vehicles. Figure 18 and Figure 19 provide altitude distributions of CO₂ and NO_x emissions loadings for each of the future scenarios.

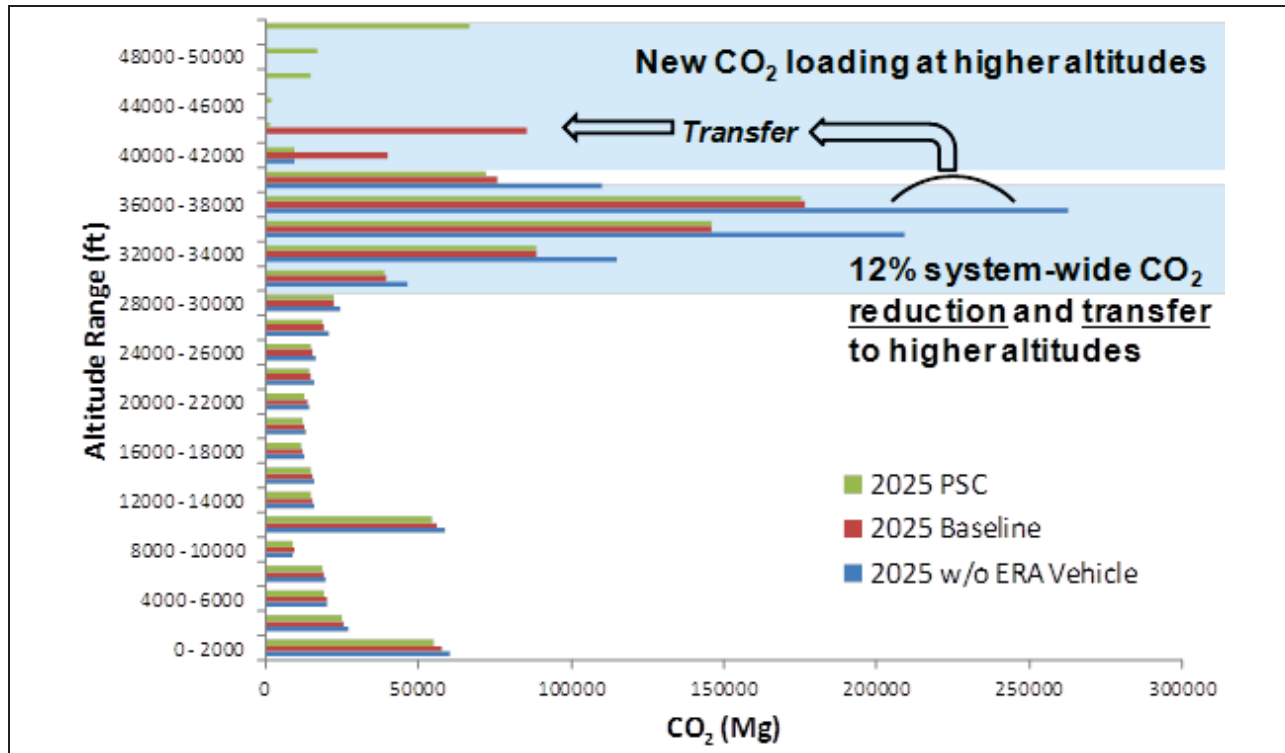


Figure 18 Altitude Distributions of CO₂ Emissions Loadings for all 2025 Scenarios

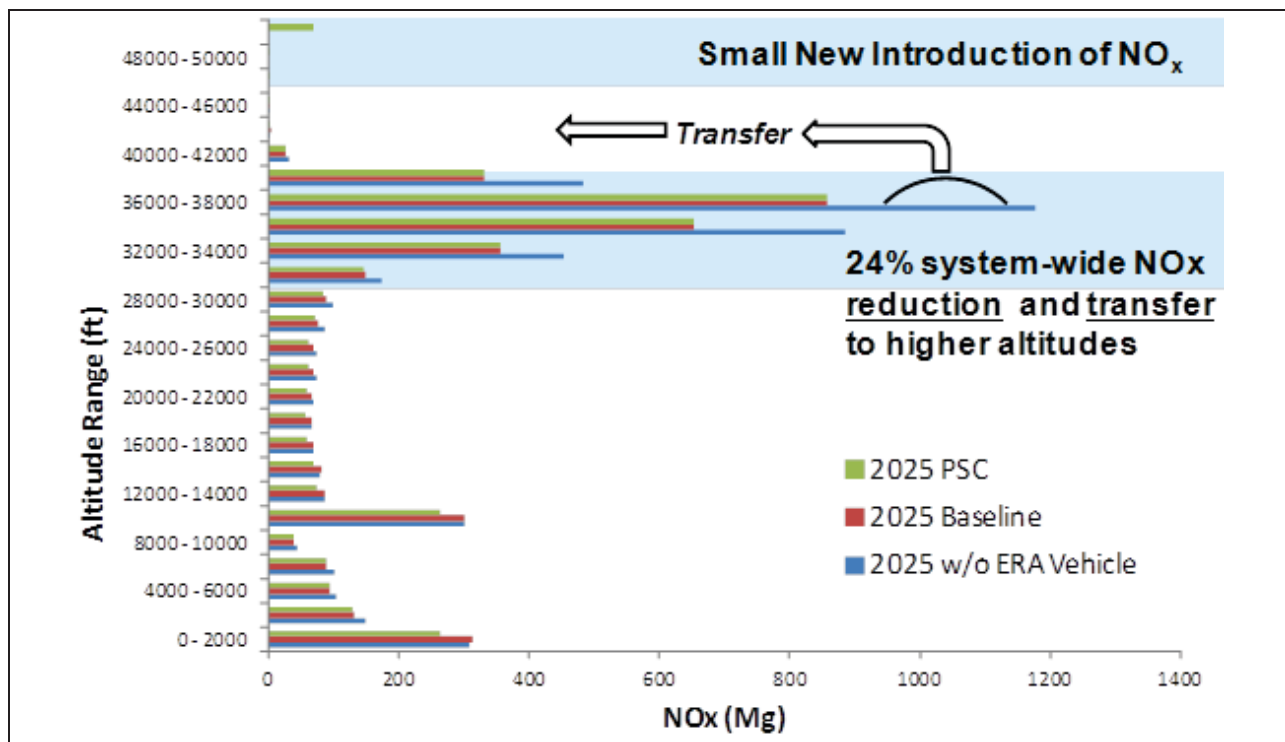


Figure 19 Altitude Distributions of NO_x Emissions Loadings for all 2025 Scenarios

As a result of inserting the 2025 PSC and the 2025 Baseline vehicle into the future scenarios, the most visible impacts as shown in Figure 18 and Figure 19 is that while emissions are reduced

predominantly in the 30,000 ft to 40,000 ft altitude range, new emissions are generated at higher altitudes. The system-wide 12% CO₂ and 24% NO_x emissions reductions due to the insertion of the 2025 PSC are replaced by smaller loadings in the 40,000 ft to 54,000 ft altitude range. Although the emissions are reduced, the higher altitude loading is noteworthy since it is unclear as to the overall global warming and climate change impacts these loadings may have. Aircraft are the only sources that directly emit pollutants in the higher levels of the troposphere and lower levels of the stratosphere.

2.6. Aircraft Noise Analysis

2.6.1. AAM Model Overview

The modeling of advanced aircraft concepts such as engine shielding and other complex design features that aim to reduce the noise footprint of the vehicle requires advanced simulation techniques for their accurate modeling beyond the integrated capabilities of AEDT. The study team used the Advanced Acoustic Model (AAM) to conduct acoustic modeling of PSC vehicle design characteristics. Limitations present in the AEDT noise engine, encompassed by a single spectral class and set of NPD curves with lateral directivity modeling based on conventional tube-and-wing aircraft, do not provide for the kind of assessment needed for the non-conventional design characteristics of the PSC.

AAM is a suite of computer programs that predict far-field noise for single or multiple flight vehicle operations of fixed wing or rotary wing aircraft. AAM calculates the noise levels in the time domain and with a variety of integrated metrics at receiver positions on or above the ground at specific points of interest and over a uniform grid. AAM is based on three dimensional noise sources defined about a vehicle moving along a trajectory. Three dimensional source modeling includes the effect of thrust vectoring, implicit for rotorcraft and present on certain fixed wing aircraft. Propagation from the vehicle to receivers accounts for geometric spreading, air absorption and finite ground impedance. Nonlinear propagation effects, usually associated with high noise levels, may be computed. It can optionally account for varying ground terrain or atmospheric gradient effects.

Sources are generally defined as three-dimensional one-third octave band spectra. Narrowband and pure tone modes are available and the Doppler shift associated with vehicle motion is included, as is the propagation time from source to the receiver. Acoustic properties of the noise source(s) are defined as sound spheres and may be obtained from flight test or wind tunnel measurements, or theoretical predictions. The vehicle source characteristics may be described in any combination of broadband (in the form of one-third octave band levels) narrow band (user defined bandwidth and spacing with arbitrary bands permitted) or as pure-tone data (in the form of specific frequency sound pressure levels and phase). Vehicle source characteristics are prescribed as a function of vehicle operating state along a defined flight trajectory. Complex source design concepts such as shielding may be accounted for in AAM by prescribing suitable 3D spectral characteristics in the source noise spheres.

2.6.2. Noise Model Assessments

A single event analysis was performed of the Northrop-Grumman PSC Passenger configuration (See Figure 40) using the Wyle Advanced Acoustic Model (AAM) to provide an aircraft-level source noise assessment. Noise spheres describing the source were developed by Northrop Grumman and provided for noise modeling. Under certain circumstances, such as when the aircraft is flying at an angle of attack and the sphere is rotated accordingly, points above the

hemisphere rim of the spheres may present noise to receivers. To avoid propagating “no data” in this situation, the data from the *waterline* (upper rim of the hemispheres) was repeated to fill in the top half of the sphere. Since the spheres are symmetric (starboard/port) the hemispheres *waterline* matches on both starboard and port sides. Spheres were re-referenced to 100 ft radius from the original 1 ft radius, a net 40 dB decrease due to spherical spreading. Figure 20 through Figure 24 display the noise spheres in A-weighted SPL (dBA) for takeoff and approach conditions. Contours are displayed both in color and in grey scales, which helps accentuate the source directivity. On the underside of the vehicle the complex shielding diffraction effects and noise sources such as landing gear creates interesting directivity patterns. There are two scales used for the approach spheres with flaps and those with flaps and gear. Noteworthy features in source characteristics include:

- Source noise in the plane of the wing increases dramatically due to lack of airframe shielding
- Regions of high noise on the underside near $\Phi=10^\circ$ to 30° and $\Theta=40^\circ$ to 90° .
- High noise regions on the underside are >40dBA louder than neighboring quiet regions.

Flight trajectories for takeoff and approach profiles were also provided. Power units of F_n/Δ (net corrected installed thrust, lb) are referenced in the noise spheres, used as lookup parameters in AAM and are consistent with AEDT and INM requirements. It was found that F_n/Δ provided a better mechanism for source lookup at various portions of the flight trajectory since it better accounted for and tracked with flight speed. Several minor adjustments were made to the provided trajectories in order to perform the AAM analysis. First the altitude was increased to the nominal engine inlet height in order to more accurately orient the noise spheres. For the PSC-passenger configuration a height of 15 ft above ground level (AGL) was utilized. The ground roll portion of the approach profiles were adapted to include a segment where thrust reversers are applied. When modeling this in AAM the configuration state was set to “clean” so that the clean spheres (which contain higher thrusts) could be used to model the thrust reversers. No additional directivity impact due to the reversers was modeled. This item could be updated in the future if thrust reverser noise spheres are made available.

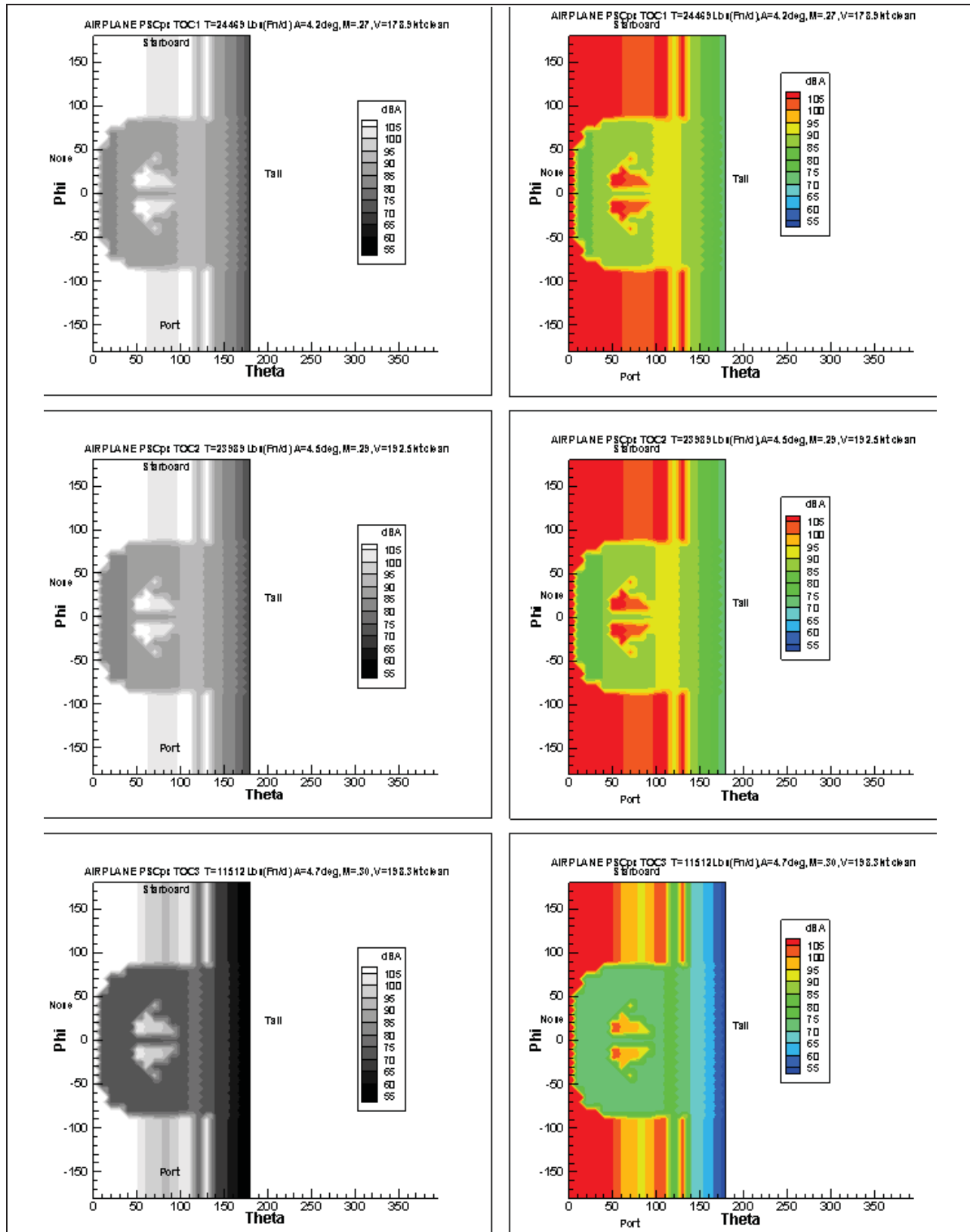


Figure 20 PSC Passenger Noise Spheres for Takeoff Conditions

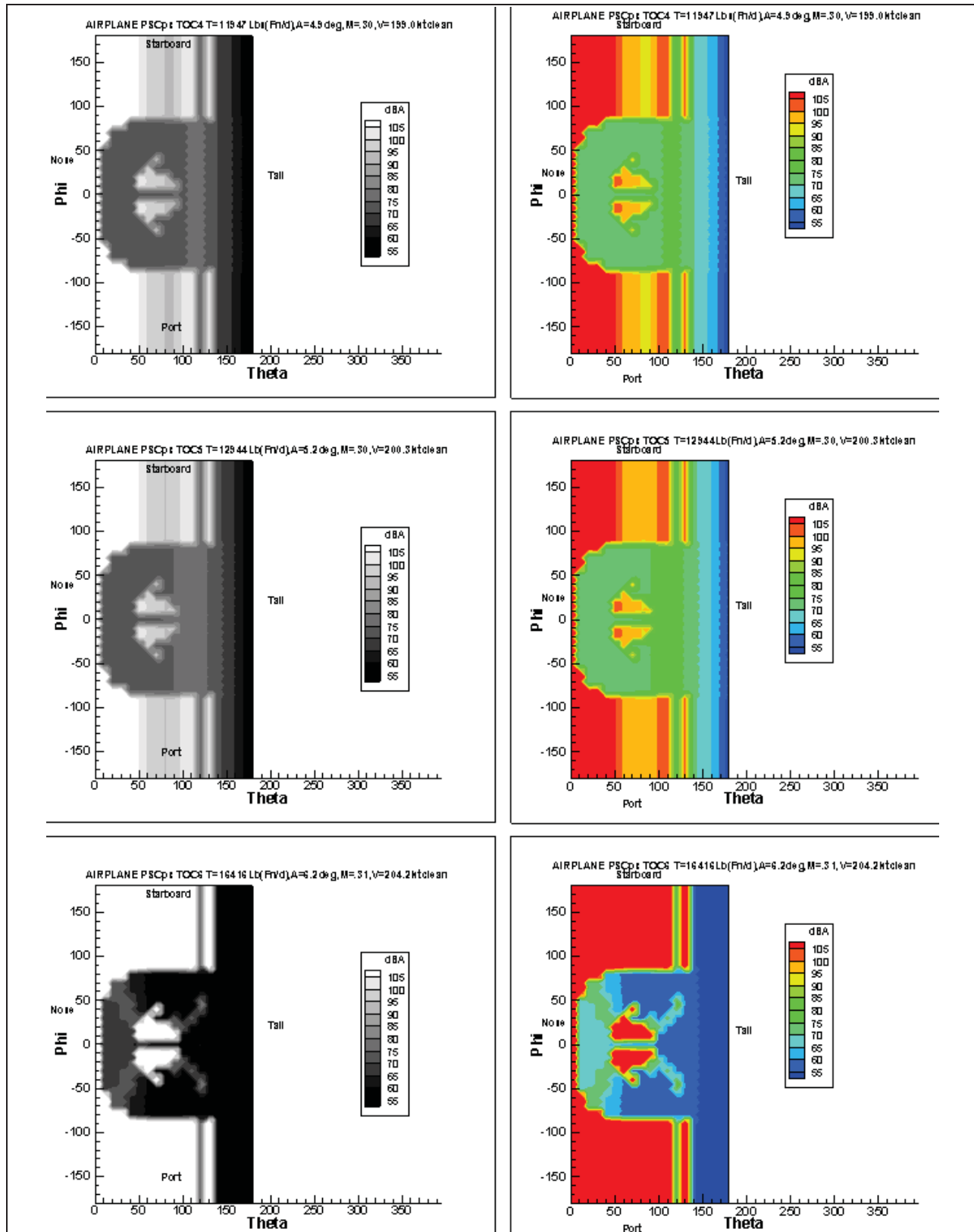


Figure 21 PSC Passenger Noise Spheres for Takeoff Conditions

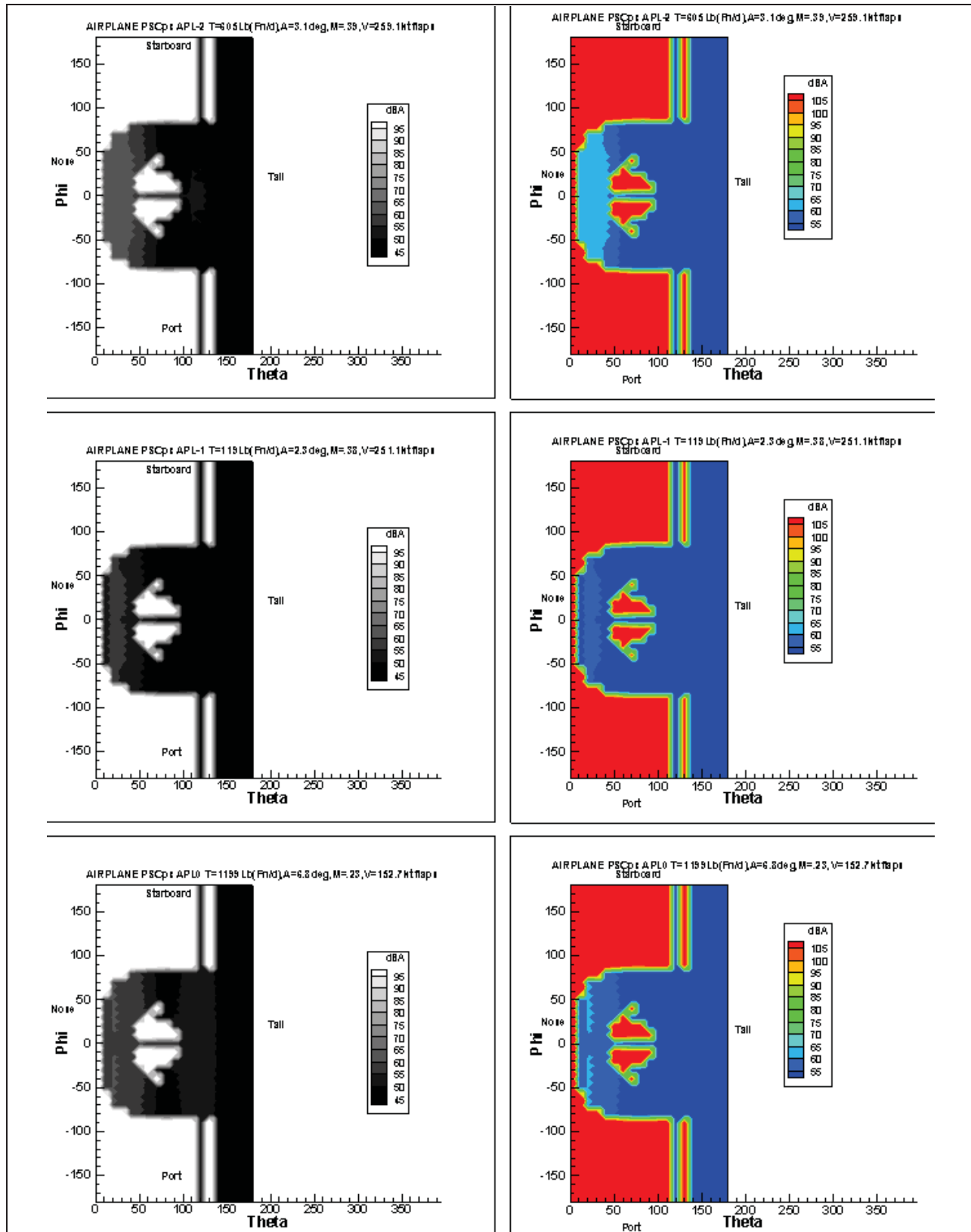


Figure 22 PSC Passenger Noise Spheres for Approach Conditions

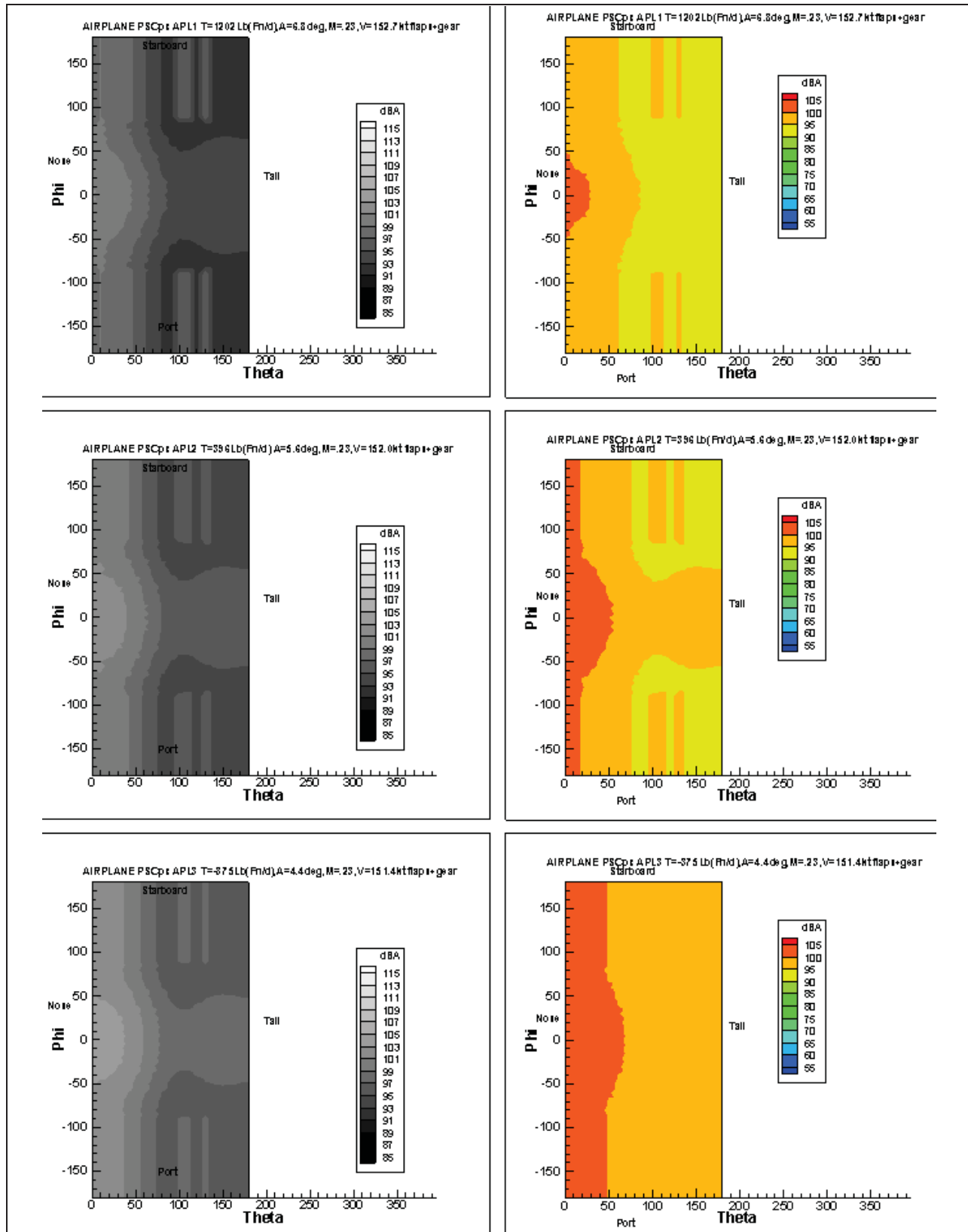


Figure 23 PSC Passenger Noise Spheres for Approach Conditions

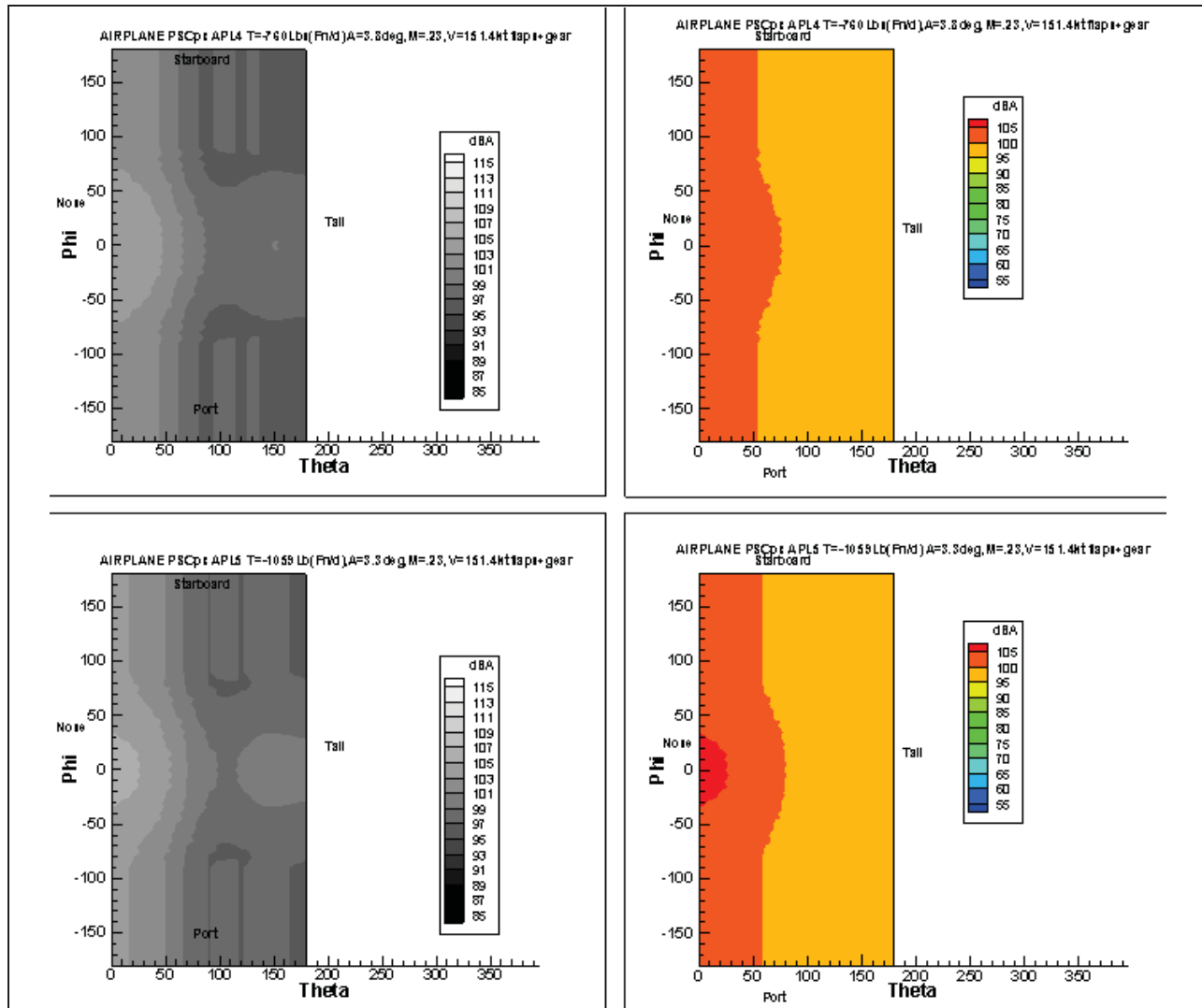


Figure 24 PSC Passenger Noise Spheres for Approach Conditions

Figure 25 shows the ground footprints (SEL-dBA, 2000 ft grid spacing) for the takeoff and landing operations of the PSC. Of particular note is the following:

- As the vehicle flies and the noise spheres are oriented with the flight path angle and the angle of attack, these fairly focused regions of highly directive noise are apparent in the ground contours and sound animations.
- There are two regions of high noise. These manifest themselves on the ground as two parallel high noise tracks which are evident when analysis is performed using a densely spaced grid.

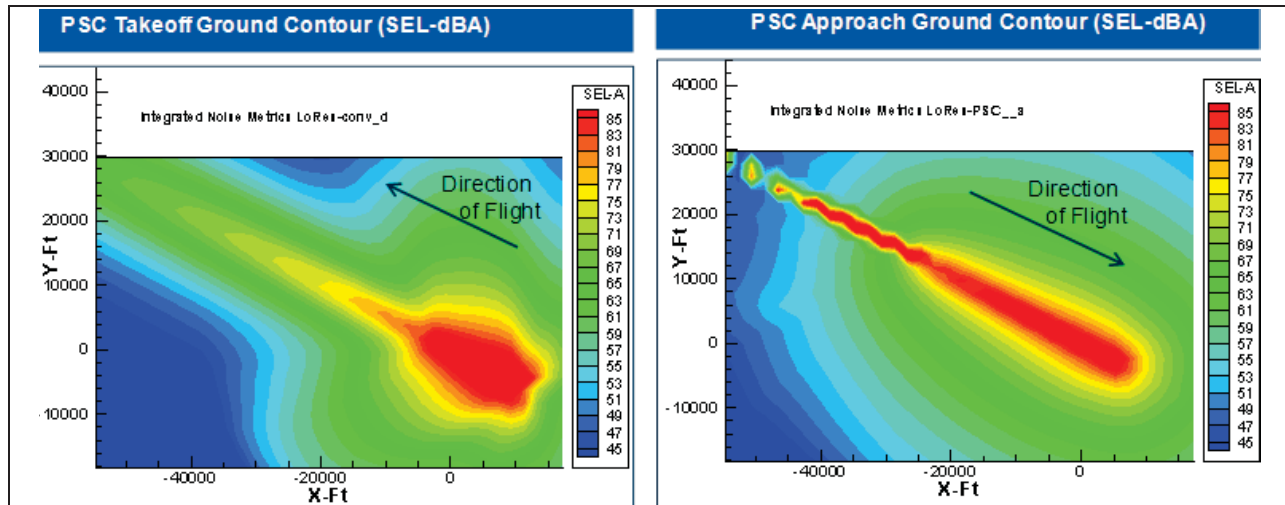


Figure 25 PSC Takeoff & Approach Ground Contours (SEL-dBA)

The approach data may also be plotted with the exact computational points indicated as shown in Figure 26, based on the 2000-ft spaced grids. The simulation was examined in order to better understand the reason for the high noise region just off the centerline of the approach trajectory. A time history of the A-weighted levels are displayed in Figure 27 for 3 points of interest located at X=-40000 and Y=20000, Y=22000 and Y=24000 ft. The narrow high amplitude noise exposure near time 600 seconds comes from sphere location $\phi \sim 60^\circ$, $\theta \sim 30^\circ$. One can see this corresponds to the high noise region on the sphere underside. Another way to view the sphere, created by “slicing” through the sphere and marching down the sphere from front to rear is presented in Figure 28. This view for $\theta = 50^\circ, 60^\circ, 70^\circ, 80^\circ, 90^\circ$ and 100° illustrates the $\sim 30\text{dBA}$ dramatic directivity “hot spots” for this configuration for sphere PSCpx011 (APL-2). At this region in the trajectory corresponding to an arrival time of $T=600$ seconds the thrust is approximately 796 lb (Fn/delta) and AAM is interpolating linearly based on power between the noise sphere PSCpx011 (APL-2) and PSCpx013 (APL0).

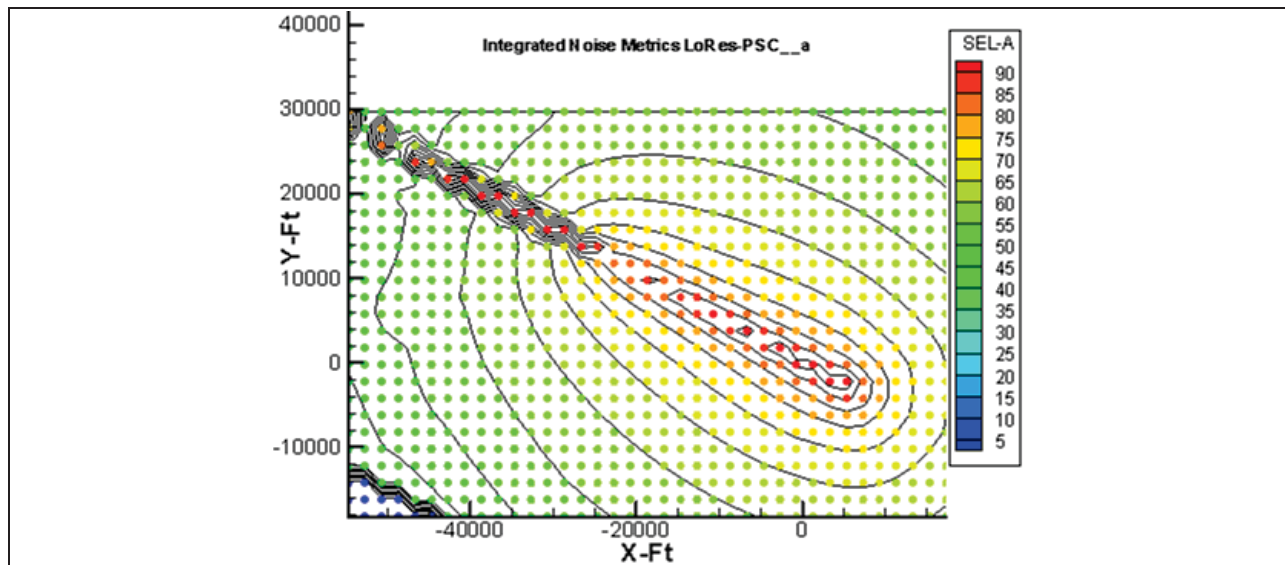


Figure 26 PSC Approach Ground Values at Computational Notes (SEL-dBA)

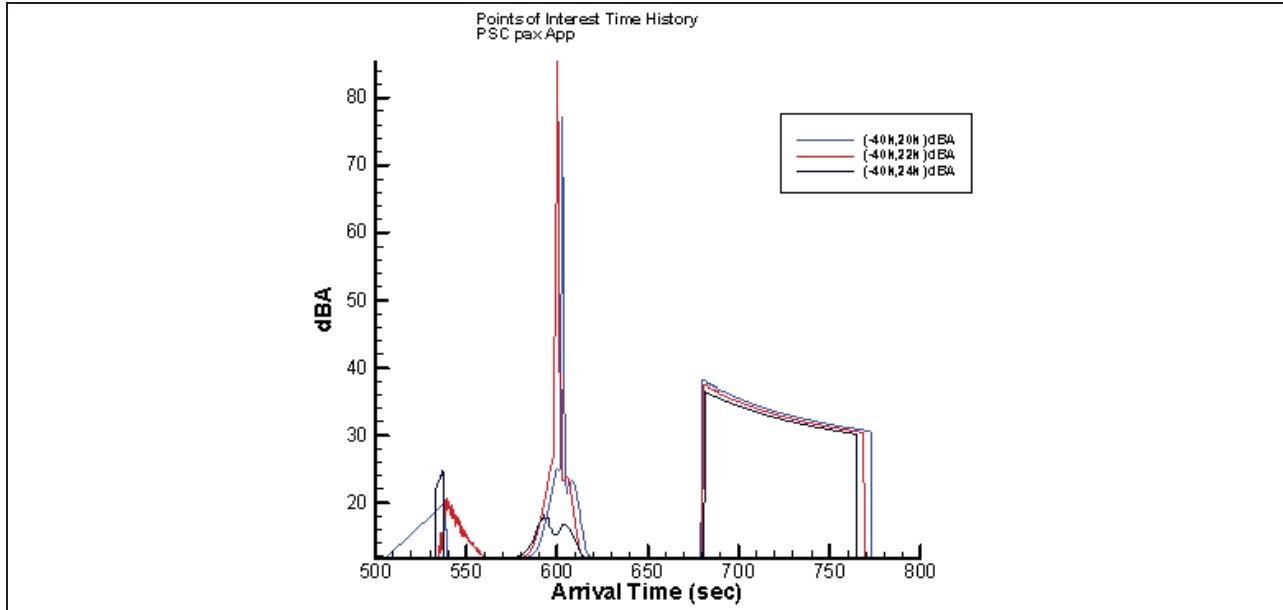


Figure 27 Time history SEL-dBA at 3 Points of Interest (40k,20k), (40k,22k), (40k,24k)Ft.

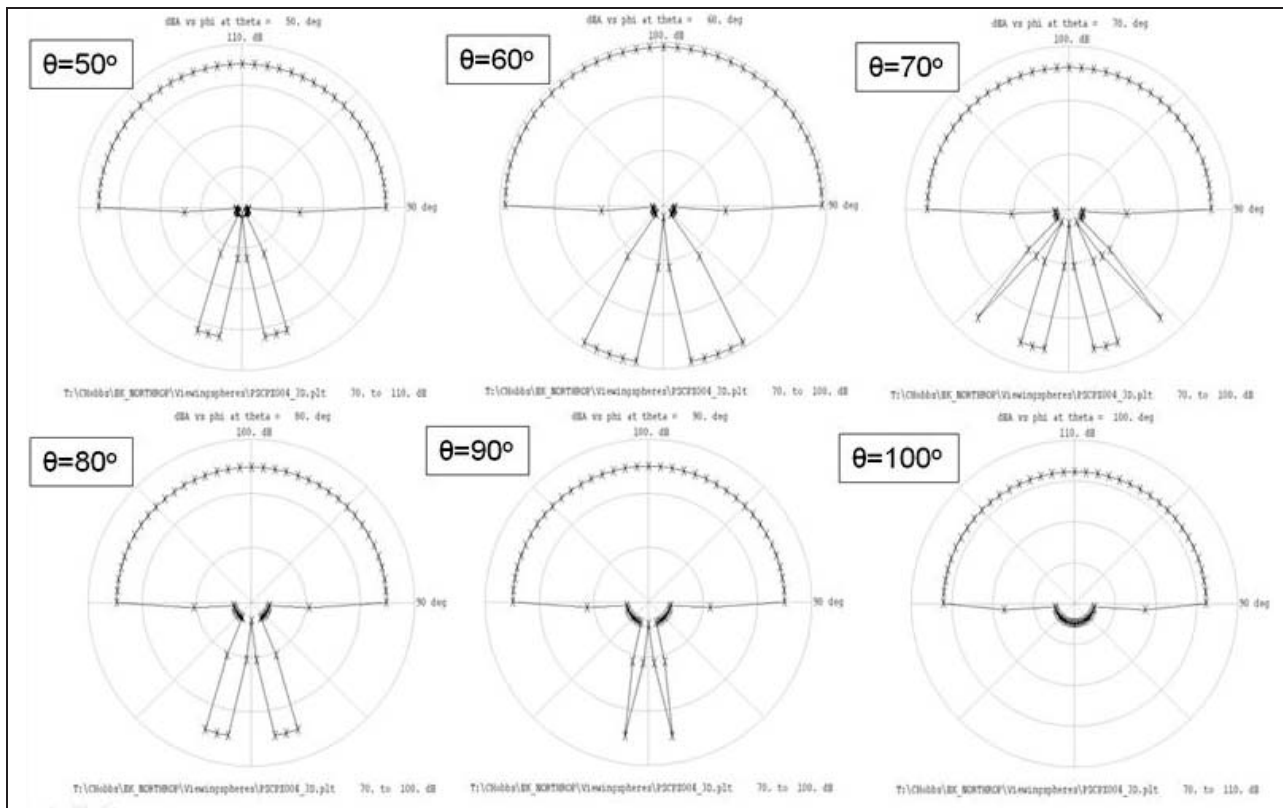


Figure 28 Sphere Slices at different theta locations, SEL-dBA (PSCpx004)

The current orientation of the trajectory is consistent with the San Francisco International Airport (SFO) analysis. In order to determine whether some of the behavior seen along the approach profile could be the result of dithering due to the alignment differences between ground track and grid orientation, a higher resolution mesh with 200 ft spacing was computed for a smaller region

and is displayed in Figure 29. Here evidence of the two highly directive regions on the noise sphere and the impact it has on the computed grid is shown.

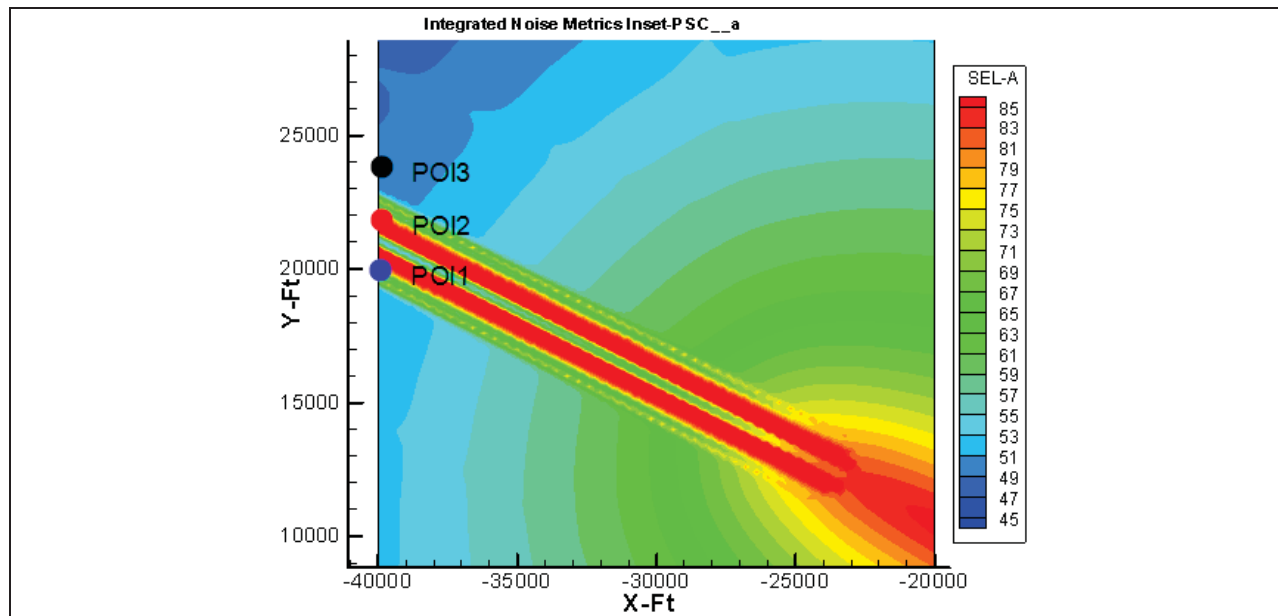


Figure 29 High resolution receiver mesh (200ft spacing) – PSC passenger, Approach, SEL-dBA

An assessment was made of airport-level noise. For this assessment, SFO was selected as a case study airport to model single-event noise exposures from operational trajectories and compare the PSC results against those for a 2025 Baseline (wing-body-tail) vehicle of the same class. Figure 30 shows the airport layout and runway configuration for SFO. This analysis allows for:

- Aircraft-to-aircraft comparison in terms of modeled A-weighted ground noise exposure
- Understanding of the effects of airport features, operational constraints, and land-use features on the relative benefits of new aircraft technologies
- Existing departure and arrival flight trajectories were modeled using AAM over flat uniform acoustically soft terrain and noise gradients were created to visualize and assess ground noise exposures from the two vehicles and contrast their differences

Figure 31 and Figure 32 provide illustrations of the SEL noise gradients for a departure operation of the PSC Vehicle and the 2025 Baseline aircraft respectively. The modeled departure track represents the existing GAP Noise Abatement Departure at SFO on Runway 28R. Figure 33 provides a difference SEL gradient (PSC minus conventional) highlighting the difference between the two aircraft in terms of single-event ground noise exposure during a standard departure operation. As is evidenced by the difference gradient, there is a marked decrease (up to 15dB) in overall SEL noise exposure for the PSC over the 2025 Baseline configuration on departure.

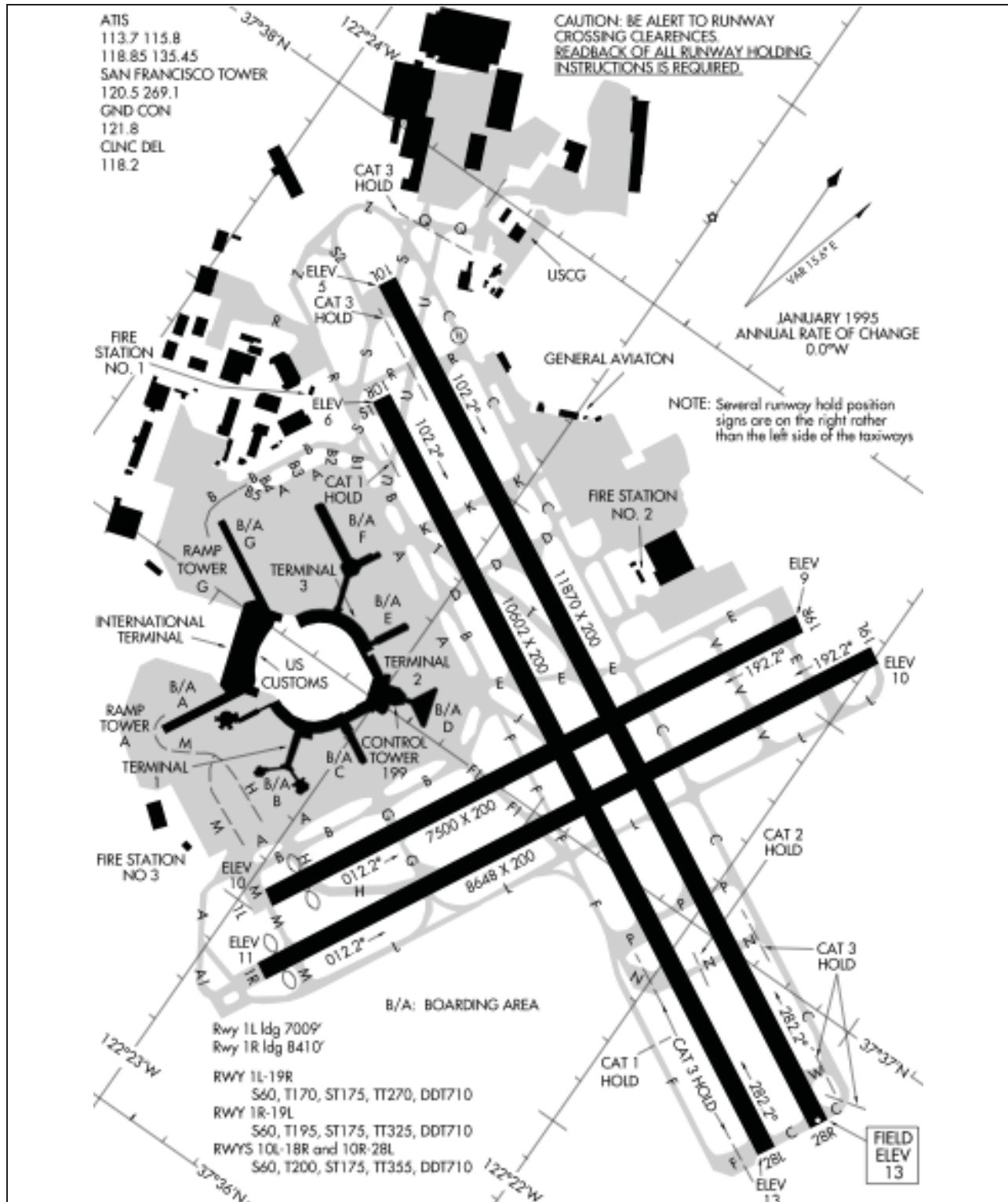


Figure 30 SFO Runway Configuration

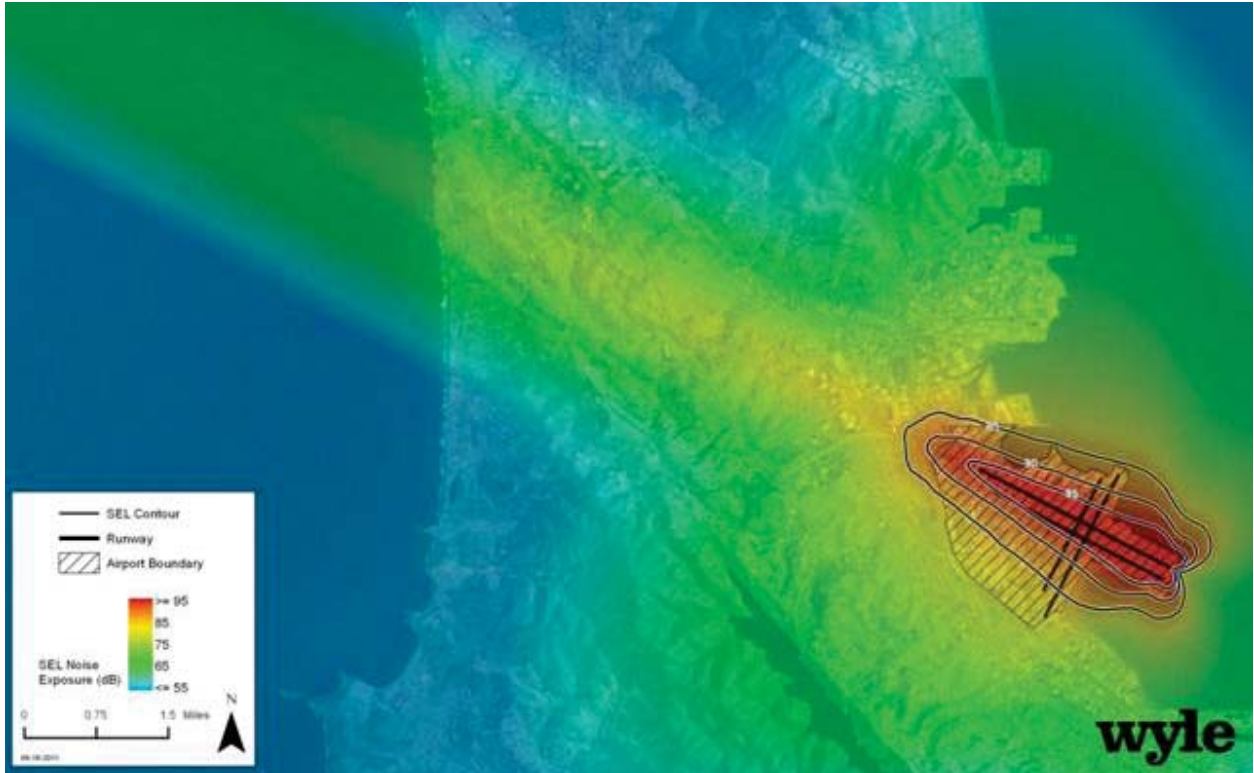


Figure 31 Single-Event Departure SEL Noise Gradient of 2025 Baseline Vehicle at SFO

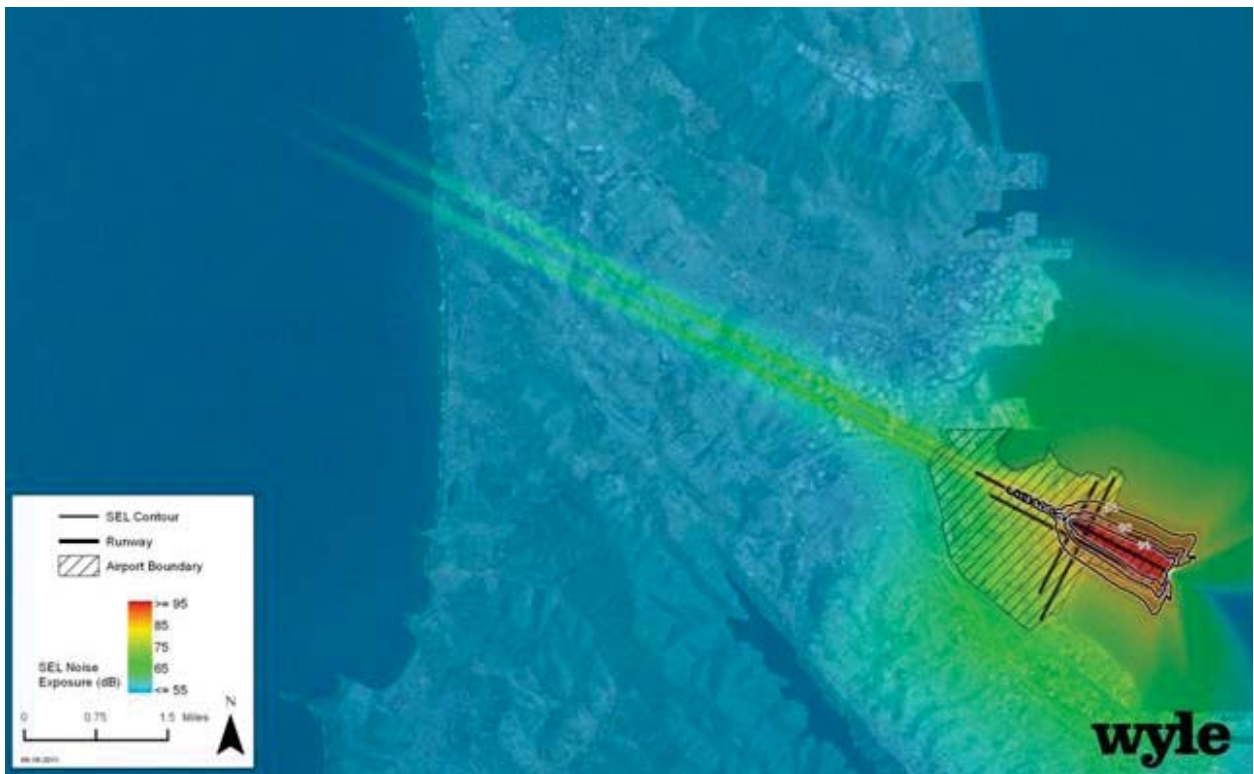


Figure 32 Single-Event Departure SEL Noise Gradient of PSC at SFO



Figure 33 Difference SEL gradient comparing 2025 Baseline Vehicle and PSC on Departure at SFO

Figure 34 and Figure 35 provide illustrations of the SEL noise gradients for an arrival operation at SFO of the PSC Vehicle and the 2025 Baseline aircraft respectively. The modeled arrival track represents an existing Standard Arrival at SFO on Runway 28R.

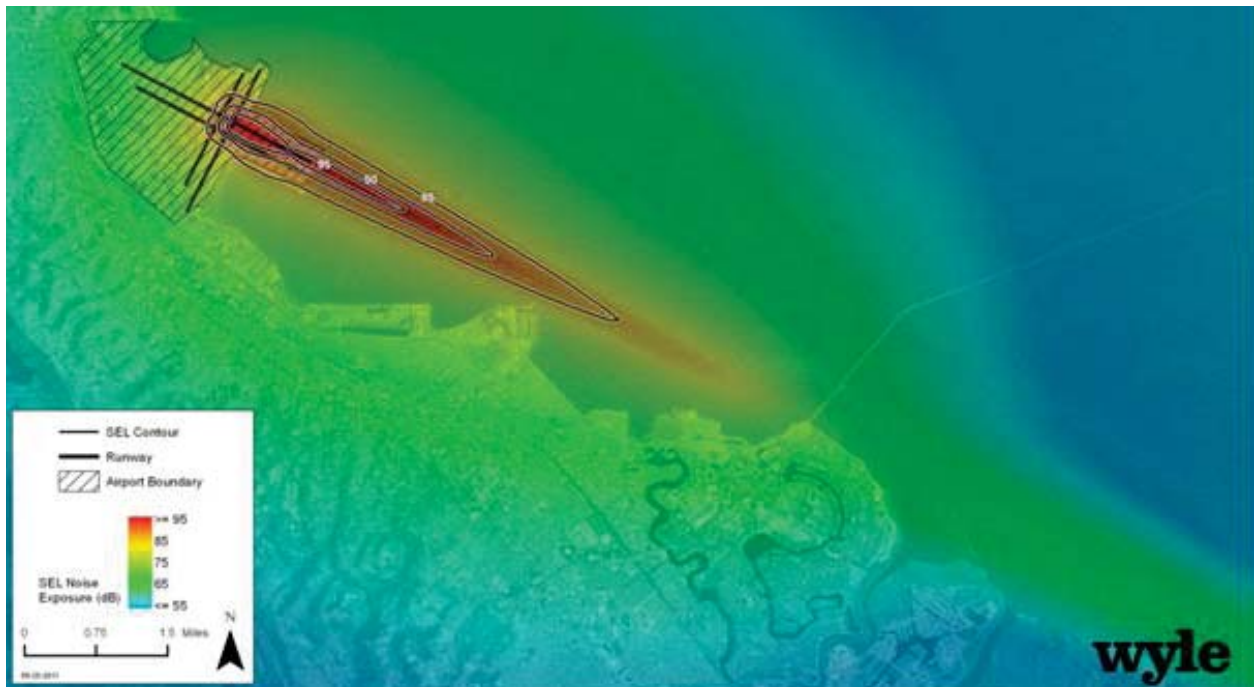


Figure 34 Single-Event Arrival SEL Noise Gradient of 2025 Baseline Vehicle at SFO

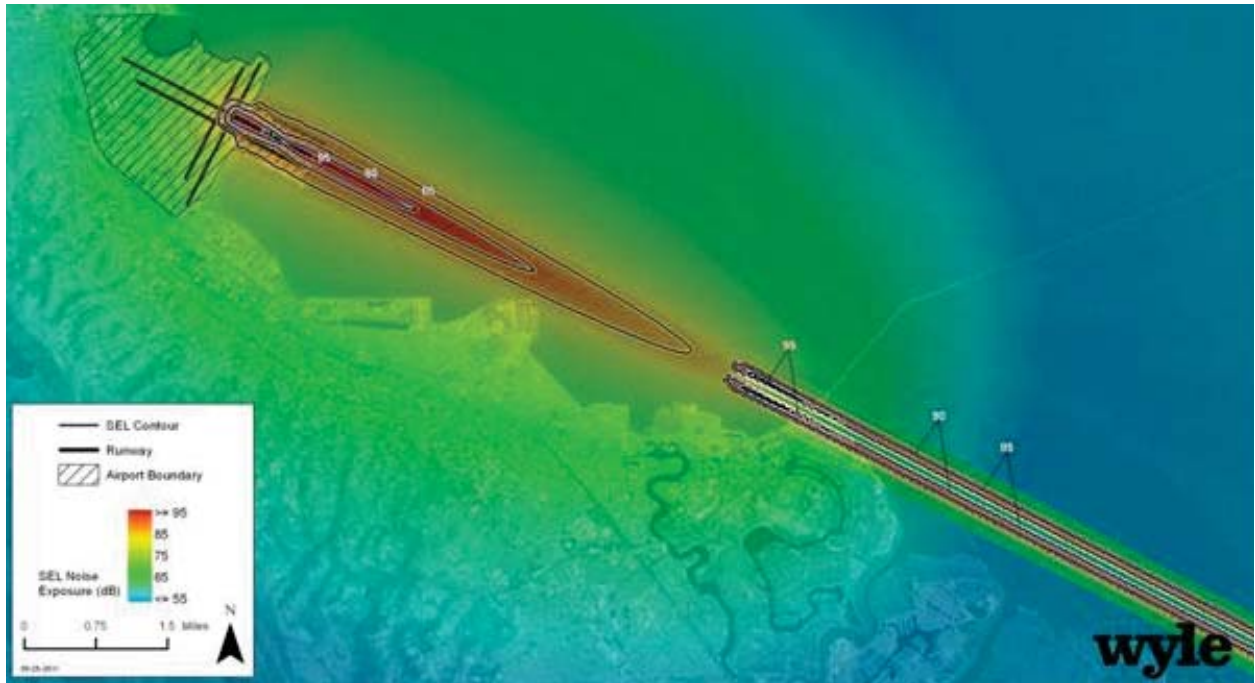


Figure 35 Single-Event Arrival SEL Noise Gradient of PSC Vehicle at SFO

As can be noted in Figure 35 and discussed in the previous section, the modeled source signature for the PSC on arrival displays shielding effects that causes two extensions of higher noise areas under the flight path. Figure 36 provides a difference SEL gradient (PSC minus conventional) highlighting the difference between the two aircraft in terms of single-event ground noise exposure during a standard arrival operation. The higher noise spikes under the flight path cause the PSC to show an increase in SEL noise exposure in some areas over the 2025 Baseline configuration on departure.

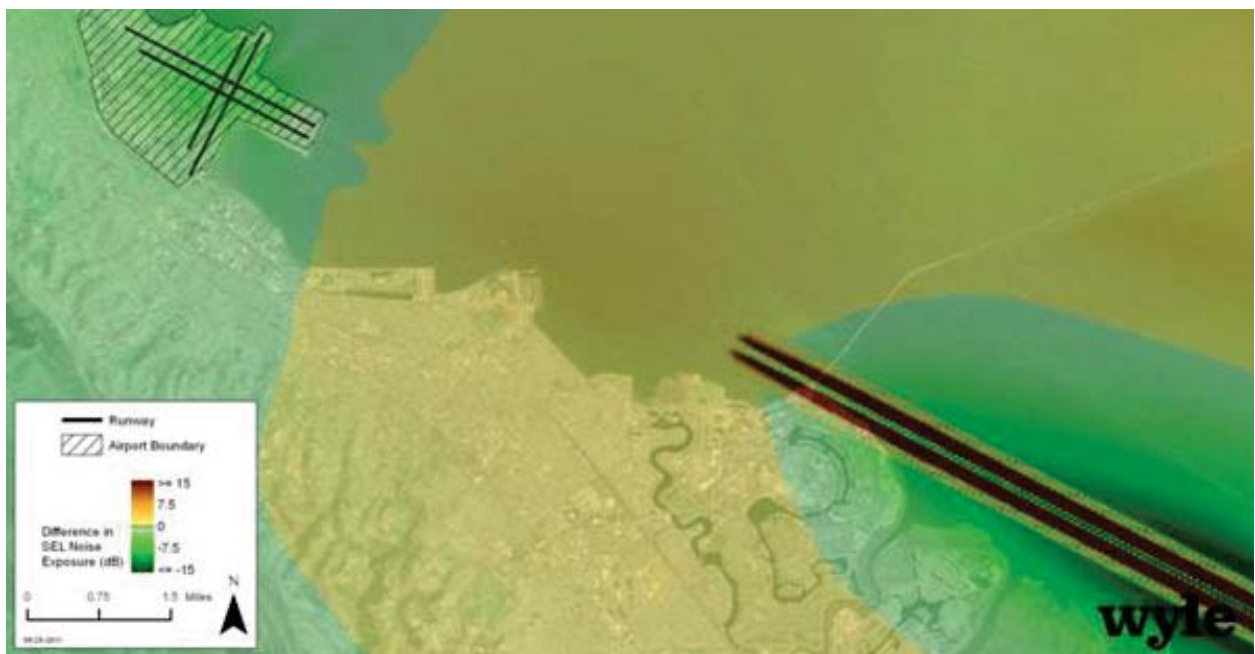


Figure 36 Difference SEL gradient comparing 2025 Baseline Vehicle and PSC on Arrival at SFO

The increase in single-event noise exposure displayed in Figure 36 may be attributable to source model issues that require further investigation. In general, as shown in Table 1, the combined exposure from arrival and departure operations provides a net improvement in total SEL exposure area, as well as in terms of exposed land area outside airport boundary. The noise reduction from the PSC is improved upon when the previously-mentioned shielding effects causing high noise spikes under arrival paths are not present (see shaded rows in Table 1).

Operation**	Change in Total Area by SEL Contour Band				
	75-80	80-85	85-90	90-95	95+
ARR	2%	11%	60%	167%	-13%
ARR*	-1%	-2%	23%	5%	-22%
DEP	-78%	-73%	-74%	-76%	-73%
ARR+DEP	-44%	-33%	-17%	3%	-60%
ARR*+DEP	-45%	-39%	-33%	-50%	-62%

Operation**	Change in Area Outside Airport Over Land by SEL Contour Band				
	75-80	80-85	85-90	90-95	95+
ARR	92%	1095%	0%	0%	0%
ARR*	77%	307%	0%	0%	0%
DEP	-100%	-100%	-100%	-100%	0%
ARR+DEP	-95%	-97%	-90%	20%	0%
ARR*+DEP	-95%	-99%	-100%	-100%	0%

* With Subtraction of shielding (diffraction) effect from contour area resulting from PSC arrival operation

** Impact area comparisons for modeled Arrivals and Departures on Runway 28R

Table 1 SEL Noise Contour Area Change from Baseline Vehicle to PSC

In addition to the technology benefits resulting from source noise reduction of PSC alternatives, there can also be additional benefits in combining new vehicle technology with environmentally-friendly operational concepts and procedures. For instance in a preferential runway situation, the PSC may be capable of operational performance on runways or along trajectories not available other aircraft in its class; hence, allowing for noise abatement over specific land uses and/or sensitive locations. This, of course, depends on the airport, its location and size, its operational environment, as well as its surrounding geography and local land-use policies and restrictions.

2.7. PSC Technology Requirements on NextGen

This study focused on the integration of a Preferred System Concept (PSC) that fulfills N+2 technology goals into the NextGen 2025 end-state as envisioned by the JPDO Concept of operations (ConOps). Task 1 of the study limited the environmental analysis to a pre-existing NextGen end-state, whereby the potential system-level impacts of the PSC on fuel burn, emissions, and noise are evaluated within a pre-defined NextGen Baseline scenario. As discussed in Section 2.1, the study team applied updates to the overall service volumes and fleet mix distributions within the Twin-Aisle vehicle class, which is the focus of the study. Underlying the analysis is the assumption that the NextGen baseline trajectories and operational concepts represent an achievable end-state for the NAS and associated technologies in 2025. Also, the

study assumes that the PSC has far-term avionics-related capabilities to perform NextGen operational procedures as outlined in the JPDO Avionics Roadmap, Version 2.0.

It is clear that the enhanced source characteristics of new vehicle technologies (N+2 and beyond) can provide a sizeable benefit to the NAS in terms of environmental impact mitigation and that such benefits can be increased with the application of smart NextGen concepts and technologies. It is important to note, however, that what may be good for the system may not always be good for a single airport community. As such, the integration of new aircraft technology and NextGen procedural concepts have to take into account local specificity, which drives concerns about noise exposure—this despite gains that can be made in improving fuel efficiency and local air quality.

While new aircraft technologies can produce significant improvements in environmental performance, non-conventional aircraft concepts can also produce challenges in terms of operational integration into the current NAS or that projected under NextGen. For instance, a non-conventional PSC may require adjustments to current ground handling and passenger loading procedures. It may require special separation assurance requirements in terminal area and transition airspace to enroute altitudes above conventional aircraft cruise bands. The latter issue may also warrant an understanding of the aircraft emission and climate impacts in lower stratosphere/upper troposphere.

Several studies have been conducted by various NAS stakeholders to quantify system performance under NextGen scenarios. The studies have focused on understanding the benefits of various technologies and advanced concepts on meeting the capacity challenge of the NAS while assessing the environmental constraints and system performance requirements of a NextGen end-state. The NASA ERA program provides an opportunity to focus on environmental performance as a driver for defining the requirements for new technology and its effective integration into the NAS. The PSC in this study is capable of meeting N+2 goals and conforming with NextGen requirements including in the performance of advanced operational concepts.

3. PREFERRED SYSTEM CONCEPTS

For the Task 2 (Preferred System Concepts Data Packages) portion of the NASA ERA AVC Study, the Northrop Grumman team produced six air vehicle concept designs. The 1998 Reference and 2025 Baseline vehicles were characterized as conventional wing-body-tail configurations. Two advanced configurations, a flying wing and a multibody configuration, were evaluated as candidates for the 2025 PSC vehicles. The major focus in developing and designing these vehicles was to meet the aggressive NASA N+2 goals for reductions in fuel burn, acoustic noise levels, and emissions.

3.1. Overview of Vehicle Designs

The Task 2 vehicle design process is outlined in Figure 37 below and includes mission requirements definition, configuration design, technology integration, propulsion system design and integration, and vehicle sizing and optimization. This section begins with a summary of the final vehicle designs and an assessment of their performance relative to the N+2 goals. It then continues with discussions of the details of the above mentioned process and summarizes the results and findings of the development of the six vehicles.

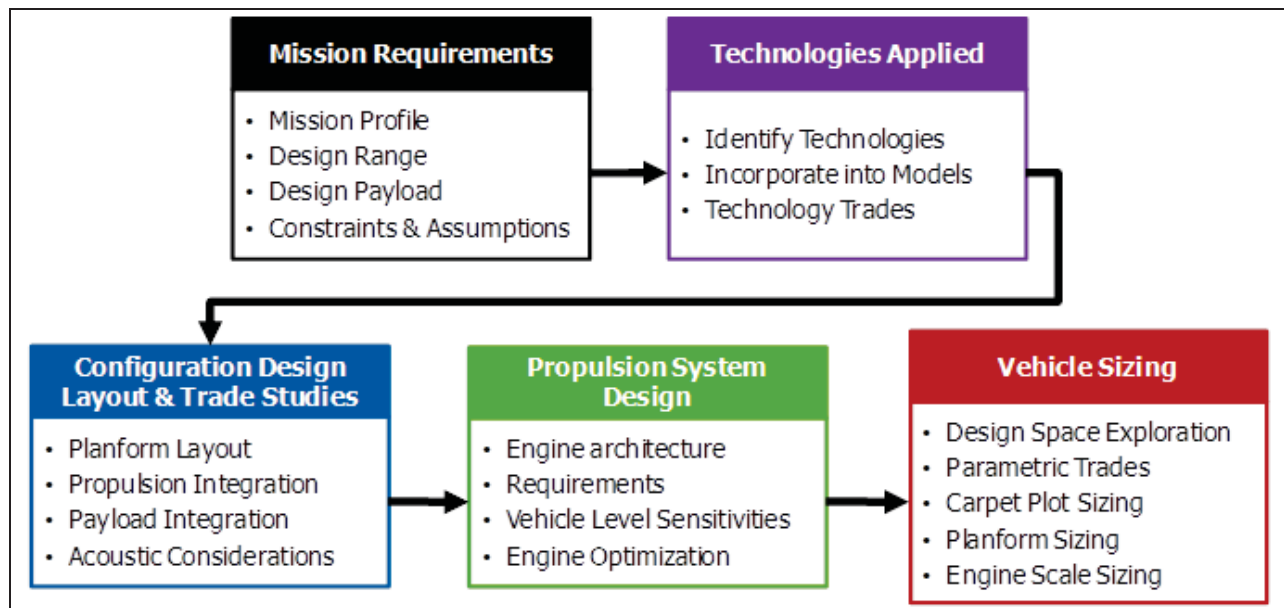


Figure 37 Concept Vehicle Design Process

3.1.1. Task 2 Concept Vehicle Designs

The set of six concept vehicle designs are shown below in Figure 38. The flying wing configuration was selected for the PSC passenger and cargo vehicles. The flying wing configuration provided the capability to take advantage of 2025 technologies and capitalize on them in ways a conventional configuration could not, to achieve reductions in fuel burn, acoustic noise levels, and emissions.

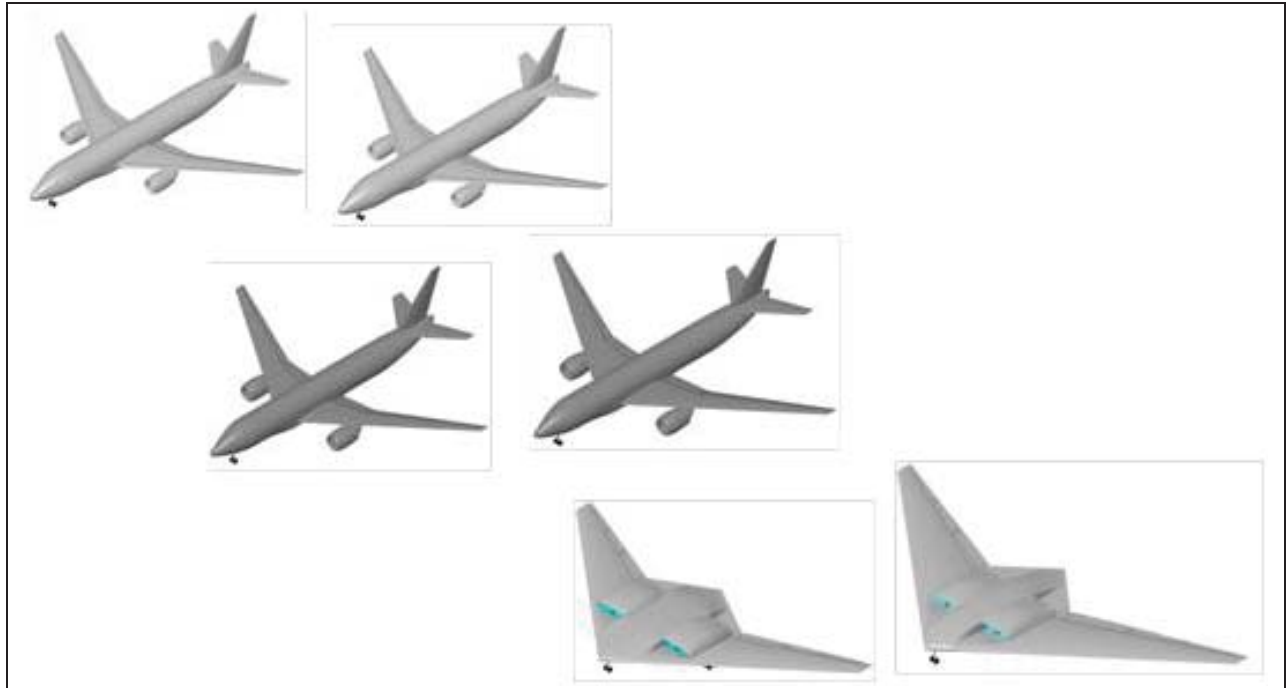


Figure 38 Task 2 Final Concept Vehicle Designs

3.1.2. Configuration Descriptions

The 1998 Reference vehicles are conventional wing-body-tail configurations that have been very popular for commercial and military transport aircraft in the past. These configurations were chosen to represent a 1998 EIS level of technologies and configuration design. Although similar aircraft were manufactured in the 1998 EIS timeframe, there were none that matched the NASA ERA payload and mission requirements. The 1998 Reference vehicles were designed based on the NASA ERA mission requirements to provide a reference point to assess the benefits in fuel burn, acoustic levels, and emissions of the 2025 Baseline and PSC vehicles.

The 2025 Baseline vehicles are also conventional wing-body-tail configurations with high bypass ratio turbofan engines. A set of 2025 technologies was applied to the 2025 Baseline vehicles to assess the impacts on fuel burn, acoustic levels, and emissions of incorporating advanced technologies into a typical conventional configuration. While these vehicles are sized differently than the 1998 Reference vehicles, they maintain the same overall configuration layout and design.

A multibody configuration was evaluated as a candidate for the 2025 PSC vehicles, as shown in Figure 39. This concept aimed to take advantage of span loading the fuselage and engine weights across the span of a high aspect ratio wing. The goal was to reduce weight through the structural relief provided by span loading and improve aerodynamic efficiency with a higher aspect ratio wing. Although this configuration performed well and produced significant improvements in the goal categories, the flying wing configuration performed significantly better.

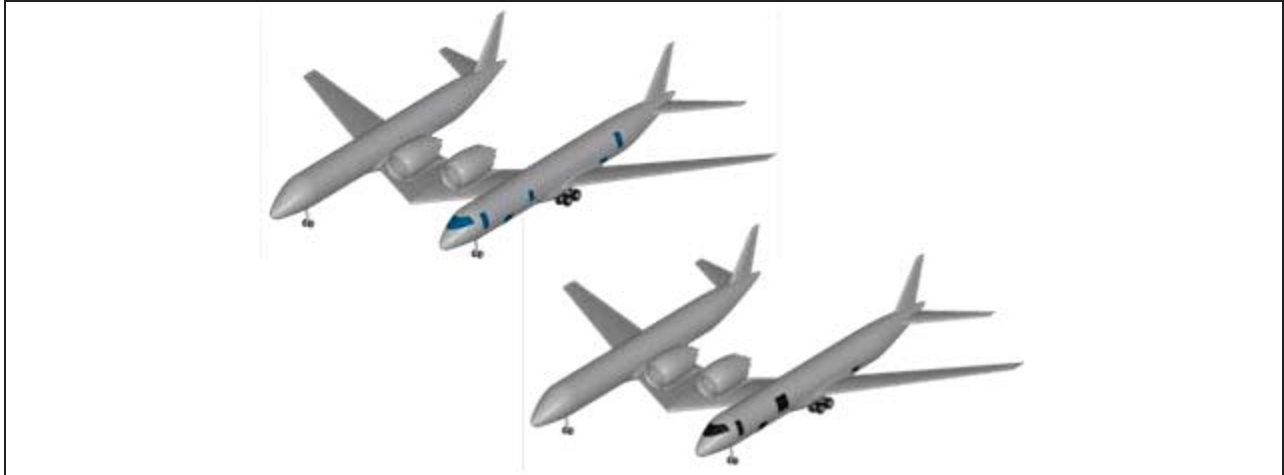


Figure 39 Multibody Configuration Vehicles

The selected 2025 PSC vehicles are flying wing configurations with four partially embedded high bypass ratio turbofan engines. The payload cabins are located along the center of the vehicle and the engines are located outboard of the cabins. This configuration was able to take advantage of the 2025 technologies in ways a conventional configuration simply could not, and in turn, achieved great benefits in the three categories of goals.

3.1.3. General Parameters and Performance Summary

A summary of geometry and performance parameters is shown in Table 2 below. The 1998 Reference vehicles are relatively similar to the families of 1998 EIS commercial airliners manufactured by major commercial airframers in terms of MTOW, empty weight, wing size, thrust class, and fuel burn. The 2025 Baseline vehicles show reductions on structural weight, improvements in engine SFC, improvements in aerodynamic efficiency, and hence, reductions in fuel burn. The PSC vehicles differ from the conventional vehicles, as expected, but include the same categories of improvements, and their performance benefits are seen in their large reductions in fuel burn. Three-views of the PSC passenger and cargo versions are shown in Figure 40 and Figure 41 below.

- Passenger, 8000 nm Mission
- Cargo, 6500 nm Mission

Parameter	Reference	Baseline	PSC	Reference	Baseline	PSC
	Passenger	Passenger	Passenger	Cargo	Cargo	Cargo
Wing Reference Area	3830 ft ²	3650 ft ²	8522 ft ²	3625 ft ²	4100 ft ²	10,313 ft ²
Wing Span	205 ft	205 ft	230 ft	200 ft	217 ft	260 ft
LE Sweep	33	33	40	33	33	40
Wing Aspect Ratio (Plan/Trap)	9.63 / 11	9.98 / 11.5	5.28 / 6.21	9.63 / 11	9.98 / 11.5	5.87 / 6.55
Taper Ratio	0.23	0.23	0.20	0.23	0.23	0.15
MTOW	595,500 lbs	466,000 lbs	427,100 lbs	611,000 lbs	509,000 lbs	473,300 lbs
OEW	284,740 lbs	253,309 lbs	225,409 lbs	283,980 lbs	259,805 lbs	231,287 lbs
Payload	50,000 lbs			100,000 lbs		
Propulsion	RR PD-684	RR PD-685	RR PD-700	RR PD-684	RR PD-685	RR PD-700
SLS Max Thrust per Engine	81,983 lbs	83,104 lbs	37,442 lbs	88,359 lbs	87,062 lbs	37,442 lbs
Number of Engines	2	2	4	2	2	4
Installed Cruise SFC	0.596	0.489	0.505	0.596	0.489	0.505
Cruise Mach	0.85	0.85	0.82	0.85	0.85	0.82
Balanced Field Length	10,088 ft	10,423 ft	7,074 ft	10,480 ft	10,468 ft	7,113 ft
Mission Fuel Burn	260,076 lbs	161,807 lbs	152,051 lbs	226,577 lbs	148,922 lbs	142,013 lbs

Table 2 Task 2 Vehicles Geometry and Performance Parameters Summary

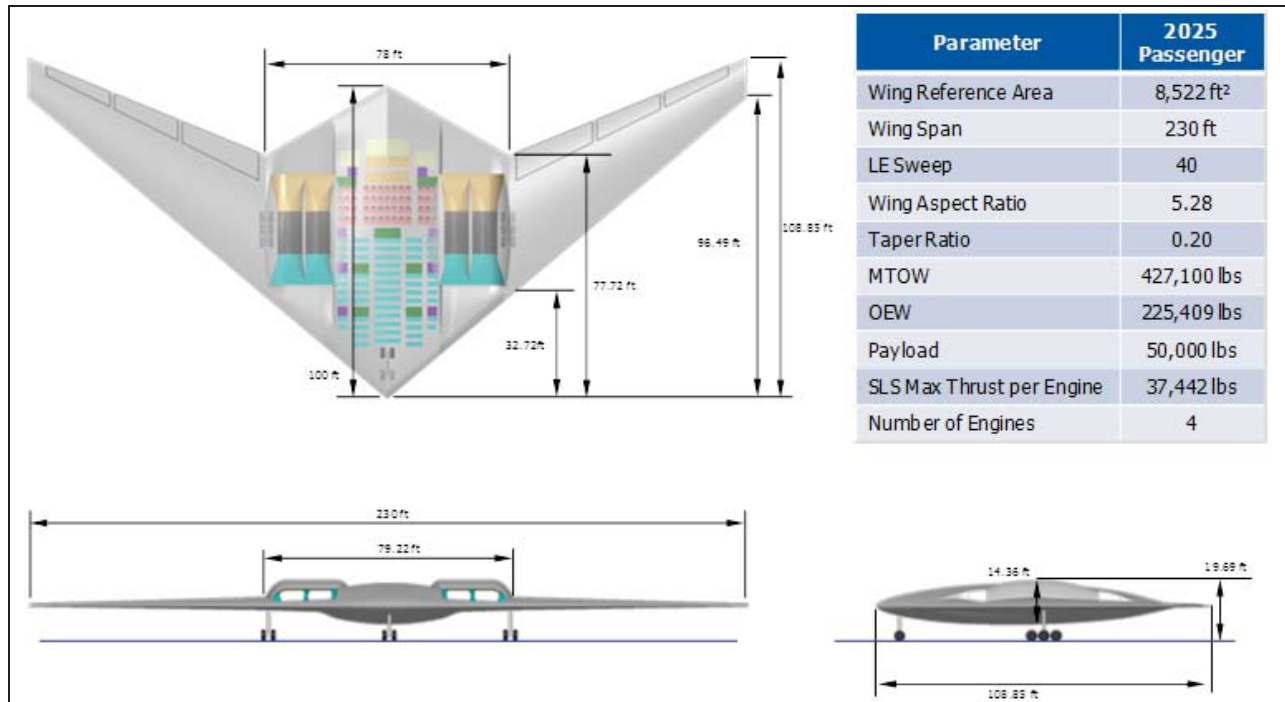


Figure 40 2025 PSC Passenger Version 3-View

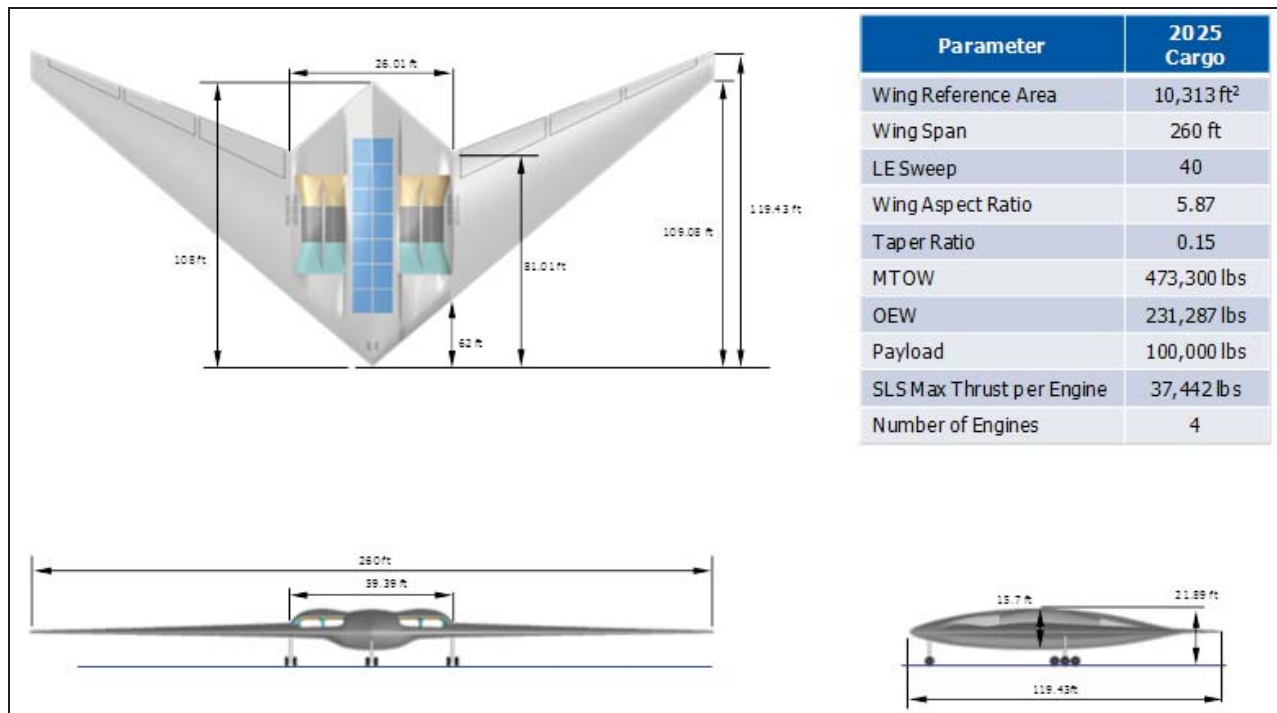


Figure 41 2025 PSC Cargo Version 3-View

3.2. Assessment of ERA Goals

The Task 2 air vehicle designs were focused on evaluating benefits to fuel burn, acoustic noise levels, and emissions, and producing benefits in these three categories to meet the challenging NASA N+2 goals. The 2025 Baseline and advanced configuration vehicles were compared with the 1998 Reference vehicles in order to assess their benefits in terms of the NASA N+2 goals. The PSC flying wing configuration was selected based on its superior performance in each of the goal categories.

3.2.1. Summary of ERA Goals

The NASA N+2 goals seek to reduce mission fuel burn by 50% relative to 1998 EIS vehicles, achieve acoustic noise levels 42 EPN db cumulative below that of Stage 4, and achieve emissions levels that are 75% below CAEP/6. These three categories of goals are major factors in the operations of commercial and military transport vehicles. Fuel burn reduction is directly related to both emissions and operating cost. Reducing the operating costs associated with fuel is a top priority for both civil and military aviation operations. Reducing acoustic noise levels is also a major concern for any type of airport operations. The commercial sector is facing particularly stringent community noise requirements and needs to address these in order to maintain operability into and out of popular airports across the world. Transport vehicles contribute greatly to emissions that are negatively impacting our environment. Conscious efforts to mitigate these effects have made emissions another major consideration in both civil and military transport operations.

The NASA N+2 goals reflect these factors impacting transport operations and aim to develop vehicles that can help realize these benefits in the future. Since all three goals have such strong influences, they are considered equally important and vehicle concepts that focus on addressing all three goals are desired, as opposed to simply optimizing on one or two of the goal categories.

These aggressive goals are challenging to meet, particularly with conventional configurations. Although advanced technologies can provide a certain level of improvements, the NASA ERA program sought to identify advanced configurations that could take advantage of these technologies more effectively to achieve these aggressive goals.

3.3. Comparison of Vehicles

Table 3 below summarizes the N+2 goals and evaluates the abilities of the 2025 Baseline and PSC vehicles to meet these goals. Although the PSC vehicles are not able to meet the 50% fuel burn reduction goal, they do achieve very significant fuel burn reductions and they exceed the reductions achieved by the conventional 2025 Baseline vehicles. The capabilities of the PSC’s advanced configuration are showcased in its ability to meet and exceed the acoustic noise level reduction goal as well as the emissions goal. Both of these goals are not met by both the 2025 Baseline vehicles.

Parameter	N+2 Goals	1998 Passenger	1998 Cargo	2025 Passenger	2025 Cargo	PSC Passenger	PSC Cargo
Fuel Burn	50% Reduction From 1998 Reference	0%	0%	37.8%	34.3%	41.5%	37.3%
Acoustic	Stage 4 -42 EPNdB Cumulative	Stage 4 -1.6 db	Stage 4 +7.3 db	Stage 4 -23.6 db	Stage 4 -20.8 db	Stage 4 -74.7 db	Stage 4 -79.5 db
Emissions	75% Below CAEP/6	9% Below CAEP/6	9% Below CAEP/6	72% Below CAEP/6	72% Below CAEP/6	88% Below CAEP/6	88% Below CAEP/6

Table 3 N+2 Goals Assessment for ERA Vehicles

Figure 42 shows a comparison of the six final vehicles as well as the two versions of the multibody configuration in terms of fuel burn and noise margin. This figure evaluates each vehicles combined benefits in the fuel burn and acoustic noise level categories of goals. This further shows the PSC vehicles’ advantage in acoustic noise reduction, while also achieving the largest fuel burn reduction. These results were the basis for selecting the flying wing configuration for the PSC vehicles.

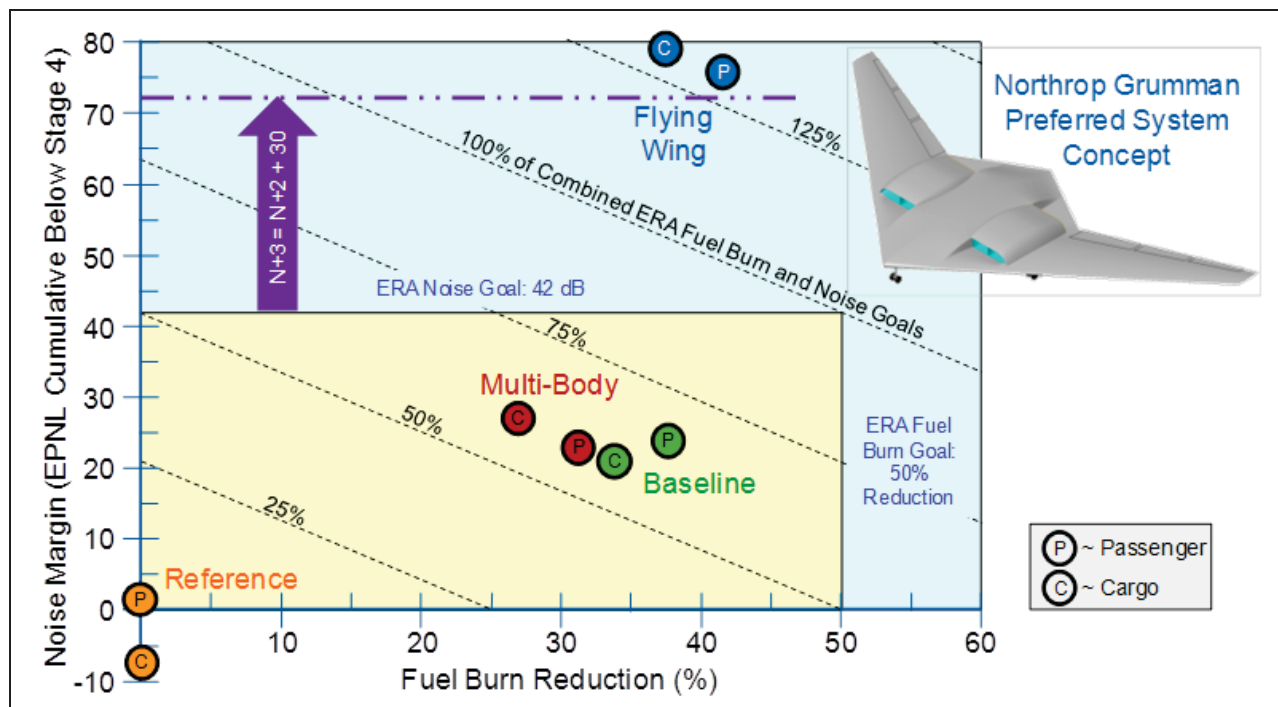


Figure 42 Comparison of Fuel Burn and Noise Margin for ERA Vehicles

3.3.1. Configuration Effects on Goals

Conventional wing-body-tail configurations represent a local optimum in commercial transport vehicles. Although the details of these vehicle designs have evolved over the decades, the overall configuration layout has not changed significantly. Advancements in composite materials and high bypass ratio turbofans have provided significant benefits for each new generation of transports. However, as this study and others indicate, even with a diverse portfolio of advanced technologies across various components of the air vehicle applied to this conventional configuration, it cannot achieve the NASA N+2 goals.

Advanced configurations that capitalize on the available set of technologies and utilize them more effectively are required to meet these goals. The flying wing configuration of the PSC vehicles takes advantage of aerodynamic, structural, and propulsion system technologies to achieve greatly improved mission fuel burn. However, the partially embedded engines integrated into the flying wing configuration provide acoustic noise level reductions through shielding and liners that otherwise would not be achievable. Furthermore, the placement of the engines distributes the load spanwise in a structurally more efficient manner, and also locates them further forward, alleviating some of the challenges in balancing a flying wing or hybrid wing body type of configuration. These configuration characteristics, when combined with advanced technologies, allow the PSC vehicle to achieve results in terms of the NASA N+2 goals that a conventional configuration simply cannot.

3.4. Mission Requirements, Constraints, and Assumptions

The first step in the vehicle design process outlined in Figure 37 is to establish the mission requirements, apply constraints, and identify any assumptions. These are described in the below section and include specific NASA ERA requirements as well as additional considerations developed by the Northrop Grumman team.

3.4.1. NASA ERA Requirements

The mission requirements for the concept vehicle designs were a combination of the NASA ERA mission requirements and other requirements and constraints established by the Northrop Grumman team. The NASA ERA requirements outlined a prescribed mission profile shown in Figure 43. The passenger version of each set of vehicles was required to carry 224 passengers weighing 50,000 lb with a mission range of 8,000 nm. The cargo versions were required to carry 100,000 lb of cargo with a mission range of 6,500 nm. The 1998 Reference and 2025 Baseline vehicles had a cruise speed of Mach 0.85. The 2025 multibody and flying wing vehicles had a cruise speed of Mach 0.82. The reduced cruise speed is based on expedited loading and unloading times for these vehicles that result in block mission times equivalent to that of the Mach 0.85 Reference and Baseline vehicles.

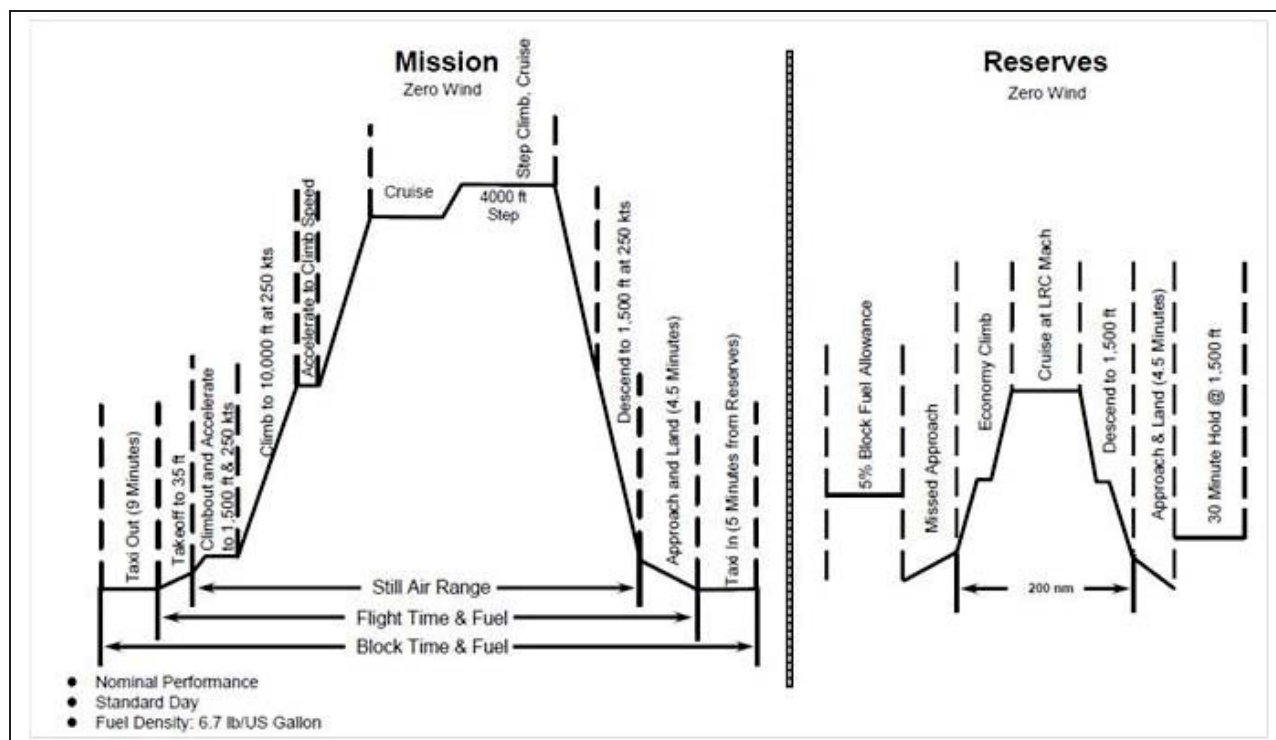


Figure 43 NASA ERA Mission Profile

3.4.2. Additional Requirements, Constraints and Assumptions

Additional requirements and constraints were established mainly to ensure the vehicle designs were appropriately representative of typical civil and military transport operations. A balanced field length requirement of no greater than 10,500 ft was included to capture the effects of vehicles that are sized by field length constraints. The vehicles were also required to meet FAA FAR 25 takeoff and landing rules to further include the effects of takeoff and landing considerations that could potentially size parts of the vehicles.

A wing span constraint of 205 ft was applied to the 1998 Reference vehicles to represent the airport ground operations conditions of 1998 EIS vehicles of a similar class as the 1998 Reference vehicles. The 2025 vehicles, both the Baselines and advanced configurations, were allowed to investigate higher aspect ratio wings; however they were constrained to a wing span of 260 ft. This constraint is based on the largest wing span of any currently operating commercial transports and is intended to apply a 2025 level of airport ground operations consideration.

All vehicles were allowed to cruise at higher altitudes than is typical for civil and military transports. This allows the vehicles to potentially fly at more optimal altitudes. These effects are also incorporated into investigation of possibilities for next generation air space operations improvements.

Lastly, each vehicle was required to meet typical operational and safety requirements for passenger and cargo revenue service. This included items such as emergency exits, passenger accommodations, cargo loading and handling equipment, loading and unloading doors and ramps, and so on. The majority of these items are accounted for in either the weights estimation tools, or in the configuration layout of the given vehicle.

3.5. Integration of Technologies into Task 2 Vehicle Models

The next step in the vehicle design process is to incorporate technologies into the vehicle models and implement them properly in designing and analyzing the vehicles. The Task 3 and 4 sections of this report discuss the technology database and the items it includes in detail for this program. The technologies identified in the technology database development effort must then be modeled in the vehicle design tools and models. This section summarizes what technologies were applied to the 2025 vehicles and how their benefits and impacts were accounted for in the vehicle models.

3.5.1. Technologies Applied, Benefits, and Penalties Implementation into Models

Table 4 summarizes the technologies accounted for in the vehicle design tools and models for the 2025 Baseline, multibody configuration, and flying wing configuration vehicles. The table also describes specifically how each technology was accounted for in the models. Many technologies have system level impacts, and any secondary impacts associated with a given technology have been accounted for as best as is possible at the conceptual design level. It is important to note that the combined benefits of applying multiple technologies that affect the same component or part of the air vehicle are not additive. Hence, in these cases, a vehicle system level benefit has been estimated to best represent the integration of the set of technologies into the air vehicle.

Technology	2025 Baseline Vehicles	2025 PSC Vehicles
Advanced 2025 Turbofan Engines	<ul style="list-style-type: none"> • ~18% SFC Improvement From 1998 EIS Engine • Engine weight and geometry models provided by RRLW 	<ul style="list-style-type: none"> • ~15% SFC Improvement From 1998 EIS Engine • Engine weight and geometry models provided by RRLW
Inlet Flow Control	<ul style="list-style-type: none"> • Not Applicable 	<ul style="list-style-type: none"> • Improved inlet pressure recovery and nozzle Cfg provided to RRLW • Allows for decreased inlet L/D
Composite Wing Structure	<ul style="list-style-type: none"> • 20% Wing weight reduction factor applied 	
Wing Maneuver Load Alleviation	<ul style="list-style-type: none"> • 1.8% Wing weight reduction factor applied 	
Composite Fuselage Structure	<ul style="list-style-type: none"> • 10% Fuselage weight reduction factor applied 	
Misc. Composite / Advanced Structure	<ul style="list-style-type: none"> • 10% Nacelle/air induction weight reduction factor applied • 3% Landing gear weight reduction factor applied 	
Swept Wing Laminar Flow Control	<ul style="list-style-type: none"> • %Chord laminar flow based on transition Reynolds Number as a function of sweep • No leading edge high lift devices • 0.1 CL_{max} penalty • No laminar flow beyond %chord location of critical sweep line 	<ul style="list-style-type: none"> • %Chord laminar flow based on transition Reynolds Number as a function of sweep • No leading edge high lift devices • No laminar flow beyond %chord location of critical sweep line
Riblets	<ul style="list-style-type: none"> • 1% Total drag reduction based on applicable wetted area 	<ul style="list-style-type: none"> • 3% Total drag reduction based on applicable wetted area
More Electric ECS System	<ul style="list-style-type: none"> • No engine bleed for ECS and increased Hp extraction • Increased number of generators • Increased generator installation, ECS, and APU system weights • Engine installation requirements reflect this system • Added ram air drag of ECS scoop 	
Carbon Nanotube Electrical Cables	<ul style="list-style-type: none"> • 20% Power distribution weight reduction factor applied 	
Spliceless Inlet Liners	<ul style="list-style-type: none"> • No weight penalty applied 	<ul style="list-style-type: none"> • Liner weight accounted for in weights model
Landing Gear Assembly Fairings	<ul style="list-style-type: none"> • 1% Landing gear weight increase factor applied 	

Table 4 Summary of 2025 Technologies Applied in Vehicle Models

3.5.2. Technology Trade Studies

The technologies applied to the vehicle design tools and models were selected from the technology database developed as part of Task 3. Certain technologies provide a definite vehicle level improvement, for example, any structural weight reduction technologies. These technologies were assessed for TRL status, applicability to the given vehicles, and any integration issues that may exist. However, certain other technologies can be traded at a vehicle level to find what provides the best performance improvement. These technologies included Swept Wing Laminar Flow Control (SWLFC), and a more electric airplane (MEA) ECS system. Furthermore, the two acoustic noise level reduction technologies, spliceless inlet liners and

landing gear fairings, are accounted for in the vehicle models. Although they provide reductions in noise levels, they add weight to the vehicle, and this is accounted for as described in Table 4.

While SWLFC provides a reduction in skin friction drag, no leading edge high lift devices can be used if it is to be implemented on a given wing. Hence, there is a potential tradeoff between the drag reduction from SWLFC and the increase in both engine thrust scale and wing area required to meet takeoff and landing requirements without any leading edge high lift devices. To examine these effects on the air vehicle’s design and performance a comparison was made between a vehicle with no SWLFC and with leading edge high lift devices, and a vehicle with SWLFC and no leading edge high lift devices. This was done on the 2025 Baseline passenger vehicle with all other technologies listed in Table 4 active. The results are summarized in Table 5 below. It was found that even without the benefits of leading edge devices for takeoff and landing driving a larger wing area and engine thrust scale, the vehicle with SWLFC active showed a greater reduction in mission fuel burn by about 9%. Hence, SWLFC was applied to the 2025 Baseline vehicles. The 2025 PSC vehicles were not sized by balanced field length as the 2025 Baseline vehicles were, hence, SWLFC was applied to the 2025 PSC vehicles as well.

	1998 Reference	2025 Baseline Sized w/o SWLFC	2025 Baseline Sized w/ SWLFC
Mission Fuel Burn (lbs)	260,076	185,474	161,807
% Mission Fuel Burn Reduction	-	28.7%	37.8%

Table 5 SWLFC Technology Trade for 2025 Baseline Vehicles

Advanced subsystem technologies were also traded similarly for the 2025 vehicles. Two main advanced subsystems architectures were considered – a fuel cell APU system and a MEA ECS system. These were traded on the 2025 Baseline and PSC passenger vehicles. The impacts to systems weights were accounted for in the weights models. Corresponding horsepower extraction and bleed air requirements were applied for each system to obtain an SFC scale factor, which was applied in the trades. The fuel cell APU system trade also included accounting for the additional fuel burned by the fuel cell APU. The MEA ECS system trade included accounting for the added drag of a ram air ECS scoop. The details of these subsystems technologies is described in Section 4 of this report, but the vehicle level trade results are summarized in Table 6 below. It was found that for both the 2025 Baseline and PSC vehicles, the fuel cell APU system actually burned more fuel relative to a 1998 EIS level conventional subsystem architecture, and the MEA ECS system showed a 0.4-0.9% fuel burn reduction for both sets of 2025 vehicles. Therefore, the MEA ECS system was applied to the 2025 Baseline and PSC vehicles.

	Fuel Cell APU		MEA ECS	
	2025 Baseline	2025 PSC	2025 Baseline	2025 PSC
% Mission Fuel Burn Reduction	-0.3%	-0.5%	0.4 - 0.5%	0.4 - 0.9%

Table 6 Advanced Subsystems Technology Trade for 2025 Vehicles

3.6. Vehicle Configuration Designs and Trade Studies

With the mission requirements established, and technologies incorporated into the vehicle models, the next step outlined in Figure 37 is to develop the configuration design layouts and execute configuration trade studies. This lays out the configurations that will be sized and optimized in the final step of the process.

3.6.1. 1998 EIS Reference Wing-Body-Tail Vehicles

As mentioned earlier, the 1998 Reference vehicle configurations were selected to represent a 1998 EIS level of aircraft that can then be sized to meet the NASA ERA mission requirements. The 1998 Reference vehicles are conventional wing-body-tail configurations with conventional cross-tail empennages. The fuselage was sized similar to that of the Boeing 787, because its passenger count is exactly the same as that of the NASA ERA requirement. The same fuselage was used for the cargo version as well to represent a typical freighter version of a commercial airliner. High bypass ratio engines with a 1998 EIS level of performance were integrated in a conventional pod mounted under-wing layout. This conventional configuration is shown in Figure 44.

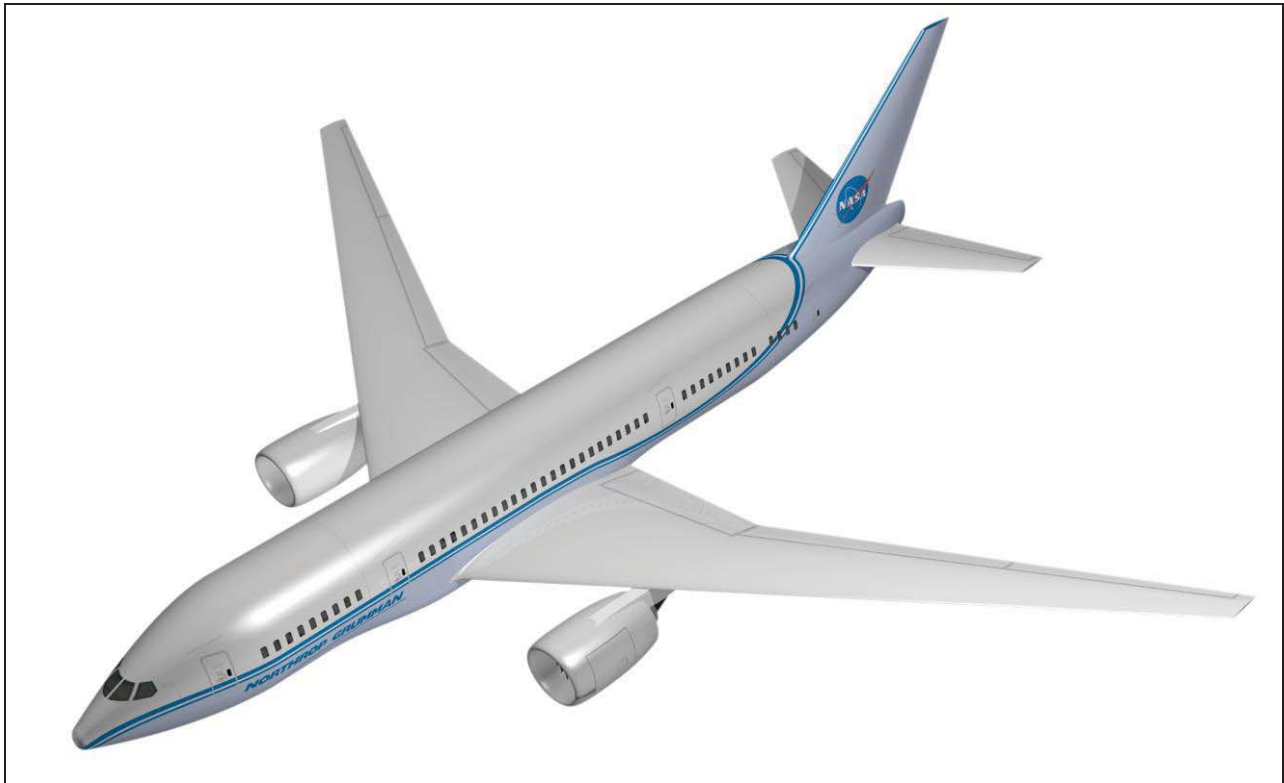


Figure 44 Conventional Wing-Body-Tail Configuration for 1998 EIS Reference Vehicles

It is important to note that civil and military transports that entered service in the 1998 time frame utilized some composite materials mainly on control surfaces, fairings, the empennage, nacelles, floor panels, and doors. The 1998 Reference vehicles include this level of composite technology in their models and designs.

3.6.2. 2025 EIS Baseline Wing-Body-Tail Vehicles

The 2025 Baseline vehicles are also conventional wing-body-tail configurations. Minor variations on this configuration were considered for these vehicles, such as T-tails, overwing engines, high wing configuration, and so on. However, the effects of these would be relatively minor and not necessarily beneficial. The chosen conventional configuration is representative of a current day optimal design to which technologies were applied, hence representing the level of benefits that can be realized from these technologies on a conventional configuration. This provides a good baseline to compare advanced configurations with, in order to evaluate if and how the advanced configurations take better advantage of 2025 technologies to achieve the N+2 goals.

3.6.3. Flying Wing Centerbody and Wing Design

The flying wing configuration that was selected for the PSC vehicles introduces interesting configuration layout challenges and is much different from a conventional wing-body-tail configuration. The flying wing configuration studied can be divided into a centerbody section and wing sections. This centerbody section includes the payload cabin, integrated propulsion system, and integrated landing gear. A schematic layout of the flying wing configuration is shown in Figure 45.

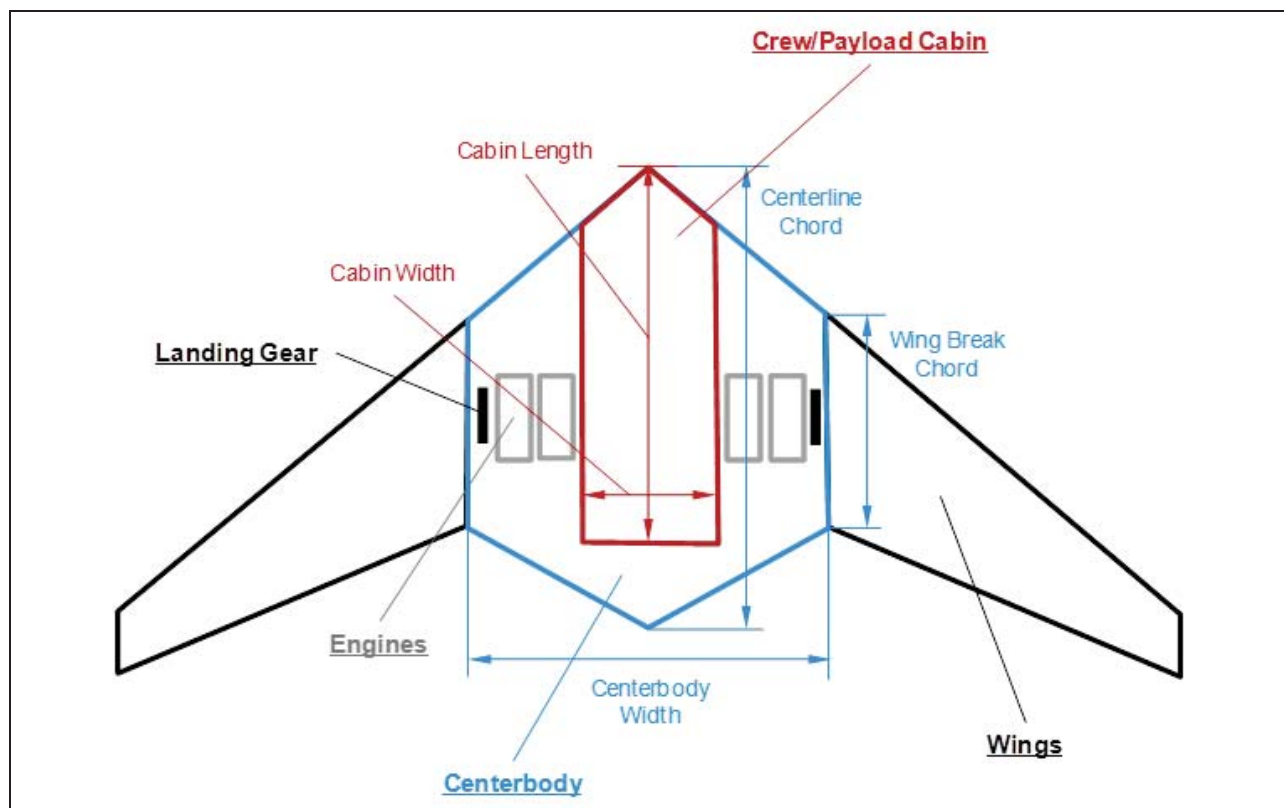


Figure 45 Schematic Layout of Flying Wing Configuration

This configuration is highly dependent on the interior arrangement of the payload cabin. The length and width of the cabin required to wrap the given payload drives the centerbody dimensions. These include the centerline chord length, the wing break chord, and the centerbody width. The integration of the cabin into the centerbody includes considerations such as thickness to chord ratios, closure angles at the trailing edge, flow path clearance from the leading and

trailing edges for the propulsion system, as well as clearance between the cabin, engines, and landing gear. Once the centerbody is configured around the payload cabin and the three centerbody dimensions are defined, the centerbody then drives the wing planform. The remaining wing geometry variables are sweep, span, and taper ratio. The flying wing configuration is highly coupled and demands close interaction between the various components in Figure 45 that define the vehicle's layout.

In this study, packaging the required 224 passengers into the payload cabin was particularly challenging, mainly due to the fact that a passenger interior arrangement is much more open ended than packing cargo payload. A database of possible payload cabins and associated centerbody dimensions was developed to ensure any vehicle geometry trades or sizing performed was done on a configuration that could properly integrate the required mission payload. These were traded as part of sizing the wing planform and the results are presented in Section 3.8.

3.6.4. Flying Wing Propulsion Integration

Three propulsion integration layouts were considered for the flying wing configuration – pod mounted overwing nacelles, partially embedded overwing engines, and a fully embedded leading edge inlet. For the pod mounted and partially embedded layouts, both two and four engine versions were considered. For the leading edge inlet layout, only a four engine version was considered, to maintain a smooth OML integration.

These five potential configurations were compared based on five metrics that represent the primary effects of the propulsion system integration layout for the flying wing vehicles. This comparison is shown in Figure 46. The pod mounted layouts were expected to achieve the best SFC due to a lack of restrictions on fan diameter, and hence, bypass ratio. The partially embedded layouts would be slightly penalized in SFC due to fan diameter restrictions in integrating into the centerbody, but more so due to reduced inlet pressure recovery and nozzle C_{fg} . The leading edge inlet layout would have greater restrictions on fan diameter and would have an even worse inlet pressure recovery than the partially embedded layouts. The installation weights associated with the pod mounted layout would be the least, and both the partially embedded and leading edge inlet layout would have added weight associated with inlet and exhaust flow paths, fire protection lining, and so on.

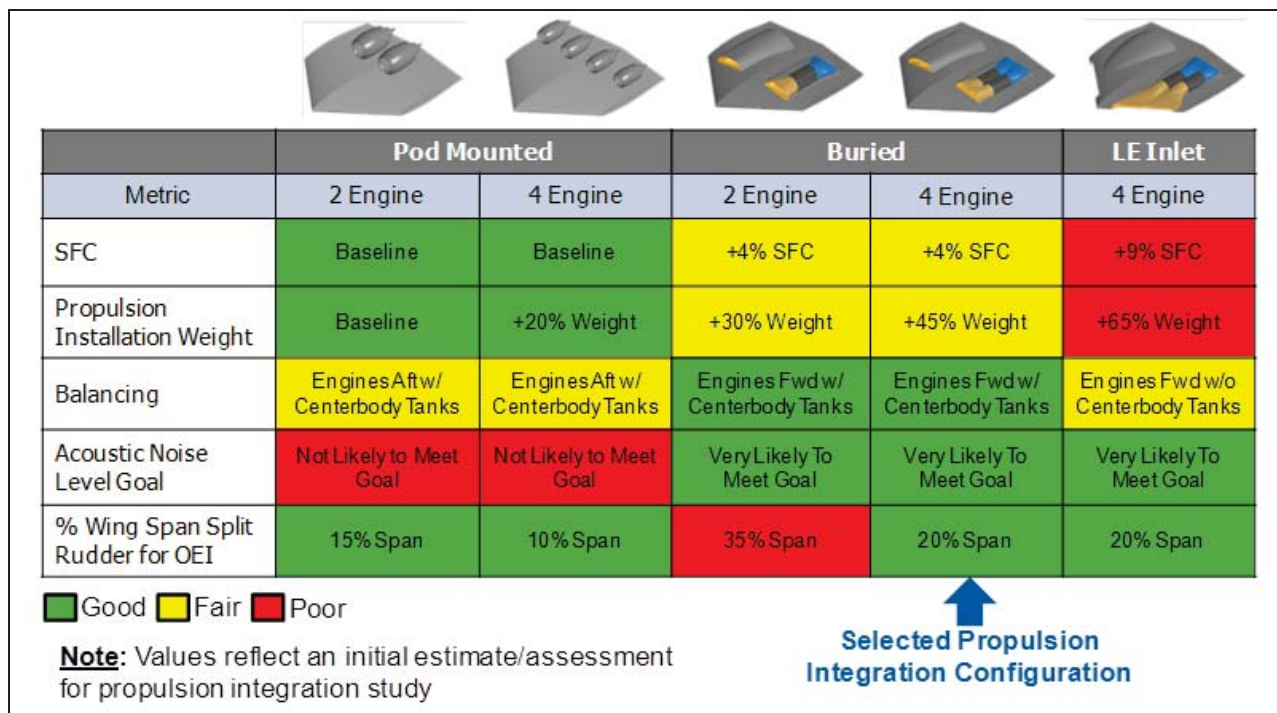


Figure 46 Flying Wing Propulsion Integration Approach Selection

In terms of balancing, pod mounted engines would be mounted further aft on the centerbody, driving the center of gravity further aft and making balancing more challenging. The partially embedded layouts place the engines much further forward making them favorable in terms of balancing. In addition, the partially embedded layout allows for the use of centerbody fuel tanks forward of the engines, helping to further shift the center of gravity forward. The leading edge inlet layout would also locate the engines more forward, but it negates the use of a centerbody fuel tank.

Another primary metric was the N+2 acoustic noise level goal. The partially embedded and leading edge inlet layouts would both most likely meet the goal with their use of inlet liners and acoustic shielding. The pod mounted layouts do take advantage of some acoustic shielding, but the benefits are minimal relative to the N+2 goals.

The final metric to consider in selecting the propulsion integration layout is that of a one engine inoperable (OEI) condition and its effects on the vehicle. The flying wing configurations implement split rudders as yaw control surfaces and these would most likely be sized by an OEI requirement. All considered layouts would have reasonably sized split rudders, except for the two engine version of the partially embedded layout. First, only having two engines puts this layout at a disadvantage. However, the difference between this and the pod mounted two engine version is that the pod mounted engines can be located much closer to the vehicle’s centerline, whereas in the partially embedded layout, they are located outboard of the payload cabin, creating a longer lever arm to counteract in an OEI condition. The required split rudders would be about 35-40% span to meet an OEI condition on the two engine partially embedded layout, and this is considered unfeasible.

The partially embedded layout was selected as the final layout. It provided favorable balancing characteristics and the potential to meet the N+2 acoustic noise level reduction goal. Although it

does have worse SFC and greater engine installation weights than a pod mounted configuration, the magnitude of these is small and is outweighed by the ability to meet the acoustic noise level reduction goal. The four engine version of the partially embedded layout was then selected based on its ability to feasibly meet requirements for an OEI condition.

3.6.5. Flying Wing Acoustics Considerations

Shielding was anticipated to be a significant contributor to the acoustic performance of the flying wing configuration. To provide guidance for engine placement with regard to airframe shielding of propulsion noise sources, a preliminary flying wing configuration was utilized for shielding analysis. (A more complete description of the code can be found in Section 3.9.7) The intent was to explore the trade space by varying the placement of an example fan noise component source (of representative size) and a jet exhaust component noise source (of representative thrust). Locations were varied chordwise and spanwise along the centerbody of the vehicle and in elevation above the planform in the range of 0.5 – 1.0 fan diameter.

The analysis showed that fan location should be inboard of 50% span, and aft of 70% chord for best airframe shielding. Additionally, analysis showed that the apparent source of the jet exhaust should be located inboard of 50% span and forward of 110% chord. The apparent source was located 5 jet diameters downstream of the nozzle, which yielded a nozzle location of less than 80% chord as a guideline. Because fan noise can also be attenuated effectively through means of an acoustic liner, for which it was anticipated substantial length would be available, the decision was made to trade fan chordwise location in favor of jet chordwise location.

As expected, the analysis also showed that placement above the airframe was to be minimized which favored embedded versus pylon mounted engines. Additionally, embedded engines afforded more area for inlet acoustic liner to be placed.

The resulting noise guidelines influenced the placement and design of the propulsion system for both PSC vehicles. A four engine embedded propulsion system was integrated as discussed in Section 3.6.4 and is shown in Figure 47. The engines were placed at 50% centerbody chord and 70% centerbody span. The placement of the engines at 50% chord allowed for an exhaust L/D of one with the exhaust plane forward of the 80% chord location specified above. The inlet plane was positioned forward of the 70% chord at approximately 25% chord, allowing for an inlet L/D of one. It was not feasible to position the inlet face at 70% chord but acoustic guidelines allowed for the trade of the inlet plane forward in order to meet the exhaust plane requirement. The engines were placed at 70% centerbody span which was further outboard than the shielding guidelines constrained. However, the acoustic shielding study showed that the sensitivity between span position and radiated acoustic field decreased as the height of the noise source relative to the vehicle OML. Therefore, the PSC's embedded propulsion system was less span constrained, with respect to acoustic considerations, than a pod mounted propulsion configuration. The placement of the propulsion system at 70% chord allowed for the integration of the passenger and cargo payloads while reducing centerbody planform area. The inlet and exhaust L/D equal to one (1) allowed for inlet and exhaust lengths of eight feet and significant noise reduction potential from inlet acoustic liners. In addition, four (4) engine configurations compare favorably to two (2) by reducing engine scale; generating higher blade passage tones and more effective inlet liners.

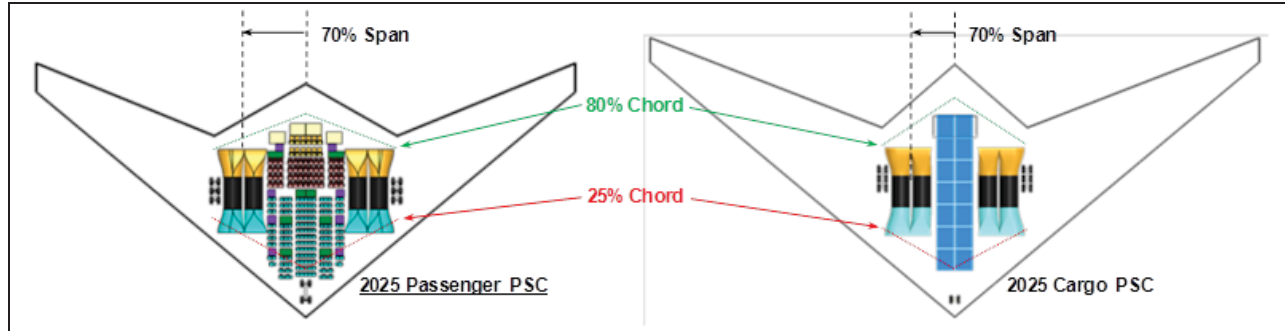


Figure 47 Flying Wing Configuration with Acoustics Considerations

3.6.6. Flying Wing Payload Integration

As mentioned in Section 3.4, the PSC passenger vehicle is required to carry a 50,000 lb payload which is comprised of 224 passengers with baggage arranged in a three-class configuration. Passengers are assumed to weigh 175 lb and their baggage to weigh 48.2 lb, satisfying the 50,000 lb payload requirement. Passenger class distribution and seat pitch is based on historical trends of vehicles of similar size and range and are shown in Table 7. Other internal arrangement requirements including galley and lavatory size and number are also based on historical trends of vehicles of similar size and range. Coat closets are not included as they do not have a significant impact on the internal arrangement or size of the vehicle.

Class	Composition (%)	Seat Pitch (in)
First	5.33	61
Business	23.11	39
Economy	71.56	32

Table 7 Passenger Class Distribution and Seat Pitch

Multiple internal arrangements were examined for various cabin sizes to determine the most optimum packaging in order to reduce centerbody size and weight. Additionally, different seat designs were examined in an effort to reduce cabin height. The aisle height on a conventional airplane seat with overhead baggage is constrained by overhead baggage container. Based on historical configurations, the minimum aisle height required to integrate an overhead baggage compartment is approximately 81 inches. The configuration shown in Figure 48 illustrates integrating the overhead baggage compartment next to the passenger instead of overhead. This constrains the aisle height to approximately 74 inches which is the height of a 95th percentile male. Additional cargo containers are required in addition to the overhead/integrated baggage containers in the event that the passenger baggage does not fit into the overhead/personal containers. LD-3 containers are used as the cargo containers on the vehicle due to being extremely common in the airline industry and integrating well into the vehicle. A LD-3 container has an internal volume of 153 cubic feet with a maximum gross weight of 3,500 lb. The PSC passenger vehicle has 4 LD-3 containers which are able to carry the passenger baggage weight and volume. In addition to cargo containers, multiple emergency exits and locations were examined in order to meet FAR requirements. Emergency exits must be placed to allow passenger and crew evacuation in the event of a crash landing with and without landing gear deployed. Far 25 requirements state that “if it is impractical to locate a side exit above the waterline, the side exits must be replaced by an equal number of readily accessible overhead

hatches of not less than the dimensions of a Type III exit". It is impractical to have side exits on the PSC passenger vehicle due to the location of the passenger cabin within the centerbody and with respect to the integrated propulsion system. Type I exits are used as a replacement for side exits. Type I exits, 48 in x 24 in, are larger than Type III exits, 36 in x 20 in, and can evacuate up to 45 passengers. Emergency exits were placed evenly throughout the cabin in order to allow evacuation of the vehicle in the fastest time possible.

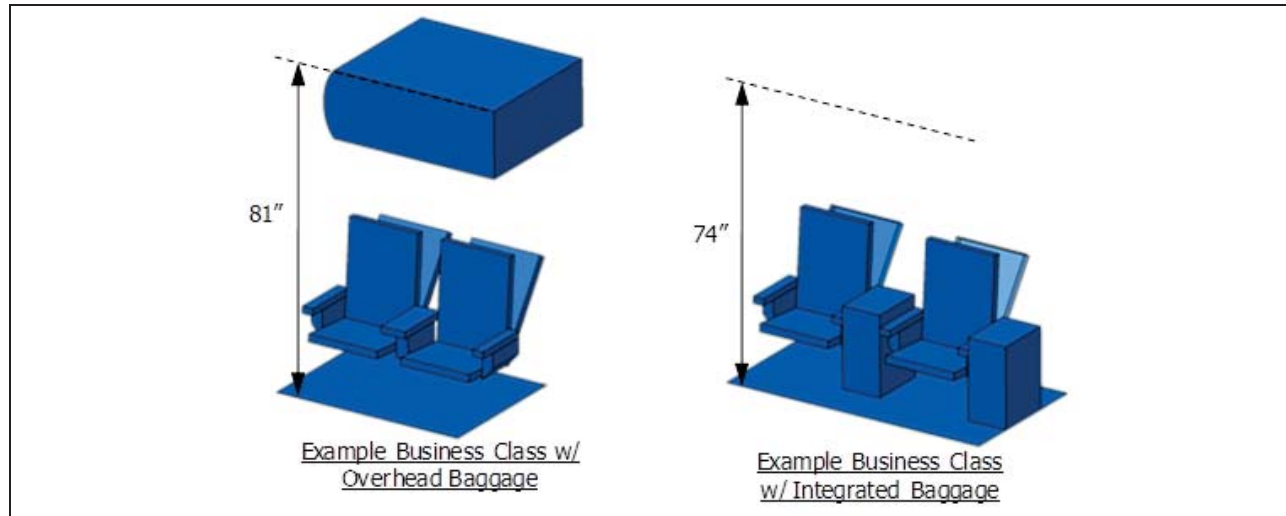


Figure 48 Example of Integrated Passenger Baggage

The internal arrangement of the PSC passenger vehicle is shown in Figure 49. The economy seats are located in the forward compartment of the cabin. The forward placement is constrained by the nose landing gear integration. Ten of the economy class seats utilize the integrated baggage seat configuration due to aisle height constraints. The business seats are located mid-cabin with the first class seats located in the aft cabin. Cargo is located aft of the first class seats. There are five telescoping and actuated loading ramps that have a maximum ramp angle of 15 degrees, which is a similar maximum ramp angle found on military cargo vehicles. Three of these ramps are used for cargo loading while the other two are used for passenger loading. Emergency exits are located in six locations throughout the cabin. Each location has a Type I exit located on the ceiling and floor to provide an exit in the event of a gear up and a gear down emergency exit.

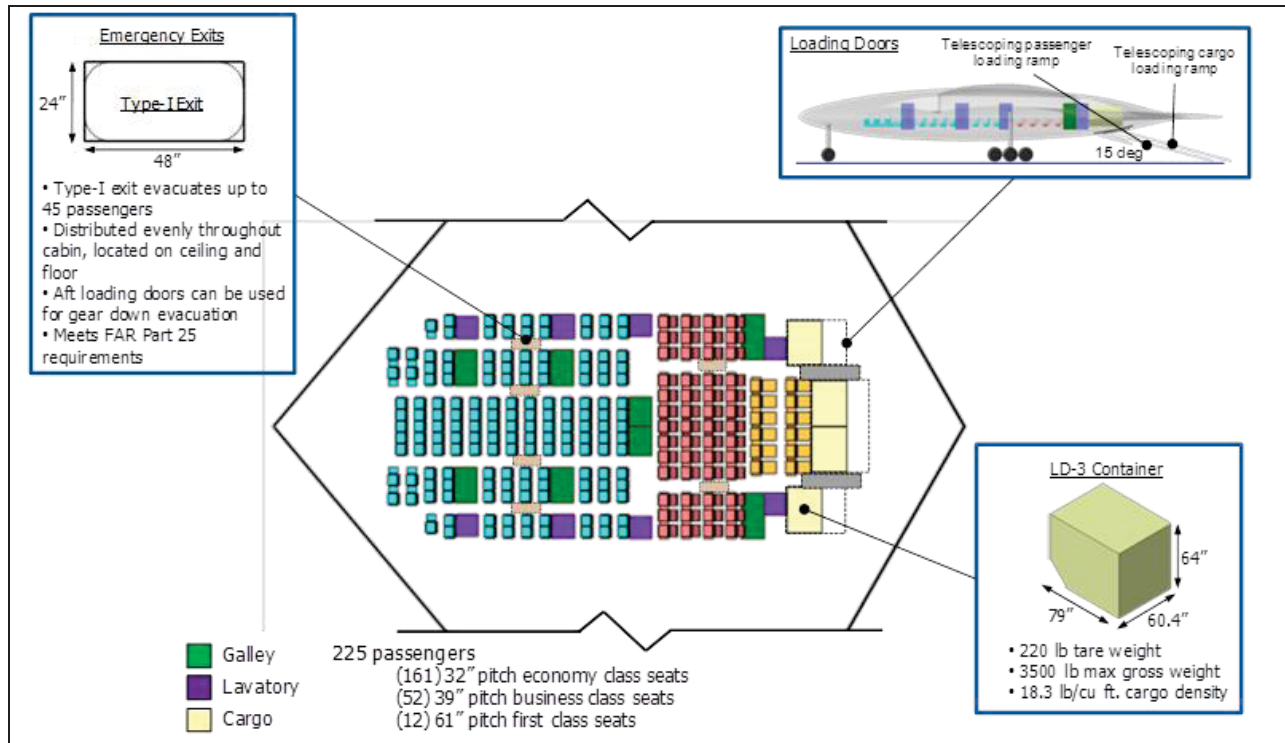


Figure 49 Flying Wing Passenger Internal Arrangement

The PSC cargo vehicle is required to carry a 100,000 lb payload. Multiple cargo containers were examined including various LD containers and military pallets. The 463L pallet was selected as the preferred cargo container due to improved integration and commonality on cargo vehicles. The full height 463L pallet has a maximum weight of 3.5 metric tons and is 88 in x 108 in x 96 in. The 50% height 463L pallet has a maximum weight of 1.75 metric tons and is 88 in x 108 in x 67 in and can be placed on the cargo loading ramp door when the door is closed.

As shown in Figure 50, the PSC cargo vehicle utilizes twelve full height 463L pallets and two 50% height 463L pallets which yield a maximum payload capacity of 105,000 lb, meeting the payload weight requirement. This arrangement minimizes cargo track weight by having two rows of pallets. Cargo track weight increases as the number of pallet rows increases. The pallets are spaced 6 inches apart and a 20 inch aisle is placed on each outboard side of the cargo which defines the outboard limits of the inner mold line. There is one telescoping and actuated loading ramp that has a maximum ramp angle of 15 degrees, which is a similar maximum ramp angle found on military cargo vehicles. The forward location of the pallets is limited by the integration of the nose landing gear.

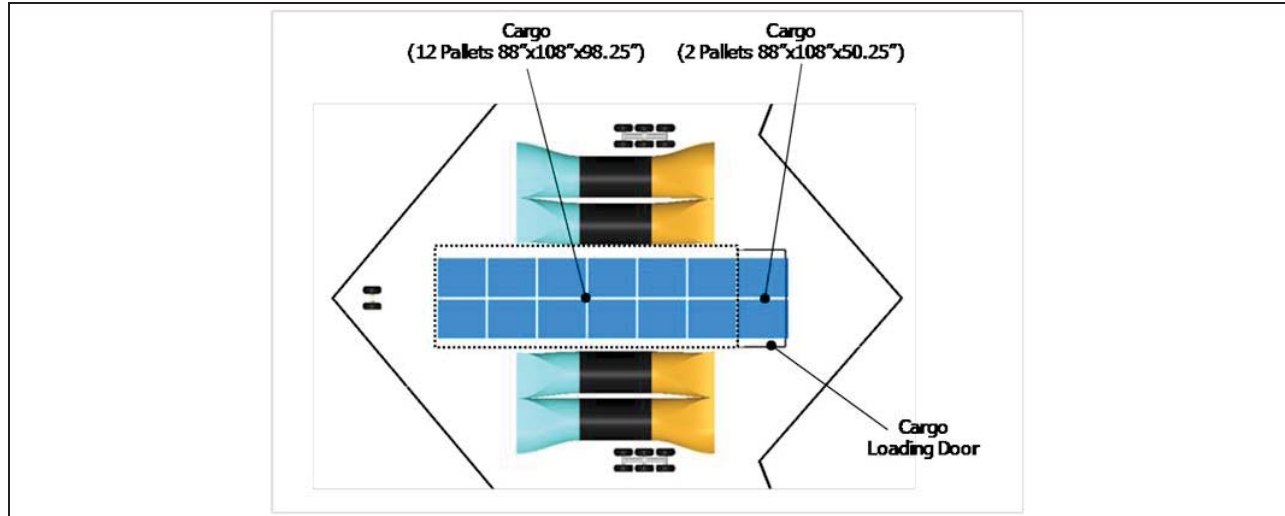


Figure 50 Flying Wing Passenger Internal Arrangement

3.6.7. Multibody Configuration

The final multibody configuration design is shown in Figure 51 below. It is characterized by two fuselage bodies and a low wing mounting. The two engines are of a pod-mounted configuration and are located above the upper surface of the center portion of the wing. The empennage is similar to a conventional tail with both horizontal tails located on the outboard sides of the two fuselage bodies. A summary of the 2025 multibody vehicles' geometry and performance parameters is shown in Table 8.



Figure 51 2025 Multibody Vehicle Configuration

The 2025 multibody vehicles were not selected as the PSC vehicles because they did not perform as well as the 2025 flying wing vehicles. Although they provided some of the expected acoustic noise level improvements over the 2025 Baseline vehicles, they did not provide the expected reductions in fuel burn. The benefits of span loading, payload packing efficiency, and wetted area reduction were not found to be as significant as expected. More detailed design work may be required to fully realize the benefits of the multibody concept. However, only marginal gains over the Baseline vehicles can be expected, unlike the flying wing concept.

Parameter	Multibody Passenger	Multibody Cargo
Wing Reference Area	3880 Ft ²	3880 Ft ²
Wing Span	205 Ft	205 Ft
LE Sweep	35	35
Wing Aspect Ratio	10.83	10.83
Taper Ratio	0.3	0.3
MTOW	461,150 lb	502,465 lb
OEW	233,275 lb	243,460 lb
Payload	50,000 lb	100,000 lb
Propulsion	RR PD-685N	RR PD-685N
SLS Max Thrust/Engine	71,235 lb	79,942 lb
Number of Engines	2	2
Installed Cruise SFC	0.489	0.489
Cruise Mach	0.82	0.82
Balanced Field Length	10,500 ft	10,500 ft
Mission Fuel Burn	162,205 lb	150,500 lb

Table 8 2025 Multibody Vehicles Geometry and Performance Summary

3.6.8. Multibody Configuration Design and Layout

The initial multibody design space was to determine possible benefits and/or disadvantages of this unique configuration. The multibody configuration is somewhere in between a full flying wing “span loader” and a standard wing, body and tail (WBT) configuration. Two design drivers surfaced – acoustic benefits with this configuration and possible structural weight savings due to discreet span loading of the fuselages. Placement of the key aircraft components such as wing, nacelles and empennage were driven by acoustic noise reduction balanced by mass properties and stability and control.

At first many different concepts were considered with regards to wing, nacelle and empennage surface placement both conventional and not. Some examples of these are shown in Figure 52 along with a table summarizing the configuration selection process. The initial offering was a high wing with below wing center mounted engines and cockpit and independent empennage V-tail surfaces. The center cockpit was abandoned early due to limited access and service.

After this many different combinations of both high and low wing and nacelle locations were evaluated. The high wing with engines below was reasonable for service with possible low clearance fuselages for cargo loading. With the high wing, however, the wing carry through structure penetrated too much of the cabin ceiling area, whereas with a low wing the spar carry through structure passed below the passenger floor and through the lower cargo hold area reducing the diameter of the fuselage pressure vessel. Also, the frontal drag area was less with the low wing. So, unless there was some particular mission that required a high wing it was ruled out.

The quadricycle, or quad, landing gear early on was a concern with a possible low approach angle of attack similar to the B-52 gear, but the design and placement of the quad gear was deemed similar to any airliners landing gear placement on take-off or landing.

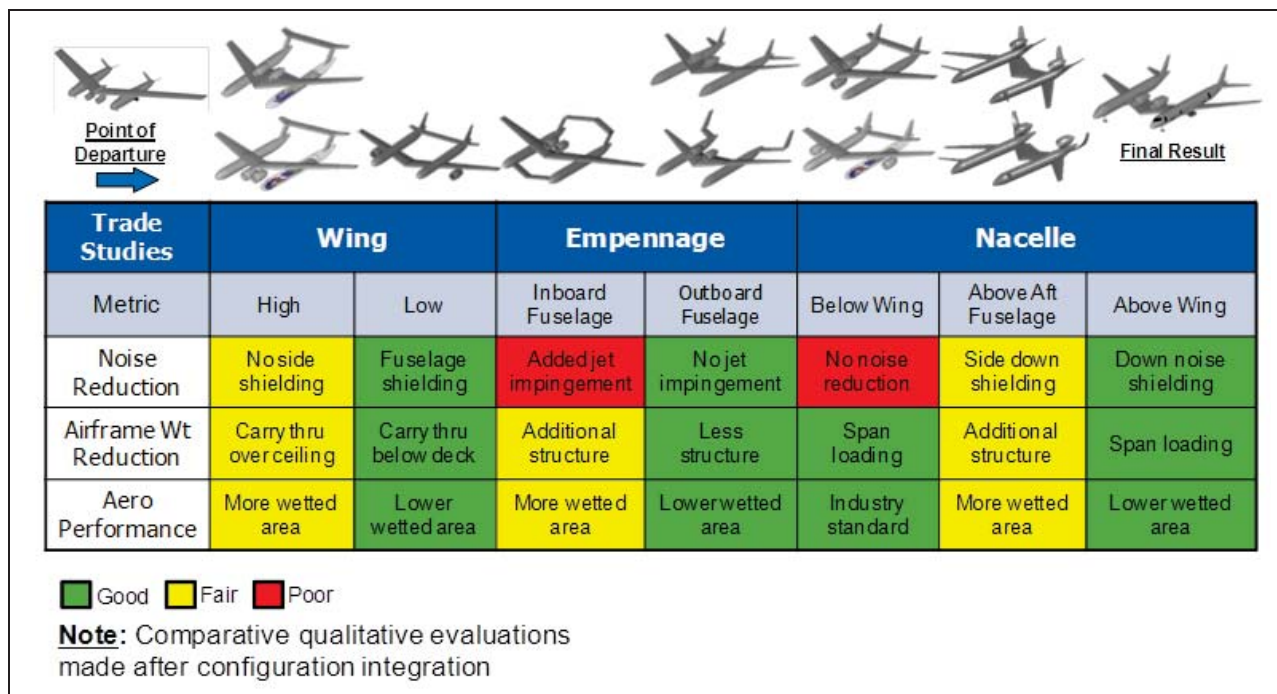


Figure 52 Multibody Configuration Design Trades

In an effort to simplify the quad landing gear into a standard tricycle gear with only one nose gear a three wing concept was evaluated, but again ruled out because of substantial drag and the structural weight required for the forward wing air and ground loads.

With the initial design space open, nearly every empennage configuration was looked at for both high and low wing placement. The challenge was placing the horizontal stabilizer out of the engine exhaust and not being blanketed out by the wing in vertical placement. All the Boeing and Airbus models were benchmarked for tail volume coefficients, wing area, sweep and loading. Simple, but conservative tail volume coefficients were used to size the empennage surfaces from industry references and the transport benchmark data.

What drove the empennage location was a required clearance of engine exhaust plume area aft of the nacelle for acoustic noise considerations. This jet plume impingement “stay out” zone required elimination of any empennage surfaces inboard of the twin fuselages favored a low wing as well.

With further acoustic noise reduction qualitative review, exhaust down and side noise and forward inlet noise from the engines necessitated nacelles on top of the wing, and in between the twin fuselages. Before this nacelles were placed inboard and outboard of the fuselages for span load wing bending reduction, service and torsional wing bending reduction. Nacelle locations outboard of the fuselages and below the wing favored lower wing bending and service, but offered no noise reduction potential. More non-conventional configurations were considered with engine nacelles mounted aft on the fuselages shielded with “bow” and straight V-tail empennage surfaces and forward swept wings outboard of the fuselage. These configurations

even though “futuristic” in style proved complicated in structure, mass balance, stability and control and did not fully address the noise reduction possible with nacelles located correctly on top of a long chord wing center section.

3.6.9. Multibody Propulsion Integration and Acoustic Considerations

As the aero-configuration design progressed the acoustic design started to affect the configuration. The jet engine exhaust plume generates an impingement volume aft of the nacelle about 14 degrees, creating a stay out guideline area. This stay out guideline was used so no airframe surfaces were allowed in these areas. To further protect from down noise and side noise the turbo fan nacelles using the PD685N engines were positioned longitudinally so the exhaust point of the engine fell at 80 percent chord in the wing center section as shown. The engine fan location at 70% of chord due to engine geometry did not align in this area. These acoustic considerations included in the configuration design are shown in Figure 53.

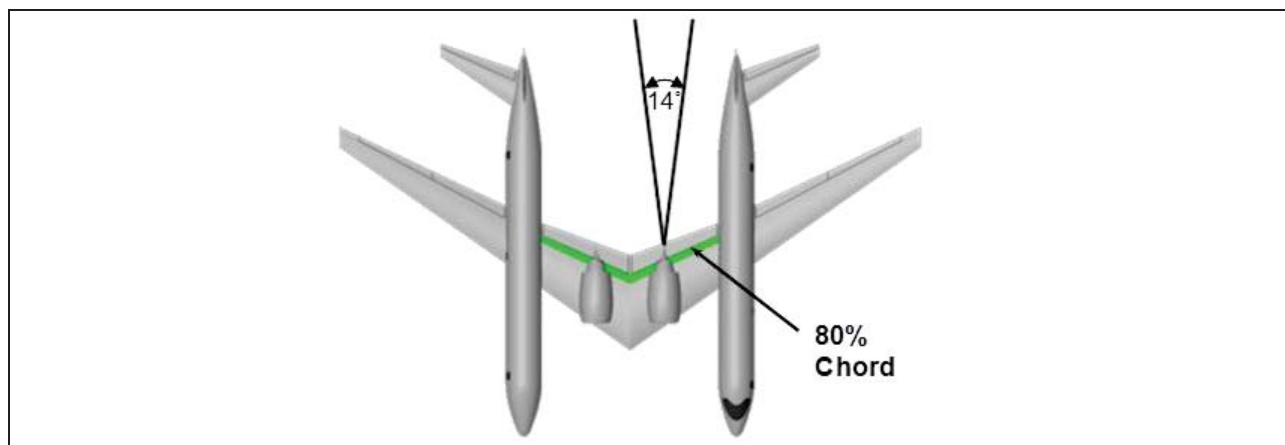


Figure 53 Multibody Acoustic Considerations

3.6.10. Multibody Payload Integration

The payload integration for the multibody vehicles was similar to that of a conventional wing-body-tail configuration, however, the multibody configuration’s twin fuselage sections provides more freedom and more options to optimally package a given payload. In performing the payload integration trade studies, the fuselage finesse ratio was optimized to minimize drag as well as weight. The passenger and cargo versions of the multibody vehicles with interior layouts are shown in Figure 54.



Figure 54 Multibody Passenger and Cargo Payload Cabins

The seats abreast for each cabin class for the passenger version are shown in Figure 55. The interior arrangement for the passenger version is shown in Figure 56. The cabin class mixes in each of the two fuselage sections was traded to find the optimal layout for packing the given payload while minimizing weight and fineness ratio.

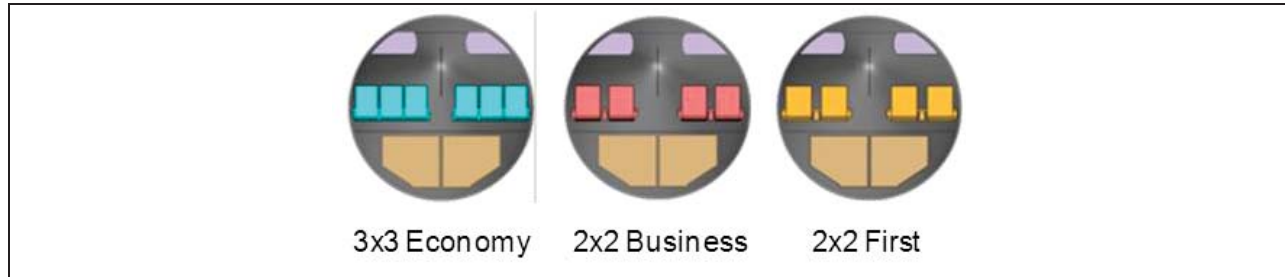


Figure 55 Multibody Passenger Cross Section Views

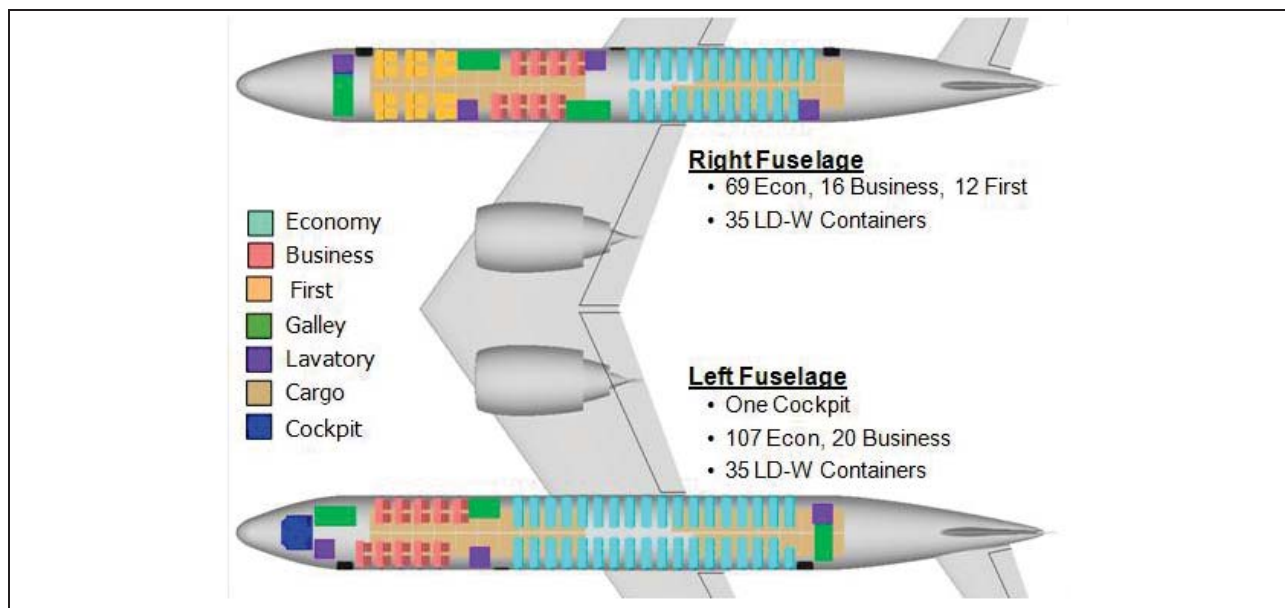


Figure 56 Multibody Passenger Interior Arrangement

The cargo version cross section is shown in Figure 57 along with an payload arrangement. A combination of LD-8 and LD-W containers was chosen to efficiently package the required payload.

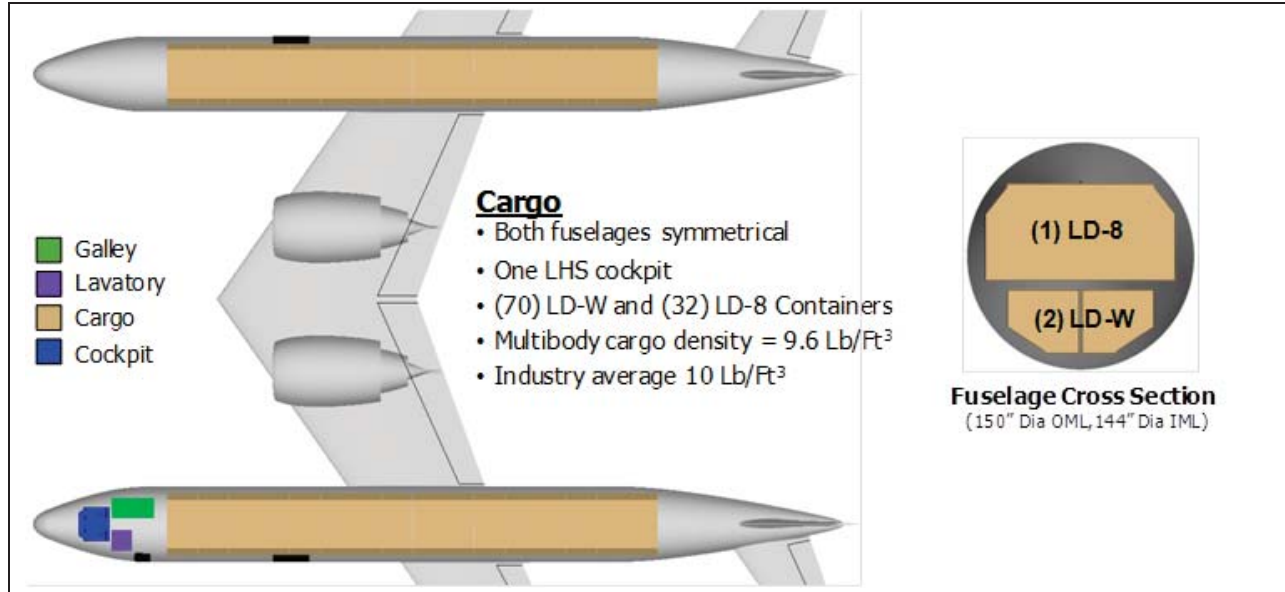


Figure 57 Multibody Cargo Cross Section and Interior Arrangement

3.7. Propulsion System Design

The next step in the vehicle design process is the propulsion system design. For each of the three given sets of Task 2 vehicles, an engine architecture was established. There were a total of three engine cycles designed – one each for the 1998 Reference, 2025 Baseline, and 2025 PSC vehicles. The wing-body-tail configurations consist of podded nacelle installations, whereas the PSC vehicles consist of partially buried engines. Based on the propulsion installation design, requirements were developed that included thrust, horsepower extraction, compressor bleed, inlet pressure recovery, and exhaust C_{fg} performance. These installation requirements are shown in Figure 58, Figure 59, and Figure 60 for each of the three sets of vehicles. Vehicle level sensitivities were also developed for each set of vehicles. These propulsion system requirements and vehicle level sensitivities were utilized to optimization and development of each engine cycle design.

- Engine technology consistent with 1998 baseline
- Two (2) engine podded installation
- Inlet Pressure Recovery: Provided by engine company
- Nozzle Performance: Provided by engine company
- Horsepower Extraction: 190 hp per engine
- Compressor Bleed: 2 pps per engine
- Trent 892 thrust class

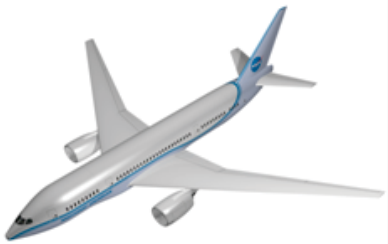


Figure 58 1998 Reference Vehicles Propulsion Installation Requirements

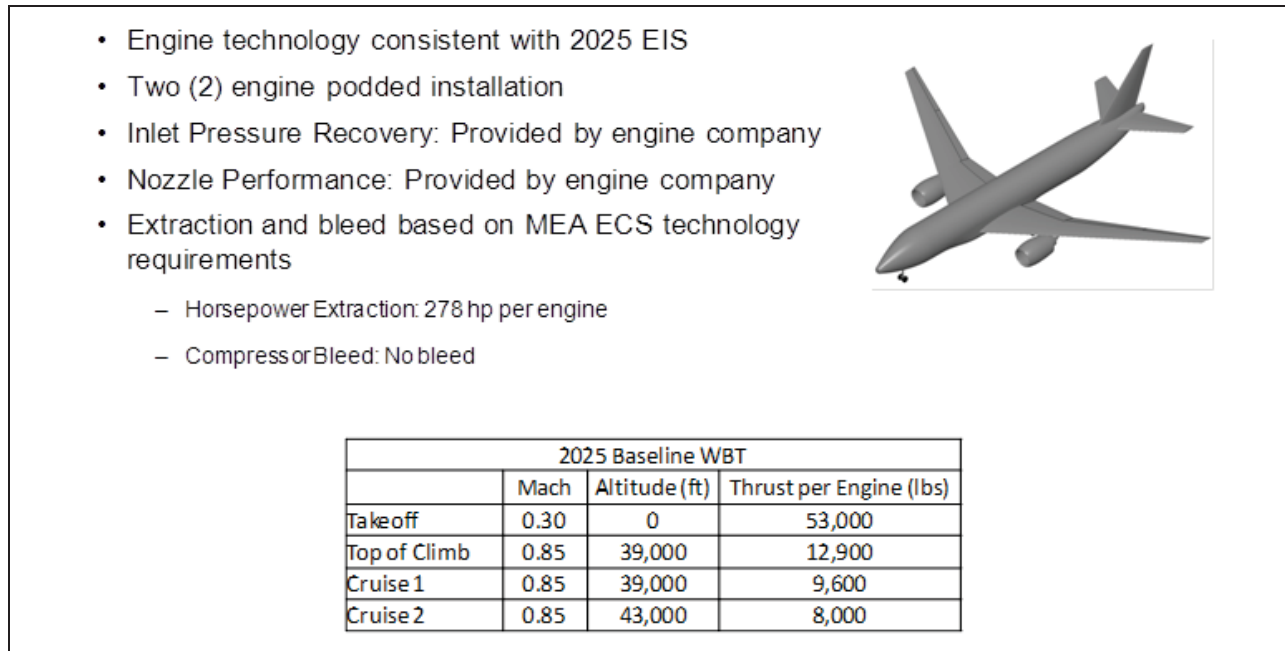


Figure 59 2025 Baseline Vehicles Propulsion Installation Requirements

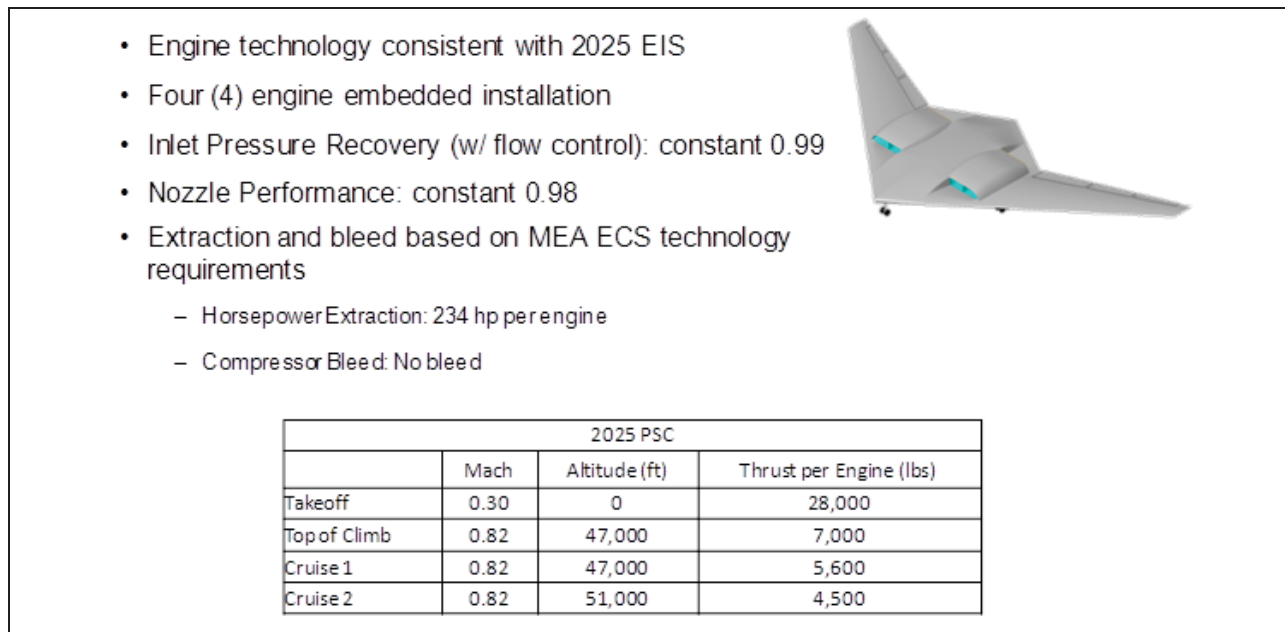


Figure 60 2025 PSC Vehicles Propulsion Installation Requirements

3.7.1. Propulsion System Design Process

The engine cycle optimization process utilized is shown in Figure 61 and was used to develop the 2025 PSC engine cycle. This process is based on using parametric models, statistical modeling, and optimization methods to rapidly model and explore the engine design space. The seven specific steps within the process are outlined in Figure 61. Realistic designs are produced by beginning the modeling with a well understood baseline and then integrating individual technologies. For this program, the applied technologies fall into two categories – company

proprietary technologies that are already being studied for 2025 EIS engines, and technologies selected primarily to meet the ERA goals.

In the modeling and simulation step, a parametric or “rubber” engine model is developed to that meets the propulsion installation requirements such as the thrust and power extractions. Parametric models for mechanical, aerodynamic, and thermodynamic effects are included in the modeling and simulation step. These parametric models are summarized in Figure 62. These models account for real world design constraints, such as minimum compressor blade height, maximum turbine speed, and turbomachinery stage loading.

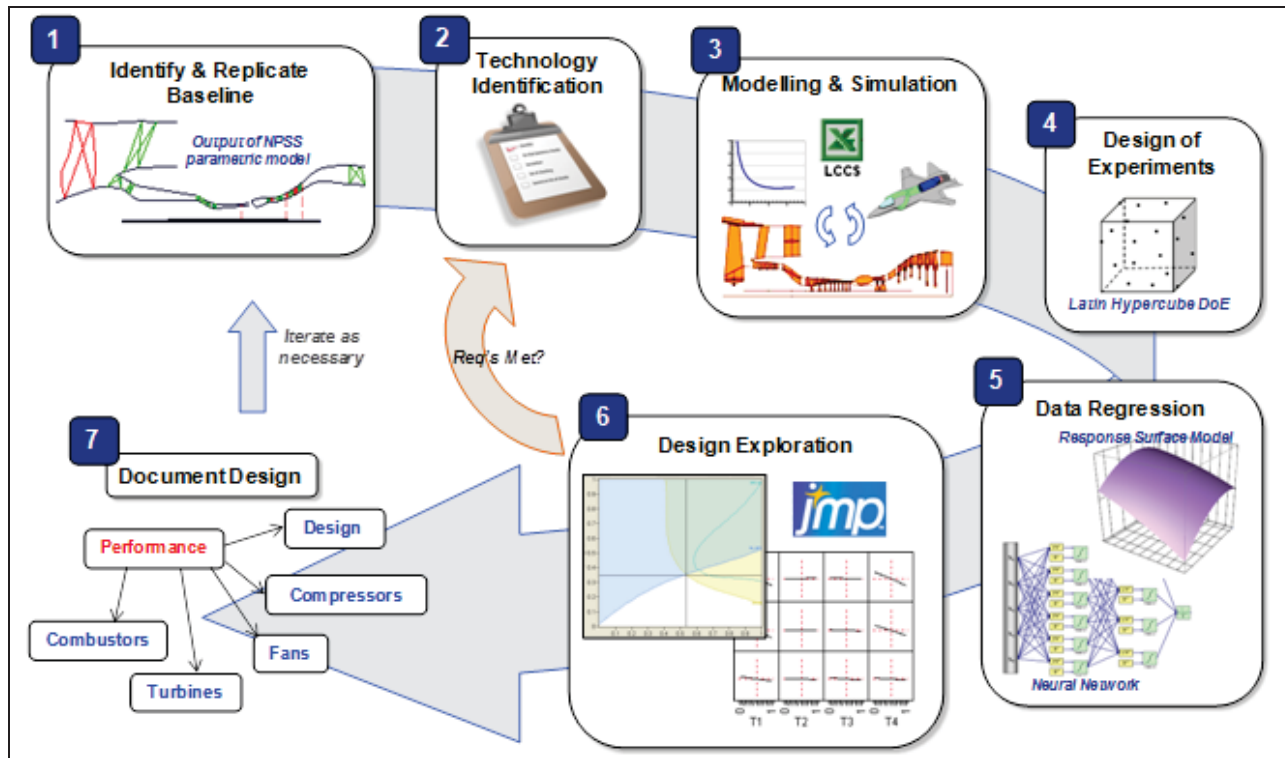


Figure 61 Engine Cycle Optimization Process

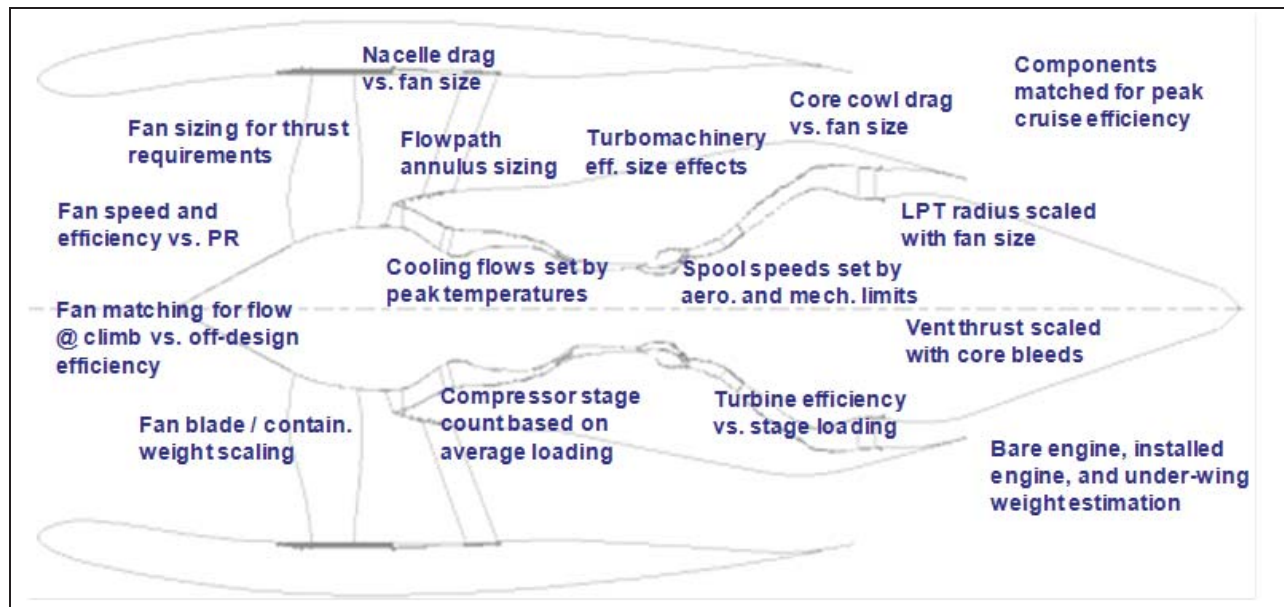


Figure 62 Parametric models included in Modeling & Simulation

A design of experiments study (DOE) is conducted where independent parameters (e.g. FPR, OPR, HP/IP work split, max T41, etc.) are varied within the engine design space. A regression model of the design space can then be created. These can be combined with models for weight, drag, and SFC, and can be used in conjunction with vehicle level sensitivities to estimate the engine design's impact on vehicle empty weight and fuel burn. The optimization process then involves minimizing the vehicle fuel burn, based on the available sensitivities, while constraining the engine design for emissions, noise, and mechanical limits.

3.7.2. 1998 EIS Reference Vehicles Engine Design

The 1998 Reference engine model is based on a combination of Trent 892 and Trent 895 engines. The Trent 892 was chosen as a basis for the 1998 Reference engine model because it had an EIS date of 1996. The Trent 895 uses the same technologies as the Trent 892, and differs only in thrust rating. A non-proprietary and representative engine model (PD684N) was generated and installed in a nominal podded installation. This was done by starting with an existing 3-shaft large turbofan model, creating a generic reference installation, aligning component efficiencies and cycle parameters, applying fuel flow scalars, and resizing the engine for specified bleed and power offtakes.

3.7.3. 2025 EIS Baseline Vehicles and Multibody Vehicles Engine Design

This 2025 Baseline engine was initially envisioned to be a scaled version of the 2025 PSC engine. However, due to differences in installation from a buried to a podded installation, a simple scaling wouldn't result in an optimum baseline engine. As a result, the 2025 Baseline engine was based off of existing 2025 podded engine models, and then resized using the requirements and sensitivities for the 2025 Baseline vehicles. This engine used podded installation requirements (ex. thrust and power extraction) and is shown in Figure 63. This engine model was used on the 2025 Baseline and the 2025 Multibody vehicles.

A sample of the optimization studies conducted is shown in Figure 64. The engine core size was driven by OPR and maxT41. High values of both are favorable for fuel burn, as they drive down

SFC and weight. For this engine, the core size has been limited by the HP compressor minimum blade height. The fan size is driven by the FPR and unmixed jet velocity ratio. The fan size is close to optimum for fuel burn, but a slightly larger fan could provide additional benefit. As this cycle was not optimized specifically for the 2025 Baseline vehicles, as mentioned above, the engine is 3% short of the emissions goal, but does provide about a 17% SFC improvement over the 1998 Reference engine.

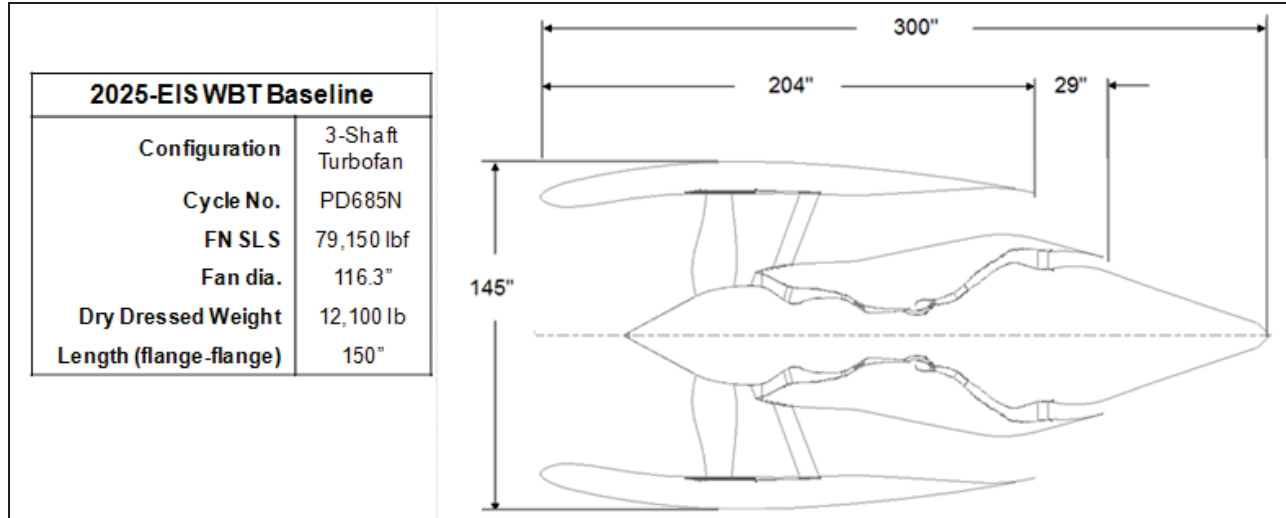


Figure 63 2025 Baseline Engine Overview

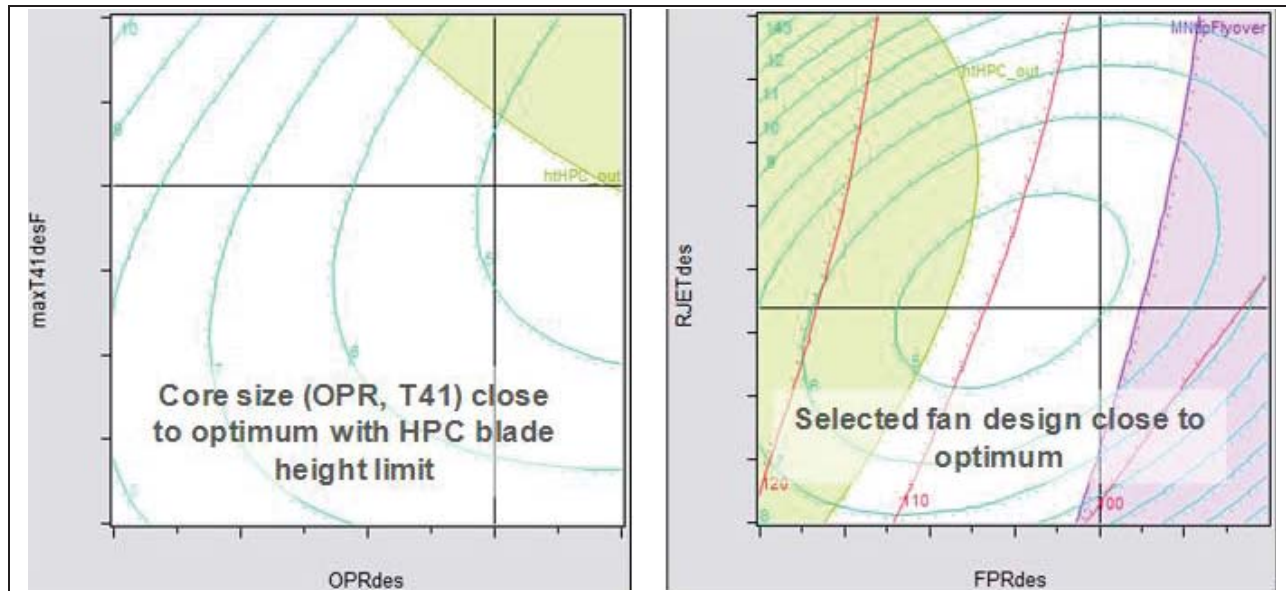


Figure 64 2025 Baseline Engine Optimization

Technologies were applied to the 2025 Baseline engine, based on existing Rolls-Royce programs that are funded outside of the ERA Program. These technologies generally focus on increasing core temperatures without increasing cooling, and increasing bypass ratio to reduce noise and SFC while also reducing weight.

3.7.4. 2025 EIS Flying Wing Vehicles Engine Design

The 2025 EIS engine (PD700) for the PSC vehicles is a large 3-shaft turbofan installed in a partially buried configuration. The PD700 engine cycle was developed and fully optimized for the 2025 PSC vehicles, based on requirements and sensitivities. This engine was designed with a mixed flow exhaust to take thermodynamic advantage of the buried installation. The engine is slightly smaller than the 2025 Baseline engine, due to the slightly lower thrust requirements of the 4-engine configuration.

The optimization results for the 2025 PSC engine design are shown in Figure 65. The PSC engine core size has been optimized for vehicle fuel burn, while constraining HP compressor blade height and LTO NO_x. The NO_x margin from the ERA goal is much higher than those of the 2025 Baseline engine because the PSC thrust requirements lead to a cycle with peak burner temperatures at climb. At takeoff, the engine is running at much lower temperatures where NO_x production is significantly lower. The fan size has been optimized based on the PSC vehicle sensitivities of SFC and empty weight to fuel burn. This results in a cycle with a higher SFC than the 2025 Baseline engine, but any fan size changes to improve SFC would result in a larger diameter and higher weight, ultimately leading to a higher mission fuel burn.

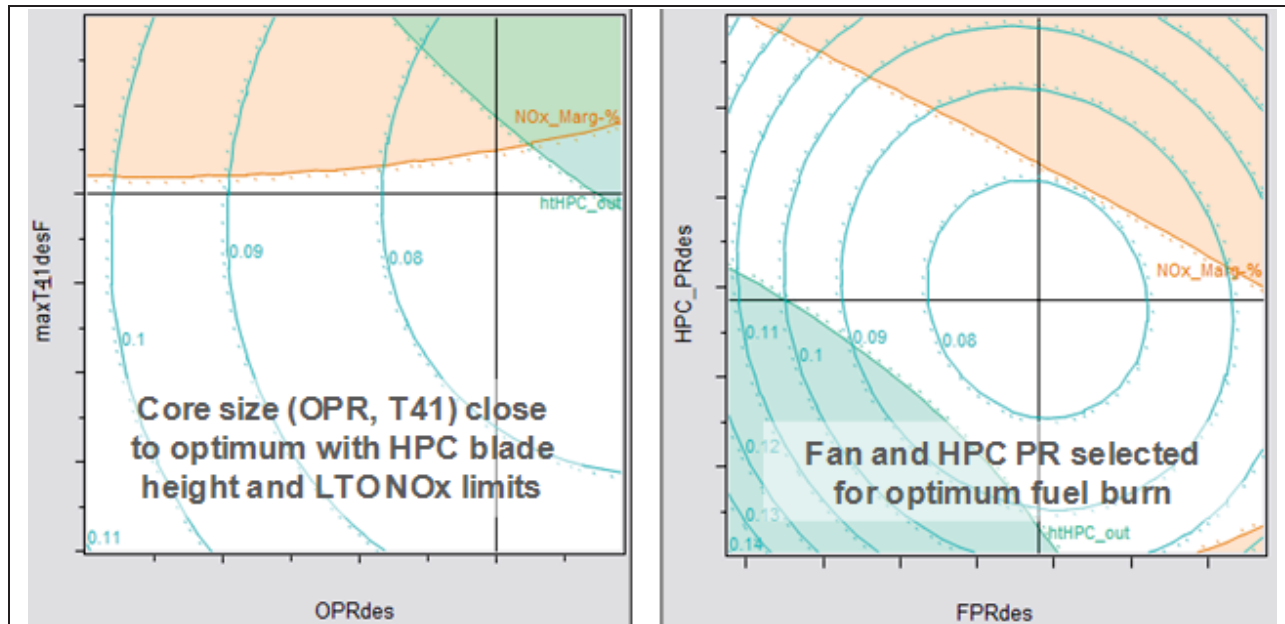


Figure 65 2025 PSC Engine Optimization

Figure 66 summarizes the technologies applied to the 2025 PSC engine. Similar to the 2025 Baseline engine, these include some technologies that are based on existing Rolls-Royce programs that are funded outside of the ERA Program, but certain ERA specific technologies critical to the PSC’s performance are also incorporated.

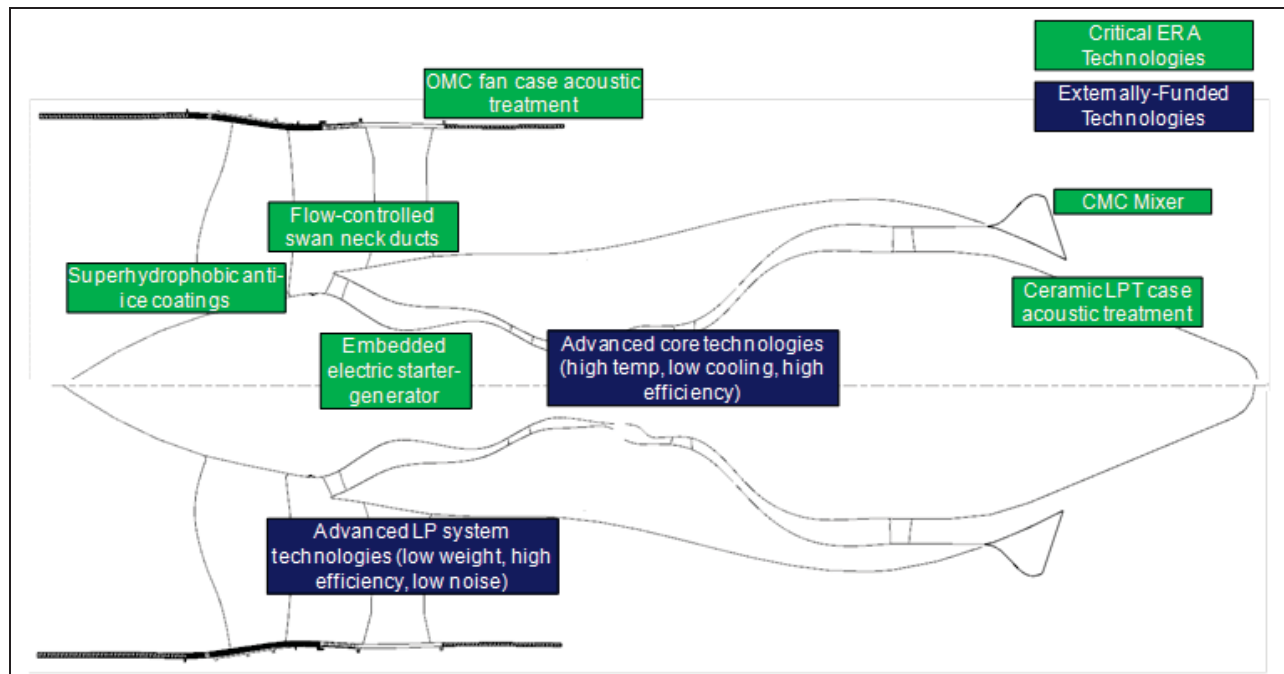


Figure 66 2025 PSC Engine Technologies

3.8. Vehicle Sizing and Results

The final step in the vehicle design process is to size and optimize the established configurations with technologies applied and integrated propulsion systems to meet the mission requirements. This section describes the sizing of the final six Task 2 vehicles as well as the multibody study vehicles. The final sized designs are then analyzed to compute their acoustic noise levels. Although the acoustic analysis is performed as an open loop process, acoustics considerations are applied in the configuration layout and design step of the vehicle design process as described throughout Section 3.6.

3.8.1. 1998 EIS Reference Vehicles Sizing

The 1998 Reference vehicles are laid out in a conventional configuration as described in Section 3.6.1. The fuselage dimensions were defined by packaging the interior arrangements required to meet the payload requirements of the mission. The components sized and optimized included the wing planform and the engine thrust scale. The empennage was sized for each design iteration using empirical tail volume trends.

Parametric studies were conducted to scope an optimal aspect ratio and leading edge sweep for these vehicles. A sample of these studies is shown for the passenger version of the 1998 Reference vehicles in Figure 67 and Figure 68. The aspect ratio study indicated optimal aspect ratios to minimize fuel burn were between approximately 11 and 12. In optimizing the aspect ratio of the wing planform, the previously discussed 205 ft wing span constraint was imposed. The optimal leading edge sweep was found to be at 33 degrees.

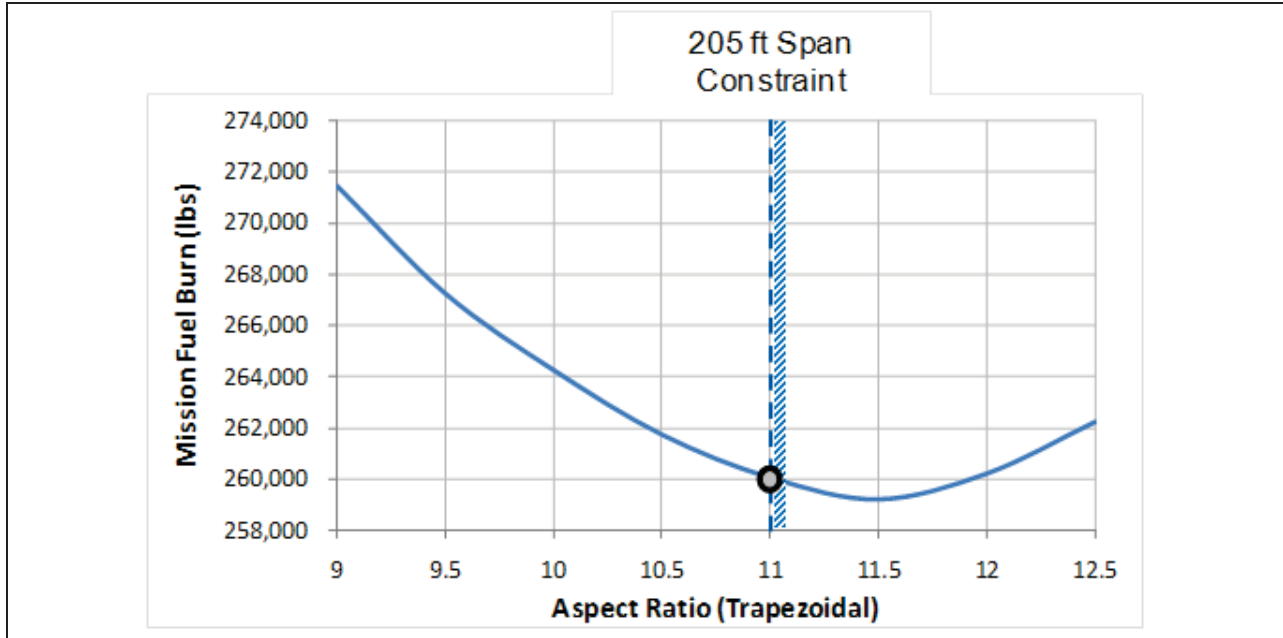


Figure 67 Wing Aspect Ratio Study for 1998 Reference Vehicles

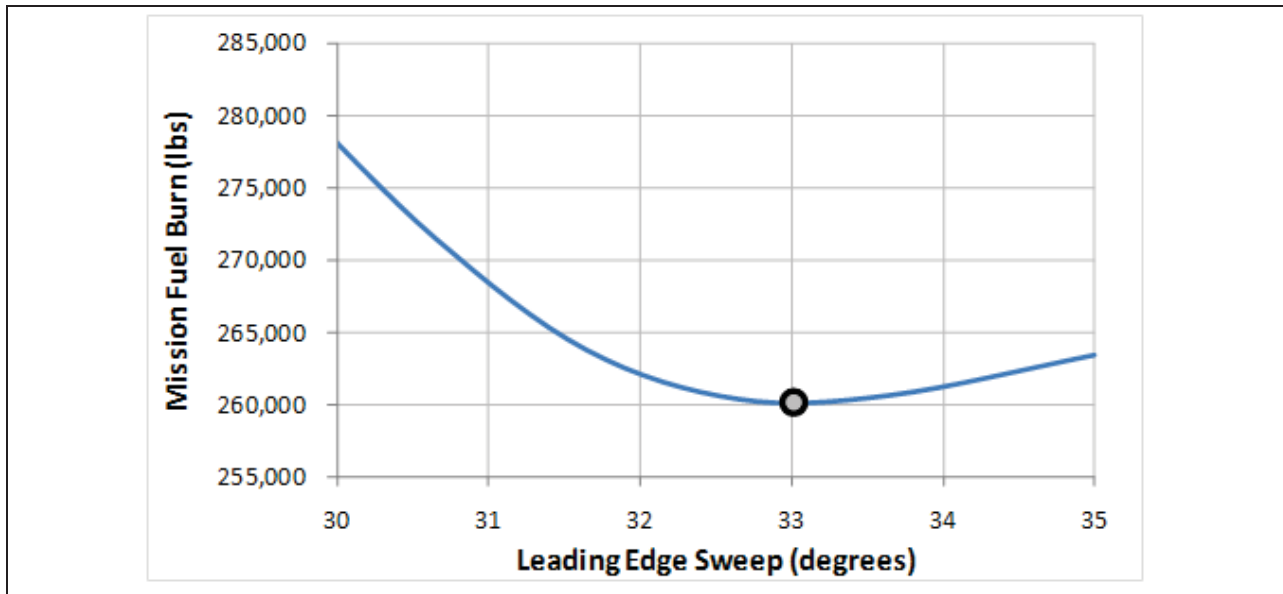


Figure 68 Wing Leading Edge Sweep Study for 1998 Reference Vehicles

The wing reference area and engine scale have the greatest effects on the geometry and performance of the vehicle. Both parameters effect parameters such as MTOW, OEW, fuel volume, balanced field length, range, and mission fuel burn. The coupled effects of wing area and engine scale on balanced field length are particularly important. To examine these effects, wing reference area and engine scale were traded in carpet plot studies for the 1998 Reference vehicles. The results of these studies are shown in Figure 69 and Figure 70 for the passenger and cargo versions, respectively.

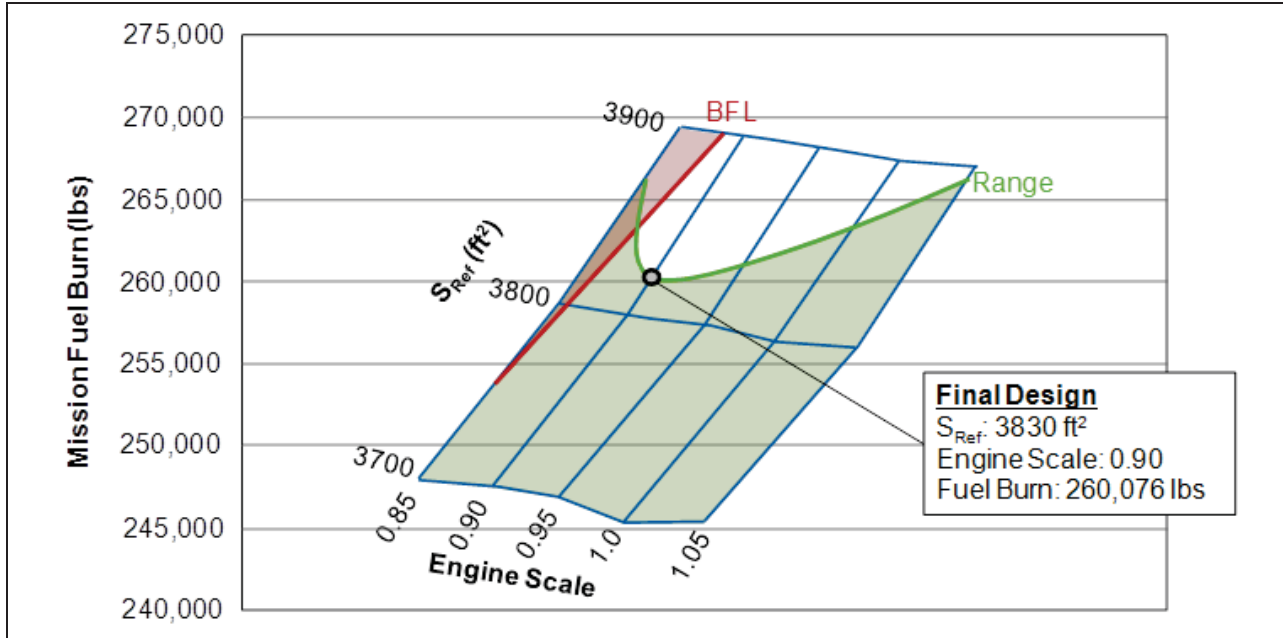


Figure 69 Wing Area and Engine Scale Carpet Plot Study for 1998 Reference Passenger

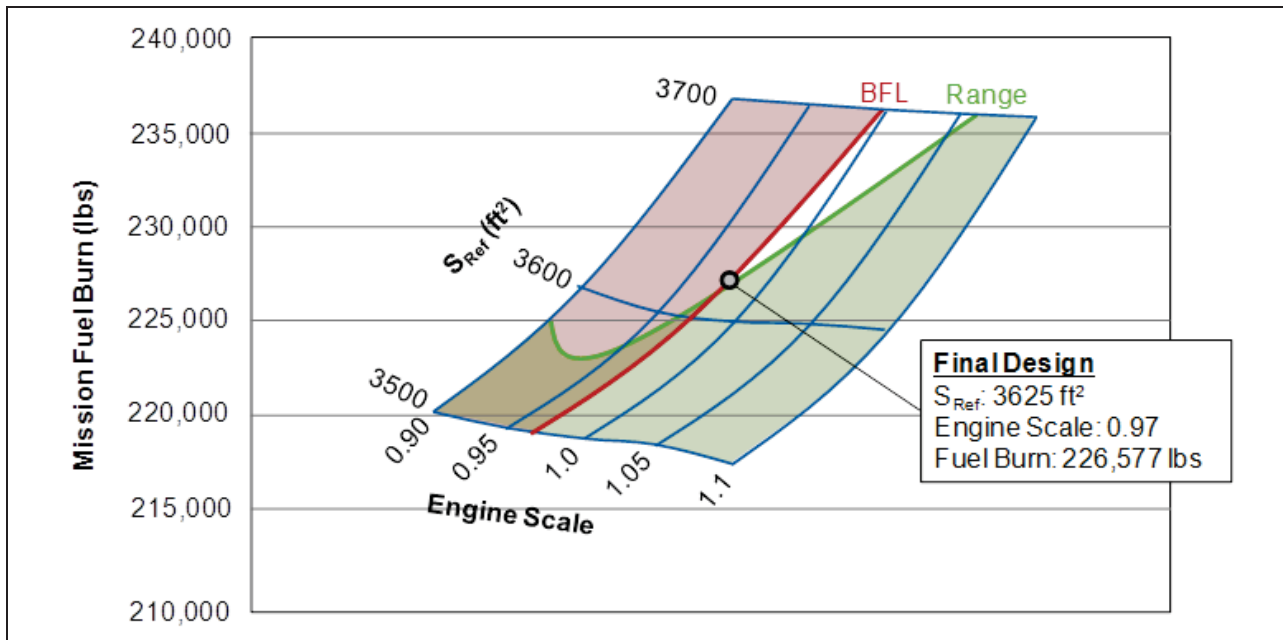


Figure 70 Wing Area and Engine Scale Carpet Plot Study for 1998 Reference Cargo

The carpet plot studies showed that the passenger version’s engine scale and wing area are sized to minimize mission fuel burn and the vehicle is not constrained by balanced field length, although just barely. The cargo version is also sized to minimize mission fuel burn; however it is sized by balanced field length.

3.8.2. 2025 EIS Baseline Vehicles Sizing

The 2025 Baseline vehicles were configured similar to the 1998 Reference vehicles, as was discussed in Section 3.6.2. The fuselage and empennage were sized in the same manner as on the 1998 Reference vehicles. Wing aspect ratio and leading edge sweep studies were conducted

and a sample of the results of these is shown in Figure 71 and Figure 72. In the case of the 2025 Baseline vehicles, the wing span constraint is 260 ft, as discussed previously.

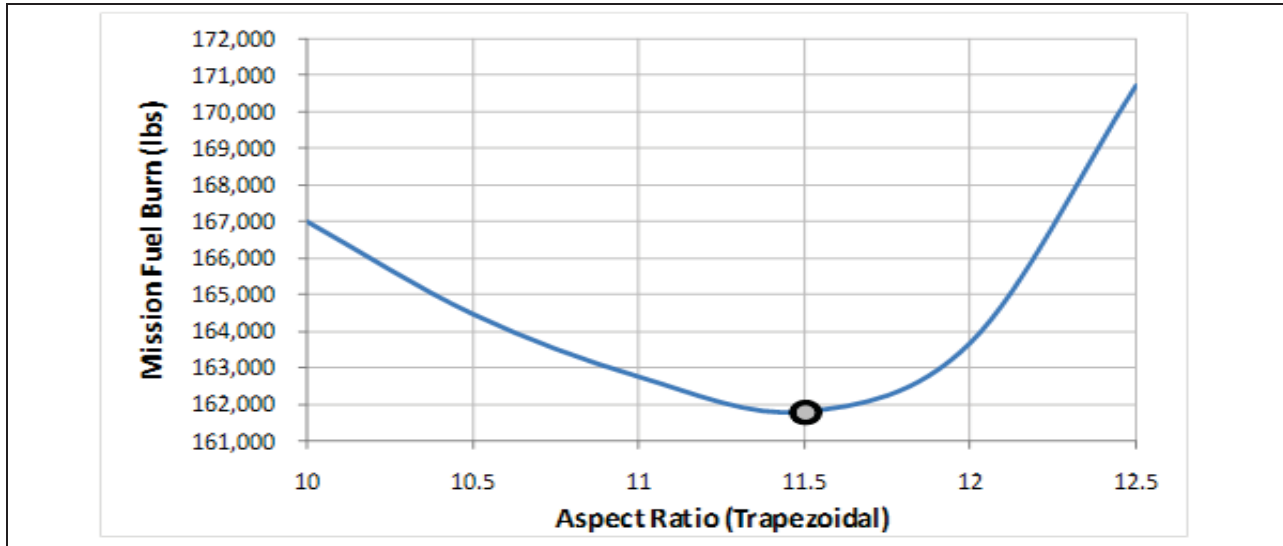


Figure 71 Wing Aspect Ratio Study for 2025 Baseline Vehicle



Figure 72 Wing Leading Edge Sweep Study for 2025 Baseline Vehicles

The wing area and engine scale were sized on the 2025 Baseline vehicles through the same type of carpet plot study as used for the 1998 Reference vehicles. However, in sizing the 2025 Baseline vehicles, it was found that they tended to have significant amounts of excess fuel volume. The reason for this is mainly attributed to the combined effects of a lack of high lift leading edge devices due to the implementation of SWLFC, and an overall more efficient vehicle. For the range of reasonable engine thrust scales, and the associated wing areas required to meet the balanced field length requirement, the available fuel volume is much larger than required to meet the mission range requirements. In other words, for each combination of wing area and engine scale, the actual fuel weight (and hence volume) can be sized to meet the balanced field length requirement, since MTOW and MLW affect field performance.

Therefore, in performing the wing area and engine scale sizing study, for each combination of wing area and engine scale, the vehicle’s actual fuel volume was sized such that it met the balanced field length requirement. For this given set of vehicles that all meet the field length requirement, mission fuel burn can then be minimized while applying the range requirement constraint. These results are shown in Figure 73 and Figure 74.

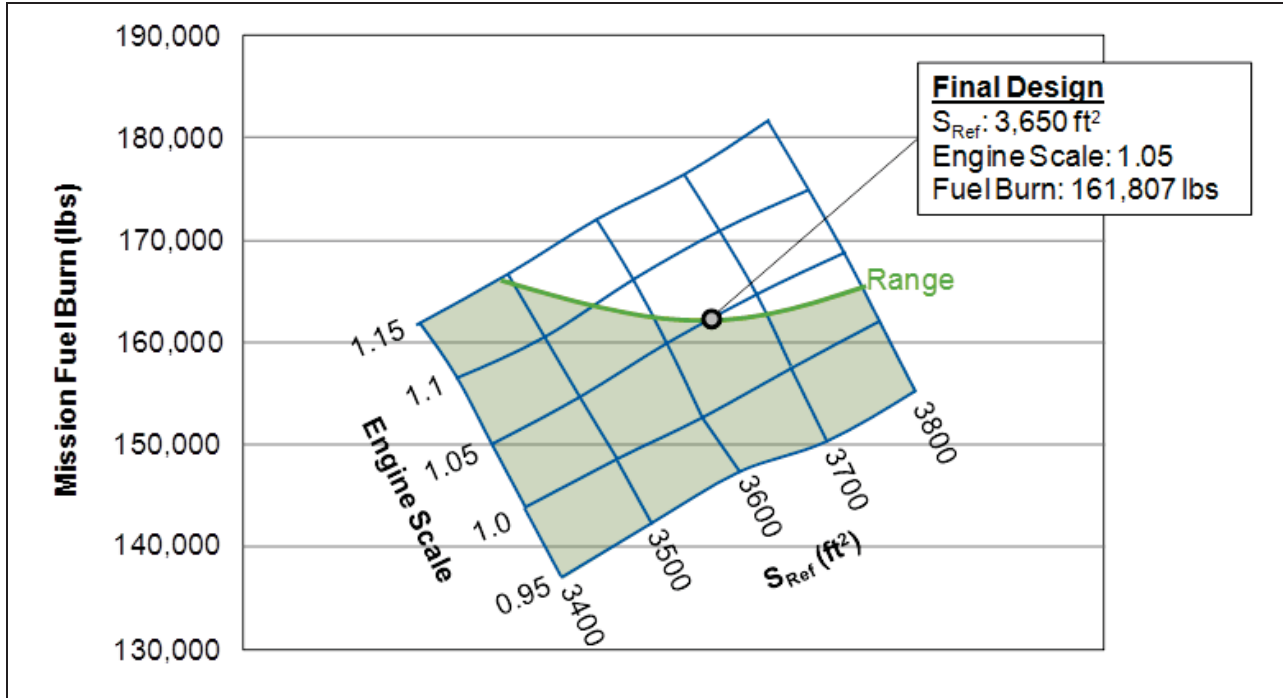


Figure 73 Wing Area and Engine Scale Carpet Plot Study for 2025 Baseline Passenger
 (Note that all designs shown in plot meet balanced field length requirement)

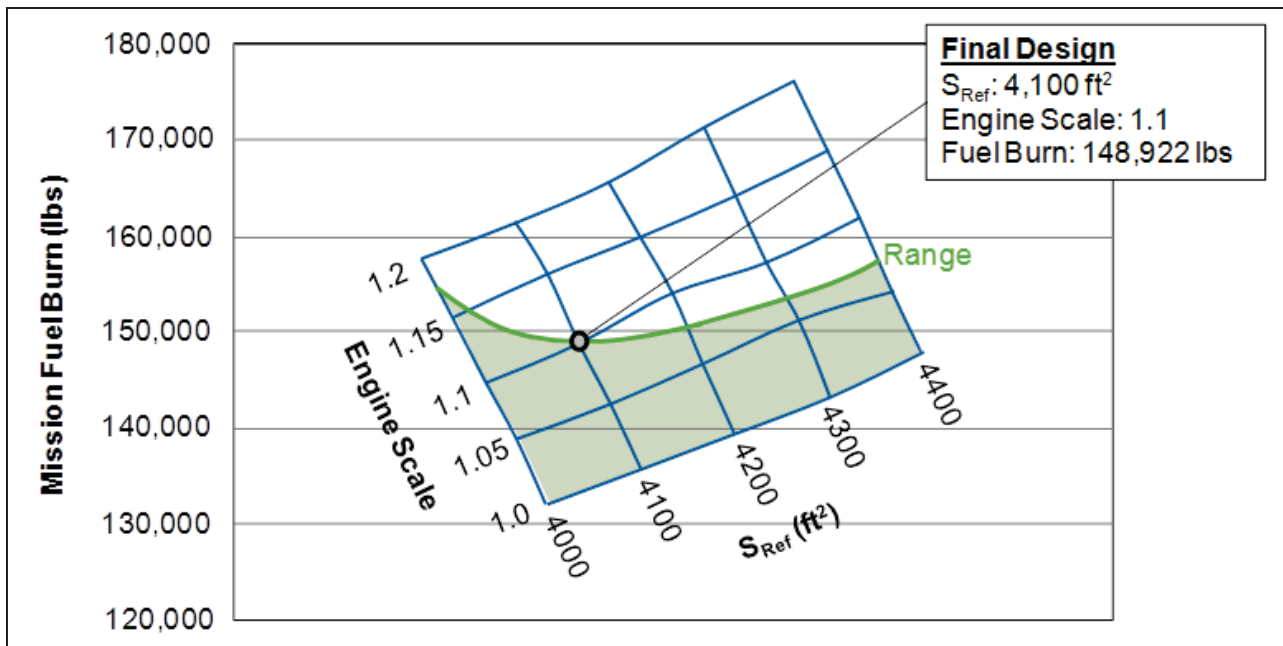


Figure 74 Wing Area and Engine Scale Carpet Plot Study for 2025 Baseline Cargo
 (Note that all designs shown in plot meet balanced field length requirement)

3.8.3. 2025 EIS PSC Flying Wing Vehicles Sizing

The 2025 PSC flying wing configurations presented more difficult payload packaging challenges than the conventional fuselage configurations. Section 3.6.3 described how the payload cabin, centerbody dimensions, and wing planform are highly coupled in this configuration. As previously mentioned, also in Section 3.6.3, a database of possible combinations of payload cabins and centerbody dimensions was developed. These possible centerbody layouts were traded to find an optimal layout. The payload version of the vehicle had fewer options and was selected through the payload integration study discussed in Section 3.6.6. The various passenger centerbody options were then studied at a vehicle level, the results of which are summarized in Figure 75. From this study, the payload cabin and associated centerbody that minimized fuel burn was selected, and is labeled configuration #7 in Figure 75. The selected centerbody layouts for both the passenger and cargo versions of the 2025 PSC vehicles are shown in Figure 76.

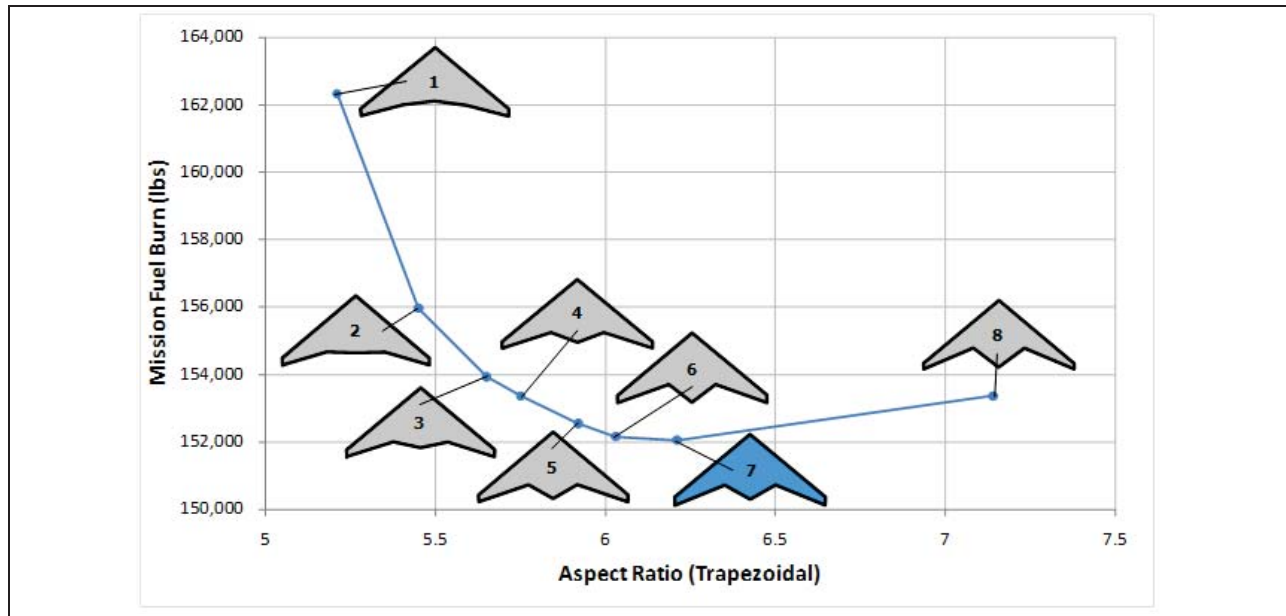


Figure 75 Payload Cabin and Centerbody Study for 2025 PSC Passenger

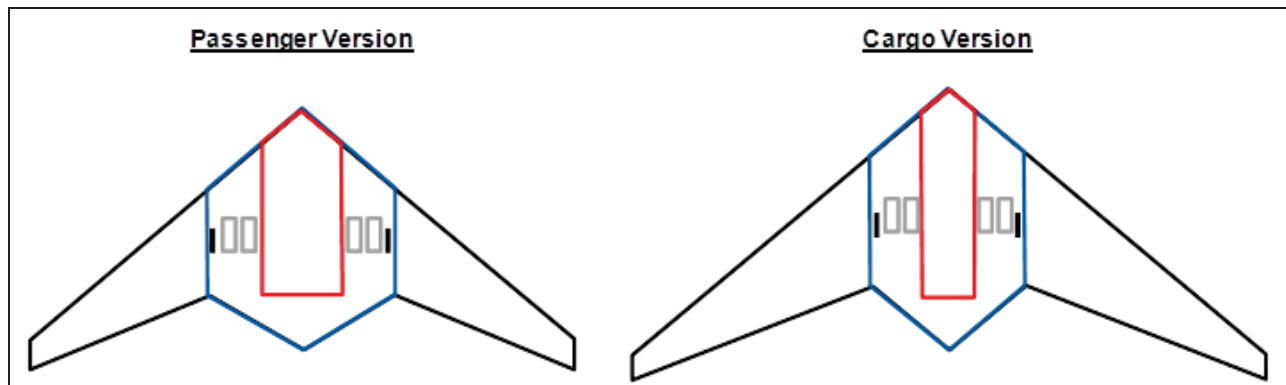


Figure 76 Schematic Layouts of Selected Centerbodies for 2025 PSC vehicles

As mentioned in Section 3.6.3, with the centerbody selected, the remaining planform variables to size are sweep, span, and taper ratio. Sweep plays a major role in effectively balancing a flying wing configuration, as it controls the aerodynamic center. The flying wing vehicles were sized for various leading edge sweep angles to investigate the effects on fuel burn and assess each

vehicle for balancing. Based on extensive experience with flying wing vehicles, a static margin of 3% at a mid-mission weight was established as a target for these vehicles. Furthermore, a positive static margin was the target at the ZFW condition. Figure 77 shows the results from this study, indicating that a leading edge sweep of 40 degrees is required to achieve the static margin targets. Any sweeps greater than 40 degrees increases fuel burn.

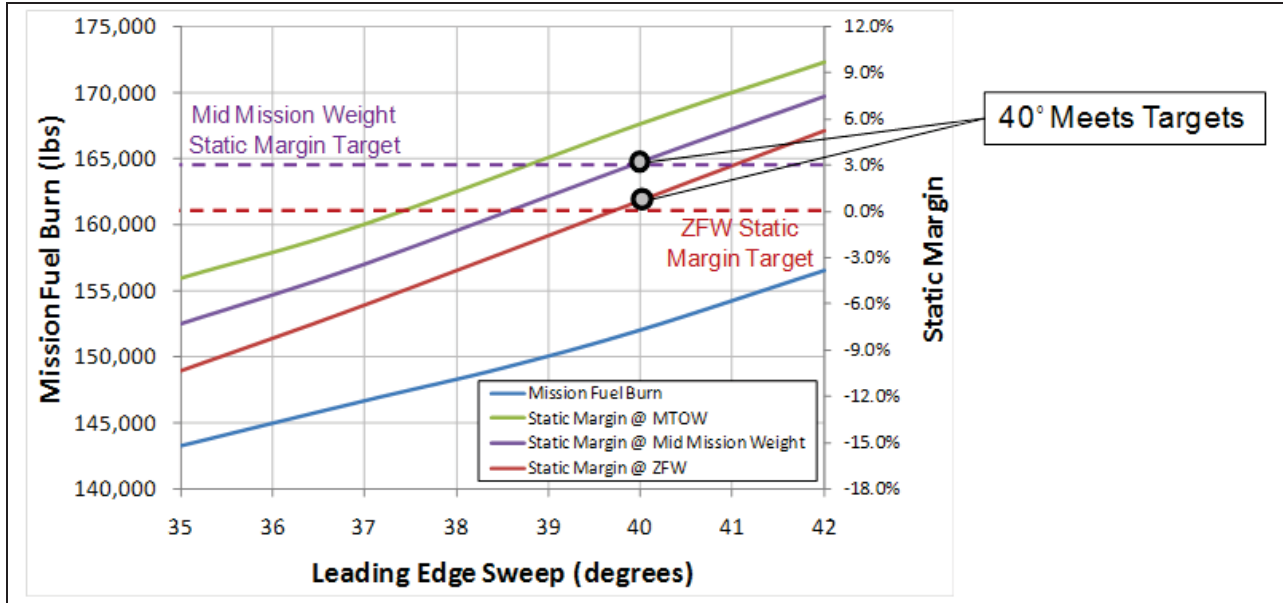


Figure 77 Leading Edge Sweep and Balancing Study Results for 2025 PSC Vehicles

The span and taper ratio of the flying wing configurations are the remaining wing planform parameters to size. Parametric studies were conducted to investigate the effects of these two parameters on mission fuel burn. These results are shown in Figure 78 and Figure 79. Increased wing spans, and in turn increased aspect ratios, reduced mission fuel burn for the overall vehicle. The 260 ft span constraint mentioned in Section 3.4.2 was also applied in these studies. Decreasing taper ratio decreased mission fuel burn for the vehicles. This is mainly due to the fact that it reduces wetted area of the wing section, reducing drag and structural weight. A minimum taper ratio limit of 0.15 is also applied for structural integration considerations.

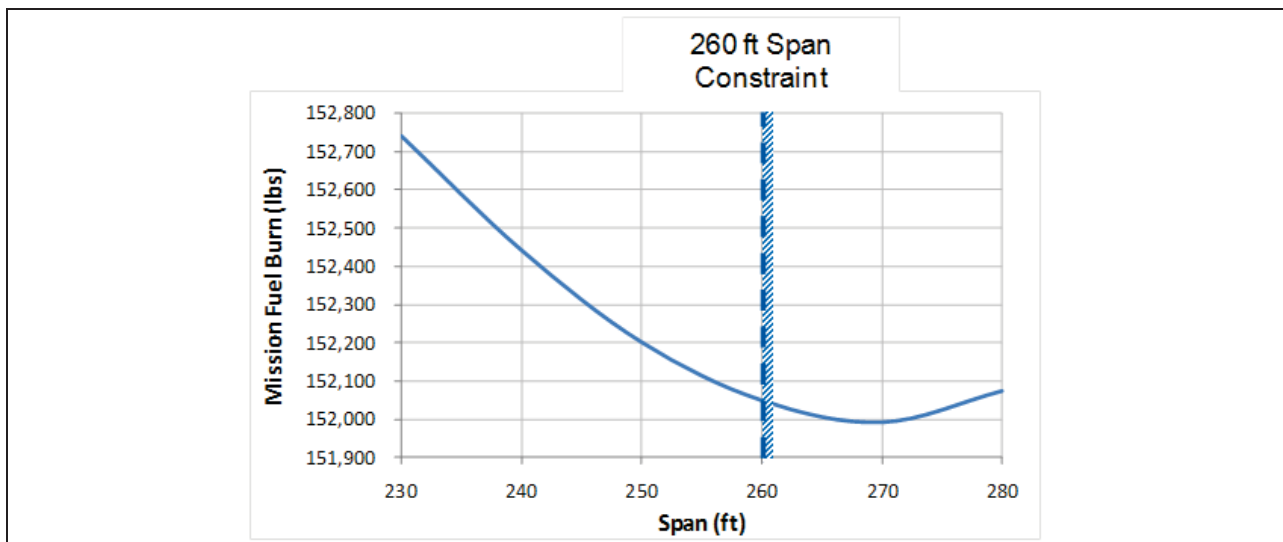


Figure 78 Span Study Results for 2025 PSC Vehicles

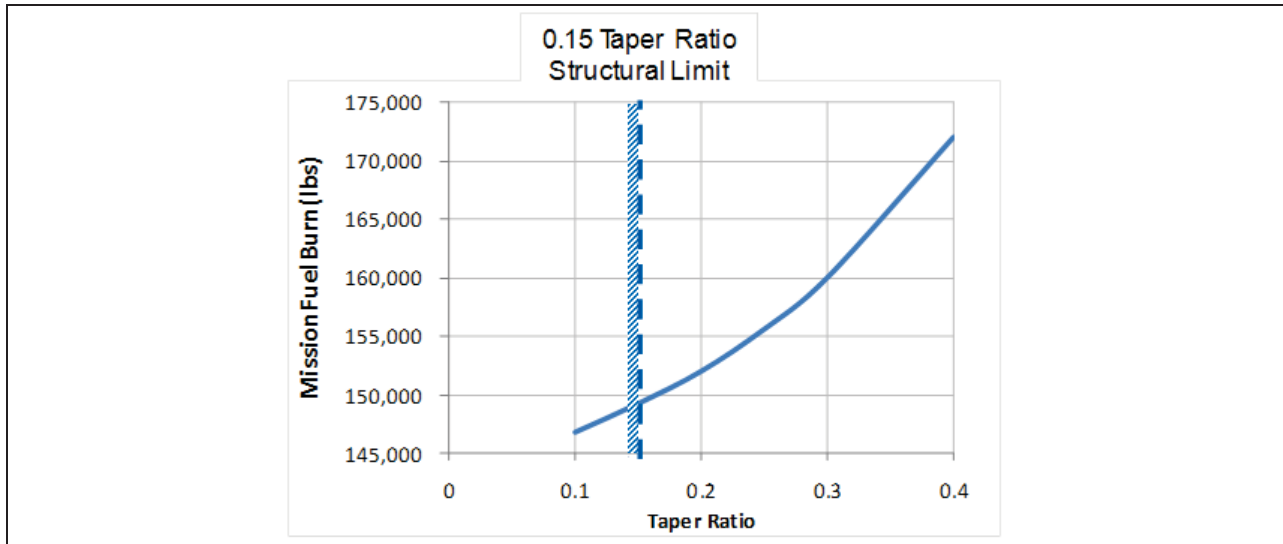


Figure 79 Taper Ratio Study Results for 2025 PSC Vehicles

However, in addition to the effects of span and taper ratio on the mission fuel burn, pitch up tendency is also directly related to the span and taper ratio of the vehicle’s planform. For a tailless flying wing configuration, it is particularly important to consider pitch up limits. Figure 80 shows historical trend lines of pitch up limits as a function of quarter chord sweep and planform based aspect ratio for various taper ratios. With the vehicle centerbodies selected and a leading edge sweep chosen, these pitch up limits were used to size the span and taper ratio of the 2025 PSC vehicles.

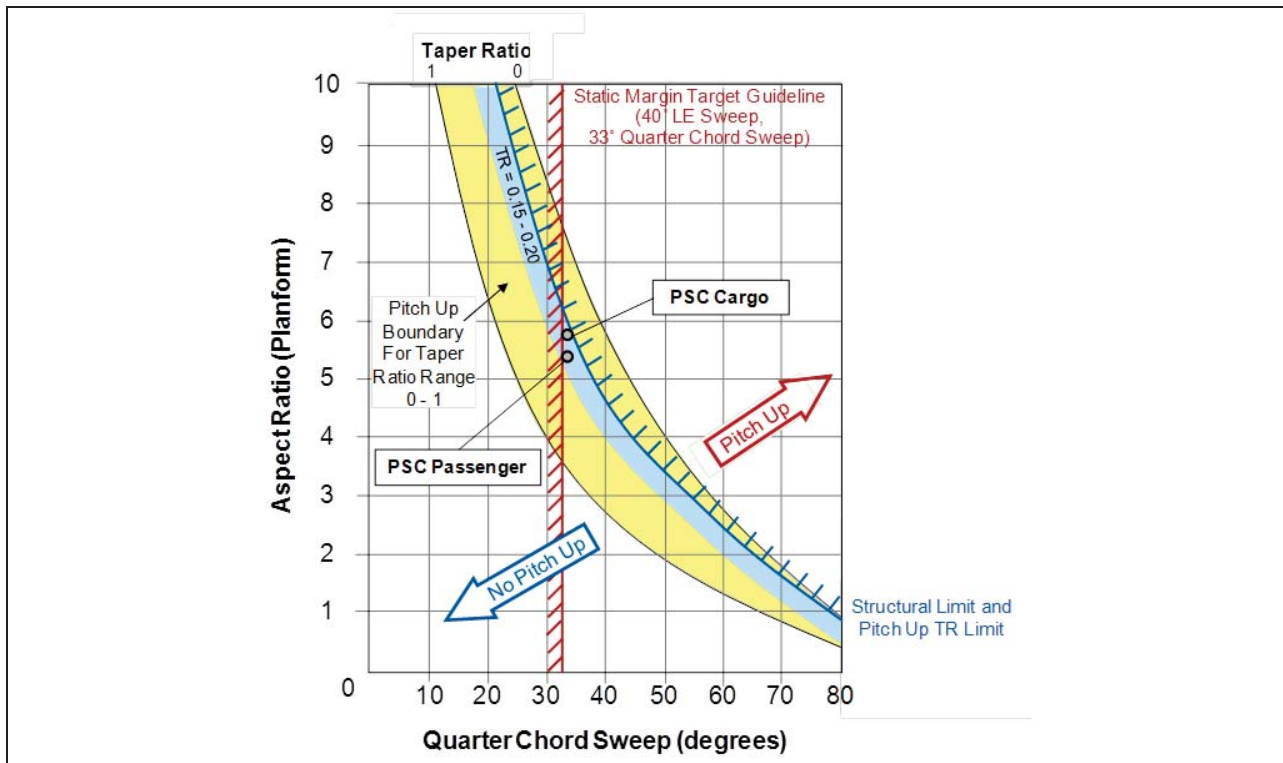


Figure 80 Pitch Up Limits Applied to 2025 PSC Vehicles

3.9. Acoustic Analysis

Acoustic analysis was performed on the Task 2 vehicles following the conceptual design process described above. The acoustic performance was assessed downstream of the aero-propulsion performance analysis, with aerodynamic inputs for Federal Aviation Administration (FAA) Federal Aviation Regulation (FAR) Part 36 profiles, engine cycle parameters, and airframe configuration geometry.

3.9.1. Vehicle Approach and Departure Profiles

Computation of effective perceived noise levels is dependent on the vehicle flying a trajectory prescribed by FAR Part 36. There are several requirements for take-off and approach, summarized below. Figure 81 shows the take-off and approach profiles for the passenger versions of each vehicle that was analyzed.

- Take-off
 - Maximum Climb Speed = $V_2 + 20$ kts
 - Minimum Climb Speed = $V_2 + 10$ kts
 - Engine Cutback Minimum Altitude
 - For Two (2) Engine Configurations = 984 feet AGL
 - For Two (4) Engine Configurations = 689 feet AGL
 - Climb Gradient = 4° with All Engines Operating or Level Flight with One Engine Operating
- Approach
 - Glide Slope = 3°
 - Descent = Constant 250q to 1500 feet AGL Based on ROA Mission Profile
 - Maximum Velocity = $V_{ref} + 10$ kts from 1500 feet AGL

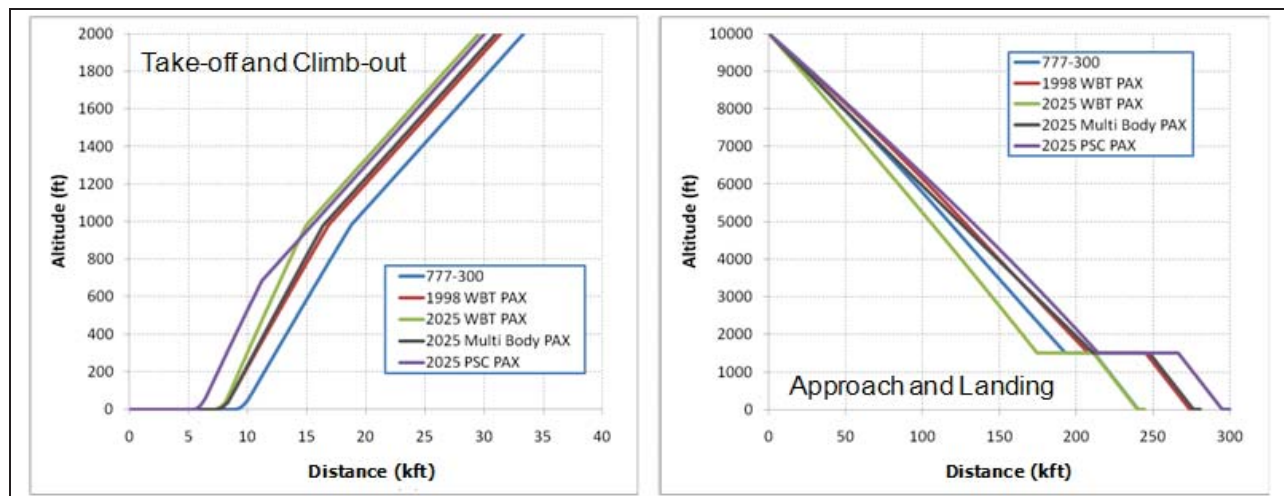


Figure 81 FAR Part 36 Take-off/Climb-out and Approach/Landing Profiles for Passenger Configurations

3.9.2. Acoustic Analysis Tools and Process

With inputs for FAR Part 36 profiles (both take-off and approach), engine cycle data linked to these profiles and the airframe configuration geometry, component noise source predictions (aka “hemispheres”) were generated using Northrop Grumman’s Model for Investigating

Detectability of Acoustic Signatures (MIDAS). Jet exhaust, fan noise sources, and airframe (lifting surface) noise sources were computed for both profiles, while gear assemblies, slats, and flaps were computed only for approach. For some configurations, certain component noise sources were necessarily neglected. Vehicle flight speed was used to compute Doppler shift, and altitude was used to compute atmospheric dependent noise parameters. Each component source was computed at five (5) stations along each profile especially at inflection points in a given profile (e.g. at engine cutback for take-off). Having computed all component sources for each profile, advanced technologies which impacted the acoustic performance of the aircraft were applied for all 2025 EIS vehicles. These technology sets were varied depending on the configuration and applied specifically for the particular implementation on a given vehicle. Different acoustic decrements were required to represent a given technological state including spectrally independent sound pressure level (SPL) shifts derived from open literature without directivity dependence, and spectrally dependent SPL shifts derived from analyses with both directivity dependence and independence.

With technologies applied, composite noise point sources were computed using summation at each station along a given profile. In this way, the total vehicle noise source hemisphere is prescribed incrementally via interpolation along each profile. Using the composite noise sources and the FAR Part 36 profiles, the vehicles were flown via simulation in MIDAS with the prescribed perceived noise level (PNL) monitors for Community, Sideline (Lateral), and Approach metrics. Respectively these were positioned at 21,325 ft from brake release for the take-off profile, every 10 ft from the end of the runway at 1,476 ft offset from the projected flight path for the take-off profile, and at 6,582 feet from the end of the runway for the approach profile. Angle of attack was also utilized to rotate the noise source hemispheres so that the directivity was appropriate for the in-flight orientation of the hemispheres was correct.

FAR Part 36 certification limits are dependent on a vehicle's weight. Figure 82 shows the Stage 3 limits for Community, Sideline (Lateral), and Approach effective perceived noise level (EPNL) metrics versus aircraft MTOW. Stage 4 is 10 EPNdB less than Stage 3 cumulative. N+2 ERA goals are 42 EPNdB less than Stage 4 cumulative. Note that the Community limit for a vehicle with four (4) engines is approximately 5 EPNdB greater than that for a vehicle with two (2) engines.

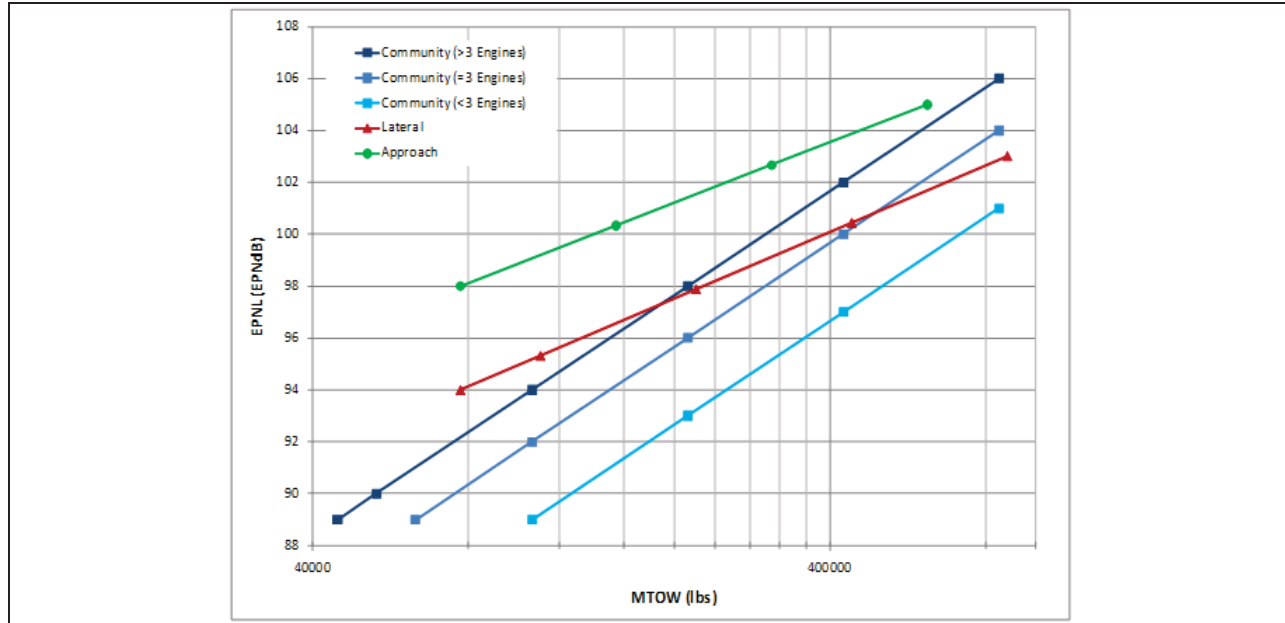


Figure 82 FAR Part 36 Stage 3 Certification Limits

3.9.3. 1998 EIS Comparison Vehicle Acoustic Analysis

Calibration of MIDAS was conducted using a 777-300 vehicle. Certification data for this vehicle are published by both the FAA and the European Aviation Safety Agency (EASA). No advanced technologies were applied to this vehicle as the acoustic noise source models were purpose built for this general configuration. As expected, propulsion sources dominated the Community and Sideline (Lateral) metrics and the landing gear assembly noise dominated the Approach metric. Figure 83 shows the predicted data versus the published data. Note that there is a 3-4 EPNdB spread between different engine installations for the Community and Sideline (Lateral) metrics, while the Approach variation is minimal. As expected, the comparison vehicle was better than the cumulative Stage 3 limit by approximately 13-14 EPNdB.

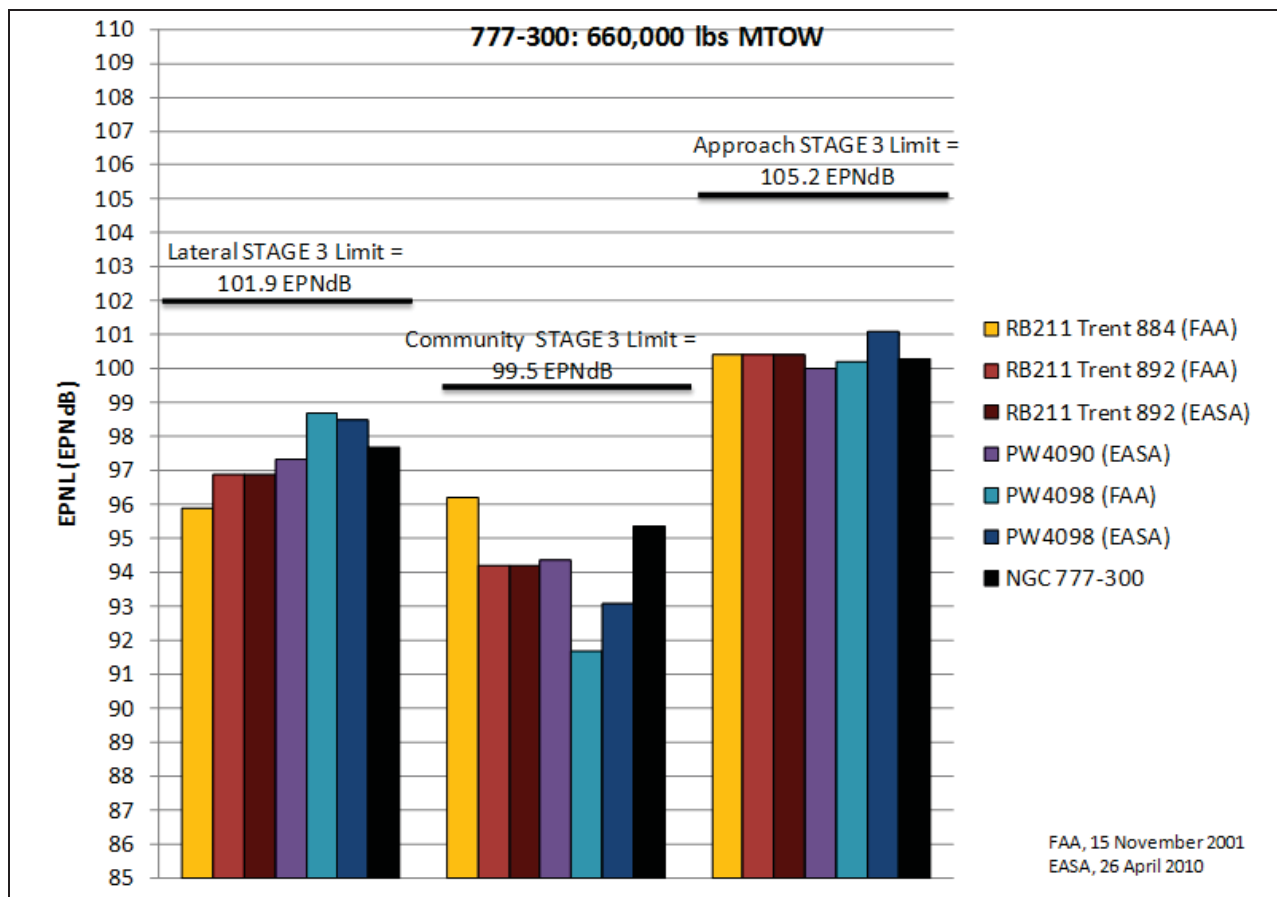


Figure 83 FAR Part 36 Stage 3 Certification Levels and Limits for 777-300

3.9.4. 1998 EIS Reference Vehicles Acoustic Analysis

Having confirmed the accuracy of MIDAS using the comparison vehicle, the 1998 Reference vehicles were analyzed. Counter intuitively, these vehicles performed acoustically worse than the 777-300. Upon investigation, it was determined that this was due to two main factors. First, the jet velocity for these vehicles contributed to a larger jet exhaust component noise source. Second, a faster approach airspeed increased the airframe, specifically the gear assembly component noise source. The issue was compounded when computing the margins versus Stage 3, Stage 4, and N+2 ERA limits due to the reduced scale MTOW. Figure 85 illustrates the EPNL levels for the 1998 EIS Reference passenger and cargo vehicles in yellow. Figure 86 illustrates the EPNL margins versus Stage 3, Stage 4, and N+2 ERA goals for the 1998 EIS Reference passenger and cargo vehicles in yellow.

3.9.5. 2025 EIS Baseline Vehicles Acoustic Analysis

Following the process which was used to analyze the Comparison vehicle and 1998 Reference vehicles, the 2025 vehicle analyses employed the additional step of advanced technology integration. These technologies were divided into two separate categories: dedicated acoustic technologies and engine-associated acoustic technologies. The latter consisted of technologies which were the responsibility of the engine manufacturer to integrate into the engine performance analysis. The former category consisted of technologies which were the responsibility of the airframer. The following is a list of the included advanced technologies in these two groups and their reduction impact on the affected component noise source.

- Dedicated Acoustic Technologies
 - Landing Gear Assembly Fairings: 3 dB
 - Adaptive Shape Memory Alloy Chevrons: 6 dB When Deployed
 - Spliceless/One-Piece Inlet Acoustic Liner: 5 dB > 2 Splice
 - Scarfed Inlet Nacelle: 4 dB @ Forward Radiated Angles
- Engine-Associated Acoustic Technologies: 7 dB Cumulative
 - Ceramic LPT Case Treatment
 - OMC Fan Case Treatment
 - Swept OGV
 - Fan Blade Shaping
 - Ceramic-metal Composite (CMC) Mixer

The advanced technologies were integrated into the component noise sources prior to compiling each composite source at each station. The landing gear assembly overall sound pressure level (OASPL) was reduced by 3 dB. The jet exhaust noise was decreased by 6 dB for the five (5) stations pertaining to the take-off profile. The fan radiated tones were modulated by an attenuation spectrum which consisted of the largest decrement of 5 dB at the BPF. Furthermore, 4 dB were removed from the OASPL of the fan noise at azimuths 0°-90°. The cumulative effect of the engine-associated acoustic technologies accounted for 7 dB reduction for the fan noise. This quantity is assumed to be conservative due to reports which conclude that Swept OGVs may independently yield up to 7 dB attenuation.

The Community, Sideline (Lateral), and Approach levels for the 2025 Baseline vehicles were expectantly less than those of the previously described vehicles. However, the integration of the advanced technology alone on the Baseline vehicles did not have a sufficient impact to reduce the cumulative EPNL levels below N+2 ERA goals. The margin was approximately 20 EPNdB.

3.9.6. 2025 EIS Multibody Vehicles Acoustic Analysis

Repeating the process which was used to analyze the 2025 Baseline vehicles, the Multi-Body vehicles were assessed. The Community, Sideline (Lateral), and Approach levels for the 2025 EIS Baseline vehicles were less than those of the previously described vehicles. Moreover, the Approach levels were less than those for the PSC Flying Wing vehicles, however like the Baseline vehicles, the integration of the advanced technology alone, nor the advanced configuration did not have a sufficient impact to reduce the cumulative EPNL levels below N+2 ERA goals. The margin was approximately 20 EPNdB. Figure 85 illustrates the EPNL levels for the 2025 EIS Baseline passenger and cargo vehicles in red. Figure 86 illustrates the EPNL margins versus Stage 3, Stage 4, and N+2 ERA goals for the 2025 Baseline passenger and cargo vehicles in red.

3.9.7. 2025 EIS PSC Flying Wing Vehicles Acoustic Analysis

Though the configuration of the Flying Wing is fundamentally different than the Wing-Body-Tail configuration, the acoustic analysis process was identical to that for the 2025 Baseline vehicles with the additional concern for airframe shielding of the propulsion system. Technologies were divided into two separate categories: dedicated acoustic technologies and engine-associated acoustic technologies. The latter consisted of technologies which were the responsibility of the engine manufacturer to integrate into the engine performance analysis. The former category consisted of technologies which were the responsibility of the airframer. The

following is a list of the included advanced technologies in these two groups and their reduction impact on the affected component noise source.

- Dedicated Acoustic Technologies
 - Landing Gear Assembly Fairings: 3 dB
 - Spliceless/One-Piece Inlet Acoustic Liner: 20 dB
- Engine-Associated Acoustic Technologies: 7 dB Cumulative
 - Ceramic LPT Case Treatment
 - OMC Fan Case Treatment
 - Swept OGV
 - Fan Blade Shaping
 - Ceramic-metal Composite (CMC) Mixer

The advanced technologies were integrated into the component noise sources prior to compiling each composite source at each station. The landing gear assembly overall sound pressure level (OASPL) was reduced by 3 dB. The fan radiated tones were modulated by an attenuation spectrum which consisted of the largest decrement of 20 dB at the BPF at 630 Hz. The spectrum was for a cylindrical duct. It was assumed that the given data were conservative for the PSC configuration, which would necessarily employ a non cylindrical inlet thus preventing certain modes. The cumulative effect of the engine-associated acoustic technologies accounted for 7 dB reduction for the fan noise. This quantity is assumed to be conservative due to reports which conclude that Swept OGVs may independently yield up to 7 dB attenuation. Though the technology suite is less substantial for the Flying Wing vehicles than for the Baseline vehicles, the elimination of the slats and tail surfaces can be considered, in effect, as additional technologies. However, the greatest contributor to the reduced noise footprint of the flying wing configuration is the effect of the airframe shielding of the propulsion system.

Acoustic shielding, though not an “advanced” technology, was integrated into the propulsion component noise sources in the same fashion. However, the data required to perform the impact analysis were derived from a separate code written and maintained by Northrop Grumman to perform such analyses. The code uses a ray-trace algorithm to propagate a point source from its location relative to the upper OML planform of the vehicle to an observation hemisphere. Rays which are shielded by the bulk of the airframe are not propagated to the observations sphere. Rays which intersect with an edge diffract from it to the observation hemisphere. The resultant sum of these two is then depropagated back to one (1) foot reference range. It was convenient to use a 0 dB noise source hemisphere in the model. The result is subsequently applied to the actual component sources.

Because both the fan component noise source and the jet exhaust noise source were affected by the presence of the airframe, each source location was computed independently for each of the passenger and cargo configurations. Figure 84 shows the locations of the fan point source (at the inlet face), and the jet exhaust point source (at the apparent source location, five (5) diameters downstream of the nozzle).

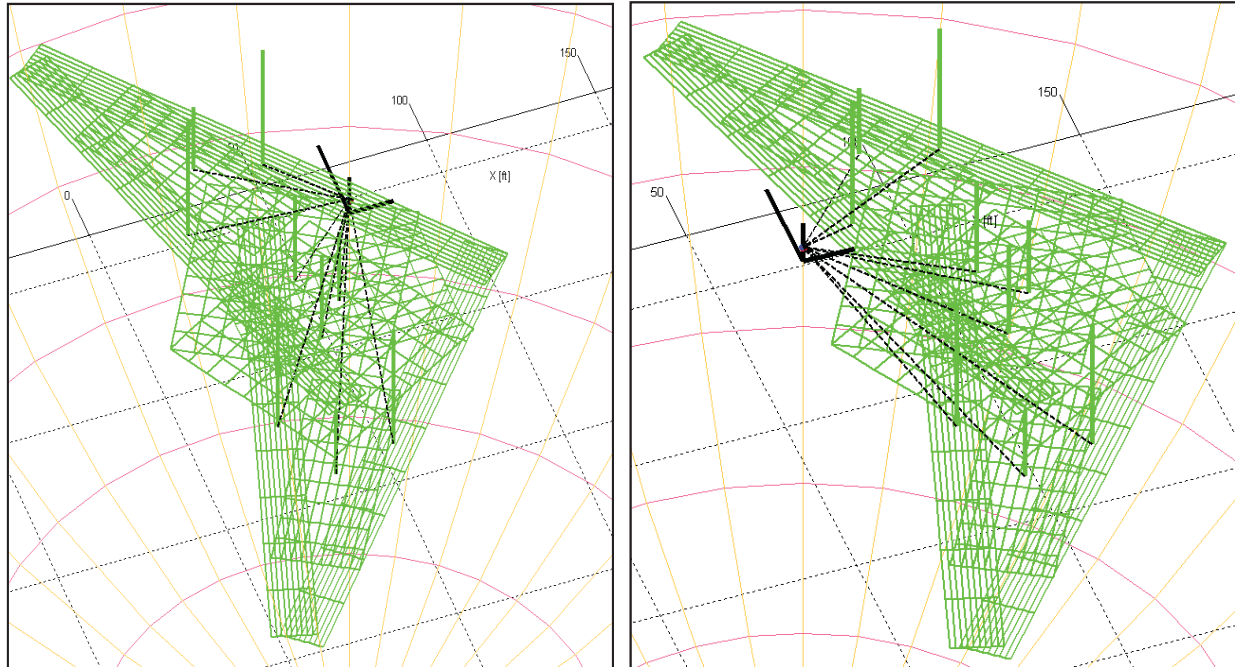


Figure 84 (L) Fan Component Noise Point Source Location (R) Jet Exhaust Component Noise Point Apparent Source Location Relative to the Passenger PSC Configuration OML

The Community, Sideline (Lateral), and Approach levels for the 2025 PSC vehicles were expectantly less than those of the previously described vehicles. The combined effect of the configuration and technology contributed to a substantial reduction in the overall noise profile of vehicle. The effect of the large airframe on the landing component noise source was inconsequential due to gear sizing being proportional to MTOW. The propulsion sources, which dominate take-off, were drastically reduced due to the effect of shielding, and particularly for the fan due to substantial acoustic liner length. The net result bettered the N+2 goals by approximately 36-41 EPNdB. In fact, the levels met the N+3 goals (Stage 4 less 72 EPNdB). Note that five (5) EPNdB in the margin are due to the increased Stage 3 limits due to the increased engine count (see Figure 82). Figure 85 illustrates the EPNL levels for the 2025 Flying Wing PSC passenger and cargo vehicles in blue. Figure 86 illustrates the EPNL margins versus Stage 3, Stage 4, and N+2 ERA goals for the 2025 Flying Wing PSC passenger and cargo vehicles in blue. Table 9 is included as a summary.

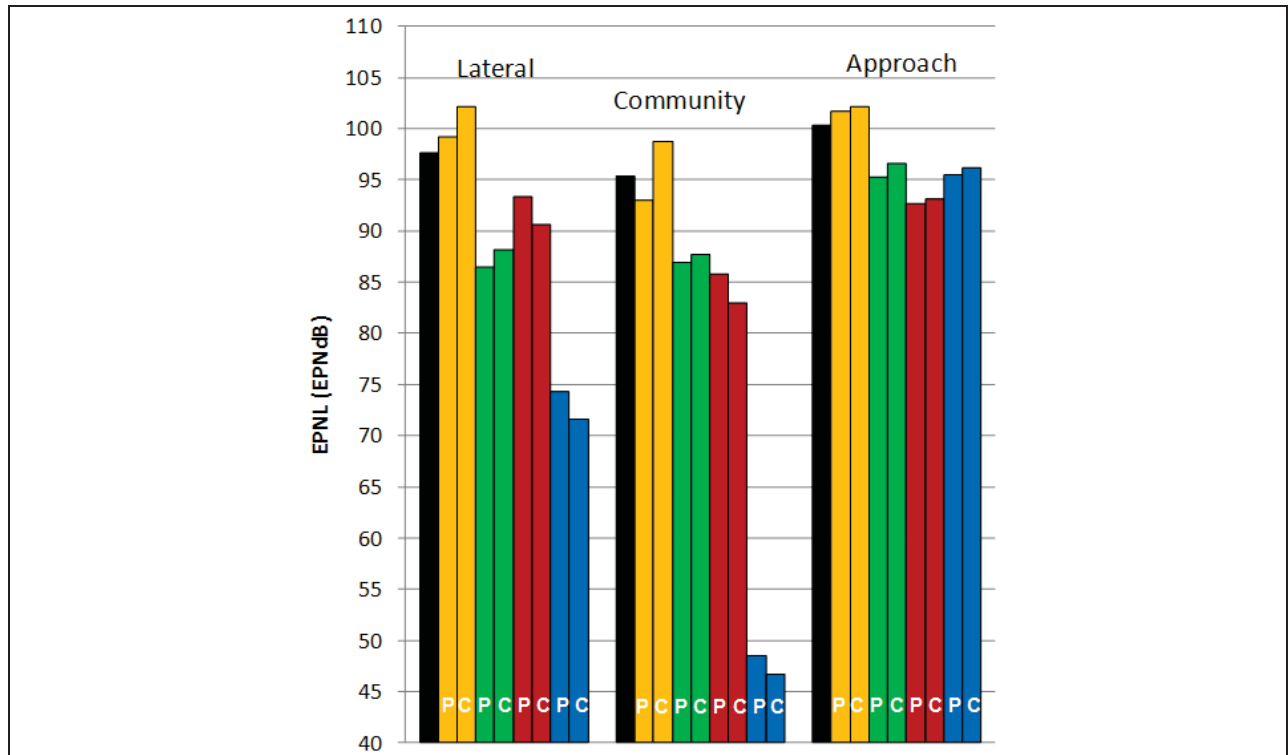


Figure 85 FAR Part 36 Stage 3 Certification Levels

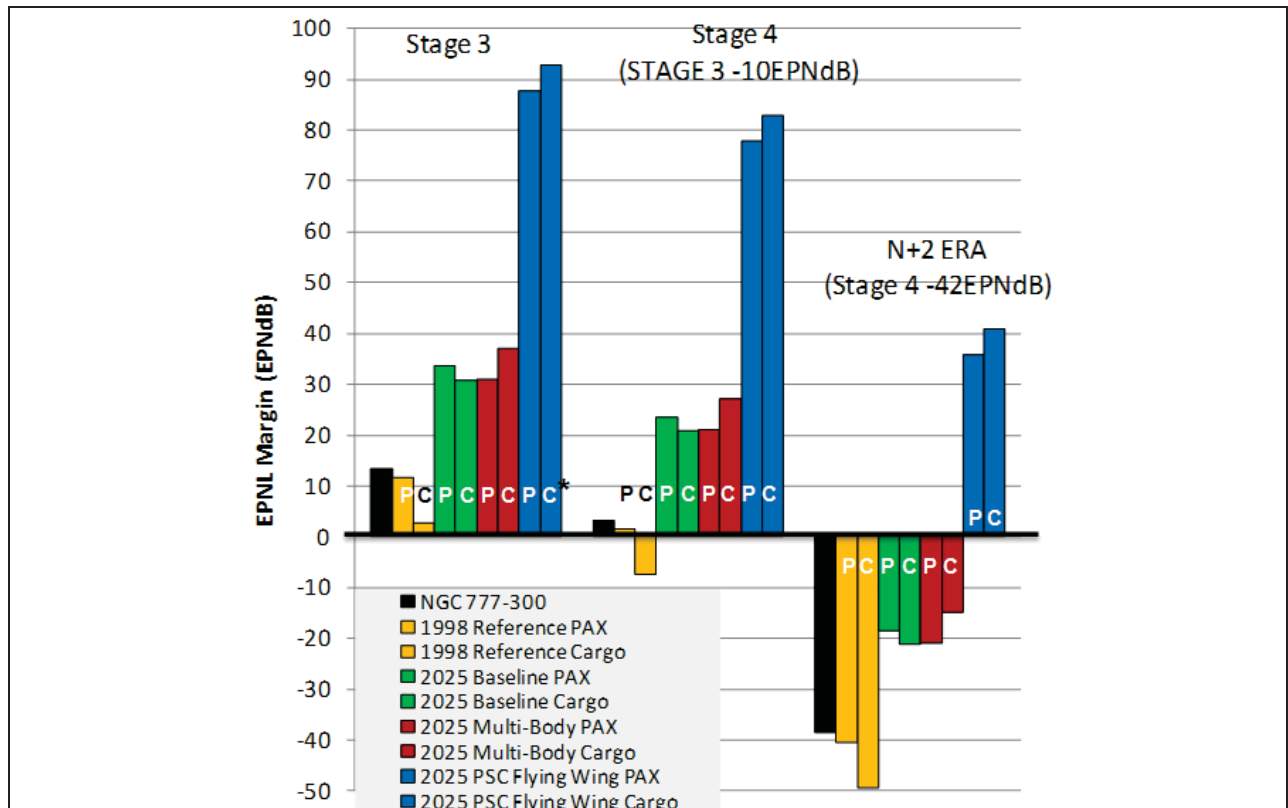


Figure 86 FAR Part 36 Stage 3, Stage 4, and N+2 ERA Certification Margins

	Max		Lateral EPNL		Flyover EPNL		Approach EPNL		Cumulative EPNL		Stage 3	Stage 4	ERA (N+2)
	TOGW (kg)	TOWG (lb)	Level	Limit	Level	Limit	Level	Limit	Level	Limit	Margin	Margin	Margin
NGC 777-300	299371.0	660000.0	97.7	101.9	95.4	99.5	100.3	105.2	293.4	306.7	13.3	3.3	-38.7
1998 Reference PAX	270114.3	595500.0	99.2	101.6	93.0	98.9	101.7	104.9	293.8	305.4	11.6	1.6	-40.4
1998 Reference Cargo	277144.9	611000.0	102.2	101.6	98.7	99.1	102.2	105.0	303.0	305.7	2.7	-7.3	-49.3
2025 Baseline PAX	211374.0	466000.0	86.5	100.6	86.9	97.5	95.3	104.1	268.7	302.2	33.6	23.6	-18.4
2025 Baseline Cargo	230878.5	509000.0	88.2	101.0	87.8	98.0	96.7	104.4	272.6	303.4	30.8	20.8	-21.2
2025 Multi-Body PAX	222351.0	490200.0	93.3	100.8	85.8	97.8	92.7	104.2	271.8	302.9	31.1	21.1	-20.9
2025 Multi-Body Cargo	237999.9	524700.0	90.6	101.1	83.0	98.2	93.1	104.5	266.7	303.8	37.1	27.1	-14.9
2025 PSC Flying WIng PAX	193729.3	427100.0	74.3	100.3	48.6	102.0	95.5	103.8	218.3	306.1	87.8	77.8	35.8
2025 PSC Flying WIng Cargo	214685.3	473300.0	71.6	100.7	46.7	102.6	96.2	104.1	214.5	307.4	92.9	82.9	40.9

Table 9 FAR Part 36 Stage 3, Stage 4, and N+2 ERA Certification Margins

4. TECHNOLOGY MATURATION PLANS

The objective of Task 3 is the development of technology maturation plans (TMPs) that outline the research required to develop the technologies and integrated aircraft systems critical to simultaneously meeting the noise, emission, and fuel burn goals for the Preferred System Concepts. This includes the development of a 15-year time phased technology maturation plan that would enable the envisioned aircraft system concept(s) by 2025. Starting and ending technology readiness level (TRL) and system readiness level (SRL) are identified as part of the technology maturation plan along with key research, analyses, tool and method development, and necessary ground and flight tests required to mature the technology or successfully address the technical challenge in time to support the EIS date. The PSC roadmaps also include credible intermediate performance objectives associated with critical tests and demonstrations along with estimated cost, schedule and expected technical outcome for each major element of the roadmap.

4.1. Technology Assessment Approach

The approach for performing the technology assessment is illustrated in Figure 87 and includes (1) identifying relevant technologies that help to meet ERA goals for fuel burn, emissions, and noise, (2) conducting trade studies to assess the TRL/maturity level for each candidate technology and provide a qualitative assessment of technology performance in helping to meet the ERA goals, (3) assessing the impact of each technology on the system level performance goals for fuel burn, NO_x emissions, and noise, and (4) developing maturation roadmaps for key relevant technologies.

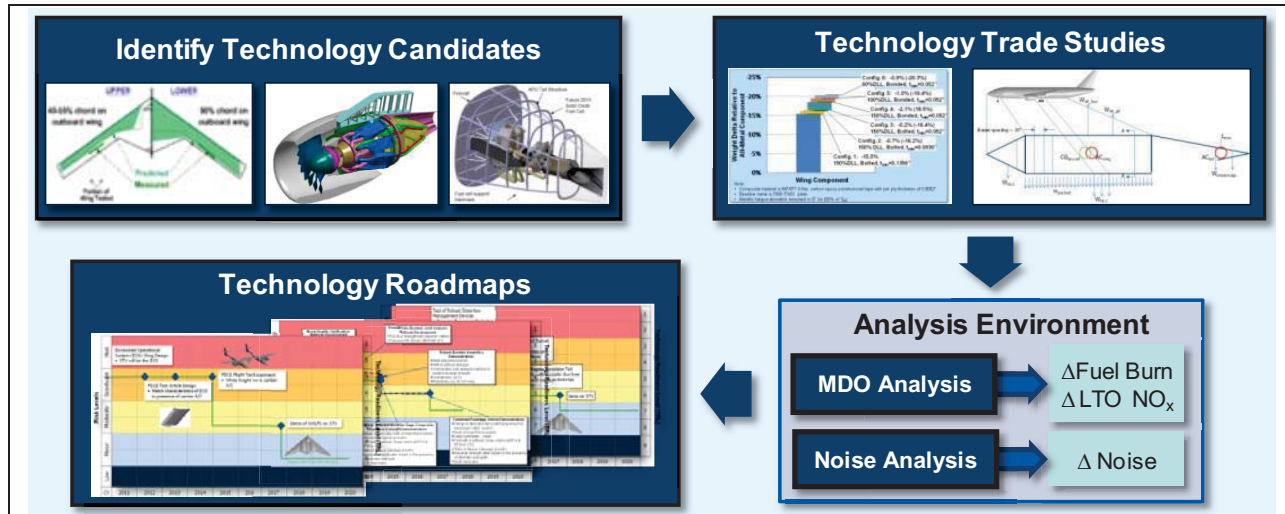


Figure 87 Technology Assessment Approach

Technology trade studies aided in providing performance data and inputs to the analysis tools in order to derive the system level benefits in terms of mission fuel burn reductions, NO_x emissions reductions, and noise SPL reductions. The studies also point out any associated penalties, integration issues, and compatibility constraints with other technologies. Selection of the candidate technologies is dependent on the technology’s capability to achieve TRL 6 by 2020 and results from the system level benefits on the overall performance of the 2025 baseline and PSC vehicles. Technologies that provide a significant positive impact in meeting ERA goals were selected for integration into the 2025 vehicles. Of those downselected technologies,

maturation roadmaps were developed for (1) relevant technologies that need to be matured to TRL 6 by 2020 or (2) enabling or risk reduction development activities specific to the PSC. The technology development roadmaps show the steps required to mature technologies to TRL 6 by 2020 and indicate performance objectives/goals for each step. For those technologies that are already at a TRL 6 or higher, no additional development path was developed, and it is assumed that sufficient investment could occur to make these available for the N+2 entry into service.

In the following subsections, technologies selected for consideration for integration into the 2025 baseline and PSC will be discussed in detail.

4.2. Structures Technology

Structures and materials technologies were focused on wing, fuselage, and landing gears because they comprise most of the structural weight for a wing-body-tail configuration as shown in Figure 88. On average for the 1998 reference vehicle passenger and cargo variants, the wing component accounts for about 43% of the structural weight while the fuselage and landing gear are approximately 31% and 14% respectively. The empennage and induction group is fairly mature in its use of composite materials in current commercial transports so further application of composite technologies to either structural group is warranted. Composite application to the wing is focused solely on the wing box primary structure. For the fuselage, it is applied to the shell which consists of the skin, rings, and stiffeners.

Technology benefit assessment is loads-based—i.e., the wing box and fuselage shell are sized based design load factors and limited set of failure modes. Note that that the sizing is done for the primary structures for the component—i.e., wing torque box for the wing component and the fuselage shell for fuselage component.

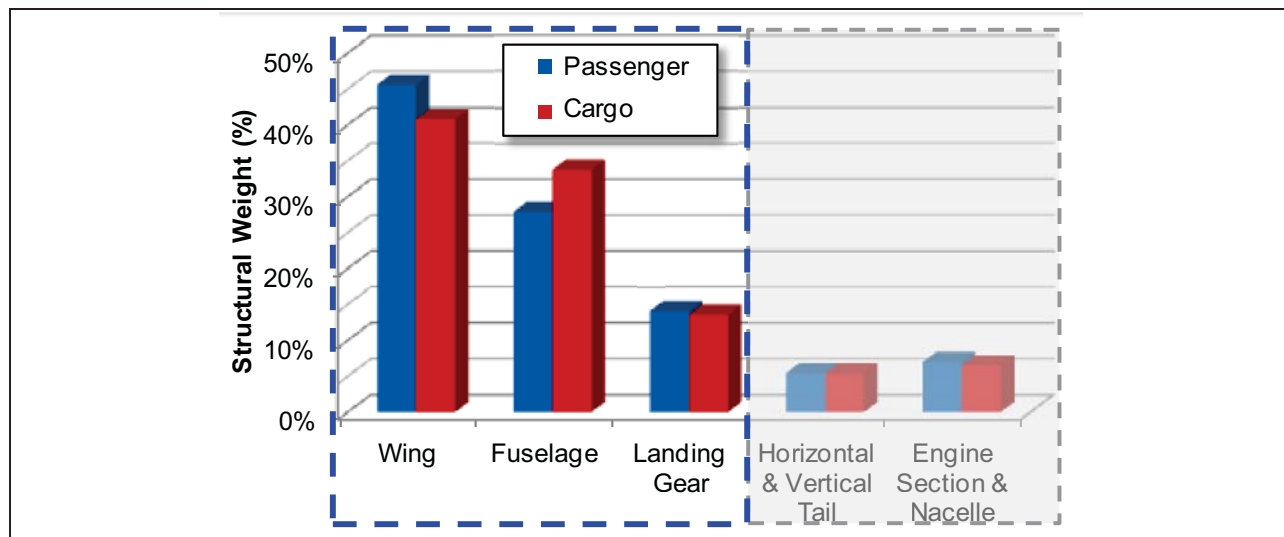


Figure 88 Major Components for Structural & Material Technologies Benefit Study

The list of candidate structural and material technologies is shown in Table 10. As weight is a strong function of density, low-density materials (carbon fiber reinforced composites (CFRC) and metal-matrix composites) and materials with improved specific properties (advanced metallics) were chosen initially. Based on lessons learned leveraged from past programs, known trends, and TRL, only CFRC and advanced titanium were downselected for final application to the PSC. Structural technologies included various structural concepts (composite bonded

assembly, postbuckling, sandwich, trussed, and stamped—e.g. beaded) and load control methods (all-inclusive in a unifying heading of integrated aeroservoelasticity or i-ASE). Of the structural concepts, primary bonded assembly, postbuckled structures, and i-ASE were chosen for further application into the PSC. Bonded assembly encourages more composites usage through reduction of high manufacturing cost associated with bolted composite assemblies. Note that this technology also includes large unitization to reduce cost associated with manufacturing of subassemblies (e.g., upper and lower skins, fuselage panels). Bonding will also aid swept wing laminar flow control by reducing/minimizing surface irregularities through the elimination of fasteners. Postbuckling is a well known technique for minimizing material, constrained to allowable minimum gauge. For deep fuselage sections/components, minimum gauge skins will dominate and the postbuckled concept is highly competitive, if not better than sandwich in terms of weight. Sandwich was not selected for this reason as well as its poor damage tolerance and durability performance. Truss and stamped structures, which would be used in substructures to replace monolithic or stiffened webs, were not selected because they would make up a smaller fraction of the total structural weight. The logic was that primary weight benefit would be achieved over metals by converting to composites. Further weight savings among composite structural concepts would be a refined trade and was deemed secondary for details that make up smaller portion of the total weight. It would be better to focus on increasing usage of composites on a majority of the airframe. Finally, i-ASE was selected for its maturity as well as necessary application in tailless (i.e., fly-wing) aircraft. In the following pages, the quantitative benefits of each selected technologies will be described, followed by discussions of technology development efforts for some of the less mature technologies.

Structures Technologies	
Technology Name	Brief Description
Primary Composite Structure	Increased composite usage for primary structures (reduced weight through density); potential weight reduction: 15-20% on wing, 8-15% on fuselage
Primary Bonded Assemblies	Bonding of composite OML shells/skins to substructures using either 2D or 3D composite joints eliminates fasteners, reduces weight and lowers manufacturing costs
Integrated Aeroservoelastic Airframe	Structural weight reduction through active control of maneuver & gust loads and flutter; improved ride and flight quality; up to 4.5% weight savings on wing component
Postbuckled Structures	Composite skins and panels capable of carrying load beyond initial buckling; allows aggressive use of minimum gage design on part that are not highly loaded resulting in part weight reduction
Advanced Metallic Alloys	Structural weight reduction using advanced metallic alloys over traditional steel or monolithic titanium, up to 21% weight savings over conventional metals
Composite Landing Gear Braces	Lightweight composite landing gear braces, up to 30% weight saving over traditional metallic braces

Table 10 Structures Technology Candidates

4.2.1. Sizing Methodology

The effect of the selected structural and material technologies on structural weight of the aircraft was determined through load-based structural sizing of the wing and fuselage of a wing-body-tail configuration. Both structures are assumed to be stringer-stiffened shells. Internal loads at various longitudinal sections of the component are obtained using flexure and shear flow methods. External loads (bending moment and shear) are obtained assuming a lift distribution for the wing and inertial relief with trim and balancing loads from wing and tail for the fuselage. More details are shown in Figure 89 and Figure 90 for the wing and fuselage, respectively.

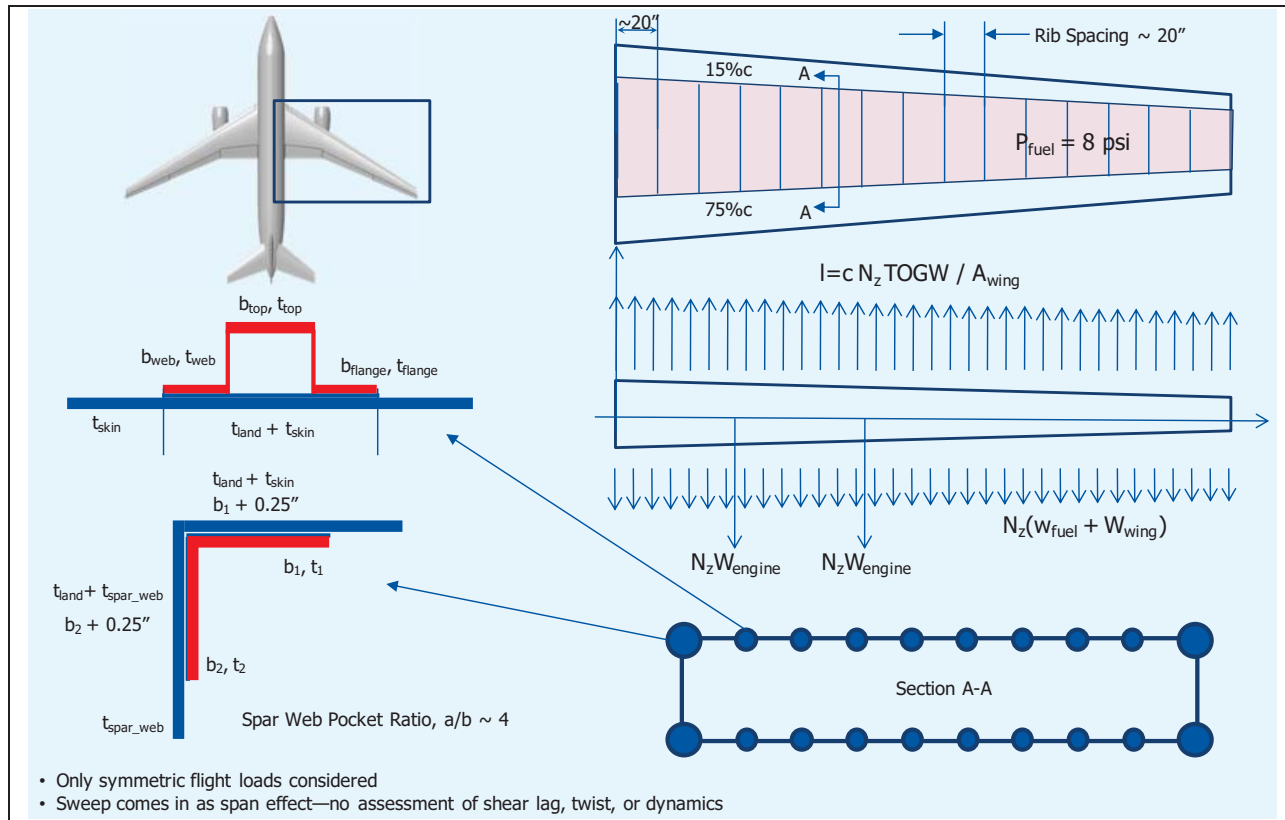


Figure 89 Set-up For Internal Loads Analysis of Wing Box

As shown in Figure 89, the wing structure is a two-spar configuration—i.e., single cell torque box—with integrally hat-stiffened upper and lower skins and angle spar caps. The spanwise-station cut cross-section is assumed to be rectangular for simplicity with depth equal to local maximum airfoil thickness. Rib spacing is variable, but for the study it was fixed at 20” based on historical usage—this spacing has been primarily set by column buckling of stiffeners. Stiffener spacing is such that the aspect ratio of the skin bay (i.e., skin between consecutive stiffeners) as defined by rib spacing to stiffener spacing is nominally around 4 for metals and 3 for composites. The lower aspect ratio for composite is to have enough skin between the hat stiffeners after accounting for drop offs from buildups in the skin under the hats and avoid non-optimal corrugated skin concept. Note that for tapered wings, each skin bay (i.e., skin between consecutive ribs) is analyzed as rectangular panel with short dimension equal to the box width at the mid-station between the ribs. Three load cases are considered: (1) symmetric maximum pull-up, (2) symmetric maximum push-over, and (3) fuel pressure. For the two flight loads, a trapezoidal lift distribution for 1-g flight at maximum fuel takeoff weight is scaled to the maximum maneuver load factor (2.5-g and -1-g). These two flight lift distributions are countered by inertial relief of fuel and wing weight distributed over the wing span as well as engine weight at appropriate stations. Wing weight distribution is determined from wing component weight from mass properties statement normalized by the wing area. Two fuel pressure cases are considered: (1) nominal pressure for skin pillowing in each bay and (2) stuck valve condition for stiffener/column bending failure. Note that ultimate pressure and flight loads are not combined.

Stringer forces are estimated using a common k-method flexure equation. Shear flow analysis is simplified by assuming a constant shear flow in the cross section and is determined by balancing external torsion to shear flow times twice the cross-section area. External torsion is determined by applying lift at ¼ chord and assuming the shear center to be at the flexural neutral axis. The vertical shear is evenly divided between the forward and aft spars. Note that wing sweep effect is limited to increase in span—i.e., the wing is de-swept to a straight wing with a longer span. Shear lag (load build up in the aft spar) and additional torsion are not considered.

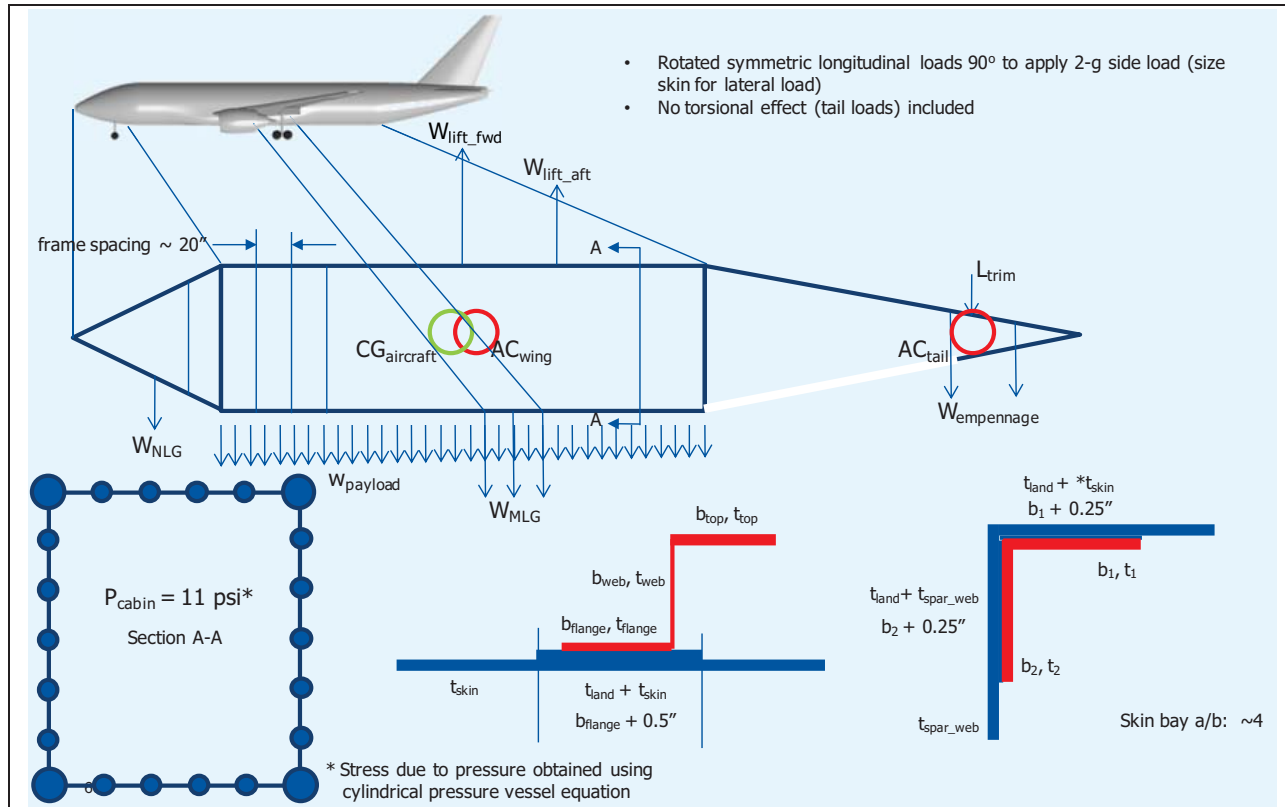


Figure 90 Set-up For Internal Loads Analysis of Fuselage Shell

The fuselage is modeled in a similar manner, but with integral z-stringers rather than integral hat stiffeners. The rectangular cross section is developed from circular fuselage by equating moment of inertia and circumference/perimeter. External loads is developed by balancing all non-wing and non-fuel mass items against lift from wing applied at estimated forward and aft spar carry-through pickup locations with tail trim. In addition to the two symmetric flight loads, one side load case is applied to size the side skins. The side load is essentially the -1-g push over case rotated 90° but with a load factor of 2. No torsion due to asymmetric flight case is applied. And, similar to the wing, internal pressure is also applied—a nominal flight pressure equivalent to 8,000 ft or about 11 psi. The stress analysis due to pressure is performed for circular fuselage, while stresses due to flight loads are performed for the rectangular equivalent. Note that the nose and aft fuselage taper, but the taper is only in depth and the width remains constant.

Two spreadsheet sizers—one for metallic wing and the other for composite wing—were developed. Shown in Figure 89 and Figure 90 are the design variables determined at each wing and fuselage bay using the gradient-based optimizer (“solver”) in Microsoft Excel. For metallic structure, the optimization problem definition was simple in that the number of design variables

was reasonable—in fact the ones shown in the figures. However, for a composite wing, all thickness-related design variables tripled from metals as 45°, 0°, and 90° plies were optimized. To reduce the optimization problem to a more manageable size, the composite wing and fuselage was sized in two nested loops, in which sizing was performed in four stages within the inner loop. The four stages consisted of optimizing the spar webs/side skins first, followed by upper skin, then the lower skin, and finally the spar caps/longerons. The outer loop controlled how many inner loops were performed—often three outer loops were enough to converge on a weight result.

	Metal	Composite
Material	• AL 7050	• IM7/epoxy unidirectional tape
Density	• 0.101 lbs/in ³	• 0.059 lbs/in ³
T_{min}	• 0.06"	• 0.052" (10-ply with 0.0052" tape
at Ultimate = 1.5 Limit	<ul style="list-style-type: none"> • tension/compression • wide column buckling • crippling (limit to 0.8S_{cy}) 	<ul style="list-style-type: none"> • FHT/OHC as a function of laminate • wide column buckling • crippling • stiffener/skin separation • bearing & bypass
at limit	<ul style="list-style-type: none"> • yield • fatigue with K_{IH}=3, K_{IL}=5.5 	• N/A
Stiffness	<ul style="list-style-type: none"> • I_v • dz waviness 	<ul style="list-style-type: none"> • I_v • dz waviness

- For bonded composites, used pi preform and assumed a minimum land thickness
- Only compression postbuckling considered

Table 11 Sizing Constraints and Failure Modes

Sizing constraints and failure modes to which the structures were sized are shown in Table 11. Materials chosen were 7050-T7451 aluminum plate and IM7/epoxy unidirectional tape. Note the density advantage of CFRP—it is 40% lighter. Minimum gauge is defined as 0.06” and 0.052” (10 plies of 0.0052” tapes) for aluminum and composites, respectively. For metals, two sets of failure analyses were performed, one at design limit load (DLL) and the other at design ultimate load (DUL=1.5 DLL).

At DUL, the structure should not fail by rupture, wide column buckling, and crippling. The crippling analysis is simplified by limiting compression stress in the stiffener to 80% of S_{cy}. Wide column buckling is performed on a unit strip of the stiffened panel, consisting of stiffener and half of the skin bay on each side. These two are the two modes of failure considered for postbuckled panels. Note that only compression postbuckling is considered—shear postbuckling and interaction are not in the interest of simplicity. Hence, postbuckling is limited to the upper and lower skins of the wing and fuselage. At DLL, fatigue and yield are checked. Fatigue is performed at the four spar caps and longerons for the wing and fuselage, respectively, and stress concentrations due to through-stress and bearing are included. For the wing, through stress is the same as the spar cap stress due to flexure while the bearing loads are determined from the forward and aft shear flow. For the fuselage, the through stress in the longerons are again due to flexure, but the bearing has two components—one due to hoop stress in the skins due to pressure and shear flow in the side skins.

For composite structures, only static failure at ultimate is considered. Fatigue (nor corrosion) is not considered as an issue for composites and hence one of the main reasons for using the material—to reduce the O&S cost. Two additional failure modes are considered for composites

at ultimate—bearing and stiffener/skin separation. If metals are weak in fatigue, composites are weak in bearing and must be considered for fair weight comparison in addition to obtaining the weight effect of bonded assembly. Stiffener/skin separation is one of the critical if not the most critical failure modes for postbuckled composite designs. Consideration of wide column buckling and crippling is not enough. Strength is checked off against stacking-sequence dependent notched allowables at appropriate environment.

4.2.2. Structures Trade Study Results

The weight effects of composite structural solutions to the wing and fuselage of the 1998 EIS aircraft were investigated. Specifically, the following were assessed using a spreadsheet-based structural sizing tool:

1. Minimum gauge
2. Bolted & bonded assembly (wing only)
3. Postbuckled structures

The results are shown in Figure 91 and Figure 92. Shown are percent weight change relative to all-metal baseline at the component-level—i.e., the weight consists of primary structure (single-cell wing torque box and the fuselage shell structure) and the remaining entities (secondary structures, any additional local “beef-ups”, high lift devices, etc) that in whole makes either the wing or the fuselage. Composite material assumed is IM7/977-3 type toughened carbon epoxy unidirectional tape with 0.0052” ply thickness. The reference metal is 7050-T7451 plate.

Weight reduction in the wing component due to composite structural technology is shown in Figure 91. For the wing, six composite structural configurations were sized. Each configuration reflects a level of risk associated with the composite technologies assumed. The least risk is associated with configuration 1 which assumes no postbuckling with bolted assembly and a thick minimum gauge at 0.14”. The highest risk configuration assumes a bonded assembly with minimum gauge of 0.052” (10-ply) and initial buckling allowed at 60%DLL (i.e., postbuckled skins which allows buckling of the skins in between the stiffeners at 60% of design limit load). As shown, the weight benefit increases with increasing risk levels. The lowest risk approach (Configuration 1) results in a weight reduction of 15.5%. Configuration 2 applies a thinner minimum gauge of 0.0936” while still bolted and non-postbuckled and results in additional 0.7% reduction over Configuration 1 resulting in 16.2% reduction relative to all-metal wing. Configuration 3 thins out the minimum gauge further to 10-ply at 0.052”. Similar to Configuration 2, the weight reduction is relatively small at 0.2%. The small changes in weight due to changes in minimum gauge definition are due to relatively small fraction of the structure being designed by minimum gauge criteria. The small depth of the wing results in low moment of inertia that can only resist bending via by adding thickness and such is the case for most of the wing span.

A decrement of 2.1% in weight is observed for converting from bolted to bonded assembly (Configuration 3 to 4) for wing structure with minimum gauge of 0.052”.

Configurations 5 and 6 reflect benefits due to post-buckled structures. The highest risk Configuration 6 with a minimum gauge of 0.052” and an initial buckling at 60% DLL results in a 20% weight reduction relative to the all-metal wing.

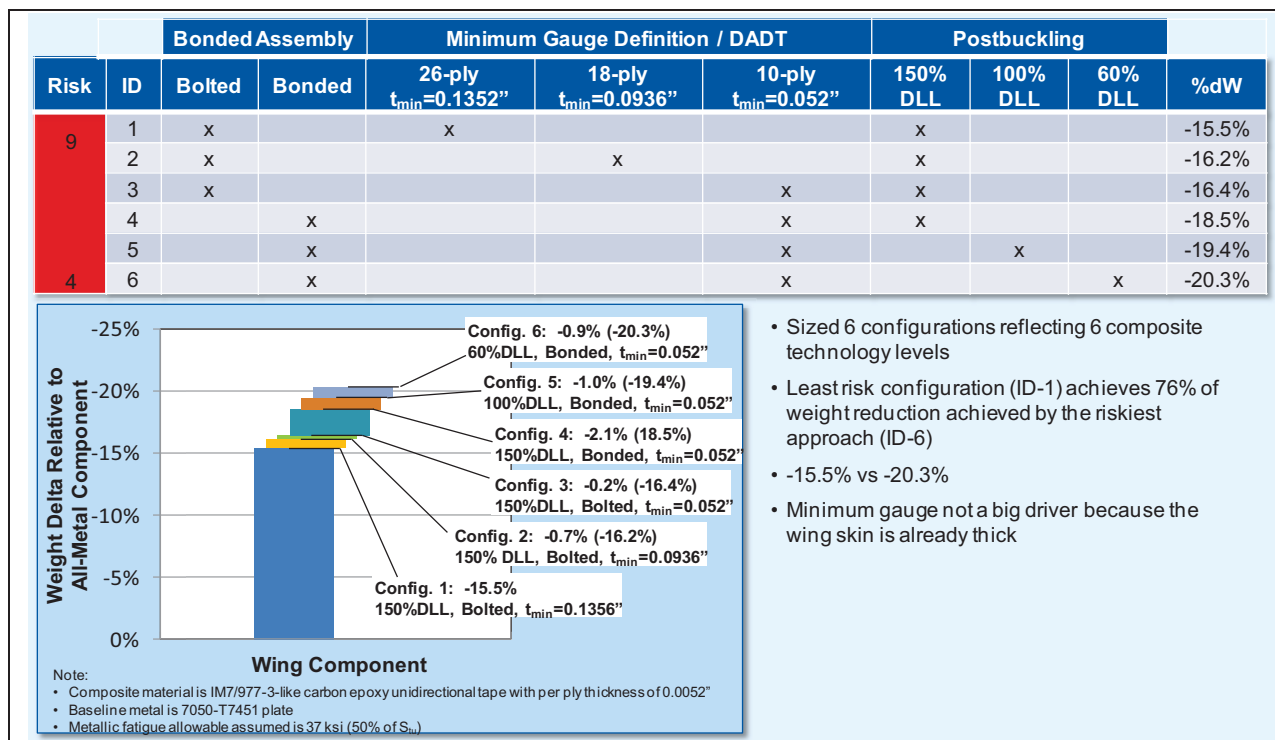


Figure 91 Wing Component Weight Reduction Due to Composite Structures Technology

Again, these six configurations reflect different levels of technology risks. The lowest risk approach—i.e., Configuration 1 with non-buckling skins with thick minimum gauge and bolted assembly is what can be done today and can be considered at a high TRL. The highest risk approach, with post-buckled skins with thin minimum gauge and bonded assembly, require some development in supporting technologies to truly enable the large weight reduction. These technologies include damage tolerant minimum gauge laminate design, bonded joint analysis methods, and bond integrity assurance methods. There are existing approaches to bonded joint analysis and bond quality inspection methods, but better approaches to the former will be required to extract the full weight benefit while enhanced interrogation methods during one or more processing phases (i.e., before-cure, during-cure, and after-cure—or pre-process, in-process, and post-process—phases) will be required for acceptance of bonded assembly by certification agencies. For reducing minimum gauge definition, laminate design concepts and improved materials concepts must be well characterized and proven, showing that less plies can still be used to meet operation in various levels of threat environment. Still, there exists many aircraft—particularly smaller commercial vehicles such as business jets—that are bonded. Military aircraft uses thin minimum gauge composite skins. For these realities balanced by the further developments required in supporting technologies for prevalent and optimized use of composite technologies for PSC, the highest benefit approach is judged to be at a moderate risk. Note, however, the comparison of TRL and weight benefit—i.e., the low-risk approach achieves 76% of weight reduction accomplished by the moderate risk approach.

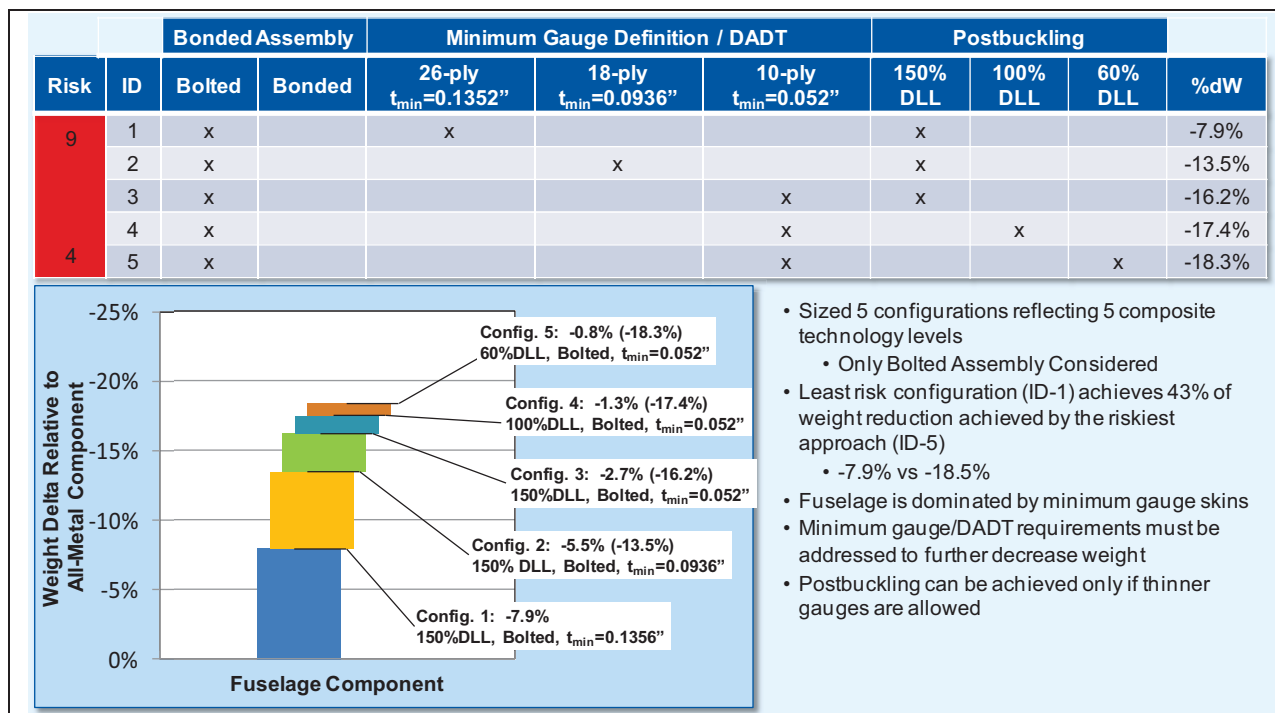


Figure 92 Fuselage Component Weight Reduction Due to Composite Structures Technology

A similar set of data is shown in Figure 92 for the fuselage component. The only exception is that the fuselage study is for a bolted assembly. Five configurations were sized, with the same range of minimum gauge thickness and initial buckling load levels, reflecting various levels of risk. Unlike the wing, the lowest risk approach with bolted assembly and thick minimum gauge at 0.1356" results in a weight reduction of 7.9% over the all-metal fuselage. Also, unlike the wing, a further reduction in minimum gauge thickness results in considerable reduction in weight. This is because bulk of the fuselage shell is dominated by minimum gauge skins as the much deeper section (as opposed to the shallower wing section) provides flexural rigidity just due to geometry and requires much less material to resist bending moment. In fact, if a 0.052" gauge is allowed with post-buckling at 60% DLL, an 18% weight reduction is anticipated. However, such aggressive application of composites to the fuselage is limited due to damage tolerance and durability reasons. For airliners concerned with operating cost of maintaining an aircraft, the fuselage structure should be tough enough to take the majority of anticipated impact threats and not require repair for the design lifetime of the structure—i.e., fly with invisible or barely visible damage. This requires a greater skin thickness that structural rigidity requirements alone. The approach is to thicken the skin and still incur benefit just due to lower density. This would be achieved by use of different minimum gauge in different regions—for example thinner gauge for upper or crown skin and thicker gauge for the lower/keel skin where most of the impact threat is likely to occur due to ground crew and debris. For the fuselage, post-buckled shell skins are less viable if not completely eliminated with increasing minimum gauge thickness. Hence, the post-buckled structure benefit shown in Figure 92 (as well as Figure 91 to some extent) is not applicable (i.e., cumulative) to the results with thicker minimum gauge.

Similar to the wing application, the five configurations can be ranked relative to TRL. Currently, thick gauged non-post-buckled bolted designs are flying. To obtain higher weight reduction, a much more aggressive use of thinner skin gauges must be allowed. For similar reasons discussed

previously, the most aggressive configuration is ranked as moderate risk. For the fuselage, however, damage tolerant minimum gauge laminate concept will be more critical than the wing.

In addition to assessing the effects of using composites, bonded assembly, and postbuckled structures, weight reduction due to i-ASE was also assessed. If materials and structural concepts address material reduction given a forcing function—i.e., load—i-ASE addresses that forcing function by use of flight controls technologies to reduce the internal loads experienced by the aircraft for same maneuver load and flight quality requirements. For this particular study, maneuver load alleviation (MLA) was mimicked by changing the lift distribution along the wing. Figure 93 shows the lift distribution and the sizing results. For this analysis, baseline lift distribution started off as elliptical. Three different lift distributions were then studied: (1) “50-50”, (2) triangular, and (3) triangular with MLA. The 50-50 distribution is an average between elliptical and triangular. The active control lift distribution was obtained by maximizing available section Cl_{max} along the span. This rigid section lift increment was modified by section elastic-to-rigid ratio assumed to be 0.9, 0.8, and 0.75 for the inboard, midboard, and outboard sections. The normalized lift distribution is shown in the upper right hand corner. The weight effect is shown in the lower left hand corner. Note that weight reduction is relative to an elliptical distribution. However, it is more likely that the actual wing will experience lift distribution closer to trapezoidal due to the tendency of swept wings to washout, resulting in reduced outboard lift. If we assume that 50-50 is the baseline lift distribution, the weight reduction at component level is estimated to be 4.5% for MLA based wing.

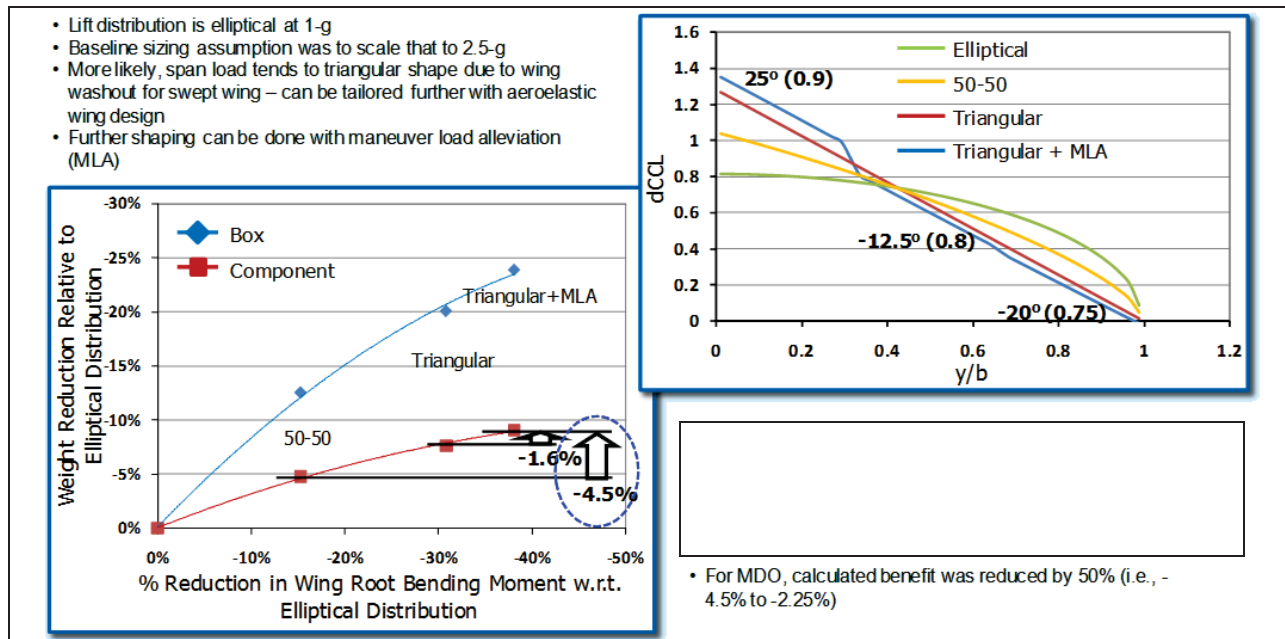


Figure 93 Effect of Maneuver Load Alleviation on Wing Weight

4.3. Aerodynamic Technology

Viscous drag is the primary contributor to the total drag of a typical transport aircraft in cruise. Of all viscous drag sources, skin friction drag is by far the largest component, accounting for as much as half of the total drag as shown in Figure 94 and as such, skin friction drag reduction has been sought for many decades as a method to reduce overall aircraft drag.

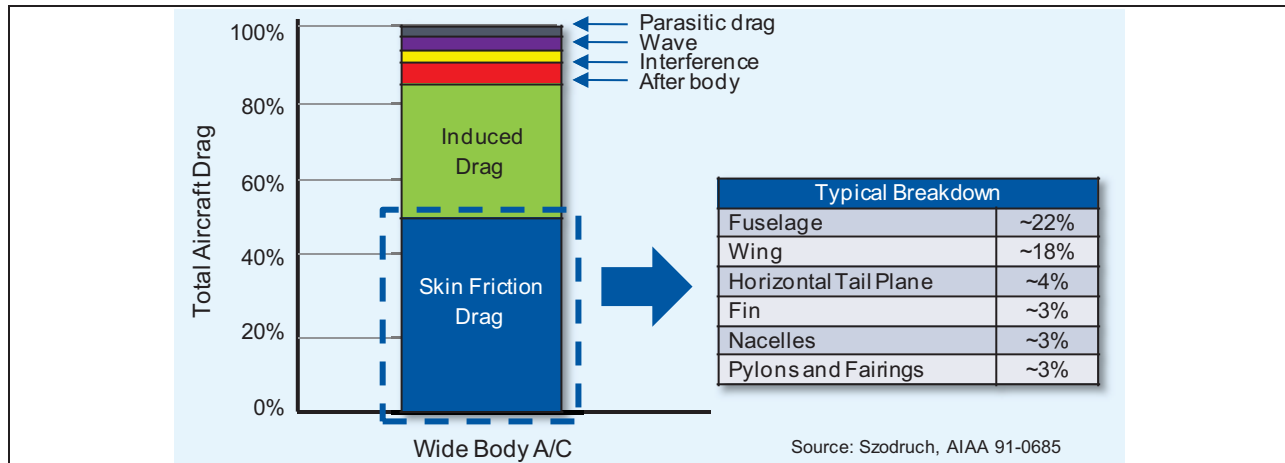


Figure 94 Typical Drag Breakdown for Wide Body Aircraft

Table 12 lists the aerodynamic technology candidates which address the reduction of skin friction drag via active and passive means. Swept wing laminar flow control and riblets offer passive solutions to reducing skin friction through shaping of pressure distributions and physical boundary layer manipulators, respectively, while hybrid laminar flow control combines passive shaping techniques with active suction to achieve the desired effects.

Aerodynamic Technologies	
Technology Name	Brief Description
Swept Wing Laminar Flow Control	Laminar flow through careful shaping of swept wing pressure distributions; up to 10% reduction in total drag
Hybrid Laminar Flow Control	Laminar flow through a combination of shaping of pressure distributions and active suction; up to 15% reduction in total drag
Riblets	Passive boundary layer manipulators, tiny grooves on the surface of an aircraft that reduce the skin-friction drag from turbulent boundary-layer airflow; 6-8% reduction in skin friction drag and 1-3% reduction in total drag

Table 12 Aerodynamic Technology Candidates

4.4. Propulsion Airframe Integration

Table 13 lists two propulsion airframe integration technologies being considered. Embedded high bypass ratio engine technology is enabled through the use of passive and active flow control techniques to prevent flow separation inside the inlet section. This provides improved pressure recovery and reduced L/D which is particularly critical for the passenger version of the PSC with its limited chord length due to the increased centerbody width over the cargo version. Shockwave boundary layer interaction control was also considered to aid in avoiding flow separation due to localized shock. This technology was eventually eliminated from the PSC technology set because the operating conditions for the PSC were subsonic at cruise and no aggressive forebody shaping was required and thus the formation of shocks are not typically present.

Propulsion Airframe Integration Technologies	
Technology Name	Brief Description
Embedded High Bypass Ratio Engine	Passive and active flow controls to prevent flow separation inside the diffuser; improves pressure recovery and reduces distortion; reduced L/D
Shockwave Boundary Layer Interaction Control	Passive and active flow controls to avoid flow separation due to localized shock; improves pressure recovery and reduces distortion

Table 13 Propulsion Airframe Technology Candidates

Embedded high bypass ratio engine technology was considered a relevant and time critical technology, particularly for the PSC passenger configuration.

4.5. Acoustic Technology

Table 14 lists the acoustic technologies evaluated for the 2025 vehicles to help reduce noise emissions and includes adaptive chevrons, airframe/pylon shielding, scarfed nacelle, spliceless inlet liner, and assembly fairings. These technology candidates which targeted acoustic source reduction were divided into two categories: “dedicated,” meaning that the technologies were essentially airframe specific and parasitic in nature and “engine-specific,” meaning that they were highly integrated into the engine architecture. Additionally, shielding effects are substantial and can be considered as an independent category. Note that each technology is not specific to every configuration. Instead, they were applied computationally as appropriate. For example, adaptive chevrons, scarfed nacelles, spliceless liners, and assembly fairings were applied to the 2025 baseline vehicles while airframe/pylon shielding, spliceless liners, and assembly fairing contributed to the PSC configurations.

The PSC configurations did not use leading edge slats or flaps for high lift on approach. While not considered a technology, the absence of these components was, in effect, the most effective reduction strategy for high lift related noise abatement. Though gear noise dominates the composite approach noise source signature, future advances in gear noise reduction technologies could reveal a clean airframe noise source with slats, flaps, gaps, and slots removed.

Acoustic Technologies	
Technology Name	Brief Description
Adaptive Chevrons	Trailing edge nacelle serrations immersed into the exhaust stream(s) producing stream-wise vorticity in the shear layer; decreased low-frequency noise intensity; moderate-minimal penetration; up to 6dB source noise reduction on take-off
Airframe Shielding, Pylon Shielding	Line-of-sight shielding of the source-receiver path; up to 10dB source noise reduction (middle frequency)
Scarfed Nacelle	Extended lower nacelle for forward radiated fan noise shielding; up to 4dB source noise reduction
Spliceless Inlet Liner	Conventional liner with zero-splice manufacturing capability; up to 14dB source noise reduction
Assembly Fairings	Wheel caps, gap fillers, component integration; up to 3dB source noise reduction

Table 14 Acoustic Technology Candidates

4.5.1. Airframe Propulsion Source Shielding

Undoubtedly, acoustic shielding is a very effective means of propulsion noise source reduction (as observed by ground-based sensors or individuals). Mass-law dependent, line-of-sight shielding presents a barrier between the fan, compressor, core, turbine, and portions of the jet plume and the observer. These effects are more prominent for high frequency components of the acoustic sources, and diffraction can reduce the effectiveness as virtual sources radiate sound toward the ground. Decreased distance between the source (i.e. the engines) and the airframe increase the effectiveness by providing greater angular coverage. Consequently, embedded engines provide the greatest amount of shielding while simultaneously yielding relatively long inlet lengths over which acoustic liners can be applied. Though the jet exhaust is a distributed source, the highest frequencies originate nearest the exhaust plane. Conveniently, these are the

easiest acoustic fluctuations to reflect via the introduction of an aft deck. Airframe shielding of propulsion associated sources is low risk.

All relevant acoustic technologies were at a sufficiently low risk and an acceptable small level of additional risk reduction activities is required for PSC integration. Therefore, no technology maturation roadmaps were developed since it is assumed the technologies are well advanced that no further investment is necessary for application into the PSC.

4.6. Subsystems Technology

Table 15 lists the subsystems technology candidates that were evaluated for inclusion into the PSC technology set. Most of the subsystems technologies were focused on the environmental control system (ECS) which, besides the engines, accounts for much of the power draw during flight. There are two ECS architectures that were assessed – an electric shaft power driven and a fuel cell based system that will be detailed in the following subsections. Carbon nanotube data cables are considered a time critical technology and are described further in Section 5.

Subsystems Technologies	
Technology Name	Brief Description
Environmental Control System Architecture	Development of electric air management system architectures focusing on both electric shaft power driven and fuel cell based environmental control systems
Efficient Power Electronics Controller	High switching speed and high temperature tolerance of silicon carbide (SiC) based power electronics can potentially reduce controller weight & volume up to ~50%
Efficient Refrigeration System	Advanced energy recovery vapor compression refrigerant cycle for reducing power input (up to ~30% over conventional system) resulting in more efficient propulsion system
Direct Jet-Fuel Fuel Cell Power	Fuel cell powered system using jet fuel directly without the need for fuel reforming; helps to eliminate the power extraction burden from the engine thus further improving propulsion system efficiency as well as reducing exhaust NOx
Fuel Cell Driven Integrated Power and Thermal System (IPTMS)	Integrated system combining APU, ECS and fuel cell functions into a single system that can significantly reduce exhaust NOx and acoustic levels during airport operation
Carbon Nanotube Data Cables	Carbon nanotubes provides good electrical conductivity and offers lightweight cabling solution for replacing copper braided shielding

Table 15 Subsystems Technology Candidates

4.7. Propulsion Technology

Table 16 lists the propulsion technology candidates. Core engine technology is a collection of 26 technologies that are being externally funded outside of NASA and thus are not evaluated in detail under this program. The benefits derived from this set of core technologies, however, were included in the engine decks. Of the six remaining advanced turbo fan technologies, embedded IP electric generator met the criteria for being a time critical technology and will be discussed in detail in Section 5 of this report.

Advanced Turbo Fan Technologies	
Technology Name	Brief Description
Ceramic Matrix Composite (CMC) Mixer	Low density ceramic matrix composite fluidic aerodynamic mixer between bypass duct air and turbine exhaust replaces heavier nickel alloys
Ceramic Low Pressure Turbine (LPT) Case Acoustic Treatment	Turbine acoustic attenuation using foamed ceramic materials
Organic Matrix Composite (OMC) Fan Case Acoustic Treatment	Acoustic attenuation using a foamed polymeric barrier that converts sound energy into low level heat energy, ~20dB attenuation
Flow Controlled Swan Neck Duct	Boundary layer control to delay flow separation to enable reduction in length of engine resulting in reduced weight
Super-Hydrophobic Anti-ice Coatings	Fan section anti-icing coating to minimize fan / stator aerodynamic effects of air foil icing
Embedded IP Electric Generator	Embedded starter/generator provide mechanical efficiency over hydraulics and eliminates traditional heavy gear box
Core Engine Technologies	Collection of 26 core technologies developed under a variety of externally funded programs

Table 16 Propulsion Technology Candidates

4.8. Technology Performance and Pareto Analysis

A Pareto analysis was performed to quantify the system level benefits of the technologies on the 2025 vehicles’ fuel burn. The analysis was performed on both variants (passenger and cargo) for the 2025 baseline and the 2025 PSC. The analysis provides the level of impact of each individual technology in reducing fuel burn by using the following process and approach:

- (1) Start with 2025 final vehicle design with all technologies activated
- (2) Deactivate given technology
- (3) Re-optimize vehicle design to minimize fuel burn
- (4) Record mission fuel burn
- (5) Reactivate given technology
- (6) Repeat steps 2 through 5 for all technologies
- (7) Find percent fuel burn increase from final design for each technology being deactivated

4.8.1. 2025 Baseline System Level Benefits – Fuel Burn

Result from Pareto analysis for the 2025 baseline for both the passenger (Figure 95) and cargo (Figure 96) show that the complete technology suite provides a 37.8% reduction in fuel burn for the passenger version and a 34.4% reduction for the cargo version. Of the candidate technologies that were integrated, advanced propulsion, swept wing laminar flow control, and composite wing structure have the most influence in reducing fuel burn in that order. It should be noted that advanced propulsion is a collection of the 33 individual engine technologies integrated together to achieve that degree of fuel savings. As expected, reduction of skin friction drag through laminar flow control played a large part in reducing fuel burn, especially since the technology had minimal weight penalties associated with it. A composite wing also had a large impact on reducing fuel burn through reduction in structural weight since the wing structures is the heaviest primary structural component of the vehicle.

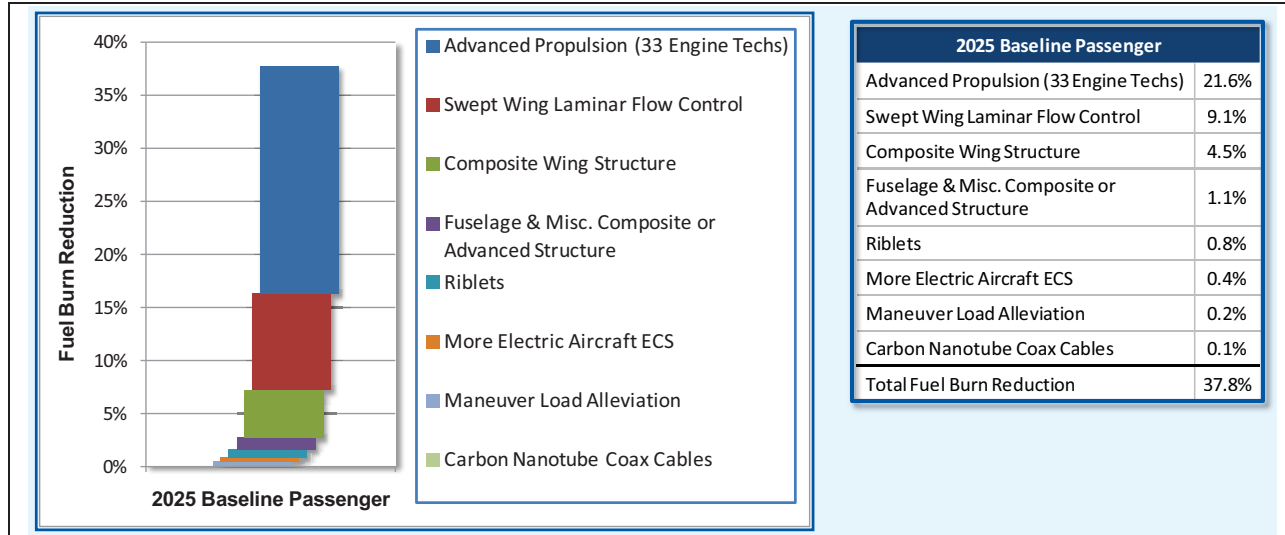


Figure 95 Pareto Analysis of Technology Benefits for 2025 Baseline Passenger

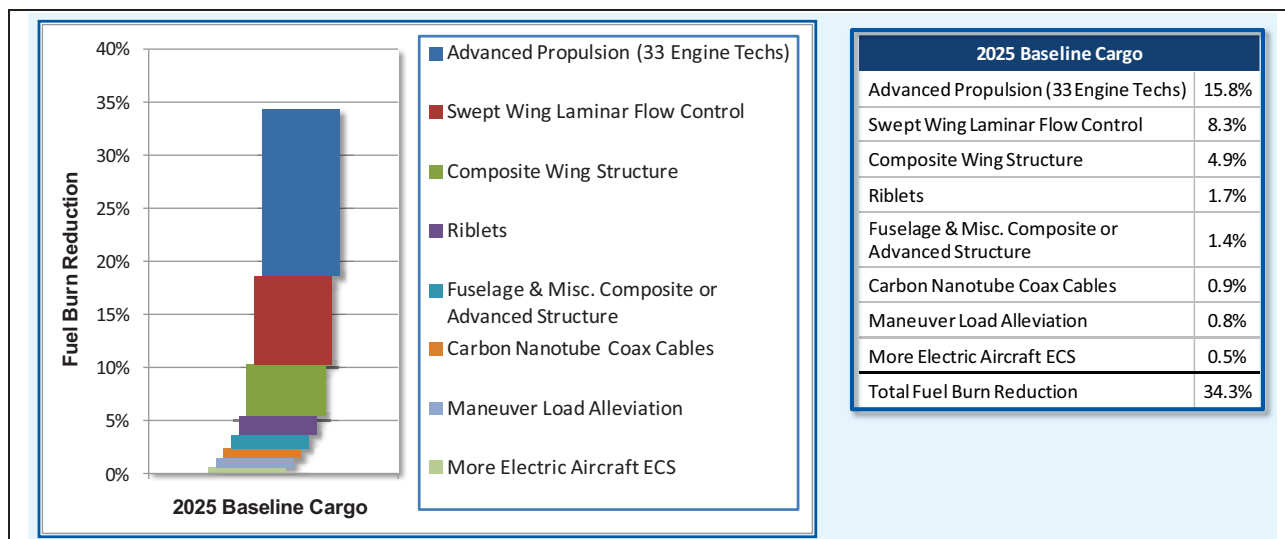


Figure 96 Pareto Analysis of Technology Benefits for 2025 Baseline Cargo

4.8.2. PSC System Level Benefits – Fuel Burn

Unlike the baseline analysis, for the PSC Pareto analysis, the embedded high bypass ratio engine technology was activated and embedded IP electric generator technology was separated out as an individual technology from the advanced propulsion technology set. Pareto analysis results for the PSC vehicles for both the passenger (Figure 97) and cargo (Figure 98) showed that the complete technology suite provided a 41.5% reduction in fuel burn for the passenger version and a 37.3% reduction for the cargo version.

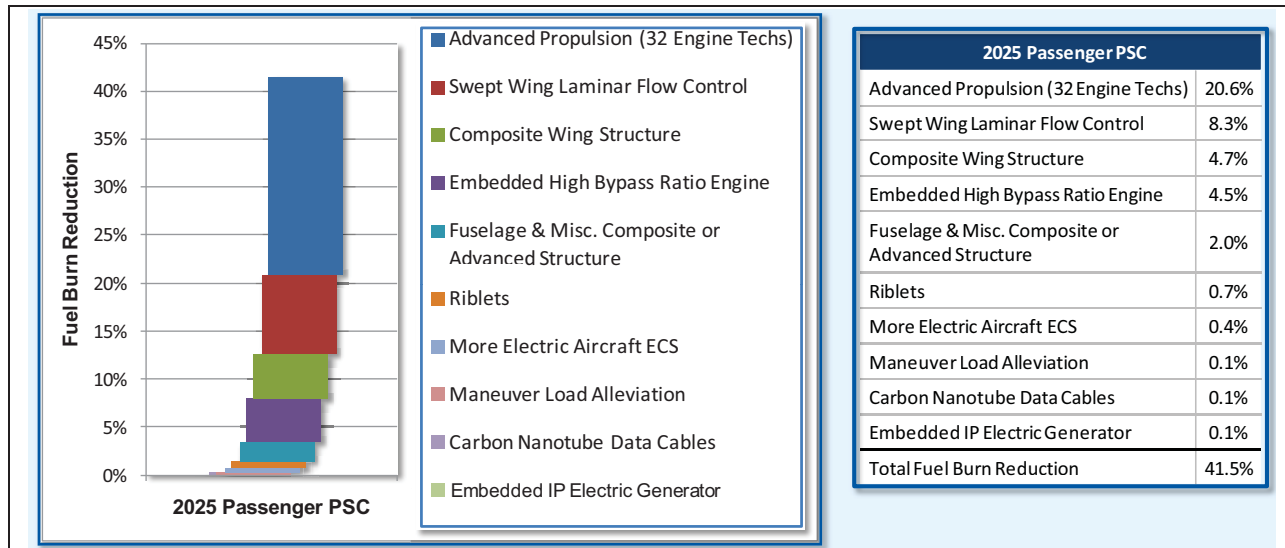


Figure 97 Pareto Analysis of Technology Benefits for Passenger PSC

Similar to the 2025 baseline Pareto analysis findings, advanced propulsion, swept wing laminar flow control, and composite wing structure also had the most influence in reducing fuel burn in that same order. However, embedded high bypass ratio engine technology played a significant role in reducing fuel burn for the PSC passenger configuration because of the limited chord length due to the wider passenger centerbody, resulting in a shorter inlet length. Inlet flow control was then critical for a constrained L/D inlet. The chord length on the cargo version was not as limited because the centerbody was narrower, allowing more room for a longer inlet and thus inlet flow control was not as crucial.

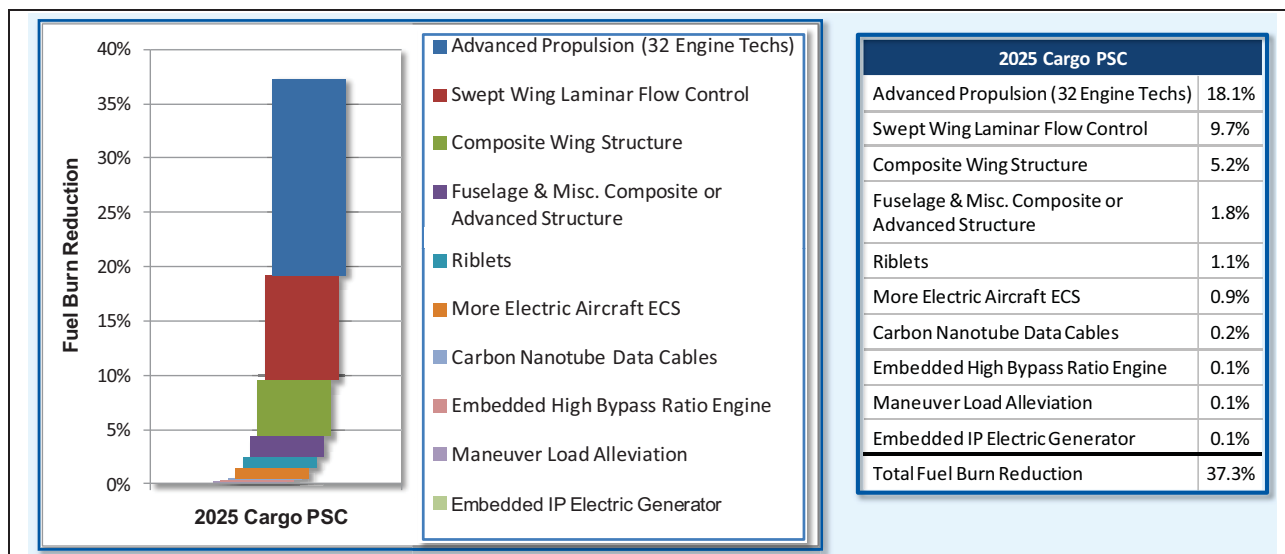


Figure 98 Pareto Analysis of Technology Benefits for Cargo PSC

4.9. System Readiness Level for PSC

The objective of implementing a system readiness level (SRL) is to provide an assessment and guideline of the risk and maturity of a system or a project. Proper SRL definitions provide exit

criteria that are used to generate metrics to help identify the level of maturity for each of the system disciplines including structures, propulsion, propulsion-airframe integration, subsystems (which also includes software, VMS, avionics), and logistics and support (which also includes testing, evaluation, training, data, and operations). The final product is to develop a system tool to help ensure that the system/project meets goals and objectives by tracking key outputs of individual disciplines at the technology, component, and subsystems levels.

Table 17 show the definition and corresponding exit criteria for each SRL level from 1 to 8. At a SRL of 1, system requirements are established and system concepts are being developed. At a SRL of 2, the architecture and system configuration design that will meet the requirements set forth at SRL 1 must be complete. Essentially, this will be the preliminary design review for the project. At SRL of 3, the exit criteria is the critical design review where the all the subsystem and component designs are complete and ready to be released for manufacturing. At SRL of 4, the hardware and associated subcomponents are built, assembled, integrated and tested for fidelity. Completion of ground testing and verification of integrated subsystems brings the project to a SRL of 5. Verification of the prototype system for its first flight takes the SRL to 6. At a SRL of 7, the system performance is assessed and validated in an operational flight environment. The results are analyzed to ensure they meet the original requirements and goals. Finally, certification and qualification in operational mission conditions brings the SRL to 8.

SRL	SRL Definition	Exit Criteria
1	System requirements established and system concepts developed	Systems concepts developed that have the potential to meet systems requirements
2	Architecture and system configuration design	Preliminary Design Review - architectural design of overall system that meets system requirements
3	Subsystem and component design; overall system performance analytically validated based on subsystem models	Critical Design Review – analytical design and validation of overall system and subsystems; detailed subsystem designs released for manufacturing
4	Hardware built and integration of subsystems	Components fabricated, assembled, integrated, and tested
5	Ground test and verification of integrated subsystem	Ground tests of integrated system in relevant environment completed and passed
6	Prototype system verified in flight	Flight readiness review; low speed/high speed taxi, first flight
7	System performance assessment and validation	Validated system performance in operational flight environment
8	System qualification and certification	FAA certification/qualification in operational mission conditions

Table 17 System Readiness Level Definition and Exit Criteria

5. TIME-CRITICAL TECHNOLOGY DEMONSTRATIONS

Task 4 identified time-critical technologies for the PSC vehicles, develops detailed roadmaps for the time-critical technologies and then prioritizes those technologies. Time-critical technologies are those that are critical to the development of the PSC vehicle(s) and that satisfy three major requirements as follows: (1) the technology benefits either PSC vehicle (passenger or cargo) in terms of meeting its goal levels for fuel reduction, NO_x emissions or noise; (2) the technology is required to meet performance objectives; and (3) the technology requires development tasks before 2016 in order to raise the TRL to 6 by 2020. Technologies that satisfy all three criteria are the “time-critical” technologies are the focus of Task 4.

Pareto analysis on the final 2025 PSC vehicles (see Section 5.1.1) has shown that the technologies of most benefit to the PSC (in terms of meeting its performance goals of reduced fuel burn, NO_x emissions and noise) are Swept Wing Laminar Flow Control (SWLFC), composite structures technologies, and engine technologies. However, benefit to the vehicle is only one characterization of the technology. To be listed on the Task 4 “time-critical” list, a technology must not only be on either PSC vehicle and benefit the vehicle and be required in terms of meeting its goals, but also be time-critical in that it requires development tasks before 2016.

This assessment of time-criticality was made based on the roadmaps developed in Task 3 as well as input from the subject matter experts (SMEs). This assessment was also made in conjunction with Task 5 and the technologies that are to be demonstrated on the STV. For instance, if a technology had a 4-year-long maturation plan to lower risk, as developed in Task 3, in theory this plan could be executed starting in 2016 and still reach TRL 6 by 2020. However, if the technology was to be demonstrated on the STV, flying in the 2016-2017 timeframe, then the maturation plan would have to be executed earlier, with some development tasks occurring before 2016, making the technology “time-critical.” It was decided to err on the side of being more inclusive of technologies in Task 4 rather than prematurely excluding technologies. Because Task 4 includes a prioritization task, less critical technologies can simply be prioritized lower than the most critical technologies.

Starting from the list of all technologies on the PSC vehicles, we excluded technologies that are already lower risk, only so only 9 technologies remained for consideration.

Reviewing the roadmaps for these 9 technologies developed in Task 3, only one technology, Embedded IP Electric Generator, has a technology maturation plan that is more than 4 years in length. However, the following technologies are slated to be demonstrated on the STV: Swept Wing Laminar Flow Control (SWLFC), Embedded High Bypass Ratio (HBR) Engine Technology, and Carbon Nanotube (CNT) Based Cables. In fact, for Swept Wing Laminar Flow Control and Embedded HBR Engine Technology, a demonstration of the technology on the STV appears on the technology development roadmap itself. Thus, each of these three technologies is also time-critical in that they require development tasks before 2016 in order to be demonstrated on the STV. Of the 6 Advanced Turbofan Technologies, only Embedded IP Electric Generator is time-critical due to the length of its technology maturation plan. The other 5 Advanced Turbofan technologies have maturation plans of 4 years or fewer and also are not slated to be demonstrated on the STV (which will have a different engine than the PSC).

Table 18 lists the subset of technologies from the PSC vehicles that are on the Task 4 time-critical technology list.

Technology Name	PSC vehicle application (cargo or passenger or both)	Current TRL	Demonstrate on STV?
<i>Aerodynamic Technologies</i>			
Swept Wing Laminar Flow Control	Both	3	Yes
<i>Propulsion Airframe Integration Technologies</i>			
Embedded High Bypass Ratio Engine Technology	Both	2	Yes
<i>Subsystems Technologies</i>			
Carbon Nanotube Based Cables	Both	4	Yes
<i>Advanced Turbofan Technologies</i>			
Embedded IP Electric Generator	Both	2	No (different engine)

Table 18 Task 4 Technologies

From the top-level roadmaps in Section 4, detailed roadmaps were made for each of the technologies in Task 4. These Task 4 roadmaps show more detail of the FY2013-FY2015 timeframe including necessary technology demonstrations.

5.1. Prioritized Technology Demonstrations

The technologies on the Task 4 time-critical technology demonstrations list are prioritized based on their overall benefit to the vehicle in meeting its goals (noise, fuel burn, and LTO NO_x emissions) and the time-criticality of the technology.

5.1.1. Benefit to Vehicle, Task 4 technologies

The overall benefit of each technology to the vehicle was determined mainly through a Pareto analysis to break out the individual technology’s benefit for both the cargo and passenger PSC vehicles. In the MDO analysis tool, starting with the 2025 final vehicle design with all technologies activated, the technology under study was then turned “off.” The vehicle was then re-optimized to minimize fuel burn and that minimum fuel burn was recorded for the technology under study. This process was followed for each Task 4 technology as well as for other major technologies on the vehicle for comparison. Thirty-two individual propulsion technologies were grouped into the “advanced propulsion” technology – this includes every propulsion technology except for Embedded IP Electric Generator, which is accounted for separately.

The individual benefits in terms of fuel burn reduction of each technology are shown in Table 19 and Table 20, for the cargo and passenger vehicle, respectively. Table 21 shows the same information, grouped by technology. Task 4 technologies are highlighted in yellow.

Technology	Fuel Burn Reduction
Advanced Propulsion (excluding Embedded IP Electric Generator)	18.1%
SWLFC	9.7%
Composite Wing Structure	5.2%
Fuselage & Misc. Composite or Advanced Structure	1.8%
Riblets	1.1%
MEA ECS	0.9%
Carbon Nanotube Based Cables	0.2%
Embedded HBR Engine Technology	0.1%
Manuever Load Alleviation	0.1%
Embedded IP Electric Generator	0.1%
Total Fuel Burn Reduction	37.3%

Table 19 2025 Cargo PSC

Technology	Fuel Burn Reduction
Advanced Propulsion (excluding Embedded IP Electric Generator)	20.6%
SWLFC	8.3%
Composite Wing Structure	4.7%
Embedded HBR Engine Technology	4.5%
Fuselage & Misc. Composite or Advanced Structure	2.0%
Riblets	0.7%
MEA ECS	0.4%
Manuever Load Alleviation	0.1%
Carbon Nanotube Based Cables	0.1%
Embedded IP Electric Generator	0.1%
Total Fuel Burn Reduction	41.5%

Table 20 2025 Passenger PSC

Technology	2025 Cargo PSC Fuel Burn Reduction	2025 Passenger PSC Fuel Burn Reduction
Advanced Propulsion	18.1%	20.6%
SWLFC	9.7%	8.3%
Composite Wing Structure	5.2%	4.7%
Embedded HBR Engine Technology	0.1%	4.5%
Fuselage & Misc. Composite or Advanced Structure	1.8%	2.0%
Riblets	1.1%	0.7%
MEA ECS	0.9%	0.4%
Manuever Load Alleviation	0.1%	0.1%
Carbon Nanotube Based Cables	0.2%	0.1%
Embedded IP Electric Generator	0.1%	0.1%

Table 21 Fuel Burn Reduction Benefit of Technologies on the PSC Vehicles

Because there are no acoustic technologies on the Task 4 time-critical technologies list, a benefit in terms of noise reduction is not shown for the Task 4 technologies of Swept Wing Laminar Flow Control, Embedded HBR Engine Technology, Carbon Nanotube Based Cables, and Embedded IP Electric Generator. The acoustic benefit of these Task 4 technologies is expected to be negligible and not a distinguisher. Likewise, the effect of the Task 4 technologies on LTO NO_x emissions is expected to be negligible and not a distinguisher. The benefits of the Task 4 technologies are best captured in the fuel burn reduction tables above.

5.1.2. Time-criticality, Task 4 technologies

The time-criticality of the technology can be determined in one of two ways. If the technology requires development tasks before 2016 in order to reach TRL 6 by 2020, then the technology is placed on the time-critical list. Or, if the technology is desired to be demonstrated on the STV, then it can also be placed on the time-critical list.

The assessment of time-criticality was based on both the roadmaps from Task 3, the overall length of the technology maturation plan, if the technology was to be demonstrated on the STV, and how critical that demonstration on the STV is to contribute to the overall maturity of the technology for the PSC. In Table 22 below, the criticality of the STV demonstration is shown as a rank from 1-3, where 1 is the most critical (relative to the other technologies) and 3 is the least critical. For instance, SWLFC is the number one priority of the STV demonstration because it involves the entire wing of the STV and therefore has interactions and integration aspects which involve many other systems on the vehicle. CNT based cables has the fewest interactions with other systems on the vehicle because it is a replacement of a subsystem component internal to the STV and therefore has the lowest rank criticality with respect to the STV demonstration.

Technology	Length of Maturation Plan to TRL 6	Demonstrate on STV?	Criticality of STV Demonstration, Rank
SWLFC	4 years	Yes	1
Embedded HBR Engine Technology	3 years	Yes	2
CNT Based Cables	4 years	Yes	3
Embedded IP Electric Generator	7 years	No, different engine	N/A

Table 22 Task 4 Technologies and STV Demonstration

5.1.3. Prioritization of Task 4 technologies

The Task 4 time-critical technology demonstrations, listed in priority order, are shown in Table 23 below. This prioritization is based on both benefit to the vehicle and time-criticality.

Priority	Technology
1	Swept Wing Laminar Flow Control (SWLFC)
2	Embedded HBR Engine Technology
3	Carbon Nanotube (CNT) Based Cables
4	Embedded IP Electric Generator

Table 23 Prioritization of Task 4 Technologies

Swept Wing Laminar Flow Control (SWLFC) is the first priority based on its benefit to the vehicle, and the time-criticality of the demonstration, and the criticality of the demonstration on the STV. SWLFC has the biggest impact on fuel burn reduction of any single technology and, as

such, is the top priority for the Task 4 time-critical technology demonstrations. Embedded High Bypass Ratio (HBR) Engine Technology is the second priority due to its benefit to fuel burn reduction, particularly for the passenger PSC. Carbon Nanotube (CNT) Based Cables is the third priority because of its benefit to fuel burn reduction is the third among Task 4 technologies. Embedded IP Electric Generator is fourth priority because its fuel burn benefit is the lowest of the Task 4 technologies. SWLFC, Embedded HBR Engine Technology, and CNT Based Cables are all planned to be demonstrated on the STV. Meanwhile, Embedded IP Electric Generator has the longest maturation plan of 7 years. The criticality of the SWLFC demonstration is the highest in Table 22 above, which only reinforces its top ranking in the technologies as shown in Table 23.

6. SUBSCALE TESTBED VEHICLE

6.1. Introduction

Task 5 developed a conceptual demonstrator aircraft representing the Task 2 Preferred System Concept (PSC) cargo aircraft (Figure 99). This demonstrator is known as the Subscale Testbed Vehicle (STV).

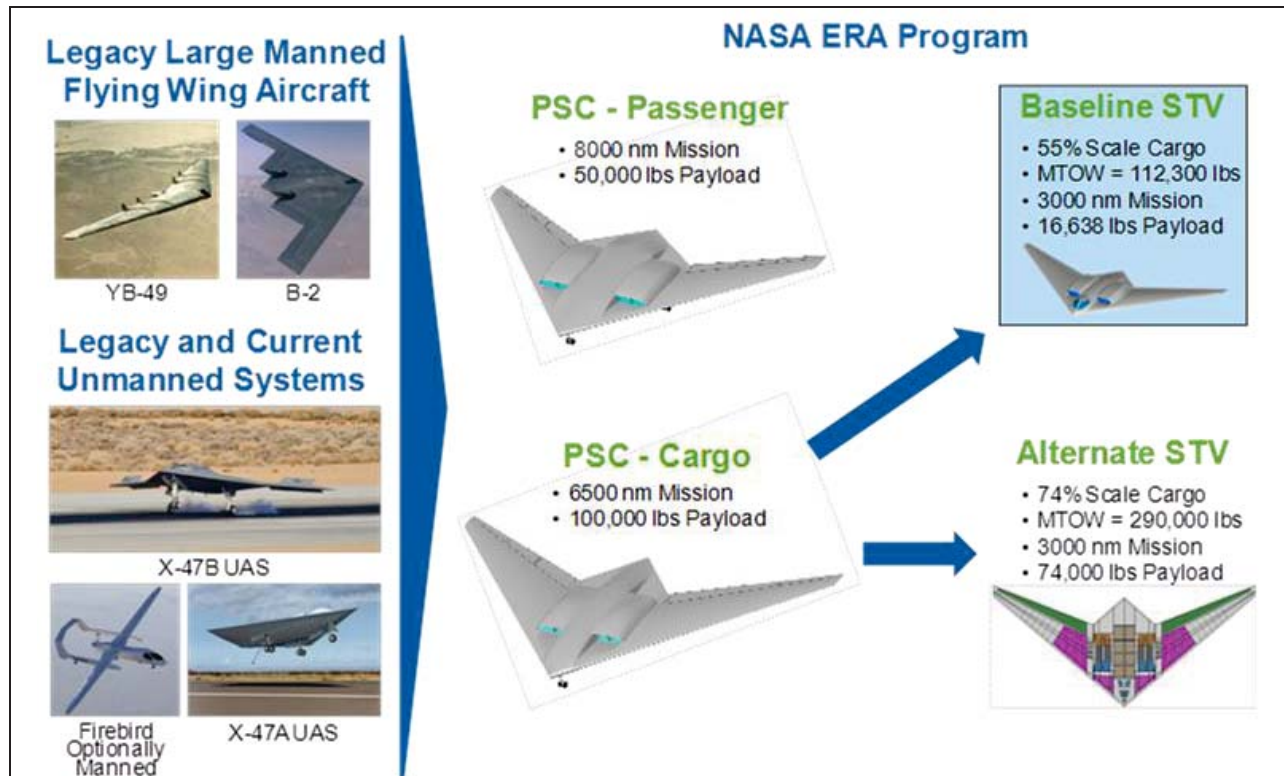


Figure 99 Vehicle Concept Lineage

Northrop Grumman has a legacy of designing and building successful large flying wing aircraft (e.g., YB-49, B-2). It was originally envisioned that the YB-49 could be developed into both a military bomber and a very efficient transport. Northrop Grumman has been the leader in unmanned air systems for many decades and continues its legacy with the X-47A and X-47B demonstrators. Recent efforts have unveiled a new type of unmanned system called “optionally manned.” This type of vehicle (Firebird shown) yields many benefits in both cost savings and versatility. This legacy of flying wing and unmanned aircraft experience was used to develop the ERA STV.

In the ERA program, Task 2 developed both a passenger and a cargo PSC. The STV is a 55% subscale demonstrator of the Cargo version (6500 nm mission range and 100,000 lb payload). The Baseline STV is has a design payload of 16,638 lb and design mission range of 3000 nm resulting in a takeoff weight of 112,300 lb. A larger 74% scale Alternate STV was designed that has a design payload of 74,000 lb and design mission range of 3000 nm resulting in a takeoff weight of 290,000 lb. The Baseline STV is the smallest design that will meet the technology demonstration objectives of the ERA program. The larger Alternate STV is the smallest design that will meet the large payload capacity that is needed for a demonstrator with significant residual operational capability.

The major features of the STV (Figure 100) enable simultaneous flight demonstrations by 2017 of an advance configuration, key efficiency technologies, noise reduction, and emissions reduction.

Key features that contribute to aircraft fuel burn reductions are:

- Efficient advanced vehicle concept (flying wing)
- Swept wing laminar flow control technology resulting in a cruise $L/D > 25$
- Advanced high bypass ratio ($BPR > 10$) commercial off-the-shelf engines

Key features that contribute to aircraft noise reductions are:

- Ultra low-noise propulsion integration
- Low-noise landing gear

Key features that contribute to LTO NO_x reductions are:

- Advanced engine technologies built into the latest generation of production engines

The STV will have operational capabilities including a state-of-the-art 2-pilot cockpit and a cargo bay with a built-in loading ramp. The STV design also has accommodations for future RPV and UAS operations.



Figure 100 STV Enables Flight Demonstration of Advance Configuration, Key Efficiency Technologies, and Noise/Emissions Reduction by 2017

During the design of the PSC cargo vehicle nominal real-world operational cargo densities were used (Figure 101). The highest cargo density transported with any regularity is 30 lb/ft^3 (e.g., alternators). For a demonstrator aircraft operational type cargo is not required, therefore a high cargo density was chosen that had an operational frequency of 1% (density = 22.6 lb/ft^3). Example types of cargo in this density class are machine parts and instruments. Both the Baseline and Alternate STVs use this density for their respective design payload, which determines cargo bay volume requirements.

The Baseline STV has a design payload represented by the following relationship:

- The STV design payload equals the PSC design payload times the scale factor cubed. This is also referred to as “volume scaling”

The Alternate STV has a design payload represented by the following relationship:

- The STV design payload equals the PSC design payload times the scale factor. This is also referred to as “linear scaling”

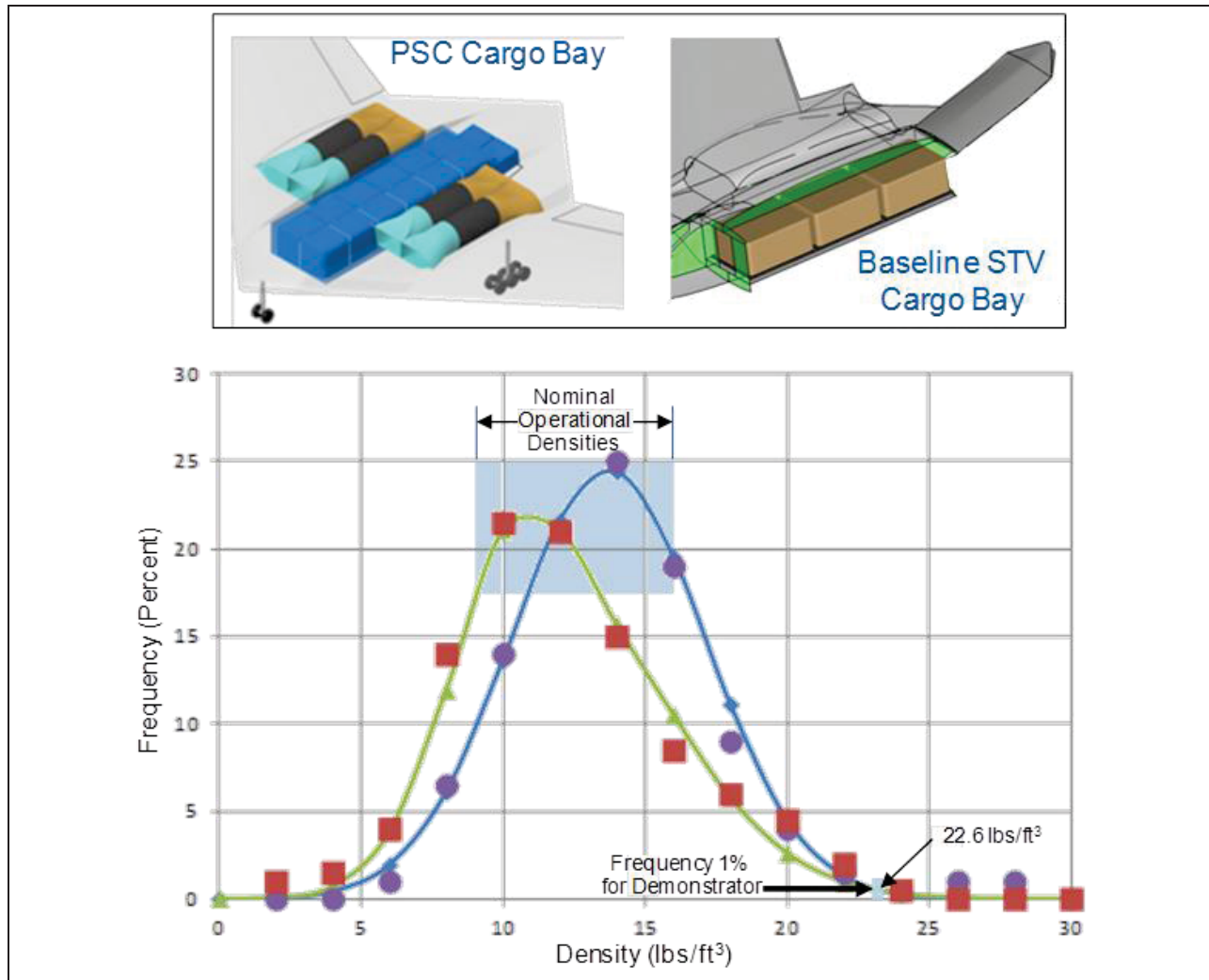


Figure 101 Frequency of Cargo Densities Transported on Operational Aircraft

6.2. System Requirements

The system requirements for the STV were derived from NASA’s program requirements for the demonstration vehicle and the concept of operation (CONOPS) guidelines developed and refined throughout the course of the program. With inputs from NASA including the statement of objectives for N+2 emission goals, the original NRA solicitation, the CONOPS and flight requirements; the system requirement specifications (SRS) were established for the STV demonstration vehicle. These specifications are the non-tradable ERA goals along with the derived specifications that define the flight capability and operation. As shown in Figure 102,

typically the SRS form the basis for the air vehicle (AV) requirement specifications, the mission control room (MCR) requirements specifications, and the support equipment (SE) requirements specifications. The figure shows the lower level of requirements for the AV generated during this conceptual design phase of the program. Initial SRS were developed and used to define the airframe, propulsion, avionics, subsystems and software design architectures. In Option 1 and 2 of the ERA program, these specifications will be formalized and put under configuration management. Other supportive plans and documents will be developed and matured as the program progresses. As the system requirements database matures it will be reported at the System Readiness Review (SRR), System Design Review (SDR), and Preliminary Design Review (PDR). Typical supportive plans and documents are listed in the figure.

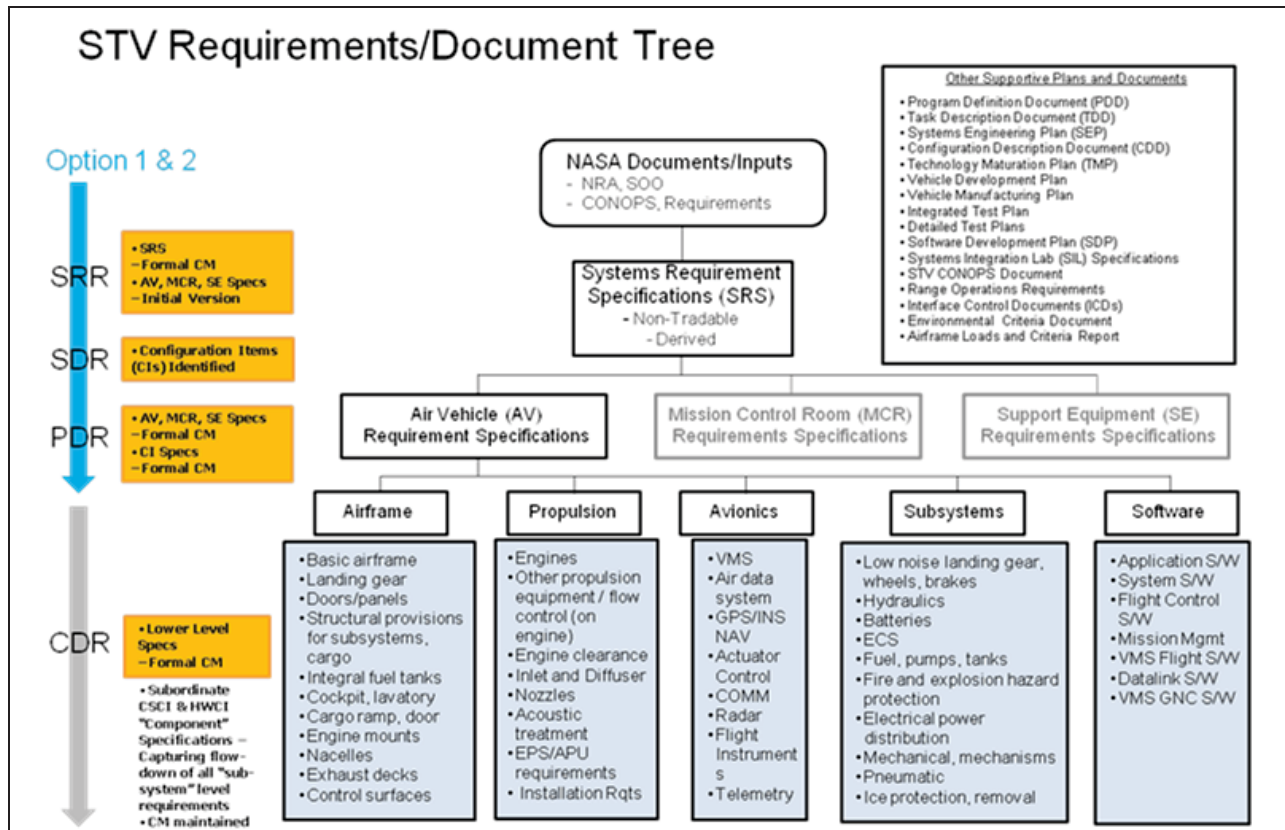


Figure 102 STV System Requirements and Document Tree

6.2.1. NASA Defined System Requirements

At the onset of the ERA program, NASA defined the mission requirements for the STV. The STV must be capable of travelling between all city pairs in the lower 48 states with the design payload and with 95% worst case winds. The design payload should scale from the PSC design payload with aircraft scale. The STV must be capable of using the top 100 busiest airports in the United States of America (US) meeting above payload/range with standard day conditions. Additionally, the STV must be capable of travelling to various domestic and foreign air shows (e.g., Farnborough, Paris).

The main objective of the STV flight program will be to provide quantitative evidence that the N+2 fuel burn, emissions, and noise goals can be met by the PSC. Also, future programs will

evaluate technologies needed for integrating unmanned aircraft systems (UAS) into the national air space (NAS).

These mission requirements govern the flight capability of the STV. The maximum speed versus altitude (right side of the flight envelope) will be determined by a constant dynamic pressure of 305 lb/ft². This number is used to size structure and determine mass properties characteristics. The minimum speed versus altitude will be determined by maximum lift coefficients versus speed, with a margin of safety. The maximum altitude performance of the STV will be determined by thrust (for selected engine) and drag of the final mission-sized STV, but will not exceed 50,000 ft altitude flight. The vehicle will be at least 50 percent scale of the PSC design and have a minimum wing span of 100 ft.

6.2.2. Concept of Operations and Derived Requirements

A concept of operations for the STV forms the basis for the derived system requirements. The STV will be operated as an experimental aircraft. It will be a piloted aircraft with crew of two and have a 20-year, 10000-hour life. Hardware and software validation and verification (V&V) will be for an operationally reliable fly-by-wire experimental aircraft.

The STV will have its crew and payload areas pressurized to allow crew and passenger comfort. Onboard ramps, doors, etc. for loading and unloading of crew, passengers and/or cargo will be provided. Pressurized crew and payload areas will be maintained at or below an 8,000 ft pressure altitude.

The STV will have some modularity features. It will provide accommodations for remotely piloted and autonomous operations for future studies. The capability for flying with the crew of two will be retained even during later autonomous operations. This allows flexibility in relocating the aircraft or returning the aircraft to maintenance facilities, as needed. The payload area will be reconfigurable allowing for passengers and/or cargo payloads. The payload area “may” also be retrofitted for military weapons bay and weapons release testing in future activities. The STV will have the capability to be re-engined during its 20-year life using commercial off the shelf (COTS) or developmental engines as they become available. The propulsion system will use engines with less than 32,000 lbf sea level static thrust.

Operationally, the STV will fly the same mission profile and reserves as the PSC. Average engine performance will be assumed. The fuel density is 6.7 lb/gallon with a 5% fuel flow rate design margin. The 1962 standard atmosphere and zero wind will be used for performance calculations. The payload of the STV will be retained for the entire mission.

Derived vehicle performance (range and field length) requirements will be based on a sizing mission and a check case. The sizing mission is a 3,000 nm range based on the worst case westbound route (Miami to Seattle: 2,400 nm great circle distance and 3000 nm equivalent still air distance (ESAD)). The field length requirement of 6,500 ft is based on worst case East coast airport. A check case for shortest West coast field length of 5,700 ft is required for a 2,400 nm mission. The STV will have the performance capability (range, balanced field length) to fly nearly all domestic mainland routes to simulate passenger and cargo service. It will be able to fly out of the 100 busiest US airports with its design payload on a standard day. It will be able to operate in all weather conditions including flying against 95% worst case winds aloft.

The STV will use standard airport support equipment with no special requirements needed. Its range capability will easily allow foreign operations (i.e., travel to air shows, etc.). Payload

requirements were derived for the STV to include weight, density, loading and payload versatility. The payload weight is defined to be 100,000 lb x (STV Scale)³ and payload density is determined to be 22.6 lb/ft³. Loading will be performed via an onboard aft ramp. The payload will use 463L pallets. Standard ground loading equipment and procedures will be used for the STV. No jacks or special landing gear will be required and no APU or ground cart will be required during loading and unloading.

The derived requirements for the avionics and subsystems architecture have been established. The STV will be required to meet high electrical power demands for a more electric vehicle. The STV will incorporate low noise landing gear and provide triple redundant flight critical actuation/hydraulic system. Due to the all weather flight capability, the IPS (Ice Protection System) must maintain laminar flow on leading edges. During flight, the STV will have electrically pressurized avionics, bays, and an electrically pressurized and conditioned cargo bay (ES/EPS). This will require four engine maintained generators. There will be an electrically pressurized and conditioned crew station. For safety, a continuous fuel tank inerting system will be required.

The derived requirements for the propulsion system will include an inlet design and bifurcated diffuser design to maximize pressure recovery. The propulsion flow path will require a buried installation to achieve pressure recovery and noise goals. A high bypass ratio engine installation has been selected to reduce temperatures for engine life and noise with the requirement for zero bleed air for more economical power extraction.

The STV will be fabricated and assembled at Northrop Grumman facilities in Palmdale, CA and transported via truck to NASA Dryden/Edwards Air Force Base (EAFB). The first flight and initial flight tests will be at NASA Dryden/EAFB.

It is envisioned that after delivery to NASA the vehicle will be based and maintained at Northrop Grumman facilities in Palmdale/Mojave, CA (on the West coast; main operational base), Baltimore, MD – BWI airport (in the Northeast US), and Melbourne, FL (in the Southeast US). These alternate basing locations would allow flexible and cost effective operations, maintenance and upgrade options during the 20-year flight program.

6.2.3. Validation and Verification

Northrop Grumman has a proven approach for verification and validation of aircraft systems. For the STV a top down allocation of requirements and bottom-up method of evaluation will be conducted to select a thorough and affordable compliance matrix and verification approach. Key features of the V&V approach will include a balanced distribution of verification methods, high fidelity modeling and simulation architecture for early system integration, followed by hardware-in-the-loop testing, including supplier components. This program will provide an assessment system using the Dynamic Object-Oriented Requirements System (DOORS).

6.3. Performance Sizing Trade Studies

The operational PSC cargo vehicle (Figure 103) was selected as the point of departure for configuration trade studies. The initial trade study STV used a preliminary PSC cargo planform. All subsequent trade study configurations were derived from the final PSC cargo vehicle. Mission sizing requirements were determined to be: 3,000 nm range using the NASA prescribed PSC profile, and 6,500 ft takeoff field length (TOFL). A check case of 2,400 nm and 5,700 ft TOFL was also imposed.

The propulsion assumptions used for the trade studies were based on the integration of five candidate engines (BR715, PW1000G, V2533, CFM56-5C and GE TechX). Note that Northrop Grumman developed an estimated model of the GE TechX engine expected performance utilizing the NASA Glenn Research Center developed Numerical Propulsion System Simulation (NPSS) software. This model is representative of the expected capabilities of the GE TechX engine; however it is not a GE issued model. The other engine models were obtained from the respective engine companies.

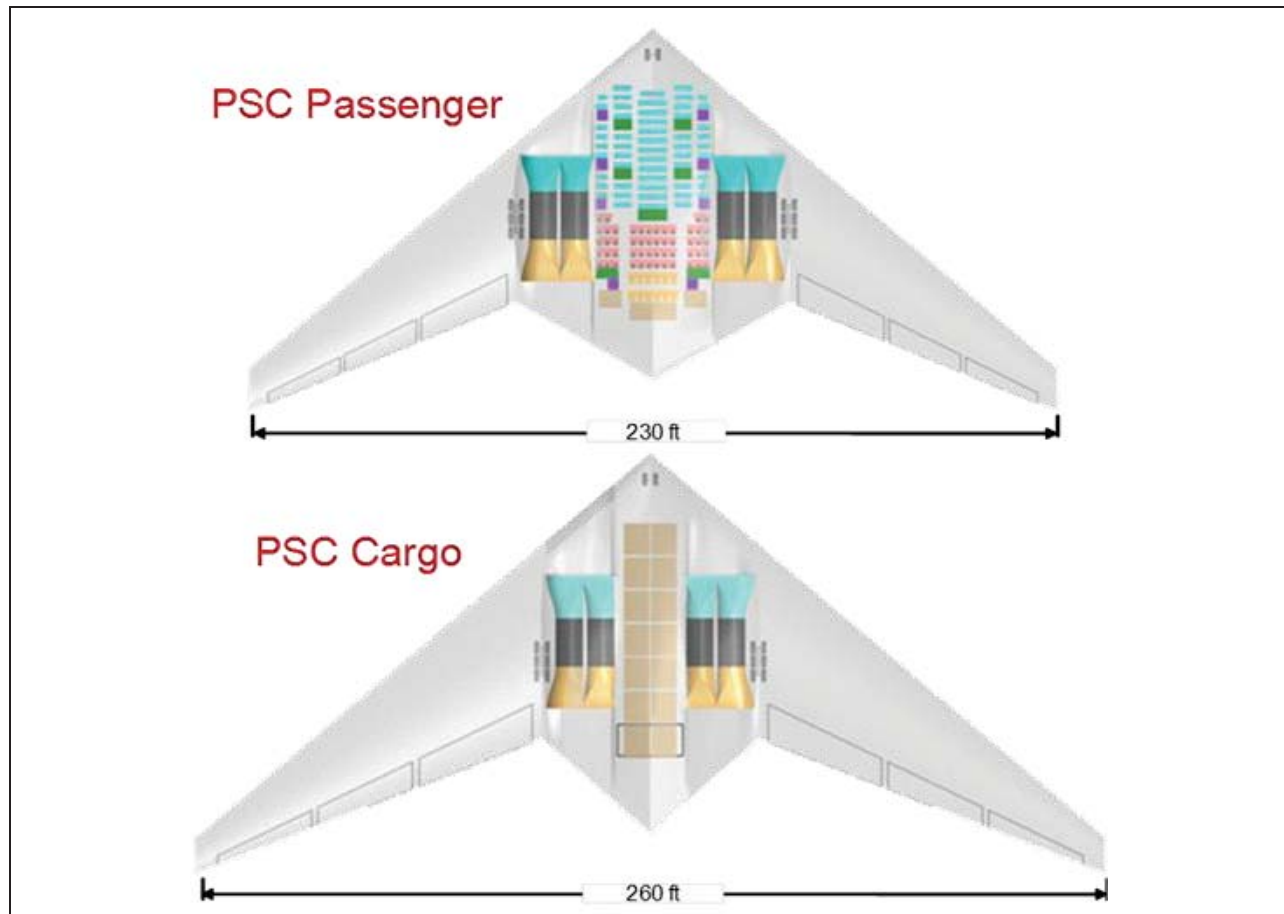


Figure 103 Sizing Trade Study Assumptions

6.3.1. Configuration Trade Space Overview

A preliminary 50% scale PSC vehicle that carried 50,000 lb of payload was initially studied and those results indicated a much bigger scale was needed to adhere to payload linear scaling. Those results led to an investigation to determine the minimum size vehicle with linear scaling of the payload using the defined density of 22.6 lb/ft³. This study revealed that a 74% scale vehicle that carried 74,000 lb of payload was the minimum size. Three candidate engines, the V2533, PW1000G and GE TechX, were examined for this configuration.

A trade study using payload volume scaling was then conducted. The objective of the volume scaling study was to determine the minimum size vehicle required to package the payload and the two leading candidate engines (PW1000G and GE TechX) within the airframe. The resulting designs were a 66% with 28,750 lb of payload for the PW100G engines, and a 55% scale factor with 16,638 lb of payload for the TechX engines.

A summary of the four configurations studied is shown in Figure 104.

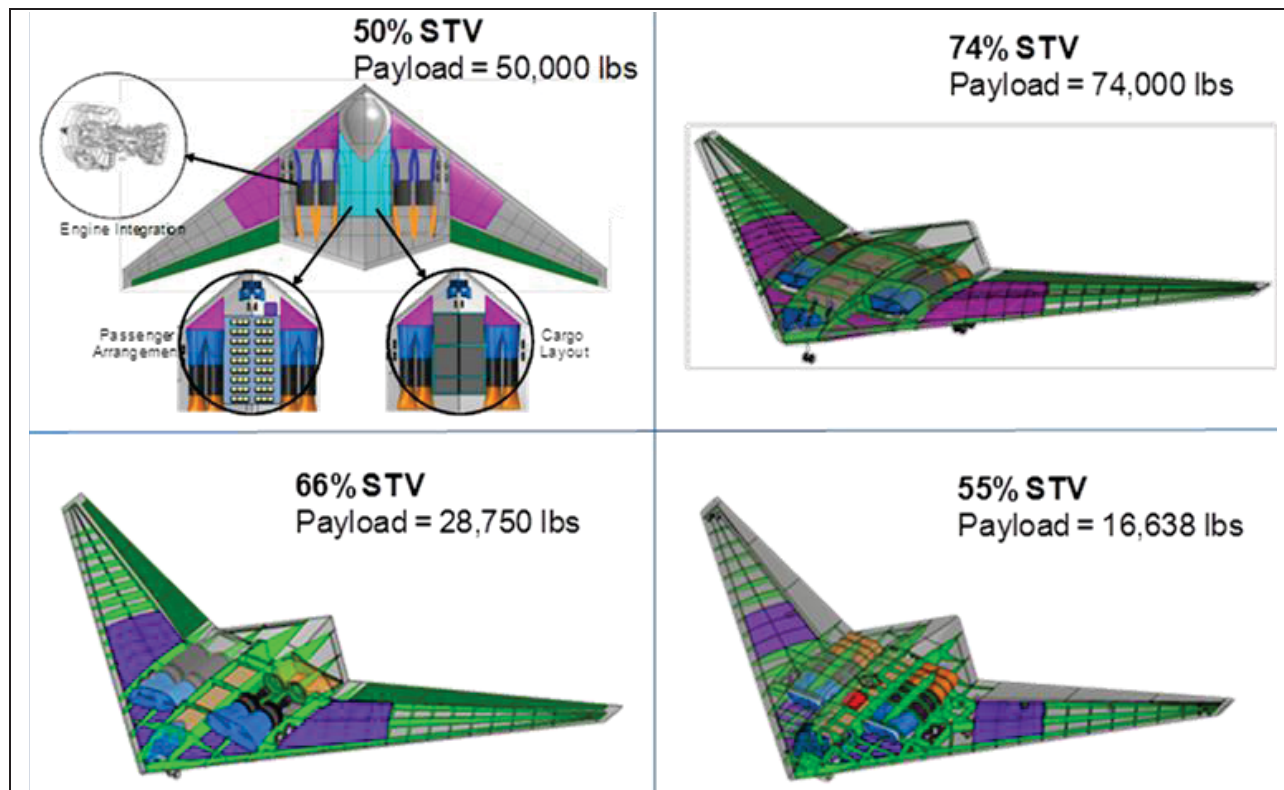


Figure 104 Configuration Trade Space Overview

6.3.2. Results for 55% Scale STV

This study found that a 55% scale vehicle with 16,638 lb of payload (linear scaling of payload) is the minimum required for integration of the GE TechX engines. An overview of the vehicle is shown in Figure 105.

The 55% scale design with GE TechX engines was selected as the Baseline STV. Overall, the STV configured with the GE TechX engine was found to be a good match between payload volume and engine integration requirements. The structural paths and details were workable and minimum OML changes from PSC vehicle were required. As the performance data in Table 24 shows, the GE TechX can easily meet the TOFL requirement. Takeoff distances with 20,000 lb and 16,000 lb engines are 2,700 ft and 3,250 ft, respectively. These thrust levels are NGC estimates of a future GE engine product, and were not provided by GE.

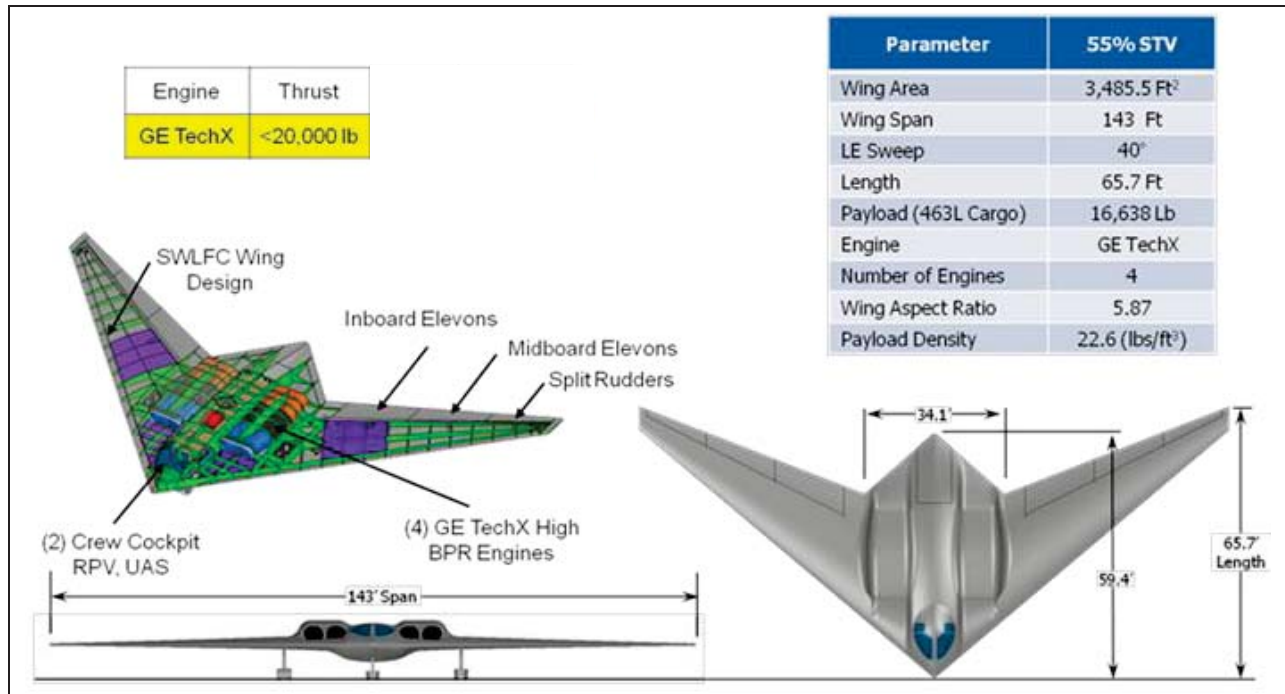


Figure 105 55% STV Overview

Parameter	Units	55% STV
Engine	-	TechX*
No. of Engines	-	4
Thrust per Engine	(lbf)	20,000
Wing Area	(ft ²)	3,485
TOGW	(lbs)	118,400
Weight Empty	(lbs)	69,405
Payload	(lbs)	16,638
Total Fuel	(lbs)	30,000
Range	(nm)	3,000
TOFL (SL, STD)	(ft)	2,700 / 3,250**
W/S	lbs/ft ²	34.0
Fuel Fraction	-	0.25

Table 24 55% STV Performance Summary

6.4. Configuration Integration and Structures

6.4.1. Configuration Design

The 55% scale Baseline STV (Figure 106 and Figure 107) evolved from the full size PSC cargo variant and trade studies described previously. The Baseline STV is the minimum size STV that can carry out the intended ERA technology demonstrations.

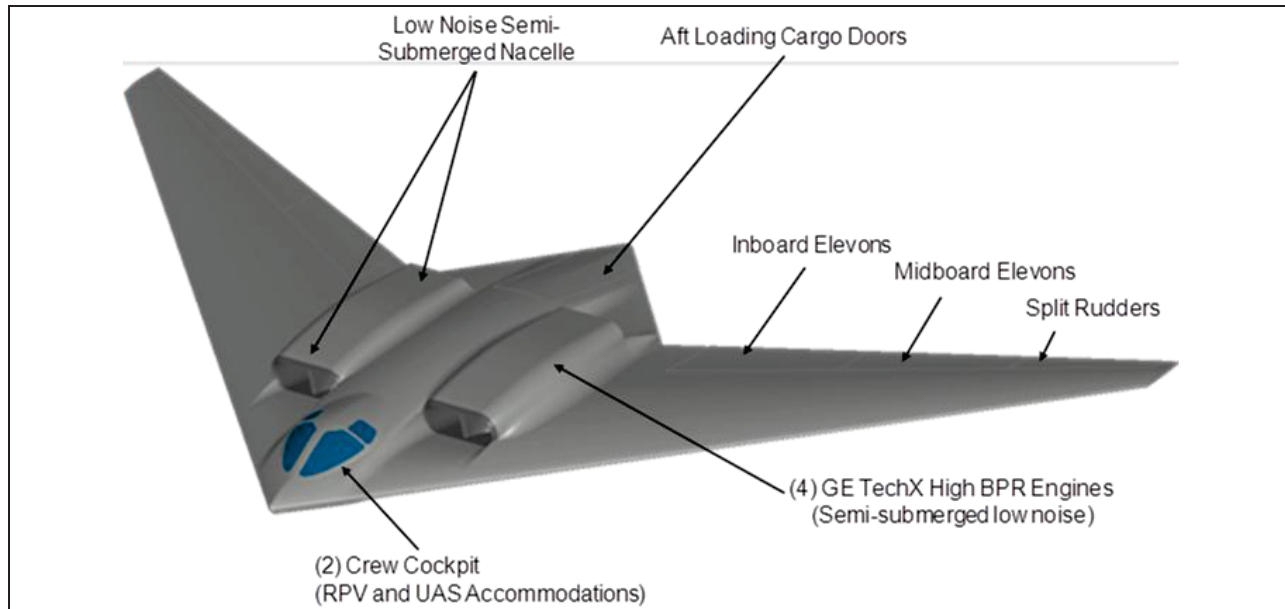


Figure 106 Baseline STV (55% Scale of PSC Cargo)

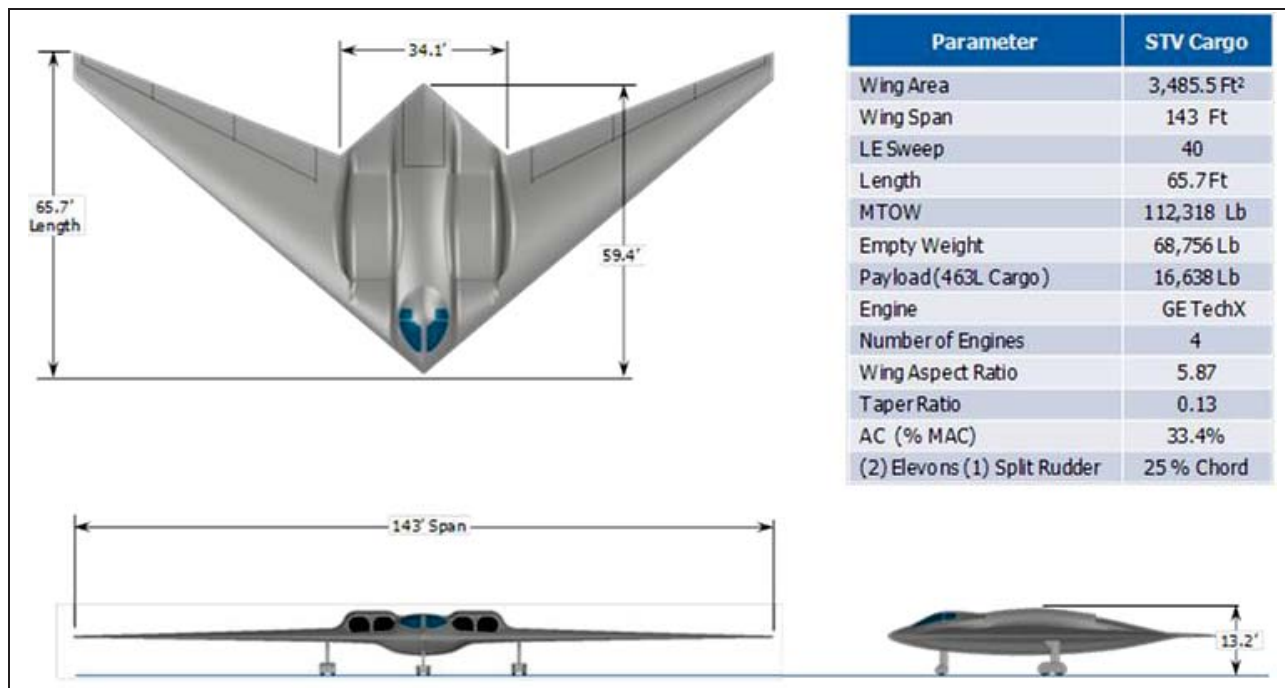


Figure 107 Baseline STV (3-View)

The sleek flying wing design can accommodate three standard military 463L pallets loaded with 5,546 pounds of cargo each. A challenge for this design was a propulsion path and structures integration of the four GE TechX engines (high pass ratio and semi-submerged approach). This integration challenge combined with the payload size and aft cargo loading drove the design and OML surface development.

The STV employs inboard and mid-board elevons, and outboard split rudder control surfaces. The initial sizing was with methods correlated to other Northrop Grumman aircraft. To provide suitable pilot visibility a raised level cockpit was required above the baseline scaled PSC OML.

This also provided enough room for nose landing gear housing and additional space for combined subsystems required for a remotely pilot vehicle and an autonomous unmanned air system. The OML of the aircraft are identical in shape to the full size PSC, except in the upper engine nacelle and cockpit areas as required to accommodate available engines and flight crew requirements.

6.4.2. Key Design Features

Key features of the Baseline STV employ technologies in fuel efficiency, noise reduction and reduced emissions (Figure 108). Semi-submerged high BPR engines coupled with low noise inlet and exhaust liner and retractable landing gear fairing technologies are planned to meet noise reduction demonstration needs. Swept wing laminar flow control combined with laminar flow compatible icing protection technologies substantially reduce drag. The cargo bay is pressurized with easy access to the avionics bay aft of the pilot in the cockpit and level with the cargo floor in the forward left corner of the cargo area. For safety, fuel tanks that are inerted with nitrogen enriched gas from the On-Board Inert Gas Generation System (OBIGGS) are used and located opposite of the avionics bay.

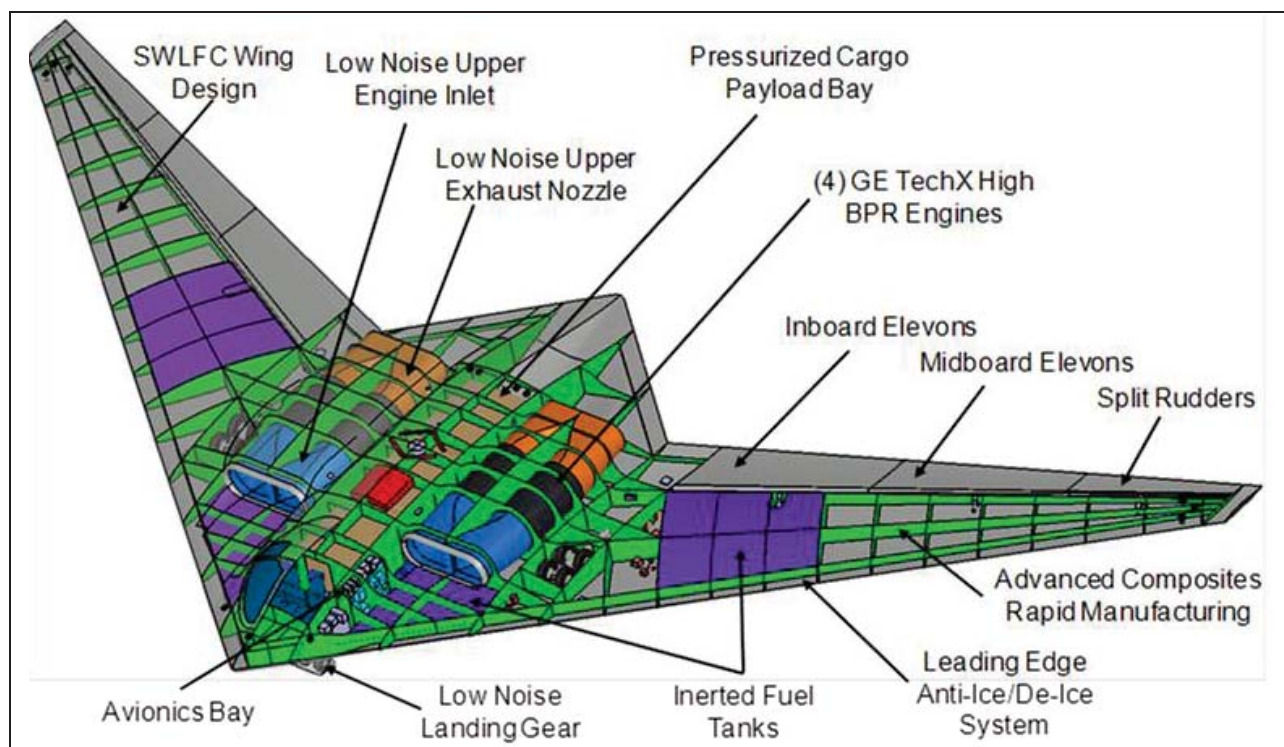


Figure 108 Baseline STV Key Features

6.4.3. STV Subsystems Integration

All required subsystems were integrated into the airframe and OML surfaces using legacy systems designs where applicable to show design feasibility (Figure 109 and Figure 110). Thought was taken to place systems for maintenance, function, service and repair. For example the centrally located avionics bay houses all VMS (vehicle management system), NAV, COMM, ADS (air data system), MM (mission management) and many support LRUs (line replaceable unit) for antennas, and many other sub-systems. With no obstructions to their view most antennas are located along the top and bottom centerline surfaces of the vehicle. The STV, even

though 55% of the PSC scale, has ample volume to house the subsystems and an OBIGGS with more than enough fuel volume. There are 22 air data probes located on the OML surfaces of the aircraft, six at each wing tip and the nose (both top and bottom), and four on top near the aft cargo bulkhead.

The green shaded areas in the figure show the cockpit and cargo floor structure. These below flight deck centerline areas also house antennas, radar and many subsystem components such as the flight actuator control system and mission management data systems. Access to these components can easily be accessed from outside or inside through removable panels. Main landing gear was logically placed outboard of the engines and the nose gear in between the radar and many other sub-systems not explicitly annotated.

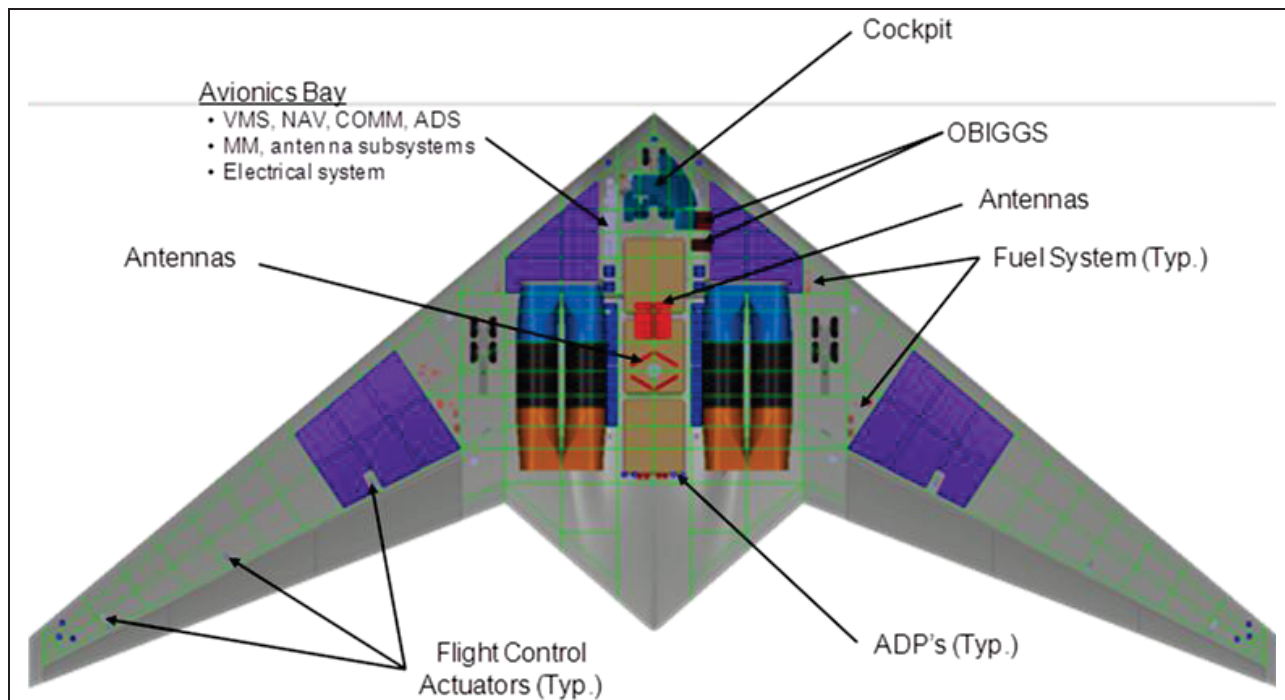


Figure 109 STV Subsystems (Plan View)

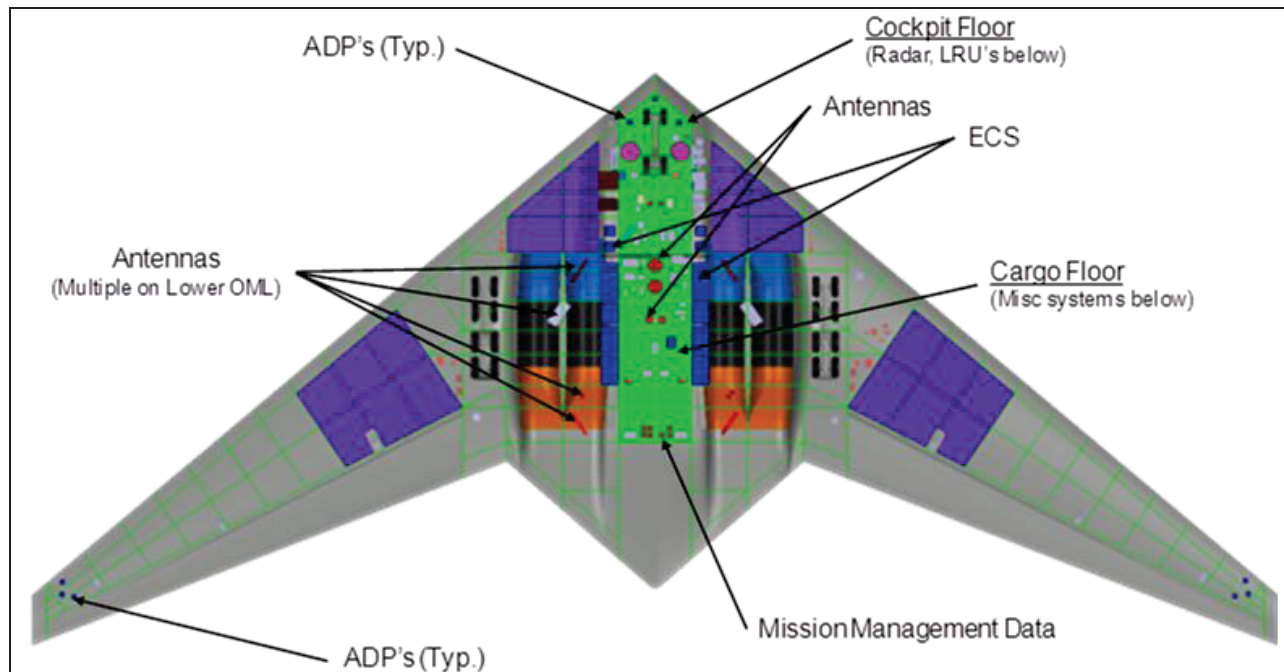


Figure 110 STV Subsystems (Bottom View)

6.4.4. Key Structures Design Drivers

A design driver was to create simple efficient primary load paths. The main internal structure of the STV consists of spanwise wing spars, frames and bulkheads, with longitudinal keel beams and wing ribs.

The challenge with integrating tall internal payloads and a large diameter engine inside the aerodynamically efficient OML is creating enough moment of inertia section depth above and below the internal components to minimize structural weight and keep wetted laminar flow areas feasible. These carry through load paths for the wing spar caps and shear-webs through the center “fuselage” section need to have adequate depth for tension and compression buckling while keeping angles shallow to allow the wing spar cap loads to go “around the corner” and gently transition from one side of the wing to the other.

Therefore, the strategy of the wing carry-through structure design is to tie into the three main wing spars and spread the spar cap loads out into multiple paths above and below the payload volume and four GE TechX engines (weight, volume, & dimensions estimated by NGC).

As shown in Figure 111, the key drivers to the structural design integration are:

- Propulsion path depth
- Military 463L pallet cargo height
- ECS depth and volume
- Main gear to wing spar attachment and depth

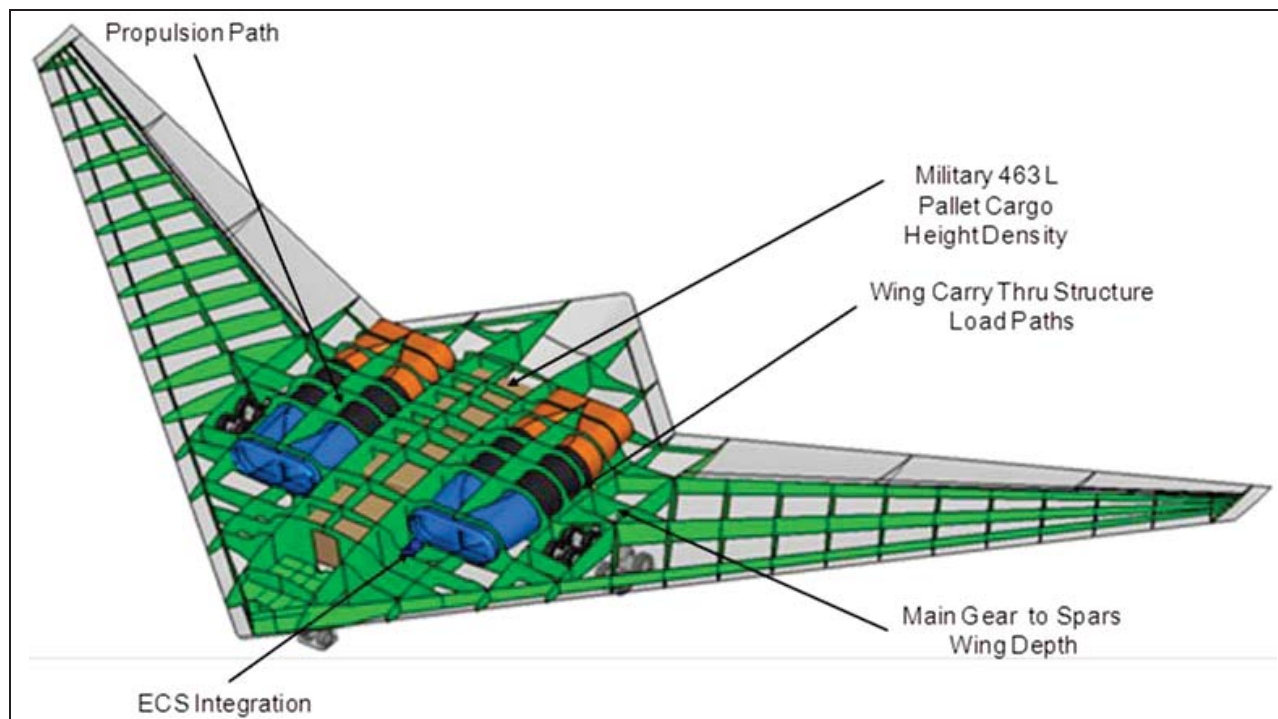


Figure 111 STV Key Structural Design Drivers

One of the main structural weight savings on the full size PSC is the use of advanced composite materials and processes. The STV airframe is to demonstrate the applicability of these structure technologies, however, due to the scaled nature of this demonstrator STV aircraft metallic materials may be utilized in certain areas due to geometric constraints around the key drivers. Material usages would be refined as the vehicle design matures in follow-on phases.

6.4.5. 1.4.5 Cockpit Design and Structures Integration

To allow for adequate pilot visibility and the envelope required for nose gear retraction a raised windshield and cockpit was required for the baseline STV (Figure 112). There is a small lavatory outboard and aft of the co-pilot with a step transition area from the cockpit floor to the cargo floor. This stepped volume aft of the pilots allows for miscellaneous storage and a small door from the cockpit to the cargo payload area. The nose gear wheel-well, cockpit and cargo floors are shown in red.

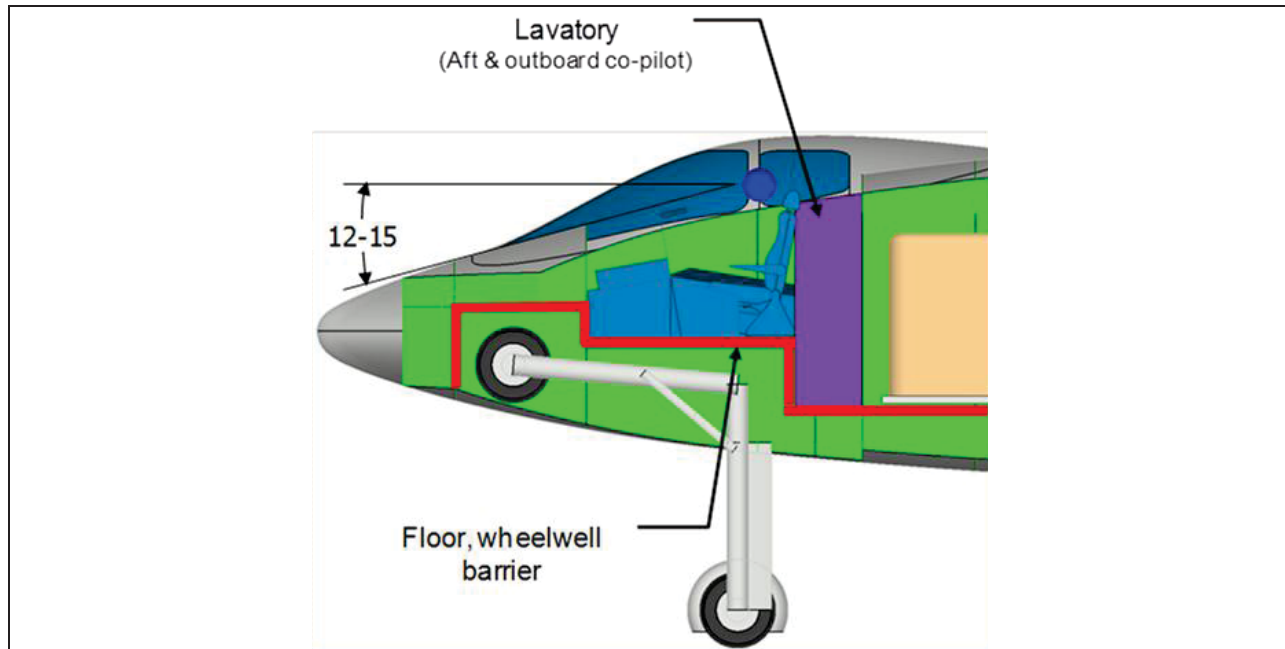


Figure 112 STV Cockpit (Centerline cross section)

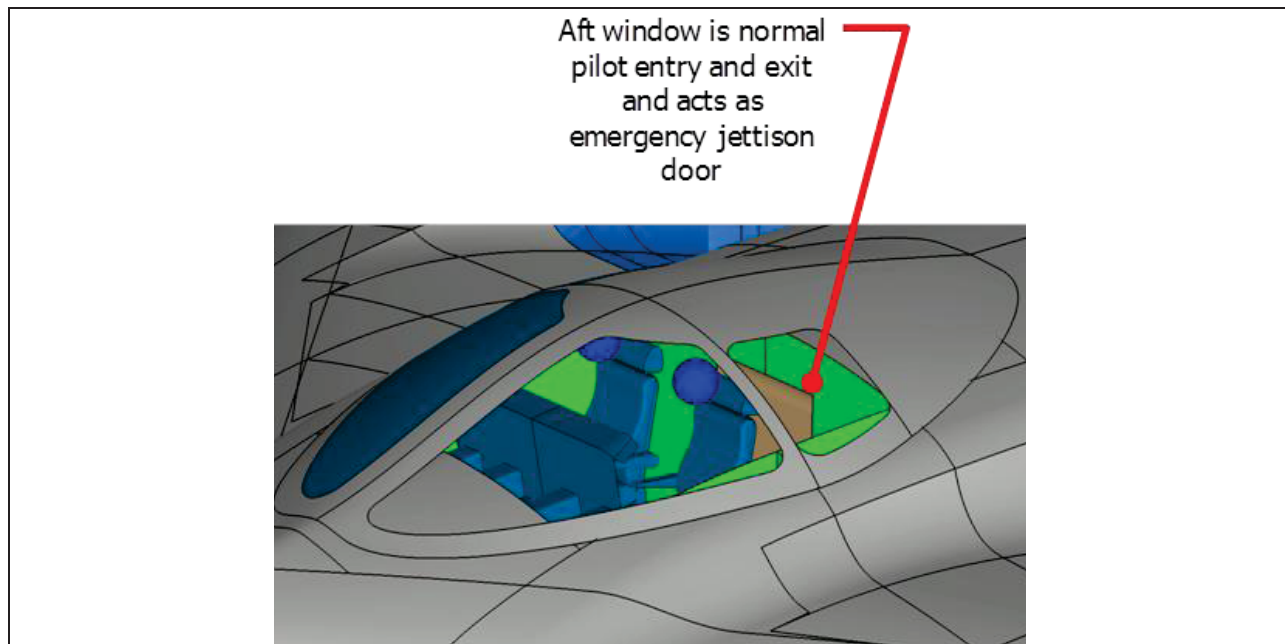


Figure 113 STV Cockpit (Isometric view)

Ingress and egress to the cockpit would be through the aft cockpit door from the cargo bay, if available, or through the aft window. In the event of an emergency the aft windows can jettison and act as escape doors (Figure 113). Visibility is also enhanced with these aft windows both in the air and on the ground.

6.4.6. Landing Gear Design and Structures Integration

The tri-cycle configuration landing gear (Figure 114) was positioned using standard conceptual landing gear layout practices. The TOGW center of gravity of the aircraft coincides well with

the aerodynamic center for the placement of the main gear. The nose gear was located to take 10% of weight of the aircraft. A conservative 14 degree angle was used for tip back and flare angle. Cargo and fuel location do not vary a great deal on flying wing aircraft. Standard off the shelf tires and wheels were chosen for the loads required. The main and nose gear use simple two piece split gear doors that close again after gear extension to close off the wheel-well cavities and reduce noise.

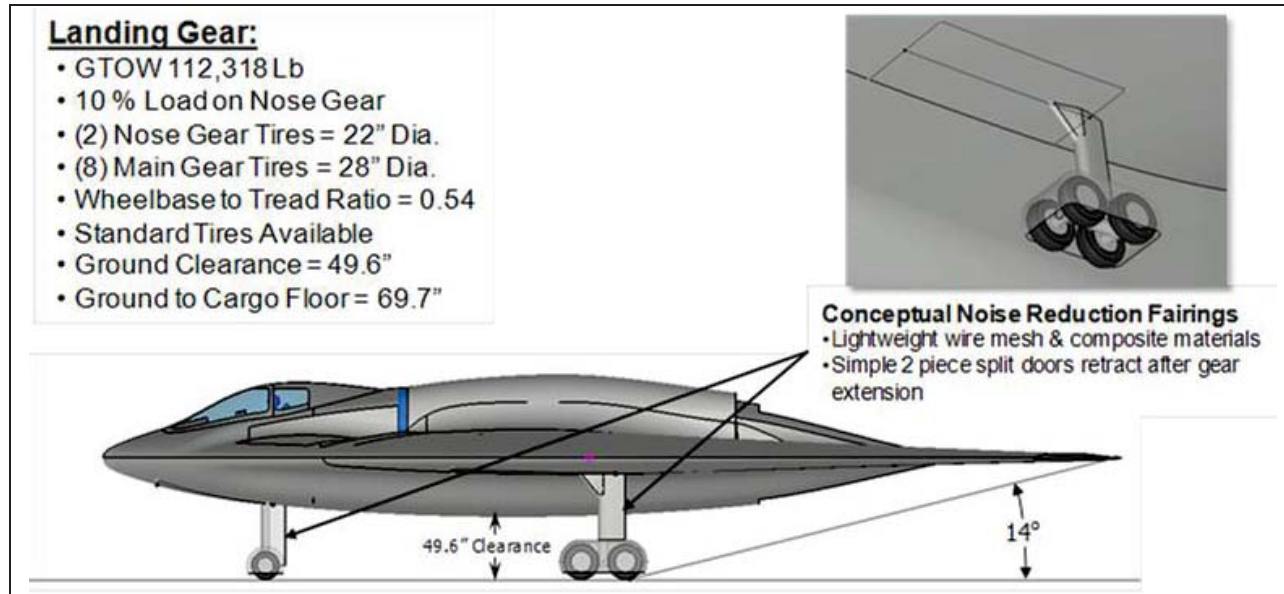


Figure 114 STV Landing Gear (left side view)

To reduce acoustic noise in the airport vicinity, aerodynamic acoustically shaped conceptual fairings were fitted to the main and nose gears. The concept consists of lightweight composite and wire mesh materials aerodynamically shaped to lower excessive noise created by exposed landing gear and retraction mechanisms. On both the nose and main gear simple inline drag braces were designed to minimize frontal area.

It is important to note the retraction and deployment of the both the landing gear mechanisms and fairings be done in parallel to create an integrated approach to simplify the design and internal volume required when the gear is retracted. The design of the fairings would be such as to be lightweight and withstand aerodynamic, dynamic and thermal loads. The service life, and maintenance requirement and overall cost of the fairings, due to the harsh environment they would be subjected to, would need further study. An easily repaired or replaceable fairing would be desirable with non-jamming reliability high.

Simple structural load paths for the nose gear and main gear loads are shown in Figure 115. The nose gear trunnion and drag brace tie into the two main keels that run full length longitudinally outboard of the payload envelope, by frames and bulkheads. In like manner the main landing gear trunnions tie into the middle wing spar via a carry through frame from side to side. Multiple load paths are available.

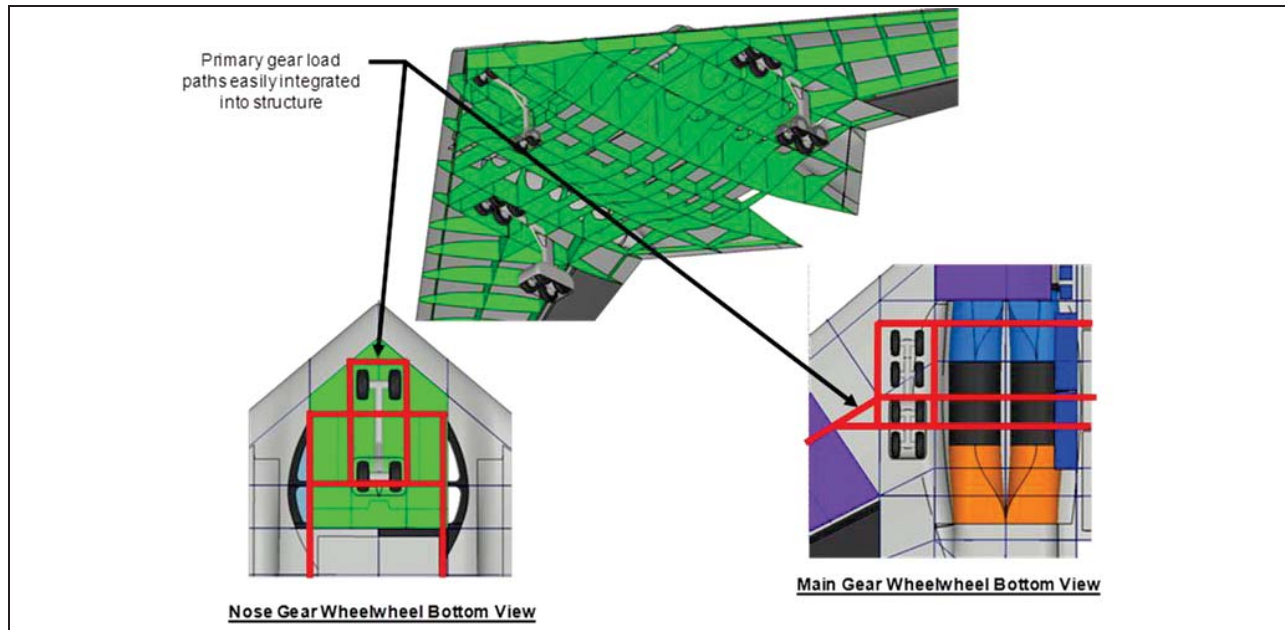


Figure 115 STV Landing Gear Structural Integration

6.4.7. Environmental Control System Structures (ECS) Integration

Another large essential subsystem was the environmental control system (ECS). Two systems are needed for redundancy. Initially a similar system to the PSC in size was considered; however, due to size constraints a re-packaged 737 system was integrated. The dual ECS system is installed just outboard of the main keels as shown in dark blue in Figure 116. An approximate 24-inch square frontal area gives the 12-inch lower spar clearance required. The volume inboard and below the inboard engines runs all along the propulsion path. No LRUs were placed inside the engine bays to allow for engine accessories and removal.

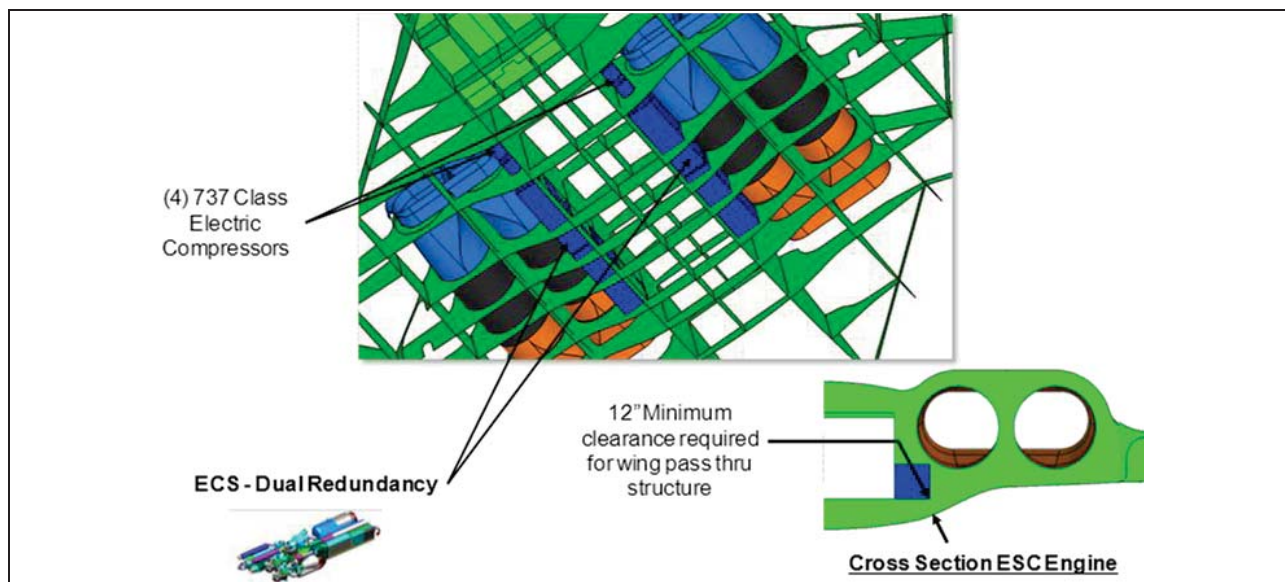


Figure 116 Environmental Control System (ECS) Structural Integration

6.4.8. Payload Structures Integration

The cargo payload volume allows for three 463L pallets 88 inches wide by 108 inches long spaced two inches apart using 2.63-in depth standard rollers in the floor structure. These rollers can be removed for other cargo types and to gain ceiling height. Ceiling and forward aft clearance is the military standard of 6 inches (Figure 117). A minimum of 12 inches was targeted for cargo structural floor depth and wing spar carry through height after trades done on the existing military cargo aircraft such as the C-130 and C-17. Spar cap depth at the wing spar carry points easily meets this similar requirement for propulsion integration.

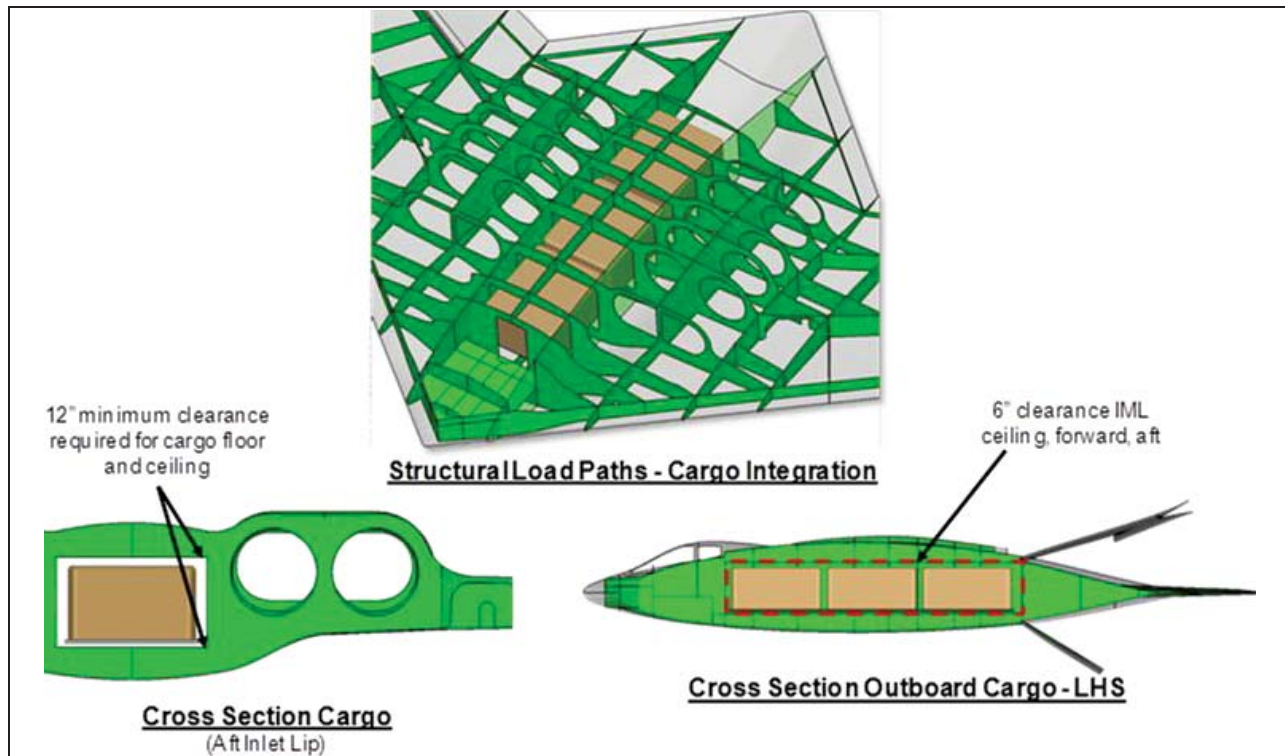


Figure 117 STV Payload Structural Integration

6.4.9. Payload Cargo Loading Integration

Standard 463L pallets were chosen as the basis for STV cargo payload. These somewhat light pallets (290 lb tare) are 2.25 inches thick by 88 inches wide by 108 inches long. The cargo is tied down with one top net and two side nets that weigh 65 lb. The cargo footprint on the pallet per Air Force standards is 84 inches by 104 inches. The maximum capacity of the HCU-6/E pallet is 10,000 lb up to a 96 inch cargo height. The three STV pallets are loaded with 5,546 lb of cargo each totaling 16,638 lb. This equates to a cargo density of 22.6 lb/ft³.

The military typically uses various forklifts and raised platform type equipment to load cargo on their freighter aircraft. A small Atlas 10K loader was used for the aft door layout. Standard practice is to load the pallets horizontally with some overhang of the forks on to the cargo floor area so the pallet can either be pushed or rolled slightly down hill onto the cargo floor. The cargo interior has extruded sidewall rails that interface with the pallets to hold them vertically and side-to-side with anchoring pins that go through the pallet and cargo floor to hold the cargo fore and aft.

To allow access to the STV internal cargo bay, an aft ramp and an upper two piece door were used as shown in Figure 118. Similar legacy cargo loading trade studies were used for the down select of this cargo door configuration. The upper door consists of two rotating doors; one is formed from the upper surface of the center section of the wing and pivots at the cargo ceiling. The other smaller auxiliary door is formed from the lower surface of the wing aft of the ramp. This auxiliary door pivots at a point to allow it to rotate flush to the larger upper door for loading equipment clearance. The actuation sequence starts with the lowering the ramp to the ground, then the upper door rotates upwards while the auxiliary door rotates flush out of the way. There is enough flexibility available in the design of the doors and their angles of operation to accommodate different ranges of motion for varying handling equipment.

The Atlas 10K loader is only one of numerous types of cargo handling equipment that are used by the military and the commercial air freight industry. In order to load and unload cargo on the STV, some form of horizontal raised platform or fork lift would be necessary. Forklifts and cargo handling equipment are available at any airport that has commercial cargo business. With routine flight planning, cargo handling equipment is easily reserved for use.

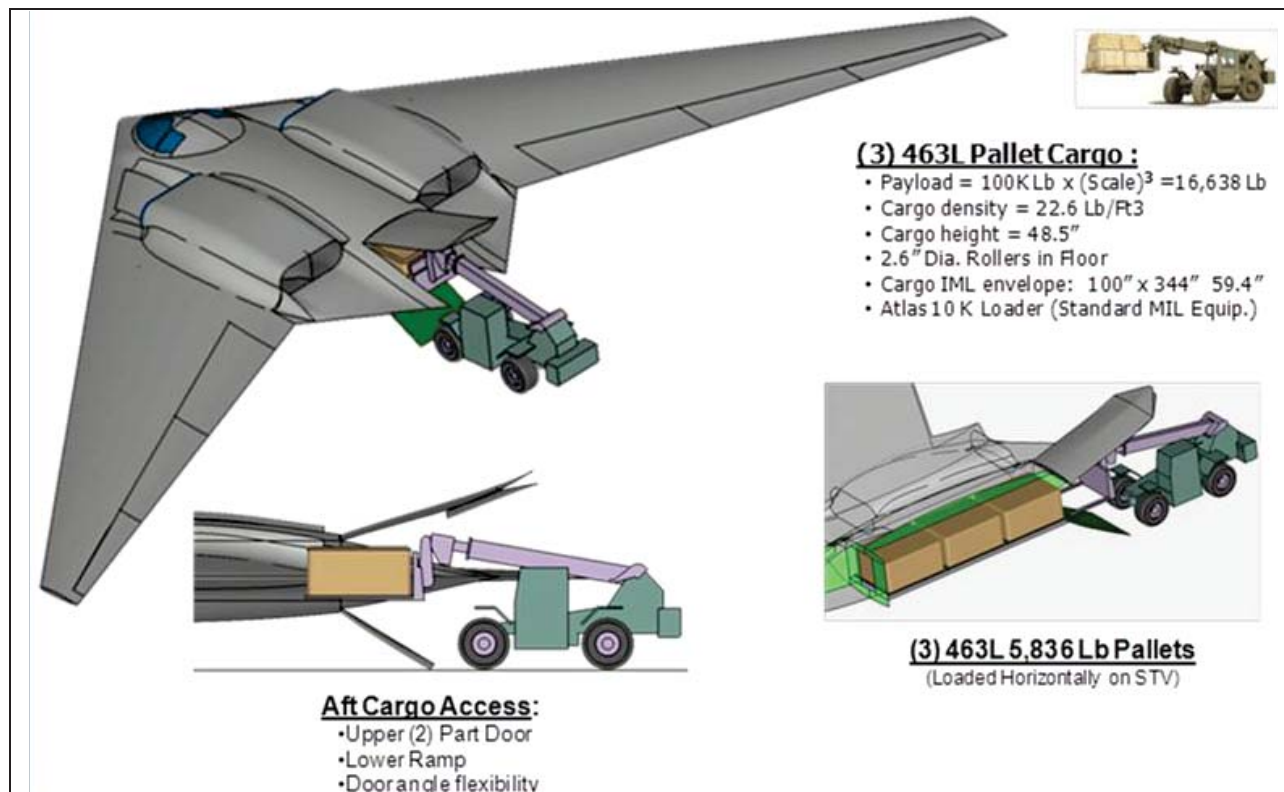


Figure 118 STV Cargo Loading (463L Military Pallets)

6.4.10. Propulsion Design and Structures Integration

The GE TechX was chosen for integration into the STV. For the inlet and exhaust sizing an L/D of 1.5 was used for this conceptual design. Due to the larger relative diameter of this engine used on the 55% STV versus the full size PSC with the Rolls Royce PD700 engines the upper aero surface of the wing in the nacelle area had to be increased in depth. This increase in depth requirement became a key structural design challenge. The STV percent scale, structural spar

depth, wing spar locations, engine location and payload envelope were iterated to make a laminar flow compliant aerodynamic shape (Figure 119).

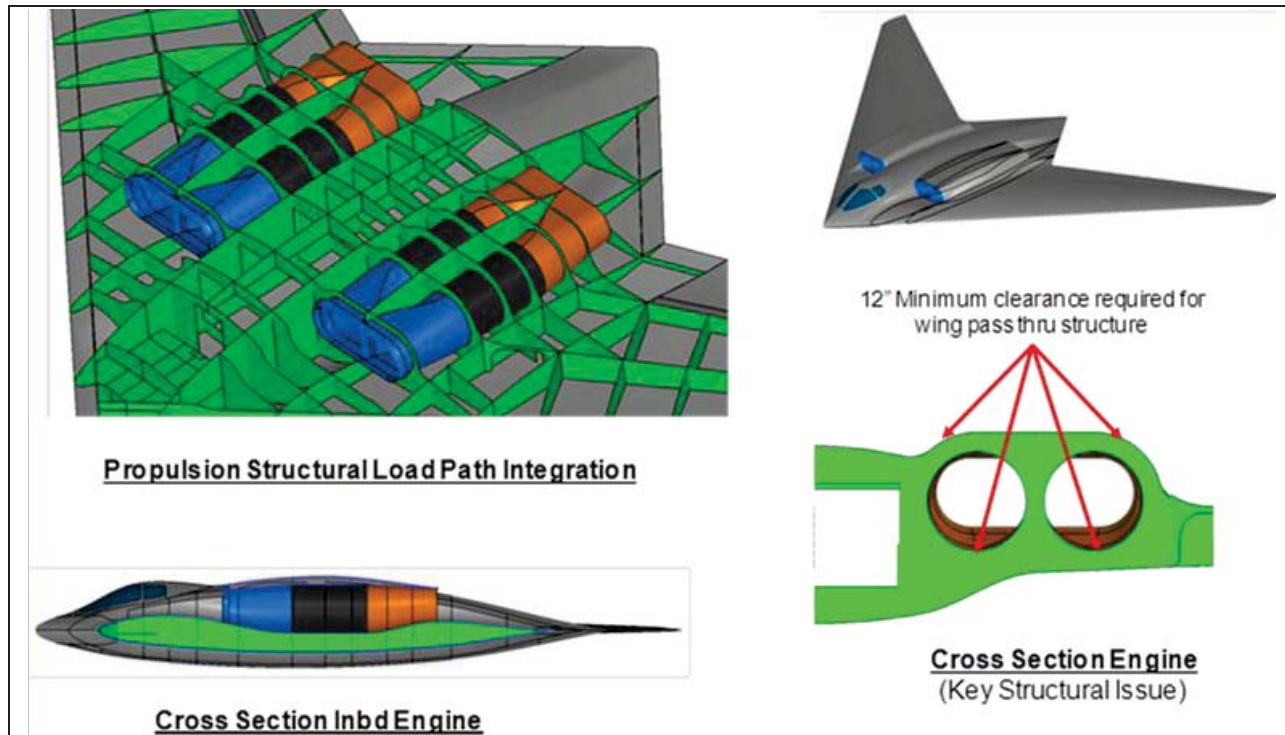


Figure 119 Propulsion Structural Integration

6.4.11. STV Configuration Integration Summary

The baseline 55% scale STV was successfully integrated with the required subsystems and aerodynamic design closure (Figure 120). Some small center body OML changes from the scaled PSC geometry were required to accommodate the estimated GE TechX engine integration and propulsion path differences. The cockpit/crew, payload bay and propulsion paths were key design drivers.



Figure 120 Baseline STV

Cargo is loaded from the aft of the aircraft for ease of access. A structural layout was developed of the entire aircraft. The wing carry through structure load paths for the GE TechX propulsion integration and payload bay were key structures design drivers. Tri-cycle landing gear was used with conceptual low noise fairing components integrated in to the design. All Master Equipment List (MEL) components were installed, which included avionics and all subsystems.

6.5. Propulsion System

A COTS engine study identified candidate engines within an appropriate range of physical constraints (fan diameter, length, weight) and performance (thrust, SFC and bypass ratio). The subset of engines identified as potential STV candidates were modeled based on nominal and anticipated performance and design specifications in cases where engine models were not available from the engine manufacturer. The GE TechX engine proved to be the most promising candidate due to the potential for flexible integration, meaning it could be installed into either a 55% or 74% STV, as well as meeting all of the STV performance goals. Initial propulsion system requirements were developed based on the conceptual design and integrated into the mission performance code.

6.5.1. Overall Propulsion System Layout

The submerged engine and inlet and exhaust ducting is shown in Figure 121. Although the exact scaled areas and T/W ratio could not be matched between the STV and PSC, the design similarity is sufficiently close to meet the integration challenges and demonstrate the configuration effectiveness. The duct length and structural clearances require the greatest deviations between the PSC and STV. Use of the TechX engines allows for an inlet L/D of approximately 1.5 or greater, while allowing for a similar exhaust L/D ratio. The amount of forebody flow acceleration and lower inlet ramp surface geometry will determine the extent to which flow control will be required to meet operational and performance targets. This was to be determined in the preliminary design. Similarly, auxiliary inlets will potentially be implemented as required to meet low speed operability requirements for takeoff.

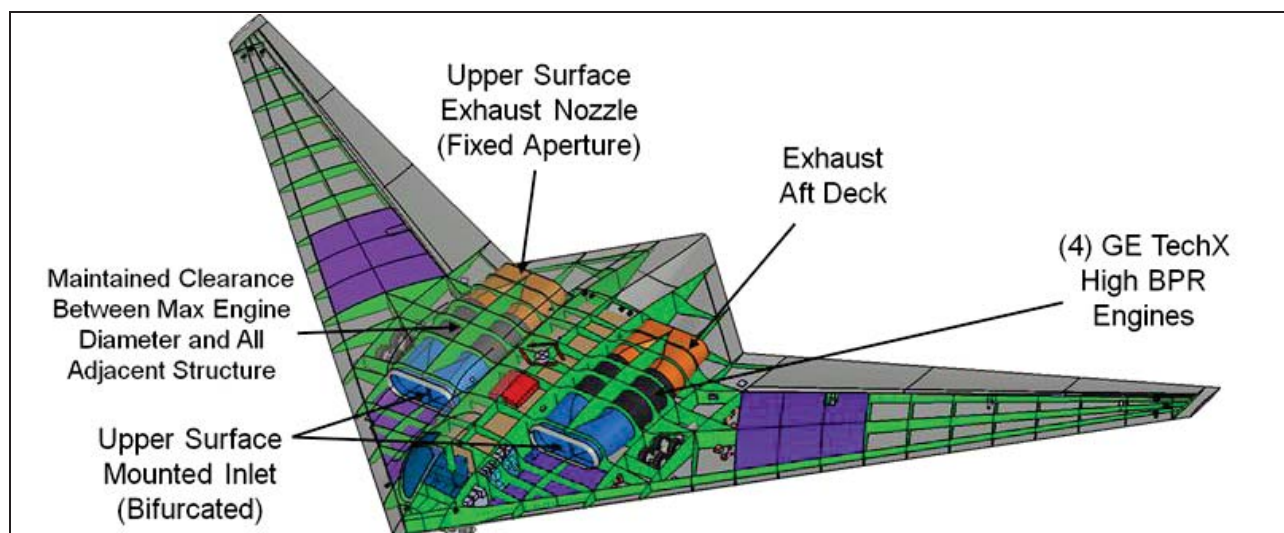


Figure 121 Baseline STV 4-Engine Propulsion Layout [Bifurcated Inlet Ducting (Blue), Engines (Gray), and Exhaust Ducting (Orange)] Are Shown With Top OML Removed

6.5.2. Propulsion Flow Path Integration and Installation Parameters

The 4-engine STV has the same leading edge sweep as the PSC, which poses design challenges for inlet integration for the outboard engines. For these outboard engines, the length between the leading edge and fan face is minimum, which imposes relatively large area changes over short distances. The flow path of the outboard engine is shown in Figure 122.

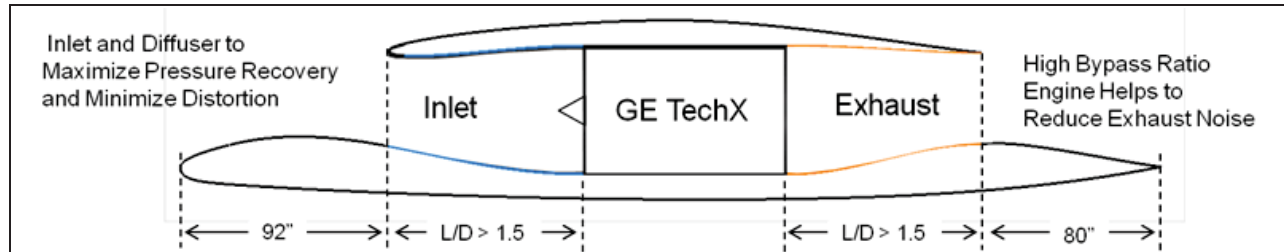


Figure 122 STV Propulsion Flow Path Cross-Section at Outboard Engine Location

Installation parameters were estimated for this configuration based on the performance of similar vehicles and the technologies that would be demonstrated on the STV. Inlet L/D ratios of about 1.5 or greater for inboard engines may require lower inlet ramp flow control to maintain a robust attached boundary layer for recovery at cruise conditions and maintaining operability margins at cruise and takeoff conditions. For the STV design a recover factor of 99% was assumed, which is less than a typical commercial pod mounted engine installation but is higher than a typical boundary-layer-submerged installation. The installation on the STV is between the two because of its forward location and the large bypass ratio that prevents the engine from being completely buried and that is not a requirement because of the good acoustic performance. Potentially, cruise conditions may produce weak shocks on the lower aircraft surface forward of the inlet, which may exacerbate the inflow condition. It is estimated that, with one of several possible techniques, this approach would be possible with only a slight degradation in recovery. To address the takeoff airflow requirements, an auxiliary inlet may be required that would allow the mass flow requirements of the engine to be met without exceeding distortion limits.

The exhaust system assumes a nozzle thrust coefficient of 0.98, which should be possible for a fixed convergent nozzle with a slightly under-expanded pressure ratio typical of commercial engines. A mixed exhaust flow design was modeled, which includes the efficiency gained by mixing the hot core flow with the cooler fan exhaust flow, improving propulsive efficiency. The benefit may also be achieved to reduce the temperatures of the materials in contact with the exhaust stream.

A fixed power extraction value of 150 hp per engine was modeled for each of the engines evaluated. A “bleedless” architecture was included that minimized the work extracted out of the HPC at the expense of additional power extraction out of the main generator.

6.6. Vehicle Subsystems

For the subsystems on the STV, the effort was intended to reasonably duplicate a typical commercial airline vehicle with its attendant flight and ground operation equipment. However it was also a goal to incorporate advanced features that would integrate optimally with the key demonstration technologies that were designed onboard. One such feature is the lack of engine bleed air utilized, in order to take advantage of more efficient power extraction methods. Also of mention is the low noise landing gear assembly, which we’ve included in order to assist other low noise design features being demonstrated elsewhere on the vehicle. Figure 123 highlights

these and other significant vehicle subsystems, their approximate location and indicates parenthetically the particular subsystem(s) involved.

The vehicle subsystems consist of the following categories and are presented in the following order in this section of this report:

- ECS (Environmental Control System)
- EPS (Electrical Power System)
- IPS (Ice Protection System)
- Fuel / OBIGGS System
- Hydraulic System
- Landing Gear
- External Interfaces

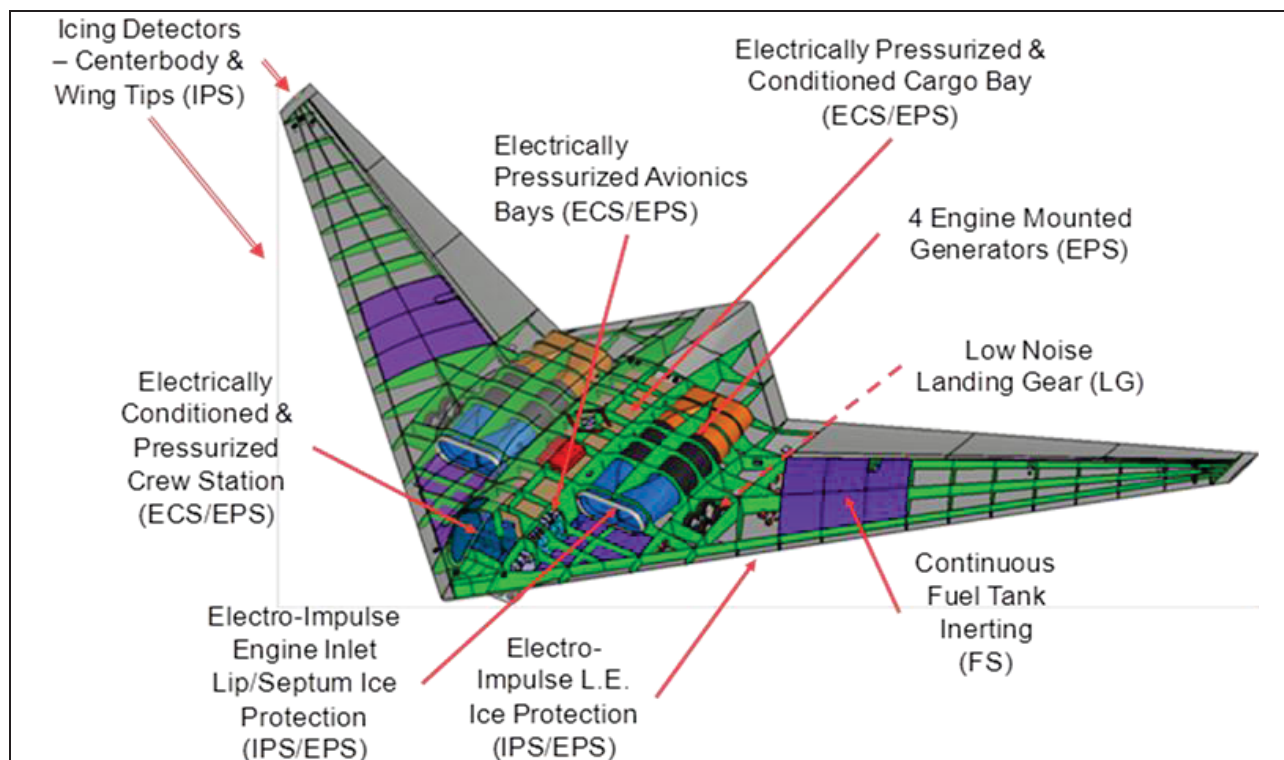


Figure 123 Key Vehicle Features

6.7. Vehicle Management Systems

This section describes the design implementation of the Vehicle Management Systems (VMS) for the use in the baseline STV. The Vehicle Management Systems (VMS) design is a highly reliable open system architecture controller, and interface to all flight critical subsystems using a Tri-redundant distributive architecture design. The primary VMS components are the Vehicle Management Computer, GPS/INS, Air Data System, Mission Management Computer, Actuator Control Unit, Remote Input Output Unit, Communications Systems (UHF, VHF, HF, Data Links, Radar Altimeter Unit, and Collision Avoidance Unit), Flight Control System, and Flight Instrumentation (Figure 124). The Vehicle Management Systems also interfaces with the following subsystems: primary and secondary Electrical Power Systems, Fuel Management, Actuator/Hydraulics Control, Propulsion Control, and other avionics subsystem sensors (Figure

125). The incorporation of these additional systems into the flight control architecture defines the VMS for the STV. In addition, the implementation of a VMS will incorporate state-of-the-art hardware technologies, and interface with the capability to operate with non-identical hardware with compatible interfaces in a redundant configuration, providing true open system architecture. Software technology will include a multiprocessor fault-tolerant executive, local area network distributed architecture synchronization and network management.

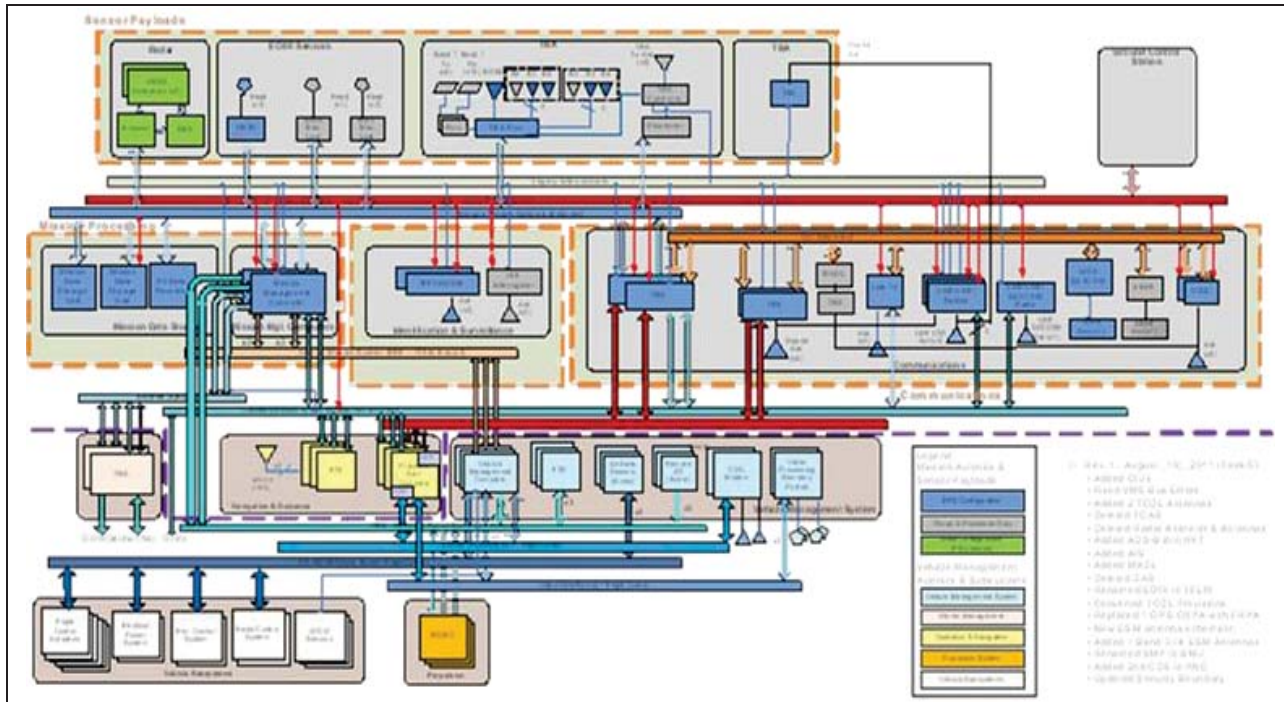


Figure 124 VMS Systems Avionics Architecture Interface

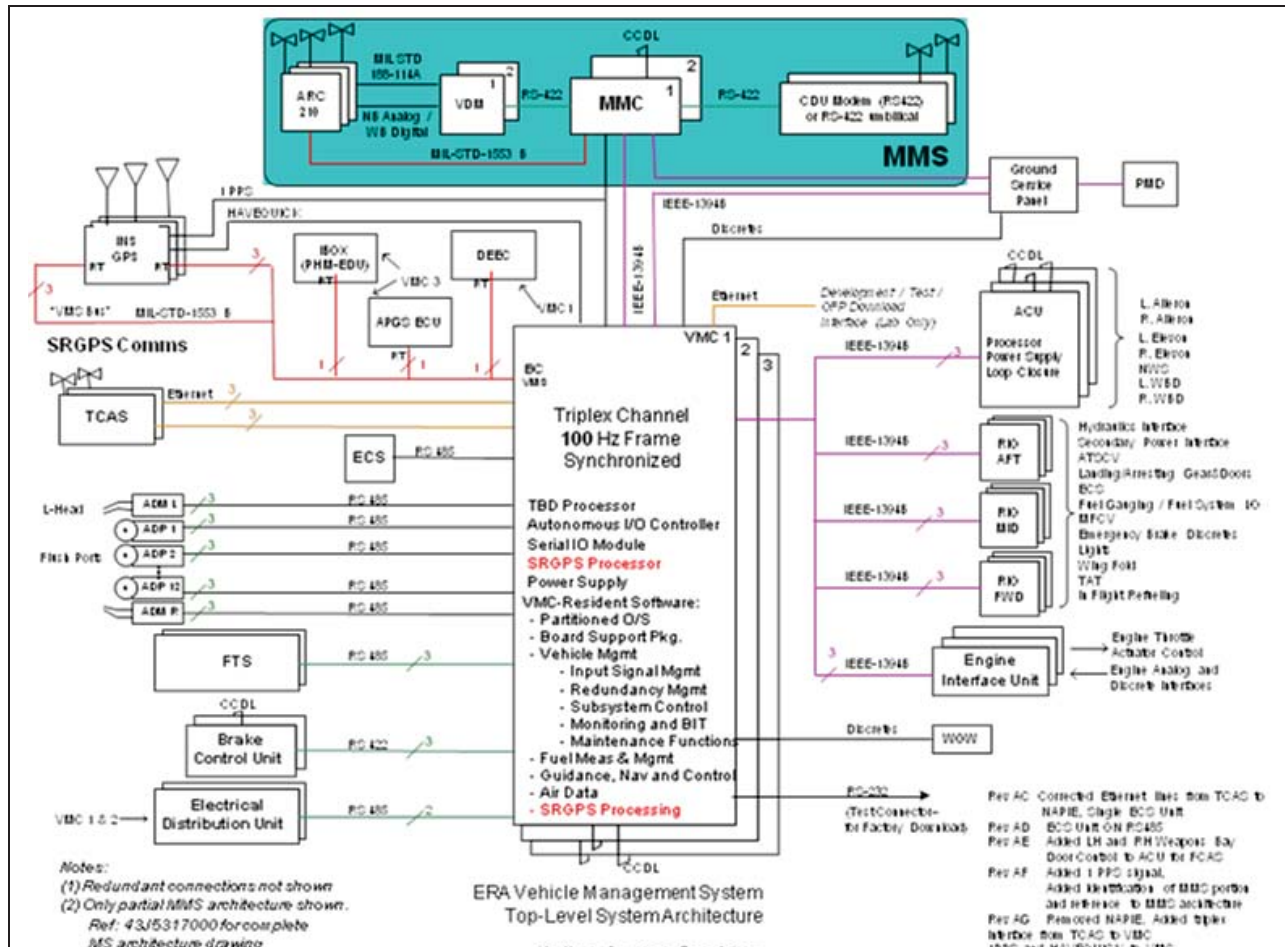


Figure 125 STV VMS Architecture

6.7.1. VMS Subsystem Equipment

The VMS subsystem equipment consists of the following:

- Environmental control system (ECS)
- Electrical power control (EPC)
- Flight control actuators
- Engine interface unit (EIU)
- Communication systems (UHF, VHF, HF, XPNDR)
- Flight instrumentation
- Weight on wheels (WOW)
- Break control unit (BCU)

6.7.2. Cockpit Location and Layout

Figure 126 and Figure 127 show the location of the crew compartment located within the STV.

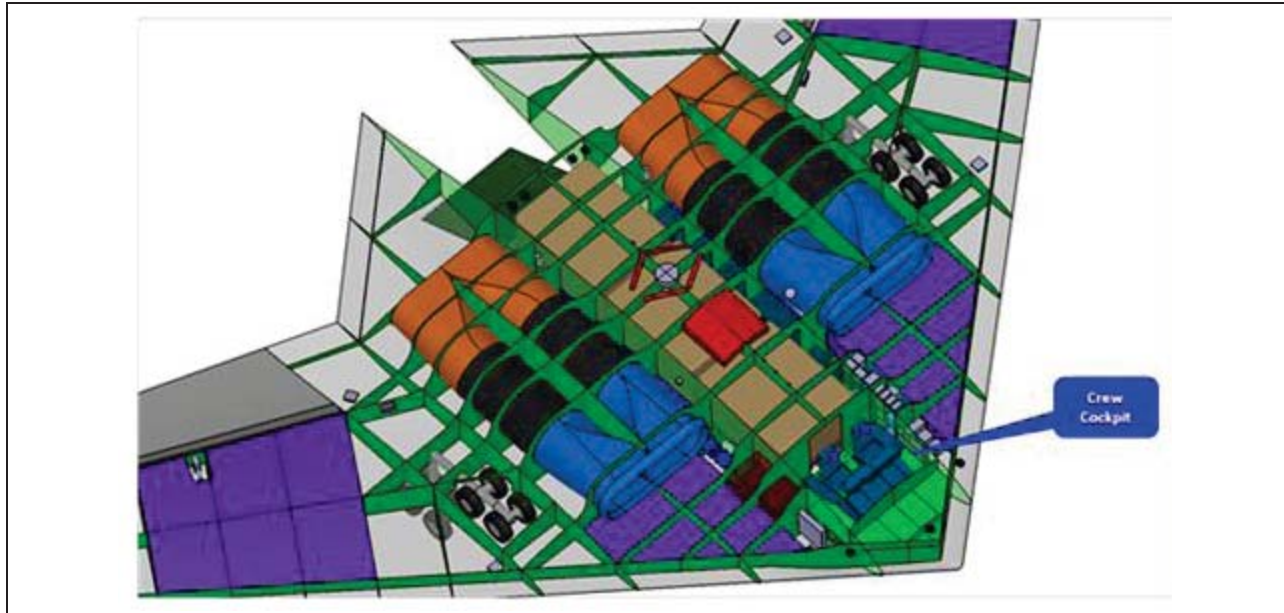


Figure 126 Crew Compartment Location on STV

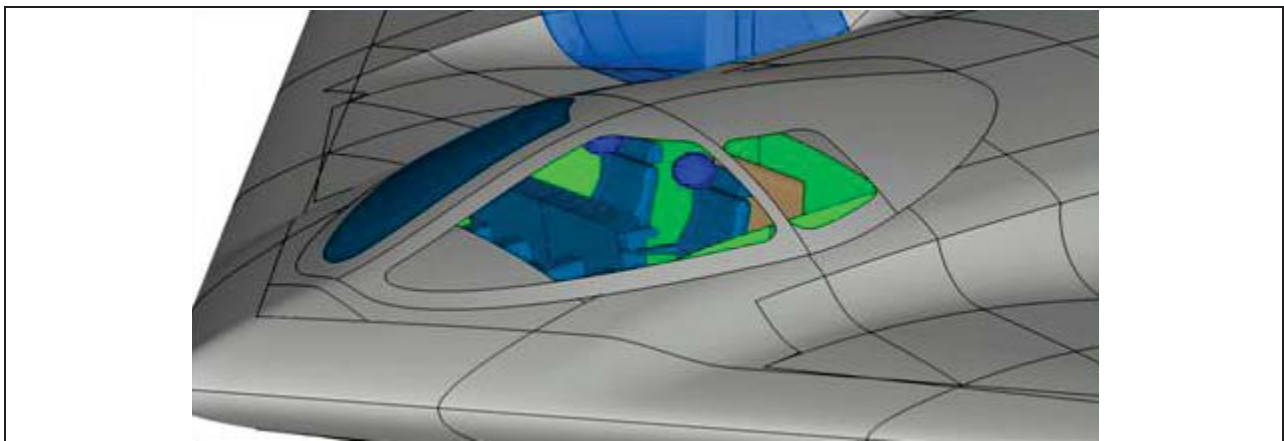


Figure 127 Cockpit Layout - External View

6.8. Mass Properties

6.8.1. STV Weight Estimate

The STV mass properties were estimated using an in-house Northrop Grumman developed tool for conceptual mass-properties estimation, an iterative system of Weight Estimation Relationships (WERS) that provides a group weight statement level weight breakdown. Figure 128 shows the group weight statement for the technology demonstrator configuration.

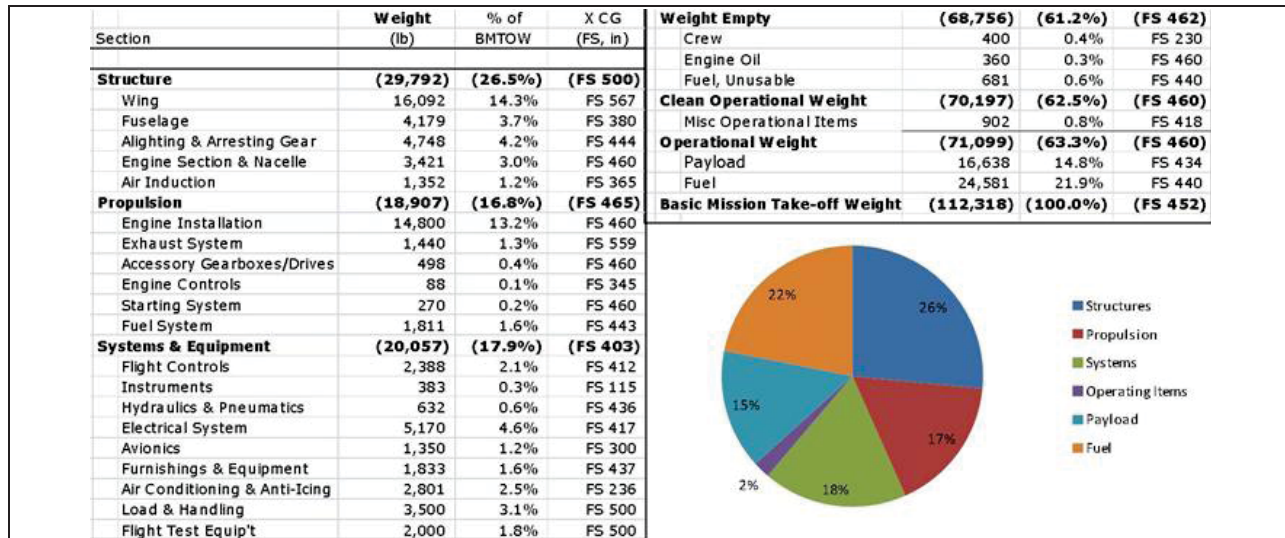


Figure 128 STV Group Weight Statement

6.8.2. Technology Weight Savings or Impacts

The Weight estimates include the effects of the addition of the technologies discussed in this report. A summary of the technology weight impacts are given in Figure 129.

Section	Weight Savings or Impact
▪ Wing	Advanced Composites Technologies : 20% Savings on Entire Wing
▪ Fuselage	Advanced Composites Technologies : 10% Savings on Entire Fuselage
▪ Engine Sect. or Nacelles	Advanced Composites Technologies : 10% Savings on Entire System
▪ Landing Gear	Advanced Composites /Advanced Metals : 3% Savings on Entire System
▪ Landing Gear	Noise Reduction Fairings: 1% Increase to Entire System
▪ Electrical	10% Savings (~250 lb)– Carbon Nano Tube Shielding on Signal Cables
▪ Fuel System	Addition of OBBIGGS – Approx 500 lb Increase to Fuel System
▪ Electrical	MEA Technologies- Growth of Power Distribution Sys-Approx +400 lbs
▪ ECS	MEA Technologies – Doubling of System Capabilities – Approx + 800 lbs

Figure 129 STV Weight Impact of Technologies

6.8.3. Weight Estimation Assumptions

The assumptions that drive the weight estimates are driven by the selection of a flying wing, partially buried engine configuration. The wing box is assumed to be high technology bonded composite structure, utilizing a variety of materials and techniques, tailored to the location on the vehicle, in order to derive the maximum weight savings benefit.

The fuselage, or center section, is mostly composite, with the exception of the cargo floor. There is a 10% penalty added to the fuselage weight for pressure loads on the flat panels on the sides of the compartment, as well as the beef-up required at the joints. There is assumed to be no weight savings benefits on other fuselage items such as windshields, mechanisms, paint, etc. The landing gear is assumed to use advanced capability metals and some composites on drag braces, but the weight savings is assumed to be very small. The addition of noise reducing fairings

around the gear's major components is assumed to cost no more than 1% the weight of the gear. The propulsion system is assumed to be mostly off-the-shelf, except for the addition of exhaust nozzles and heat resistant materials over the deck where the hot engine exhaust passes over the wing structure.

The fuel systems is assumed to incorporate a dump system for emergency landings, OBIGGS for tank inerting, and is based on integral tanks placed such that the forward and outboard tanks provide sufficient center of gravity shifting capability for C.G. management during all phases of the flight. The flight control system is hydraulically based, assuming a 3,000 psi system. The electrical system is comprised of four 120 kVa generators, eight 22 amp-hr and four 270 V DC batteries, carbon-nanotube shielded signal wiring, and standard wiring and lighting elsewhere. The avionics and instrumentation suites are assumed to be modern technology, highly integrated systems, with the baseline avionics LRUs given an allocation of 1,000 lb and an installation of 35% (local wiring and brackets). Additional pilot and air data instruments are assumed to be 383 lb.

Any flight-test-specific LRUs are accounted for in the flight test equipment allocation which is set at 2,000 lb at this time. The ECS system is comprised of two 500 lb cooling units, ram air ducts, associated plumbing, ducting, installation, windshield defog, and anti-icing system. Furnishings and equipment weights provide for a lavatory, seats for 2 crew, oxygen system, fire detection, fire suppression and limited emergency equipment. Load and handling weight provides allocations for floor rollers, winches, cargo tie-down hard points, jacking and hoisting points, and other cargo handling equipment. Additional operating items are comprised of the crew weight, engine oil, unusable fuel and allocations for 2 flight kits plus the weight of cargo pallet structures and tie-down cables.

6.9. Baseline STV

The performance trade studies were discussed in a previous section of this report. Upon completion of those trades studies and selection of the Baseline STV, the baseline design was refined. Refinements to the baseline STV included: (1) a review and update of our aerodynamics assessment based on refined definition of the extent of laminar flow on the surfaces and on OML differences compared to the PSC, (2) an update to the mass properties predictions, which included an update to the subsystems definition and technology benefits assumptions, and (3) an update from a 20,000 lb to a 16,000 lb thrust class GE TechX engine.

The baseline vehicle has a wing area of 3,485 ft² and a wing span of 143 ft. This vehicle is powered by four GE TechX engines and is designed to carry 16,638 lb of payload for 3,000 nm range. Additional details of this configuration are shown in Figure 130.

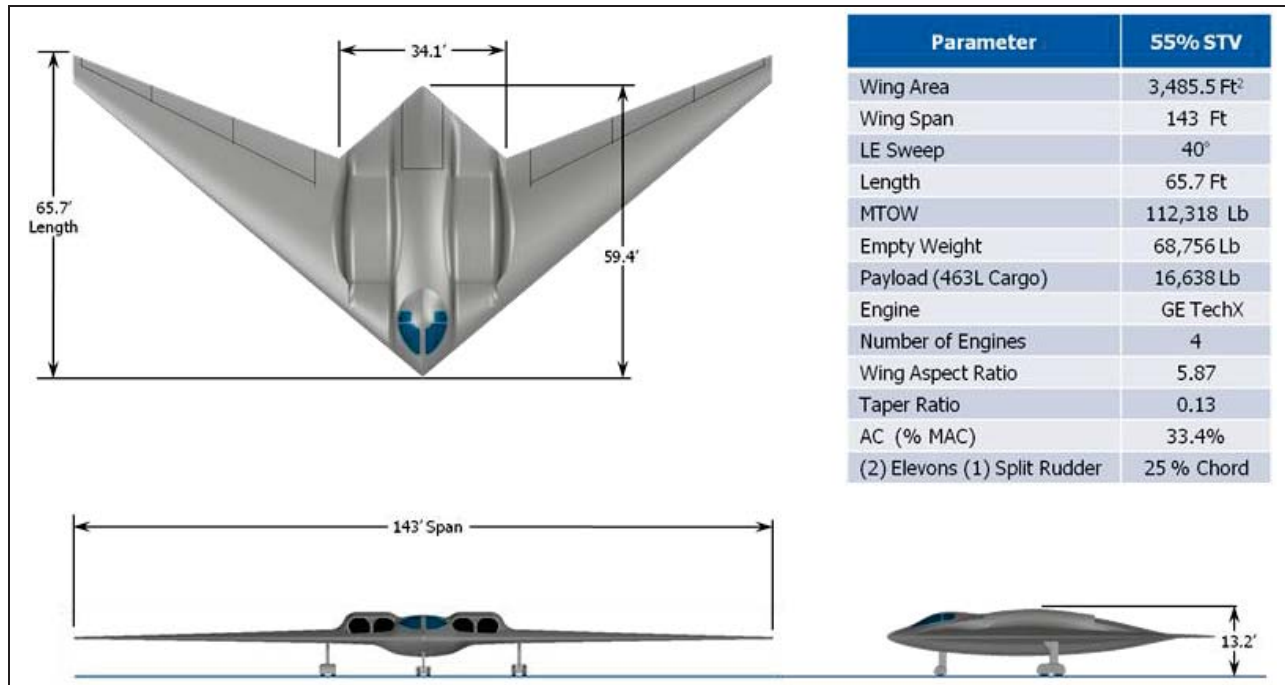


Figure 130 Baseline STV 3-View

6.9.1. Baseline STV Aerodynamics

Laminar flow areas on the STV are predicted using Swept Wing Laminar Flow Control technology inputs and likely causes of turbulent transition (e.g., doors, hinge lines) (Figure 131).

Aerodynamics characteristics of the vehicle were estimated based on empirical methods and historical data. Plots of aerodynamics efficiency M^*L/D and L/Ds are shown in Figure 132. The cruise C_L for this vehicle at Mach 0.82 is approximately 0.23 to 0.25. The vehicle skin friction drag correlates well with other vehicle and due to the STV unique design; it has low minimum drag to extensive laminar flow. Similarly, lift-to-drag (L/D) of the vehicle at 40,000 ft cruise and Mach 0.80 shows similar efficiency trend as other laminar flow aircraft such as sailplanes as shown in Figure 133.

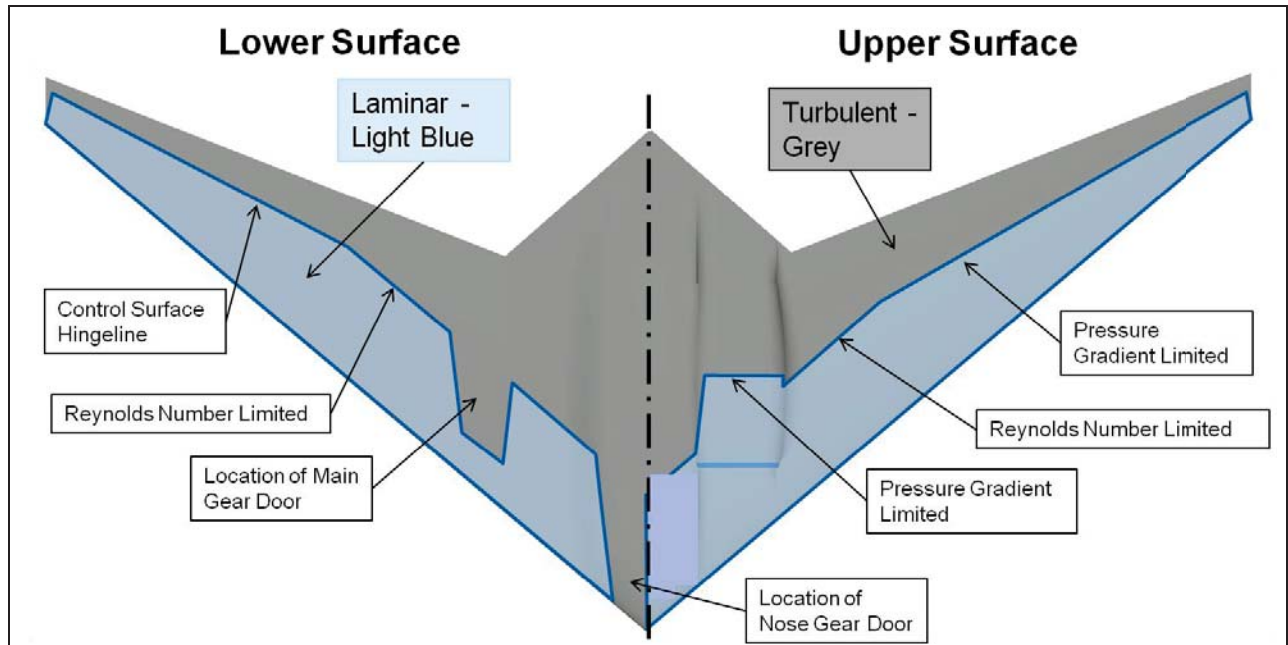


Figure 131 STV Baseline Laminar Flow

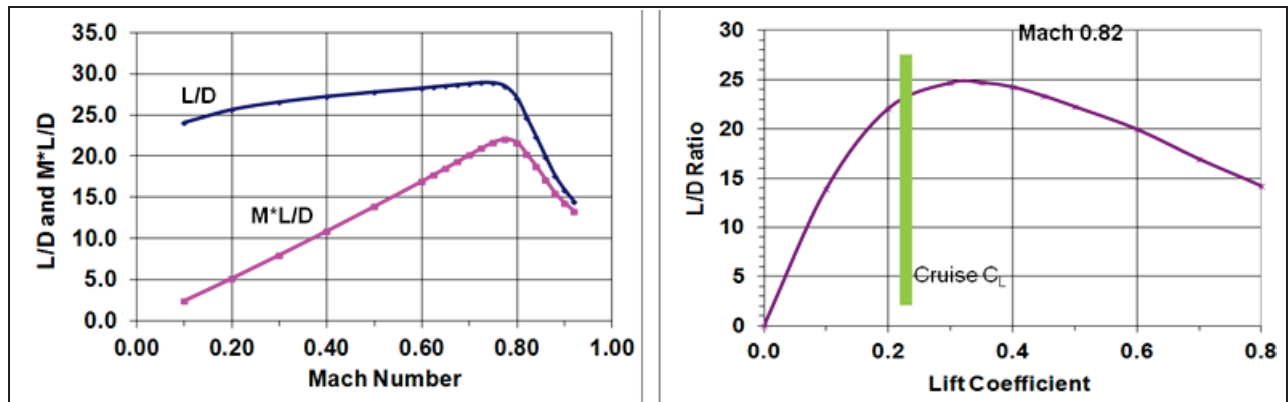


Figure 132 STV Baseline L/D

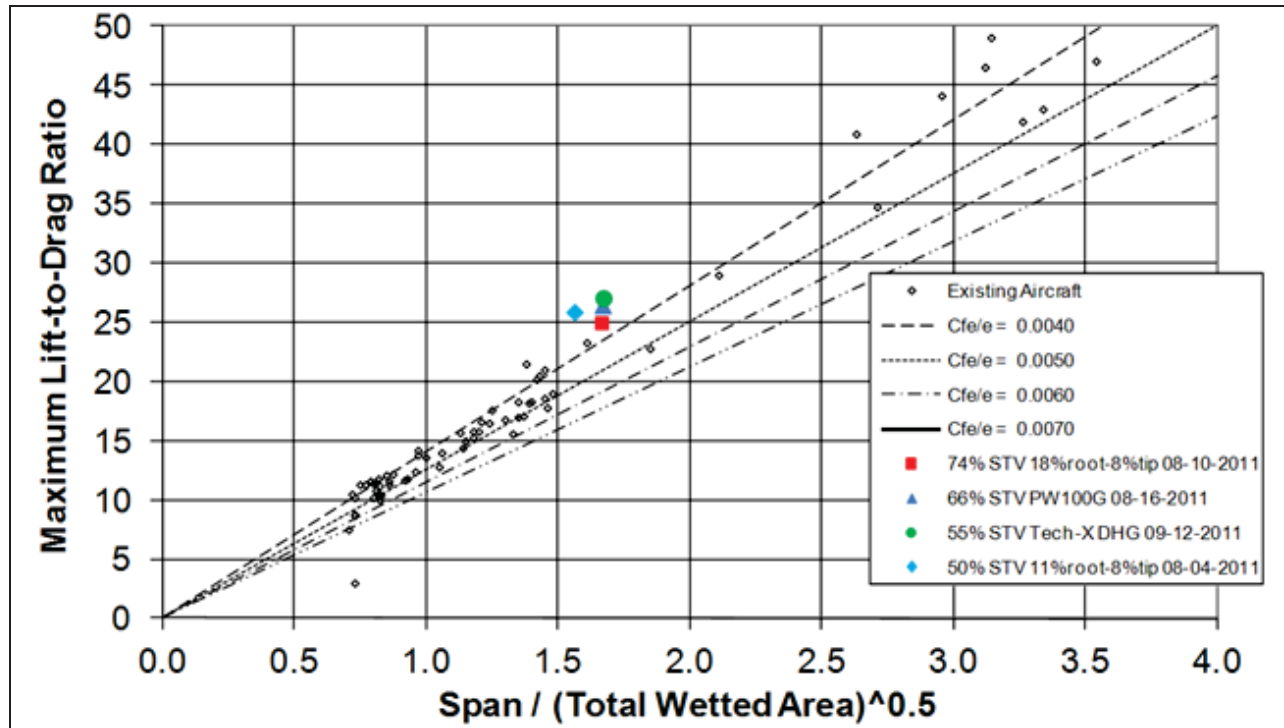


Figure 133 M=0.80, 40,000 ft. Altitude STV L/D Correlation

6.9.2. Baseline STV Propulsion

The baseline vehicle is powered by four GE TechX with a sea level static thrust of 16,000 lb per engine. The TechX engine performance data is an estimate generated using NPSS method by Northrop Grumman and hence no GE proprietary data was used.

6.9.3. Baseline STV Performance

The final performance for the 55% STV vehicle was generated based on the following set of requirements.

- Engines: Four (4) GE TechX engines
- Mission requirements:
 - Same as PSC mission profile
- 200 nm alternate and 30 min hold
 - Mission range = 3,000 nm EASD
 - TOFL = 5,700 ft sea level, standard day
 - 50,000 ft altitude limit
 - Mach cruise = 0.82

The baseline vehicle cruises at 49,000 ft and has a flight time of 6.8 hrs. The total fuel spent (minus reserves) is about 19,000 lb. Plots of Altitude vs. Distance, Flight time vs. Distance and Fuel vs. Distance are shown in Figure 134. Additionally, fuel spent and time spent for each of mission segments (taxi, climb, cruise, descent and reserves) are shown in Figure 135. The fuel spent during cruise is approximately 15,000 lb.

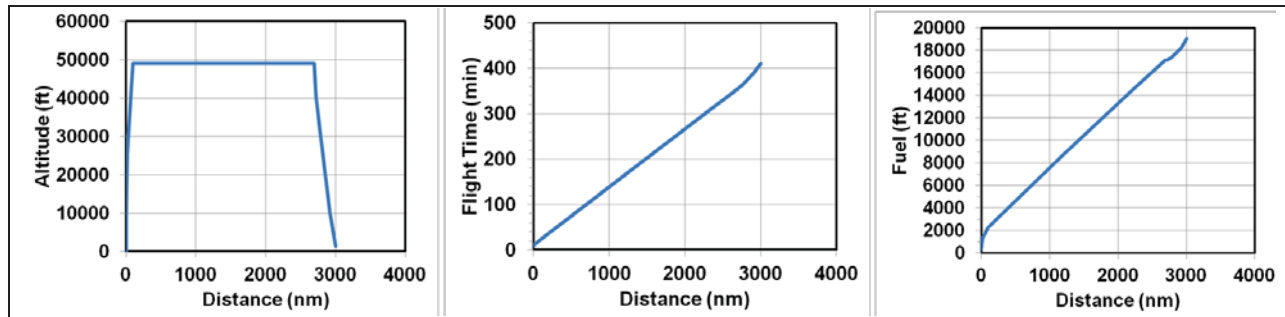


Figure 134 STV Baseline Mission Profiles

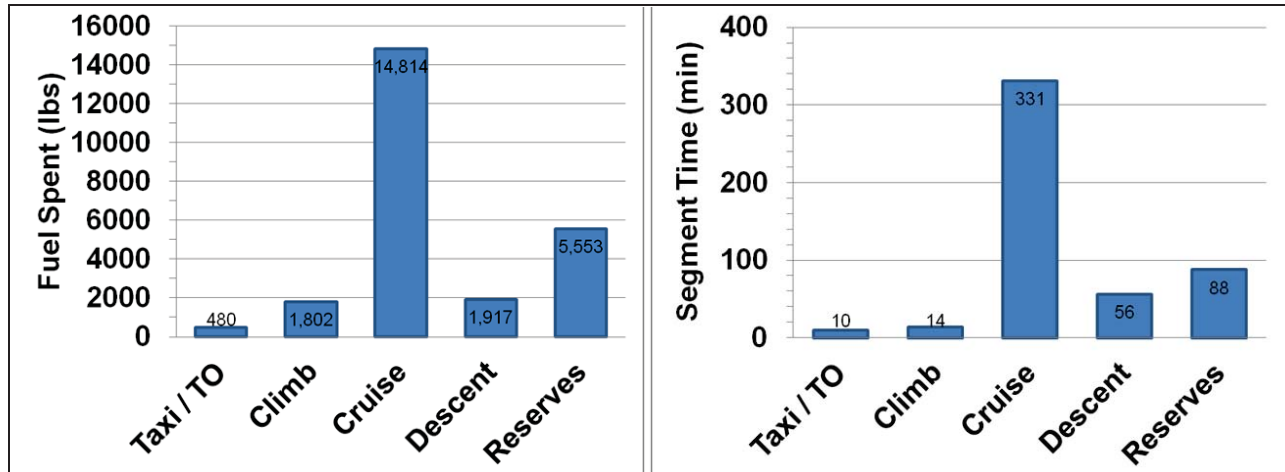


Figure 135 STV Baseline Fuel and Time Spent

A flight envelope for the baseline vehicle was developed using a mid-mission weight (Figure 136). On the left-hand side of the envelope, it is limited by a combination of stall speed and 1.0-g limit. The right hand side is set by structural limit of 305 lb/ft² or 300 KEAS. The horizontal line is a 50,000 ft limit and the maximum Mach number line of 0.85 is defined by approximate thrust equals to drag and as a safety margin for potential control reversal at higher transonic speeds. These will be refined in later phases of the design maturation.

Finally, the baseline vehicle cruises at a constant cruise altitude of 49,000 ft at Mach 0.82 (470 kts). The total mission fuel is approximately 25,000 lb. The baseline STV has a TOGW of 112,300 lb and carries 16,638 lb of payload for 3,000 nm. Takeoff distance at max TOGW is about 3,000 ft which is below the 6,500/5,700-ft requirement. A summary of the baseline performance is shown in Table 25.

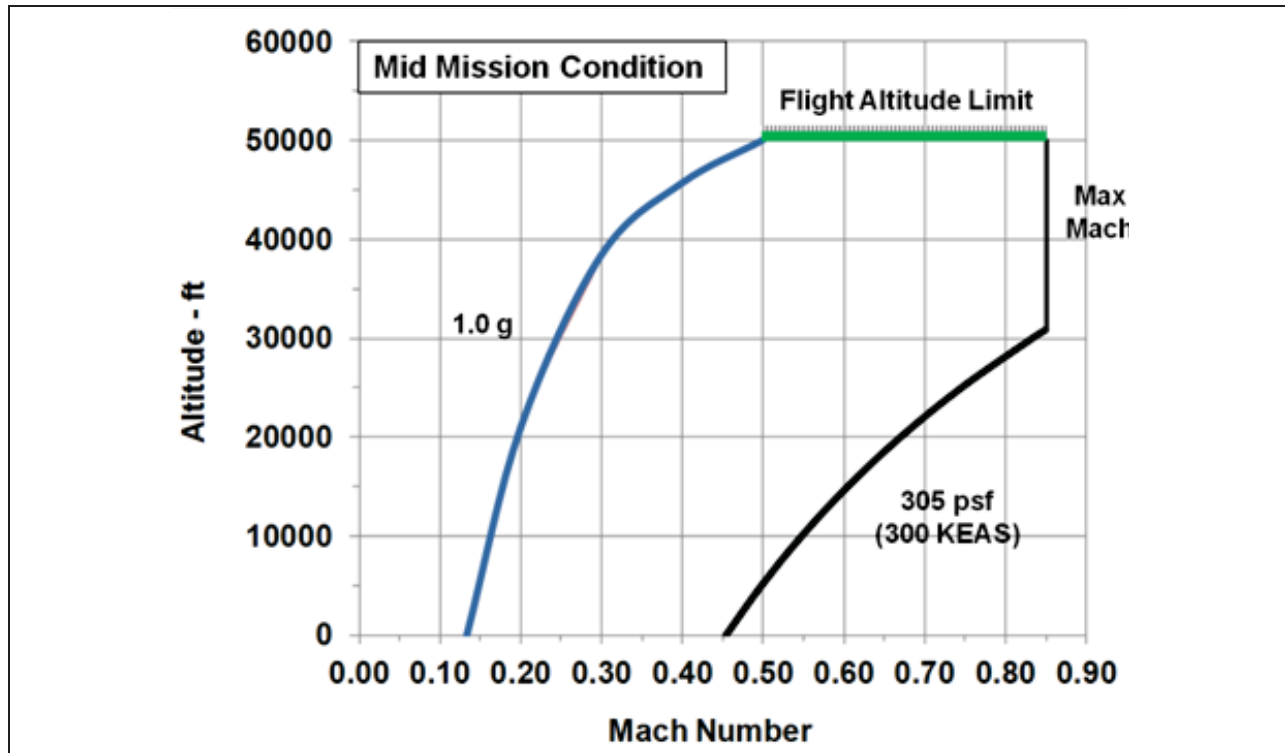


Figure 136 STV Baseline Flight Envelope

Engine	-	TechX*
No. of Engines	-	4
Thrust per Engine	lbf	16,000
Wing Area	ft ²	3,485
TOGW	lbs	112,300
Weight Empty	lbs	68,800
Payload	lbs	16,638
Range	nm	3,000
Total Fuel	lbs	24,600
TOFL (SL, STD)	ft	2,950
Fuel Fraction		0.22

Table 25 STV Baseline Performance Summary (*NGC Estimated)

7. Conclusions

The AVC study program identified advanced integrated PSC passenger and cargo vehicles with component technology concepts and showed how these vehicles will efficiently operate within the NextGen that is currently being developed. The study defined what NextGen will be in 2025 for both en route mission segments and terminal area segments, and a scenario was developed that establishes a context within which the passenger and cargo PSC vehicles may meet a market need and enter into service. The study results show how the PSC vehicles, when integrated into the fleet, affect noise contours and LTO NO_x and particulate and carbon emissions at a relevant airport (SFO) and provide key requirements to NASA's Airspace Systems Program and to the Joint Planning and Development Office (JPDO) to enable optimal integration of the PSC vehicles into the NextGen environment. For the cargo PSC, key requirements were identified to enable the aircraft to operate autonomously in the NAS in 2025 or beyond.

The study identified technologies required to meet the aggregate N+2 goals. To meet the noise goal, component technologies and propulsion integration concepts were identified to reduce cumulative noise below Stage 4 by greater than 42 dB. To meet the emissions goal, technologies were identified to reduce cruise NO_x and CO₂, mitigate global warming effects of water vapor, reduce aerosols and solid particulates that contribute to the formation of aircraft-induced cirrus clouds, and reduce the emission of particulate matter by 75 percent. The study produced optimal combinations of airframe, engine, and integrated vehicle efficiency improvements, including the use of an unconventional airframe configuration—a flying wing—to reduce fuel-burn by 42 percent.

The study developed and documented technology maturation plans that outline the research required to develop the critical technologies and integrated aircraft systems. A time-phased 15-year technology maturation plan was defined that establishes credibility and provides traceability for PSC benefits that will enable the envisioned aircraft system concepts to enter service by 2025. Results of the study show how much of the improvement toward the N+2 goals are attributable to the use of advanced technologies and how much is attributable to the vehicle configurations defined for the PSC vehicles. The maturation plan contains roadmaps that define credible intermediate performance objectives (go/no-go criteria) associated with critical tests and demonstrations and is of sufficient detail to support the advocacy and strategic program planning of possible follow-on Integrated Systems Research Program (ISRP) (or other NASA Program) projects. A prioritized list of time-critical technology demonstrations that must be performed in the Fiscal Year (FY) 2013 through FY 2015 time frame was documented. A set of coherent, comprehensive roadmaps were completed containing a matrix of options starting with an ideal list of critical demonstrations for FY 2013 through FY 2015 and showing trade-offs among scale, complexity, schedule, cost, and risk for each major element. Alternate test techniques, ranges, test assets, and risk levels were developed for each of the key technical challenges. Collaborative research opportunities were highlighted in the roadmaps.

The AVC study produced a conceptual design of a testbed vehicle to focus research efforts leading to multiple integrated research experiments at the TRL level of 6. The testbed design is a subscale version of the PSC that demonstrates in an integrated fashion key enabling technologies required to simultaneously meet the N+2 noise, emissions, and fuel-burn goals. The testbed was designed to provide flexibility for future flight campaigns to investigate UAS integration into the NAS.

The ERA program has identified future efforts intended to follow the AVC study. These efforts will provide critical validation data for predictive methods required for design of a full-scale PSC, and provide quantitative evidence that the N+2 fuel-burn, emissions, and noise goals can be met by the PSC. Under the primary effort a preliminary design of a subscale testbed vehicle for future flight campaigns will be provided. Demonstrations using the testbed will reduce the risk for the technologies/integrations that are critical enablers for the proposed 2025 EIS of the PSC. The testbed is also a key enabler for a new project under ISRP that will develop and assess technologies and techniques to allow the routine operation of a UAS in the NAS. The companion effort will focus on key early technology maturation demonstrations to increase the probability of the subscale testbed vehicle successfully meeting its goals.

7.1. Significance of the AVC Study

The most significant aspect of the AVC study program is that its results will help guide future ERA (and other NASA aeronautics) investment decisions for the next 15 years. This program set the stage for an ERA/UAS subscale testbed vehicle aircraft that will through flight research reduce the risks associated with designing and building a full-scale vehicle based on the PSC conceptual design. The subscale flight test vehicle was designed to demonstrate a subscale version of the PSC. Once the testbed demonstrates in an integrated fashion key enabling technologies required to simultaneously meet the ERA noise, emissions, and fuel-burn goals, NASA and industry can move forward to realize a marketable EIS 2025 efficient aircraft for our nation and the world.

7.2. Perceived Impact of Work

The ERA AVC Study program developed a scenario for the next generation of civilian transport aircraft to operate with maximum efficiency in the NextGen airspace. The program conceptualized two preferred system concepts (one passenger, and one cargo) that meet the aggregate N+2 goals for fuel burn, noise, emissions, and field length and documents in this report the feasibility, benefits, and technical risks of these concepts. This program leveraged and built upon significant previous and ongoing research in advanced configurations and the technology areas related to these goals. Programs such as ADVENT, HEETE, RCEE, CLEEN, Subsonic Fixed Wing (SFW), and the recently started ERA technology development work are building on past significant NASA, Air Force, and industry investments. The AVC Study program developed technology roadmaps that set the stage for the later work in ERA and follow-on efforts over the next 15 years. As a start to furthering technology maturation of time-critical technologies to TRL 6 by 2015, this study produced a testbed aircraft concept that was designed to enable demonstrations of these technologies in an integrated fashion. Overall, the AVC Study program significantly increased the state of knowledge for advanced efficient transport aircraft and their critical enabling technologies.

REPORT DOCUMENTATION PAGE

Form Approved
OMB No. 0704-0188

Public reporting burden for this collection of information is estimated to average 1 hour per response, including the time for reviewing instructions, searching existing data sources, gathering and maintaining the data needed, and completing and reviewing this collection of information. Send comments regarding this burden estimate or any other aspect of this collection of information, including suggestions for reducing this burden to Department of Defense, Washington Headquarters Services, Directorate for Information Operations and Reports (0704-0188), 1215 Jefferson Davis Highway, Suite 1204, Arlington, VA 22202-4302. Respondents should be aware that notwithstanding any other provision of law, no person shall be subject to any penalty for failing to comply with a collection of information if it does not display a currently valid OMB control number. **PLEASE DO NOT RETURN YOUR FORM TO THE ABOVE ADDRESS.**

1. REPORT DATE (DD-MM-YYYY) 30-04-2013		2. REPORT TYPE Final Technical Report		3. DATES COVERED (From - To) Nov 2010 - Apr 2013	
4. TITLE AND SUBTITLE Environmentally Responsible Aviation N+2 Advanced Vehicle Study				5a. CONTRACT NUMBER NND11AG02C	
				5b. GRANT NUMBER •	
				5c. PROGRAM ELEMENT NUMBER	
6. AUTHOR(S) Drake, Aaron Harris, Christopher A. Komadina, Steven C. Wang, Donny P. Bender, Anne M.				5d. PROJECT NUMBER	
				5e. TASK NUMBER NNL10AD11T	
				5f. WORK UNIT NUMBER	
7. PERFORMING ORGANIZATION NAME(S) AND ADDRESS(ES) Aerospace Systems Northrop Grumman Systems Corporation One Hornet Way El Segundo, CA 90245-2804				8. PERFORMING ORGANIZATION REPORT NUMBER	
9. SPONSORING / MONITORING AGENCY NAME(S) AND ADDRESS(ES) NASA Dryden Flight Research Center P.O Box 273 M/S 1422 Edwards, CA 93523-0273				10. SPONSOR/MONITOR'S ACRONYM(S) NASA DFRC	
				11. SPONSOR/MONITOR'S REPORT NUMBER(S)	
12. DISTRIBUTION / AVAILABILITY STATEMENT					
13. SUPPLEMENTARY NOTES					
14. ABSTRACT This is the Northrop Grumman final report for the Environmentally Responsible Aviation (ERA) N+2 Advanced Vehicle Study performed for the National Aeronautics and Space Administration (NASA). Northrop Grumman developed advanced vehicle concepts and associated enabling technologies with a high potential for simultaneously achieving significant reductions in emissions, airport area noise, and fuel consumption for transport aircraft entering service in 2025. A Preferred System Concept (PSC) conceptual design has been completed showing a 42% reduction in fuel burn compared to 1998 technology, and noise 75dB below Stage 4 for a 224-passenger, 8,000 nm cruise transport aircraft. Roadmaps have been developed for the necessary technology maturation to support the PSC. A conceptual design for a 55%-scale demonstrator aircraft to reduce development risk for the PSC has been completed.					
15. SUBJECT TERMS Transport Aircraft Configurations, Reduced Fuel Burn, Reduced Emissions, Noise Reduction, Technology Maturation Roadmaps, Preferred System Concept (PSC), Subscale Testbed Vehicle (STV), National Aeronautics and Space Administration (NASA), Northrop Grumman					
16. SECURITY CLASSIFICATION OF:			17. LIMITATION OF ABSTRACT UU	18. NUMBER OF PAGES 235	19a. NAME OF RESPONSIBLE PERSON Lisa A. Jackson, CO
a. REPORT U	b. ABSTRACT U	c. THIS PAGE SAR			19b. TELEPHONE NUMBER (include area code) 661-276-2154

INSTRUCTIONS FOR COMPLETING SF 298

1. REPORT DATE. Full publication date, including day, month, if available. Must cite at least the year and be Year 2000 compliant, e.g. 30-06-1998; xx-06-1998-, xx-xx-1998.

2. REPORT TYPE. State the type of report, such as final, technical, interim, memorandum, master's thesis, progress, quarterly, research, special, group study, etc.

3. DATES COVERED. Indicate the time during which the work was performed and the report was written, e.g., Jun 1997 - Jun 1998; 1-10 Jun 1996; May - Nov 1998; Nov 1998.

4. TITLE. Enter title and subtitle with volume number and part number, if applicable. On classified documents, enter the title classification in parentheses.

Ba. CONTRACT NUMBER. Enter all contract numbers as they appear in the report, e.g. F33615-86-C-5169.

5b. GRANT NUMBER. Enter all grant numbers as they appear in the report, e.g. AFOSR-82-1234.

5c. PROGRAM ELEMENT NUMBER. Enter all program element numbers as they appear in the report, e.g. 61101A.

5d. PROJECT NUMBER. Enter all project numbers as they appear in the report, e.g. 1F665702D1257; ILIR.

5e. TASK NUMBER. Enter all task numbers as they appear in the report, e.g. 05; RF0330201; T4112.

5f. WORK UNIT NUMBER. Enter all work unit numbers as they appear in the report, e.g. 001; AFAPL30480105.

6. AUTHOR(S). Enter name(s) of person(s) responsible for writing the report, performing the research, or credited with the content of the report. The form of entry is the last name, first name, middle initial, and additional qualifiers separated by commas, e.g. Smith, Richard, J, Jr.

7. PERFORMING ORGANIZATION NAME(S) AND ADDRESS(ES). Self-explanatory.

8. PERFORMING ORGANIZATION REPORT NUMBER.

Enter all unique alphanumeric report numbers assigned by the performing organization, e.g. BRL-1234; AFWL-TR-85-4017-Vol-21-PT-2.

9. SPONSORING/MONITORING AGENCY NAME(S) AND ADDRESS(ES). Enter the name and address of the organization(s) financially responsible for and monitoring the work.

10. SPONSOR/MONITOR'S ACRONYM(S). Enter, if available, e.g. BRL, ARDEC, NADC.

11. SPONSOR/MONITOR'S REPORT NUMBER(S).

Enter report number as assigned by the sponsoring/monitoring agency, if available, e.g. BRL-TR-829; -21 5.

12. DISTRIBUTION/AVAILABILITY STATEMENT. Use agency-mandated availability statements to indicate the public availability or distribution limitations of the report. If additional limitations/ restrictions or special markings are indicated, follow agency authorization procedures, e.g. RD/FRD, PROPIN, ITAR, etc. Include copyright information.

13. SUPPLEMENTARY NOTES. Enter information not included elsewhere such as: prepared in cooperation with; translation of; report supersedes; old edition number, etc.

14. ABSTRACT. A brief (approximately 200 words) factual summary of the most significant information.

15. SUBJECT TERMS. Key words or phrases identifying major concepts in the report.

16. SECURITY CLASSIFICATION. Enter security classification in accordance with security classification regulations, e.g. U, C, S, etc. If this form contains classified information, stamp classification level on the top and bottom of this page.

17. LIMITATION OF ABSTRACT. This block must be completed to assign a distribution limitation to the abstract. Enter UU (Unclassified Unlimited) or SAR (Same as Report). An entry in this block is necessary if the abstract is to be limited.